

**THE DEVELOPMENT OF COASTAL SANDY SOIL AGE SEQUENCES
IN AUSTRALIA :
WITH EMPHASIS ON HEAVY MINERAL WEATHERING**

A thesis submitted in fulfilment of the requirements for
the Degree of Doctor of Philosophy,
Faculty of Agricultural Science,
The University of Adelaide

by
MUSTAPHA S. TEJAN-KELLA

Department of Soil Science
Waite Agricultural Research Institute
The University of Adelaide

MARCH 1990.

TABLE OF CONTENTS

List of Figures	viii
List of Tables	xiii
List of Plates	xv
List of Appendices	xxii
Abstract	xxiii
Statement	xxvi
Acknowledgements	xxvii
CHAPTER 1 INTRODUCTION	1
CHAPTER 2 SITE DESCRIPTIONS, SOIL PROPERTIES AND SOIL CLASSIFICATION	6
2.1. Site descriptions	6
2.1.1. Introduction	6
2.1.2. Location and general description	6
2.1.2.1. Cooloola and North Stradbroke Island	6
2.1.2.2. LeFevre Peninsula and Mount Compass	8
2.1.2.3. Canunda and Mount Burr	13
2.1.3. Geology and geomorphology	13
2.1.3.1. Introduction	13
2.1.3.2. Cooloola and North Stradbroke Island	13
2.1.3.3. LeFevre Peninsula and Mount Compass	16
2.1.3.4. Canunda and Mount Burr	19
2.1.4. Climate	21
2.1.4.1. Introduction	21
2.1.4.2. Rainfall	24
2.1.4.3. Evapotranspiration	25
2.1.4.4. Temperature and relative humidity	25
2.1.4.5. Wind	27

TABLE OF CONTENTS (contd.)

2.1.4.6. Vegetation	28
2.2. Soil properties	30
2.2.1. Introduction	30
2.2.2. Soil sample collection and profile description	30
2.2.3. Laboratory analyses	31
2.2.3.1. Physical analyses	31
2.2.3.2. Chemical analyses	32
2.2.4. Results and discussion	34
2.2.4.1. Calcareous soils	34
2.2.4.2. Siliceous soils	36
2.3. Soil classification and pedogenic processes	38
2.3.1. Introduction	38
2.3.2. Uniform textured soils	41
2.3.2.1. Calcareous sands	41
2.3.2.2. Siliceous sands	42
2.3.2.3. Podzols	42
2.4. Summary	44
CHAPTER 3 AGE SEQUENCES	45
3.1. Introduction	45
3.2. Cooloola - North Stradbroke Island sequence	47
3.2.1. Introduction	47
3.2.2. Materials and methods	50
3.2.2.1. Site description	50
3.2.2.2. Sampling	50
3.2.2.3. Laboratory analysis	52
3.2.3. Results and Discussion	53
3.2.3.1. TL measurements	54
3.2.3.2. DTA-TGA and SEM analysis	57

TABLE OF CONTENTS (contd.)	
3.2.3.3. Annual dose rate measurements	62
3.2.3.4. Age determination	67
3.2.4. Conclusions	70
3.3. LeFevre Peninsula-Mount Compass sequence	70
3.3.1. Introduction	70
3.3.2. Inferred ages	71
3.3.3. Absolute radiocarbon ages	73
3.3.4. Absolute thermoluminescence ages	74
3.4. Canunda-Mount Burr sequence	74
3.4.1. Inferred ages	75
3.4.2. Absolute radiocarbon ages	76
3.5. Summary	77
CHAPTER 4 MICROMORPHOLOGY	80
4.1. Introduction	80
4.2. Materials and methods	81
4.2.1. Soils	81
4.2.2. Sampling	81
4.2.3. Impregnation	82
4.2.4. Sawing, mounting and lapping	82
4.2.5. Descriptive methods and terminology	82
4.3. Results	84
4.3.1. Micromorphology of the Cooloola-North Stradbroke Island sequence	84
4.3.2. Micromorphology of the LeFevre Peninsula-Mount Compass sequence	100
4.3.3. Micromorphology of the Canunda-Mount Burr sequence	113
4.4. Discussion	120

TABLE OF CONTENTS (contd.)

4.4.1. Cooloola-North Stradbroke Island sequence	120
4.4.2. LeFevre Peninsula-Mount Compass sequence	122
4.4.3. Canunda-Mount Burr sequence	124
4.4.4. General discussion	125
4.5. Conclusions	128
CHAPTER 5 WEATHERING ASSESSMENT USING SCANNING	
ELECTRON MICROSCOPY	129
5.1. Introduction	129
5.2. Materials and methods	130
5.2.1. Soil Samples	130
5.2.2. Laboratory analysis	131
5.2.3. Weathering assessment	132
5.2.3.1. Point value score (PVS) method	135
5.2.3.2. Value assessment score (VAS) method	135
5.2.3.3. Statistical analysis	137
5.3. Results	138
5.3.1. X-ray diffraction and SEM-EDAX	138
5.3.2. Relative weathering assessment	138
5.3.2.1. Weathering trends between minerals	145
5.3.2.2. Weathering trends within profiles	151
5.3.2.3. Weathering trends between profiles	151
5.3.3. Assessment of weathering patterns from statistical analysis of PVS and VAS data	157
5.4. Discussion	163
5.4.1. Mineral identification	163
5.4.2. Numerical and statistical weathering assessment	163
5.4.2.1. Physical characteristics of minerals	164
5.4.2.2. Chemical characteristics of minerals	167

TABLE OF CONTENTS (contd.)	
5.4.2.3. Geologic history of sediment	167
5.4.2.4. Soil weathering	168
5.5. Conclusions	171
CHAPTER 6 PRE- AND POST-DEPOSITIONAL WEATHERING	
CHARACTERISTICS OF ZIRCON AND RUTILE	
6.1. Introduction	173
6.2. Materials and Methods	175
6.2.1. Study area and Materials	175
6.2.2. Methods	176
6.3. Results	176
6.3.1. Scanning electron microscopy	176
6.3.1.1. Qualitative analysis of surface microtextures	176
6.3.1.2. Quantitative analysis of surface microtextures	180
6.4. Discussion	187
6.4.1. Chemical weathering features and pedogenic processes	187
6.4.2. Mechanical/physical weathering features and other environmental processes	189
6.4.3. Physico-chemical weathering features and other environmental processes	190
6.5. Conclusions	192
CHAPTER 7 MINERALOGY AND CHEMISTRY OF HEAVY	
MINERAL FRACTION	
7.1. Introduction	194
7.2. Materials and methods	197
7.2.1. Materials	197
7.2.2. Methods	198
7.2.2.1. Heavy mineral separation and fractionation	198
7.2.2.2. Grain impregnation and mounting	198

TABLE OF CONTENTS (contd.)	
7.2.2.3. Electron microprobe analysis	199
7.2.2.4. X-ray fluorescence spectroscopy	200
7.3. Results and discussion	200
7.3.1. Parent material uniformity	200
7.3.1.1. 53-125 μm fraction percent	200
7.3.1.2. Total heavy mineral (THM) percent	206
7.3.1.3. Magnetic mineral fraction percent	211
7.3.1.4. Zircon:rutile ratio	218
7.3.1.5. Zirconium:titanium ratio	221
7.3.1.6. Summary	229
7.3.1.7. Statistical evaluation	230
7.4.1. Weathering	237
7.4.1.1. 53-125 μm and THM fractions	237
7.4.1.2. Magnetic fractions	239
7.4.1.3. Zircon:rutile and zirconium:titanium ratios	240
7.5.1. Nature of zircons in soils	242
7.5.1.1. Zirconium and hafnium contents, and Zr:Hf ratios of zircon grains	243
7.6. Conclusions	247
CHAPTER 8 GENERAL DISCUSSION AND CONCLUSION	249
8.1. Introduction	249
8.2. Thermoluminescence dating and related studies, and weathering rates with time	250
8.3. Stages of soil development based on micromorphology and SEM	252
8.4. Environmental effects of mineral weathering based on SEM studies	254
8.5. Mineral distribution and characteristics in soils	258

TABLE OF CONTENTS (contd.)

8.6. General conclusions	264
8.7. Suggestions for future work	266
APPENDICES	267
REFERENCES	278

LIST OF FIGURES

Fig.	Title	Page
1.1.	Distribution of calcareous and siliceous sands in the south eastern region of Australia.	3
1.2.	Extent of Podzol development associated with the south eastern region of Australia.	5
2.1.	Locality map of sampling areas.	7
2.2.	Location of soil sample sites at Cooloola.	9
2.3.	Location of soil sample site at North Stradbroke Island.	10
2.4.	Location of soil sample sites at LeFevre Peninsula.	11
2.5.	Location of soil sample site at Mount Compass.	12
2.6.	Location of soil sample sites at Canunda and Mount Burr.	14
2.71.	Particle size distributions of horizons within Canunda soil profile (untreated samples).	35
2.72.	Particle size distributions of horizons within Canunda soil profile (acid treated samples).	35
3.1.	Schematic cross-section of the soil profiles sampled showing the increase in delopment with age (modified from Thompson, 1983).	51
3.2.	Glow curve for Amity sample which has received only the natural dose.	54
3.3.	Dose plateau for Amity sample with natural glow curve superimposed. The error bars are assigned by the curve fitting programme.	55
3.4.	Regenerative TL data for Amity sample used for calculating ED at peak temperature (○, natural sample; □, bleached sample).	56
3.5.	DTA (—) and TGA (- -) traces for (A) Kings Bore, (B) Warrawonga, (C) Amity and (D) Kabali samples for pre-treatment (b): the 90-125 μm non-magnetic fraction, HF and HCl treated, used in TL dating.	58
3.6.	DTA (—) and TGA (- -) traces for (A) Kings Bore, (B) Warrawonga, (C) Amity and (D) Kabali samples for pre-treatment (a): the 90-125 μm non-magnetic fraction, untreated.	59
3.7.	Schematic time diagram for a post-incisive chronosequence. The bars represent time intervals of soil development (after Vreeken, 1975).	73
3.8.	The Holocene marine transgression. Alternative interpretations of sea level changes during the past 6000 years are indicated. Fairbridge considers that the sea rose to higher levels (O.P. = Older Peron, Y.P. = Younger Peron, A = Abrolhos, and R = Rottnest stages); Shepard thinks it attained present level without exceeding it during Recent times (after Bird, 1976).	79

LIST OF FIGURES (Contd.)

Fig.	Title	Page
4.1.	The simple arrangements of coarse to fine components observed in soil thin sections (after Murphy <i>et al.</i> , 1985).	83
5.1.	Flow chart of laboratory methods.	133
5.21.	Powder x-ray diffraction pattern of non-magnetic heavy mineral fraction in the E horizon of Kings Bore profile.	139
5.22.	Powder x-ray diffraction pattern of non-magnetic heavy mineral fraction in the E horizon of Chalambar profile.	139
5.3.	EDAX spectrum for monazite from E horizon of Seacliffs profile.	142
5.40.	Weathering of different minerals in soils from the south east coast of Queensland based on the mean point value and value assessment scores of 30 grains (5.401, Kings Bore profile, mean point value scores), (5.402, Chalambar profile, mean point value scores), (5.403, Seacliffs profile, mean point value scores), (5.404, Kings Bore profile, mean value assessment scores), (5.405, Chalambar profile, mean value assessment scores), (5.406, Seacliffs profile, mean value assessment scores), (5.407, Warrawonga profile, mean point value scores), (5.408, Amity profile, mean point value scores), (5.409, Warrawonga profile, mean value assessment scores), (5.410, Amity profile, mean value assessment scores).	146
5.41.	Weathering of different minerals in soils from the central South Australian coast based on the mean point value and value assessment scores of 30 grains (5.411, LeFevre Peninsula 2 profile, mean point value scores), (5.412, Mount Compass profile, mean point value scores), (5.413, LeFevre Peninsula 2 profile, mean value assessment scores), (5.414, Mount Compass profile, mean value assessment scores).	149
5.42.	Weathering of different minerals in soils from the south east South Australian coast based on the mean point value and value assessment scores of 30 grains (5.421, Canunda profile, mean point value scores), (5.422, Mount Burr profile, mean point value scores), (5.423, Canunda profile, mean value assessment scores), (5.424, Mount Burr profile, mean value assessment scores).	150
5.43.	Weathering of different minerals in soils from A horizons of different profiles based on the mean point value and value assessment scores of 30 grains (5.431, A horizons of different profiles, mean point value scores), (5.432, A horizons of different profiles, mean value assessment scores).	152

LIST OF FIGURES (Contd.)

Fig.	Title	Page
5.44.	Weathering of different minerals in soils from E horizons of different profiles based on the mean point value and value assessment scores of 30 grains (5.441, E horizons of different profiles, mean point value scores), (5.442, E horizons of different profiles, mean value assessment scores).	153
5.45.	Weathering of different minerals in soils from B horizons of different profiles based on the mean point value and value assessment scores of 30 grains (5.451, Bhs2 horizons of different profiles, mean point value scores), (5.452, B2 horizons of different profiles, mean point value scores), (5.453, Bhs2 horizons of different profiles, mean value assessment scores), (5.454, B2 horizons of different profiles, mean value assessment scores).	154
5.46.	Weathering of different minerals in soils from B3 and C horizons of different profiles based on the mean point value and value assessment scores of 30 grains (5.461, B3 horizons of different profiles, mean point value scores), (5.462, C horizons of different profiles, mean point value scores), (5.463, B3 horizons of different profiles, mean value assessment scores), (5.464, C horizons of different profiles, mean value assessment scores).	155
5.47.	Weathering of different minerals in AC horizons of soils from Carlo and Canunda sites based on the mean point value and value assessment scores of 30 grains (5.471, AC horizons of different profiles, mean point value scores), (5.472, AC horizons of different profiles, mean value assessment scores).	156
6.1.	Occurrence of microtextural features on grain surfaces from selected horizons.	179
6.21.	EDAX spectrum for zircon from E horizon of Seacliffs profile.	181
6.22.	EDAX spectrum for rutile from E horizon of Seacliffs profile.	181
7.10.	Percent weight of 53-125 μm fraction and total heavy mineral fraction in the < 2 mm fraction of soils from the south east coast of Queensland (7.101, Kings Bore profile), (7.102, Chalambar profile), (7.103, Warrawonga and Seacliffs profiles), (7.104, Amity profile).	201
7.11.	Percent weight of 53-125 μm fraction and total heavy mineral fraction in the < 2 mm fraction of soils from the central South Australian coast (7.111, LeFevre Peninsula 1 and LeFevre Peninsula 2 profiles, (7.112, Mount Compass profile).	202

LIST OF FIGURES (Contd.)

Fig.	Title	Page
7.12.	Percent weight of 53-125 μm fraction and total heavy mineral fraction in the < 2 mm fraction of soils from the south east South Australian coast (7.121, Canunda site), (7.122, Mount Burr profile).	202
7.13.	Percent weight of 53-125 μm fraction and total heavy mineral fraction in the < 2 mm fraction of soils from comparable horizons of different profiles (7.131, A horizons of different profiles), (7.132, E horizons of different profiles), (7.133, B2 horizons of different profiles), (7.134, B3 horizons of different profiles), (7.135, C horizons of different profiles).	207
7.20.	Percent weight of NM, SM and VM heavy mineral fraction in the <2 mm fraction of soils from the south east coast of Queensland (7.201, Kings Bore profile), (7.202, Chalambar profile), (7.203, Warrawonga profile), (7.204, Seacliffs profile), (7.205, Amity profile).	212
7.21.	Percent weight of NM, SM and VM heavy mineral fraction in the <2 mm fraction of soils from the central South Australian coast (7.211, LeFevre Peninsula 1 and LeFevre Peninsula 2 profiles, (7.212, Mount Compass profile).	213
7.22.	Percent weight of NM, SM and VM heavy mineral fraction in the <2 mm fraction of soils from the south east South Australian coast (7.221, Canunda site), (7.222, Mount Burr profile).	214
7.23.	Percent weight of NM, SM and VM heavy mineral fraction in the <2 mm fraction of soils from comparable horizons of different profiles (7.231, A horizons of different profiles), (7.232, E horizons of different profiles), (7.233, B2 horizons of different profiles), (7.234, B3 horizons of different profiles), (7.235, C horizons of different profiles).	215
7.30.	Zircon:rutile ratio of the 53-125 μm fraction of soils from the south east coast of Queensland (7.301, Kings Bore profile), (7.302, Chalambar profile), (7.303, Warrawonga and Seacliffs profiles), (7.304, Amity profile).	219
7.31.	Zircon:rutile ratio of the 53-125 μm fraction of soils from the central South Australian coast (7.311, LeFevre Peninsula 1 and LeFevre Peninsula 2 profiles, (7.312, Mount Compass profile).	220
7.32.	Zircon:rutile ratio of the 53-125 μm fraction of soils from the south east South Australian coast (7.321, Canunda site), (7.322, Mount Burr profile).	220

LIST OF FIGURES (Contd.)

Fig.	Title	Page
7.33.	Zircon:rutile ratio of the 53-125 μm fraction of soils from comparable horizons of different profiles (7.331, A horizons of different profiles), (7.332, E horizons of different profiles), (7.333, B2 horizons of different profiles), (7.334, Bhs2 horizons of different profiles), (7.335, B3 horizons of different profiles), (7.336, C horizons of different profiles).	222
7.40.	Zirconium:titanium ratio of the 53-125 μm fraction of soils from the south east coast of Queensland (7.401, Kings Bore profile), (7.402, Chalambar profile), (7.403, Warrawonga and Seacliffs profiles), (7.404, Amity profile).	224
7.41.	Zirconium:titanium ratio of the 53-125 μm fraction of soils from the central South Australian coast (7.411, LeFevre Peninsula 2 profile, (7.412, Mount Compass profile).	225
7.42.	Zirconium:titanium ratio of the 53-125 μm fraction of soils from comparable horizons of different profiles (7.421, A horizons of different profiles), (7.422, E horizons of different profiles), (7.423, Bhs2 horizons of different (7.424, C horizons of different profiles).	227

LIST OF TABLES

Table	Title	Page
2.1.	Mean annual climatic data for stations nearby sampling sites (Bureau of Meteorology, 1988).	22
2.2.	Summary of selected environmental characteristics at each sampling location.	23
2.3.	Comparison of the approximate classification of soils studied, using different system.	40
3.1.	Percent weight losses for 40 mg air dried samples subjected to four different pre-treatments, based on TGA curves.	60
3.2.	Major element composition of ignited samples.	63
3.3.	Comparison of U and Th concentrations ($\mu\text{g g}^{-1}$) using XRF, TSAC and γ -spectroscopy.	64
3.4.	Comparison of TL, inferred and isotope dates for samples.	65
3.5.	Summary comparison of ages for samples from LeFevre Peninsula-Mount Compass and Canunda-Mount Burr sequences.	72
4.1.	Classification of related distribution patterns of soils (modified from Murphy <i>et al.</i> , 1985).	85
4.2.	Comparison of selected soil and micromorphological data for the different section.	86
5.1.	Surface microtextural features of heavy mineral grains used in assessing weathering class.	134
5.2.	Weathering classification of heavy mineral grains.	135
5.3.	Value assessment of heavy mineral grain micro-textures (after Setlow and Karpovich, 1972).	136
5.4.	Weathering classification of minerals based on mean point value score (MPVS) and mean value assessment score (MVAS).	144
5.5.	Results of the Kruskal-Wallis non-parametric test based on the hypothesis that no significant difference existed in the degree of weathering between different mineral types within the same horizon of a profile.	158
5.6.	Results of the Kruskal-Wallis test based on the hypothesis that no significant difference existed between weathering of different mineral types within the different horizons of a profile.	160

LIST OF TABLES (contd.)

Table	Title	Page
5.7.	Results of the Kruskal-Wallis test based on the hypothesis that there were no significant differences between weathering of the same mineral type in similar horizons between different soil profiles in regionalised sequences.	162
6.1.	Soils associated with the different profiles in the dunes studied.	175
6.2.	Comparison of surface features between grains within the same soil profile.	182
6.3.	Comparison of surface features between grains within the same horizons in different soil profiles using Carlo as a reference profile.	183
6.4.	Comparison of surface features on zircon and rutile in the same horizons of different soil profiles using Carlo as a reference profile.	184
7.1.	Percent 53-125 μm fraction particles and heavy minerals in the < 2 mm fraction, and ratio data for individual soil profiles. Means, Standard deviations and coefficients of variation.	203
7.2.	Percent by weight of (a) 53-125 μm fraction, (b) total heavy mineral, (c) zircon and (d) rutile in the < 2 mm soil fraction, and ratio data for comparable horizons of different soil profiles. Means, Standard deviations and coefficients of variation.	209
7.3.	Percent 53-125 μm fraction particles and heavy minerals in the < 2 mm soil fraction, and ratio data for soil sequences based on locations. Means, Standard deviations and coefficients of variation.	231
7.4.	Percent 53-125 μm fraction particles and heavy minerals in the < 2 mm soil fraction, and ratio data for soil horizons from all locations combined. Means, Standard deviations and coefficients of variation.	233
7.5.	The zirconium and hafnium content and the zirconium:hafnium ratio of zircon in selected horizons from different sites.	244
7.6.	Comparison of variances of zirconium and hafnium contents, and Zr:Hf ratios of zircon grains in selected horizons of soils from south east coastal region of Queensland.	245
7.7.	Comparison of variances of zirconium and hafnium contents, and Zr:Hf ratios of zircon grains in selected horizons of soils from central and south east coastal region of South Australia, and in all horizons analysed.	246

LIST OF PLATES

Plate	Title	Page
3.1.	Scanning electron micrographs of quartz grains after different pre-treatments (A) 90-125 μm , non-magnetic fraction (pre-treatment a) for Kings Bore, (B) 90-125 μm , non-magnetic fraction (pre-treatment a) for Amity and (C) 90-125 μm , non-magnetic fraction (pre-treatment b) for Kings Bore. Note, in (A) arrow indicates natural crack in quartz grain and boxed area indicates a portion of the surface coatings, and in (B) arrow indicates accentuated crack after HF etching.	61
4.1.	Photomicrograph showing single grain structure in section from Bhs2 (A)/B3 (B) horizon of Kings Bore. Quartz and heavy mineral grains (a = zircon, b = rutile, c = ilmenite) loosely arranged with little or no fine material around grains. <i>PPL</i> . Bar scale 100 μm .	91
4.2.	Photomicrograph of monic related distribution pattern in section from Bhs2/B3 horizon of Kings Bore with a large fragment of weakly to moderately altered plant tissue. <i>PPL</i> . Bar scale 100 μm .	91
4.3.	Photomicrograph of monic related distribution pattern in section from A1/E horizon of Chalambar. Locally a tendency to chitonic with quartz and heavy mineral grains (a = zircon, b = rutile, c = ilmenite) partly or wholly surrounded by dark yellow brown fine material. <i>PPL</i> . Bar scale 100 μm .	91
4.4.	Photomicrograph of monic related distribution pattern in section from A1/E horizon of Chalambar. Note, highly altered plant fragments and moderately coalesced excrements. <i>PPL</i> . Bar scale 100 μm .	91
4.5.	Photomicrograph of chitonic related distribution pattern in section from Bhs2 horizon of Chalambar. Coarse quartz grain wholly or partly coated with dark yellowish brown fine material. <i>PPL</i> . Bar scale 100 μm .	91
4.6.	Photomicrograph of dense incomplete and loose infillings in the Bhs2 horizon of Chalambar. Dense strongly coalesced excrements (arrow) masked by organic rich fine material. <i>XPL</i> . Bar scale 100 μm .	91
4.7.	Photomicrograph of monic related distribution pattern in section from E/B1 horizon of Seacliffs. Mineral grains show high degree of alteration (c = irregular linear, d = dotted) patterns. <i>XPL</i> . Bar scale 100 μm .	96

LIST OF PLATES (contd.)

Plate	Title	Page
4.8.	Photomicrograph of monic related distribution pattern in section from E/B1 horizon of Amity. In section A = E horizon and B = B1 horizon. Quartz and heavy mineral (e.g. a = zircon, b = rutile, c = ilmenite with rutile inclusion) grains show irregular linear alteration patterns. <i>XPL</i> . Bar scale 100 μ m.	96
4.9.	Photomicrograph of gefuric related distribution in section from Bhs2 portion of E(pipe)/Bhs2 horizon of Amity. The bridging fine material comprises mainly opaque organic components. <i>XPL</i> . Bar scale 100 μ m.	96
4.10.	Photomicrograph of a combination of monic, gefuric and enaulic related distribution in section from E(pipe)/Bhs2 horizon of Amity. Note, A part of section is E horizon (monic) and B part is Bhs2 (gefuric and enaulic). Pigmentation of quartz grains with dark brown coloured organic fine material. <i>PPL</i> . Bar scale 100 μ m.	96
4.11.	Photomicrograph of enaulic related distribution in section from central Bhs2 horizon of Amity. Note, irregularly shaped aggregates of dark stained fine material in inter-granular spaces of quartz grains. <i>XPL</i> . Bar scale 100 μ m.	96
4.12.	Photomicrograph of coarse mineral grains wholly or partly surrounded by fragmented dark fine material. Section of lower Bhs2 horizon of Amity. Note, z = zircon grain. <i>XPL</i> . Bar scale 100 μ m.	96
4.13.	Photomicrograph of coarse mineral grains from section of the lower Bs horizon of Amity showing chitonic related distribution and pellicular microstructure. The grains are surrounded by thin sesquioxidic coatings. Note, r = rutilated-quartz grain. <i>XPL</i> . Bar scale 100 μ m.	101
4.14.	Photomicrograph showing monic related distribution, locally tending to chitonic. The fine material surrounding and pigmenting the coarse grains is yellowish brown organo-mineral complex. Coarse grains exhibit complex alteration patterns. Section from B3 horizon of Amity. <i>XPL</i> . Bar scale 100 μ m.	101
4.15.	Photomicrograph showing inter-grain micro-aggregate structure from section of A2 horizon of LeFevre Peninsula 1. Generally uncoated mineral grains (e.g. f = plagioclase feldspar) and inorganic residues of gastropods with numerous organic micro-aggregates in the inter-granular spaces. <i>XPL</i> . Bar scale 100 μ m.	101

LIST OF PLATES (contd.)

Plate	Title	Page
4.16.	Photomicrograph showing single grain structure from section of A2 horizon of LeFevre Peninsula 1. Quartz grains, gastropods and plant remains loosely arranged with little or no fine material to provide aggregation. <i>XPL</i> . Bar scale 100 μm .	101
4.17.	Photomicrograph of open porphyric related distribution in section from E(pipe)/B1 horizon of Mount Compass. The coarse grains are embedded in a dense ferruginous matrix. <i>XPL</i> . Bar scale 100 μm .	101
4.18.	Photomicrograph of gefuric and chitonic related distribution in section from Bhsb2/Bhsb3 horizon of Mount Compass. The coatings and infillings comprise dark organo-mineral fine material in places pigmenting coarse grains. <i>XPL</i> . Bar scale 100 μm .	101
4.19.	Photomicrograph showing chitonic related distribution in section from Bhsb2/Bhsb3 horizon of Mount Compass. Note, altered plant tissue (organic residue) with deposits of dark coloured organic matter occupying the outer layer (arrow) of the organ fragment. Organic pigments also stain grains. <i>XPL</i> . Bar scale 100 μm .	106
4.20.	Photomicrograph showing open porphyric related distribution in section from Bhsb2/Bhsb3 horizon of Mount Compass. Note, the quartz grains are embedded in a dense ferruginous (F) and manganiferous (M) matrix forming a large impregnative nodule. <i>XPL</i> . Bar scale 100 μm .	106
4.21.	Photomicrograph showing dense complete void infillings with bow-like distribution pattern (arrow) in section from Bhsb2/Bhsb3 horizon of Mount Compass. The microlaminated infillings consist of deposits of dark coloured organic matter plus clay. <i>PPL</i> . Bar scale 100 μm .	106
4.22.	Photomicrograph of compound manganiferous and ferruginous strong impregnative nodule in a section from Bhsb2/Bhsb3 horizon of Mount Compass. Note, the ferruginous outer component diffuses into the manganiferous inner member. <i>XPL</i> . Bar scale 100 μm .	106
4.23.	Photomicrograph showing chitonic related distribution in section from Bhsb3 horizon of Mount Compass. The strong orientation of the fine material around the coarse grains (a = zircon) causes micro-channel formation in voids (arrow). <i>XPL</i> . Bar scale 100 μm .	106

LIST OF PLATES (contd.)

Plate	Title	Page
4.24.	Photomicrograph showing vughy microstructure in section from Bhsb3 horizon of Mount Compass. The continuity of the organic rich fine mass is broken by irregularly shaped vughs (e.g. v). Note, large channel (c) with walls coated with organic rich fine material. <i>PPL</i> . Bar scale 100 μm .	106
4.25.	Photomicrograph of microlaminated organic and clay rich infilling in section from Bsb3 horizon of Mount Compass. The layered infillings around grains and walls of voids (v) show complex replicated zones of dark and bright coloured organic and clay rich deposits respectively (A) Note, dessication cracks (arrow). <i>PPL</i> . Bar scale 100 μm .	112
4.26.	Organic-clay rich void infillings and coatings similar to that in Plate 4.25, but with more distinct zones of accumulation of organic and clay rich fine material. Replicated boundary layers between organic and clay rich fine material. <i>XPL</i> . Bar scale 100 μm .	112
4.27.	Photomicrograph of pellicular microstructure in section from Bb4 horizon of Mount Compass. The quartz grains are completely surrounded by organo-mineral fine material which bridges and welds the grains together. <i>PPL</i> . Bar scale 100 μm .	112
4.28.	Photomicrograph of vughy microstructure in section from Bb4 horizon of Mount Compass. The continuity of the organic fine material is broken up by irregular shaped vughs as in Plate 4.24. Note, the dark coloured organic deposit has condensed earlier deposits of yellow coloured clayey fine material (e.g. arrow). <i>XPL</i> . Bar scale 100 μm .	112
4.29.	Photomicrograph of gefuric related distribution in section from Ab2 horizon of Canunda. Organic and carbonate rich fine material forms bridges between coarse grain carbonate inorganic residues. Distinctive carbonate deposit (a) in void space. Coarse grains are stained by organic pigments. <i>XPL</i> . Bar scale 100 μm .	112
4.30.	Photomicrograph of inter-grain micro-aggregate structure in section from Bb1 horizon of Canunda. The mostly uncoated grains have numerous organic micro-aggregates (possibly soil animal excrements) in the inter-grain spaces. Organic pigmentation of coarse grains. <i>XPL</i> . Bar scale 100 μm .	112
4.31.	Photomicrograph of monic related distribution in section from Bb3 horizon of Canunda. The inorganic residues are highly altered, with distinctive carbonate rich deposits in inter-granular spaces. Organic pigmentation of coarse grains. <i>XPL</i> . Bar scale 100 μm .	117

LIST OF PLATES (contd.)

Plate	Title	Page
4.32.	Photomicrograph showing chitonic related distribution in section from Bhs2 horizon of Mount Burr. The quartz grains are partly or wholly surrounded by dark organic rich fine material. Locally tending to gefuric, with organic pigmentation of coarser grains. <i>XPL</i> . Bar scale 100 μm .	117
4.33.	Photomicrograph of microlaminated clay rich infilling of void in section from Bs horizon of Mount Burr. Note, complete infilling of inter-granular spaces, and alternating layers of impure clay and silt (arrow). <i>XPL</i> . Bar scale 100 μm .	117
5.1.	Scanning electron micrograph of rutilated-quartz grain from E horizon of Kings Bore. Note, (A) and (B) indicate portions of rutile and quartz respectively.	140
5.2.	X-ray diffraction patterns of rutilated-quartz and heavy minerals: (A) rutilated quartz from E horizon of Kings Bore, (B) sillimanite from A1 horizon of LeFevre Peninsula 2, (C) garnet (grossularite) from Bhs2 horizon of Kings Bore, (D) spinel (Cr-spinel) from E horizon of Chalambar and (E) epidote (zoisite) from C horizon of Chalambar. Note, all patterns taken using a Gandolfi single-grain camera and $\text{CoK}\alpha$ radiation.	141
5.3.	Scanning electron micrographs of selected heavy mineral grains: (A) zircon, (B) rutile, (C) sillimanite, (D) garnet, (E) monazite, (F) spinel and (G) epidote used for weathering classification system outlined in Table 5.5.	143
5.41.	Scanning electron micrograph of spinel grain from Bs2 horizon of Seacliffs, minor etch pits and slightly rounded edges showing traces of octahedral habit.	165
5.42.	Scanning electron micrograph of garnet grain from C horizon of Kings Bore showing rounded edges and slightly more severe etch pits.	165
5.43.	Scanning electron micrograph of garnet grain from E horizon of Kings Bore showing the development of well defined etch and delicate needle-like terminations during dissolution.	165
5.44.	Scanning electron micrograph of epidote grain from E horizon of Kings Bore showing mamillary and virtually unetched features.	165
5.45.	Scanning electron micrograph of epidote grain from Bhs2 horizon of Seacliffs showing severely etched and rounded features.	165

LIST OF PLATES (contd.)

Plate	Title	Page
5.46.	Scanning electron micrograph of monazite grain from E horizon of Chalambar showing well rounded and etched features.	165
5.47.	Scanning electron micrograph of zircon grain from A1 horizon of Canunda showing rare etch pits and euhedral surface features and crystal form respectively.	166
5.48.	Scanning electron micrograph of zircon grain from E horizon of Mount Compass showing unetched and euhedral surface features and crystal form respectively.	166
5.49.	Scanning electron micrograph of rutile grain from C horizon of LeFevre Peninsula 2 showing slight etching at fractured surfaces.	166
5.410.	Scanning electron micrograph of rutile grain from E(pipe) horizon of Mount Compass showing angular form and rarely any etch pits.	166
5.411.	Scanning electron micrograph of sillimanite grain from A1 horizon of Mount Compass showing fresh unetched crystal faces.	166
5.412.	Scanning electron micrograph of sillimanite grain from A1 horizon of LeFevre Peninsula 2 showing etching and dissolution at grain terminations.	166
5.413.	Scanning electron micrograph of rutile grain from E horizon of Kabali showing intense dissolution of silicon rich portions, leaving skeletal titanium rich grain.	166
6.1.	Zircon grain from B3 horizon of Chalambar soil profile with high relief, clean/smooth surfaces, conchoidal fracture/breakage blocks, etch pits, subdued/rounded edges and hairline cracks.	177
6.2.	Zircon grain from Carlo soil with high relief, clean/smooth surfaces, conchoidal fractures, etch pits and subdued edges.	177
6.3.	Zircon grain from A1 horizon of Chalambar soil profile with clean/smooth surfaces, angular/sharp edges and etch pits.	177
6.4.	Zircon grains from A1 horizon of Chalambar soil profile with clean/smooth surfaces, angular/sharp edges and some adhered particles (left grain); clean/smooth surfaces, subdued/rounded edges and hairline cracks (right grain).	177

LIST OF PLATES (contd.)

Plate	Title	Page
6.5.	Zircon grain from A1 horizon of Chalambar soil profile with scaled surfaces, etch pits, subdued/rounded edges and hairline cracks.	177
6.6.	Zircon grain from C horizon of Chalambar soil profile with clean/smooth surfaces, breakage blocks, scaled/rough surfaces, etch pits, subdued/rounded edges and hairline cracks.	177
6.7.	Rutile grain from E horizon of Chalambar soil profile with breakage block, precipitation surfaces, rough surfaces, etch pits and subdued edges.	178
6.8.	Rutile grain from E horizon of Kings Bore soil profile with solution/precipitation surfaces, scaled surfaces and subdued/rounded edges.	178
6.9.	Rutile grain from C horizon of Kings Bore soil profile with solution/precipitation surfaces, scaled surfaces and subdued/rounded edges.	178
6.10.	Rutile grain from Bhs2 horizon of Seacliffs soil profile with etch pits, subdued/rounded edges and coated surfaces.	178
6.11.	Rutile grain from A1 horizon of Kings Bore soil profile with high relief, clean surfaces, solution/precipitation surfaces, scaled surfaces and subdued/rounded edges.	178
6.12.	Rutile grain from E horizon of Chalambar soil profile with clean surfaces, breakage block, scaled surfaces, etch pits, subdued/rounded edges and hairline cracks.	178

LIST OF APPENDICES

Appendix	Title	Page
1.	Monthly and annual climatic data for stations nearby sampling sites (Bureau of Meteorology, 1988).	267
2.	Selected morphological data for samples associated with profiles studied.	272
3.	Physical and chemical analytical data for selected soil samples.	275

Abstract

Heavy minerals (s.g. > 2.9) often play a central role in pedological and sedimentological studies because of their supposed resistance to chemical and physical breakdown, and because they are indicators of the provenance of a sediment. However, despite the widely acceptable use of heavy minerals as pedogenic indices, the nature and weathering characteristics of key index heavy minerals (in particular zircon and rutile) in different soil weathering environments is not fully documented. In view of the paucity of systematic quantitative studies on the nature and extent of weathering of heavy minerals, the objectives of this thesis are (i) to apply a range of microscopic (optical and electron), thermal, mineralo-chemical and statistical techniques to characterize non opaque heavy minerals and quartz from a range of sandy soils (predominantly Entisols and Spodosols) within six age sequences from different regions consisting of different source materials and climatic conditions in the south eastern half of Australia (South Australia and Queensland) and (ii) to use these methods to determine, semi-quantitatively, weathering patterns of heavy mineral grains and apply them to investigations involving the uniformity of parent materials and weathering trends within soil profiles.

One factor of soil formation which is known to influence mineral weathering in soils is time. Even though inferred ages based on stratigraphic, geomorphic and denudational relationships with dated sequences were available for most of the soils studied, there were few absolute age determinations for most of the samples. For this reason thermoluminescence (TL) dating was successfully applied to establish an absolute age sequence for a Podzol chronosequence in Queensland.

Using micromorphological evidence, it was suggested that (i) two broad categories of soil development prevailed and (ii) the coarse to fine (c/f) related distribution pattern (rdp) became more complex (usually with more than one type of rdp present) as profile age increased. The presence of grain coatings and void infillings were used to explain differences in weathering characteristics of heavy mineral grains. A complex relationship was observed between the role of these features in absolutely

inhibiting or promoting the weathering of heavy mineral grains, presumably because of the effects of other soil forming processes on mineral weathering.

Using scanning electron microscopy (SEM), ten classes of surface microtextural features of mineral grains were quantified by two scaling methods. Based on these methods, a weathering classification scheme was developed. The following order of mineral resistance to weathering was established (starting with the most resistant) zircon > sillimanite \geq spinel \geq rutile > garnet > epidote > monazite. The two methods used proved useful in assessing pedogenic weathering trends between and within profiles from the different age sequences. These methods confirmed that, of the minerals examined, zircon was the most reliable mineral on which to base a pedogenetic index. However, the separation of pedogenetic and inherited lithological features proved difficult even in the chronosequence at Cooloola.

Zircon and rutile were studied more closely in a podzol chronosequence to investigate further the possible pedogenic changes associated with these two minerals with age. The frequency of occurrence of the ten classes of surface features used in the weathering class determination were adapted using the χ^2 distribution test. Pedogenic changes were quantified and differences between horizons within profiles, within the same horizon between profiles and between minerals, tested for significance. The results indicated that zircons were less chemically weathered than rutile, and that the presence of grain coatings did not seem to have prevented the surfaces of grains from developing solution pits. Zircons tend to show more features which are associated with physical alteration. Rutile grains in the illuviated Bhs2 horizons of the podzols were more thickly coated with poorly crystalline iron and alumino-silicate compounds compared with zircon grains. With increasing age there was a preponderance of 'weathering' features on grains of both minerals. The presence of various shapes and surface microtextures on grains from the different soils suggested a multiple grain source for zircon and rutile, and a complex predepositional history for these minerals.

The uniformity of parent material and weathering trends in all soils was investigated using a combination of weight fractionation, and mineral and elemental

ratio data of soil and heavy mineral separates. Except for one profile, the parent materials of all soils are uniform. Also, all soils showed some evidence of sedimentary layering or stratification. The use of these methods to investigate weathering trends in the soils studied was difficult to quantify, but did show broad trends. Elemental analysis of individual zircon grains suggested a multiple grain source for this mineral in all the soils examined.

In this thesis, the techniques used were effectively applied to the understanding of aspects relating to provenance, parent material uniformity and weathering of soil mineral constituents, particularly heavy mineral grains. It was concluded that the weathering patterns of different heavy minerals in the soils studied were complex. Although zircon was found to be the *most* resistant to weathering, no general rule can be applied which will be suitable for all soils. The choice of a heavy mineral for use as a pedogenetic indice should not be automatic (as has usually been the case), but should be justified by a study of its grain surface morphology by SEM or, at the very least, reflected light microscopy. This investigation could be carried out relatively quickly and would usually involve only a small amount of time relative to the overall weathering study. If there are differences in surface microtextures between horizons, further evaluation of the minerals, by weight fractionation and elemental analysis may be required.

STATEMENT

This thesis contains no material which has been accepted for the award of any other degree or diploma in any University. To the best of my knowledge this thesis contains no material published previously or written by any other person, except where due reference is made in the text of the thesis.

I consent to this thesis being made available for photocopying and loan.

MUSTAPHA S. TEJAN-KELLA

March, 1990.

ACKNOWLEDGEMENTS

I wish to thank my supervisors, Dr. D.J. Chittleborough (Department of Soil Science) and Dr. R.W. Fitzpatrick (CSIRO, Division of Soils) for their interest, guidance and invaluable discussions throughout this research.

I would also like to thank Mr. C.H. Thompson (CSIRO, Brisbane) for his assistance in the collection of the samples from Queensland, and for offering useful comments on some of the chapters in this dissertation. I am also grateful to Professor J.R. Prescott and Mr. J.T. Hutton (Department of Physics and Mathematical Physics, University of Adelaide) for introducing me to thermoluminescence work and for their cooperation and assistance in conducting research in their department.

Grateful acknowledgement is made to individuals of various sections of the CSIRO Division of Soils, Adelaide; Dr. P. Slade and Mr. M. Raven for assistance with single grain X-ray diffraction analysis; Messrs S. McClure, J.M. Thompson and P. Fazey for their help with scanning electron microscopy, thermal analyses and X-ray fluorescence analysis respectively; staff of the drawing office for producing some of the figures.

Thanks are also due to the following people: Miss S. Othams and Mrs. B. Goldsmith (Biometry Section, Waite Institute) for time devoted to typing portions of this thesis; Mr. J. Denholm (Department of Soil Science) for his assistance with laboratory work at various stages of the research; Mr. H. Rosser (Electron Optical Centre, University of Adelaide) for time spent with me on the electron microprobe; Mr. T. Hancock (Biometry Section, Waite Institute) for assisting, at various times, with the statistical analysis of my data. Mr. A. Dunbar (Photography Section, Waite Institute) helped prepare the photographs in this thesis.

I would like to thank other members of the Department of Soil Science for providing helpful discussions and an amicable working condition throughout the entire period of my program. Particular thanks go to Mrs. J. Ditchfield for her assistance with typing scores of manuscripts, as well as official correspondence.

I am indebted to the Australian International Assistance Bureau (AIDAB) for funding my study in Australia, and the Government of the Republic of Sierra Leone for allowing this program to go through.

The patience, understanding and invaluable support of my wife, Amie and son, Quanmalo shall always be remembered.

CHAPTER 1

INTRODUCTION

Heavy minerals (s.g. > 2.9) constitute only about 2 % or less of the total mineral fraction of most soils. The identification and study of heavy minerals in soils dates back to 1899, when Steinriede separated and identified heavy minerals (Mitchell, 1975). Since then many studies have been carried out in which heavy minerals have been used as indicators of provenance (origin of parent material) and weathering indices based on the assumption that they are resistant to weathering (Barshad, 1964). This assumption arises from the observation that the concentration of "resistant" species of heavy minerals is higher in older soils or parent materials than in younger types (Mitchell, 1975).

In many soil formation studies, the establishment of parent material uniformity and assessment of pedogenic weathering have been important objectives, the realization of which heavy minerals (or their constituent elements) have played a central role (Barshad, 1964; Brewer, 1976). In Australia, quantitative methods have been used by a number of researchers to study pedogenic changes in a range of soils (e.g. Brewer, 1955; Green, 1966; Chittleborough and Oades, 1980; Chittleborough *et al.*, 1984 and Chittleborough 1989). Such studies involved mineral and elemental analyses for which petrographic microscopic, x-ray diffraction (XRD) and x-ray fluorescence spectroscopic (XRF) techniques were widely used.

Over the past 25 years, more sophisticated techniques especially those involving electron microscopy have emerged to augment mineralogical analyses. In this regard transmission electron microscopy (TEM) and scanning electron microscopy (SEM), in addition to electron probe analysis provide information on the physical and chemical modifications of individual mineral grains (e.g. Lin *et al.*, 1974; Jung and Peacor, 1987; Morton, 1985; Allan *et al.*, 1988). Many of these studies have involved geologic sediments and/or rocks. Use of these sophisticated techniques in Australia is well established both in studies involving rock samples or their derivatives (e.g. Milnes

and Hutton, 1974; Hollis *et al.*, 1986; Dragovich, 1988) and in soils (e.g. Fordham and Norrish, 1979; Anand and Gilkes, 1984). From SEM studies it is generally believed that weathering is usually accompanied by characteristic developmental sequence of surface textures (Bateman and Catt, 1985).

I hypothesized that the integration of these more sophisticated electron optical techniques together with the relatively older traditional methods (such as petrographic microscopy), XRD and XRF could facilitate the understanding of the various processes encountered by mineral grains in the weathering environment.

Despite roles which conventional heavy mineral analysis can and do play in pedological and geological studies, their analysis is now perceived by most workers as inferior to other sophisticated and often automated techniques (Bateman, 1989). This decline has been worsened by failure of most workers to fully exploit the data obtained from heavy mineral analysis, especially by using appropriate statistical methods to facilitate better quantitative interpretation.

Different soils react to weathering processes differently. The weathering rates of most minerals are probably determined by a range of soil forming factors (e.g. nature of parent material, time, vegetation, climate), soil environmental factors (e.g. pH, Eh, permeability) and mineral characteristics (e.g. physical characteristics such as shape, size and roughness, chemical composition). Because of the complex interaction between several or all of these factors during mineral weathering, it is appropriate to develop suitable research techniques for each peculiar type of condition to be investigated. Little or no work has been done to test the resistance to weathering of heavy minerals in chronosequences developed on similar parent materials and similar climatic conditions or age sequences of different soils in different climatic conditions with a view to determining the weathering pattern of various minerals and/or pedogenic changes which occur in the different soil horizons.

The soils to be used in this study are calcareous and siliceous sands (Stace *et al.*, 1968) or Entisols (Soil Management Support Services, 1987), the latter having developed into Podzols or Spodosols to different degrees and magnitudes. Fig. 1.1

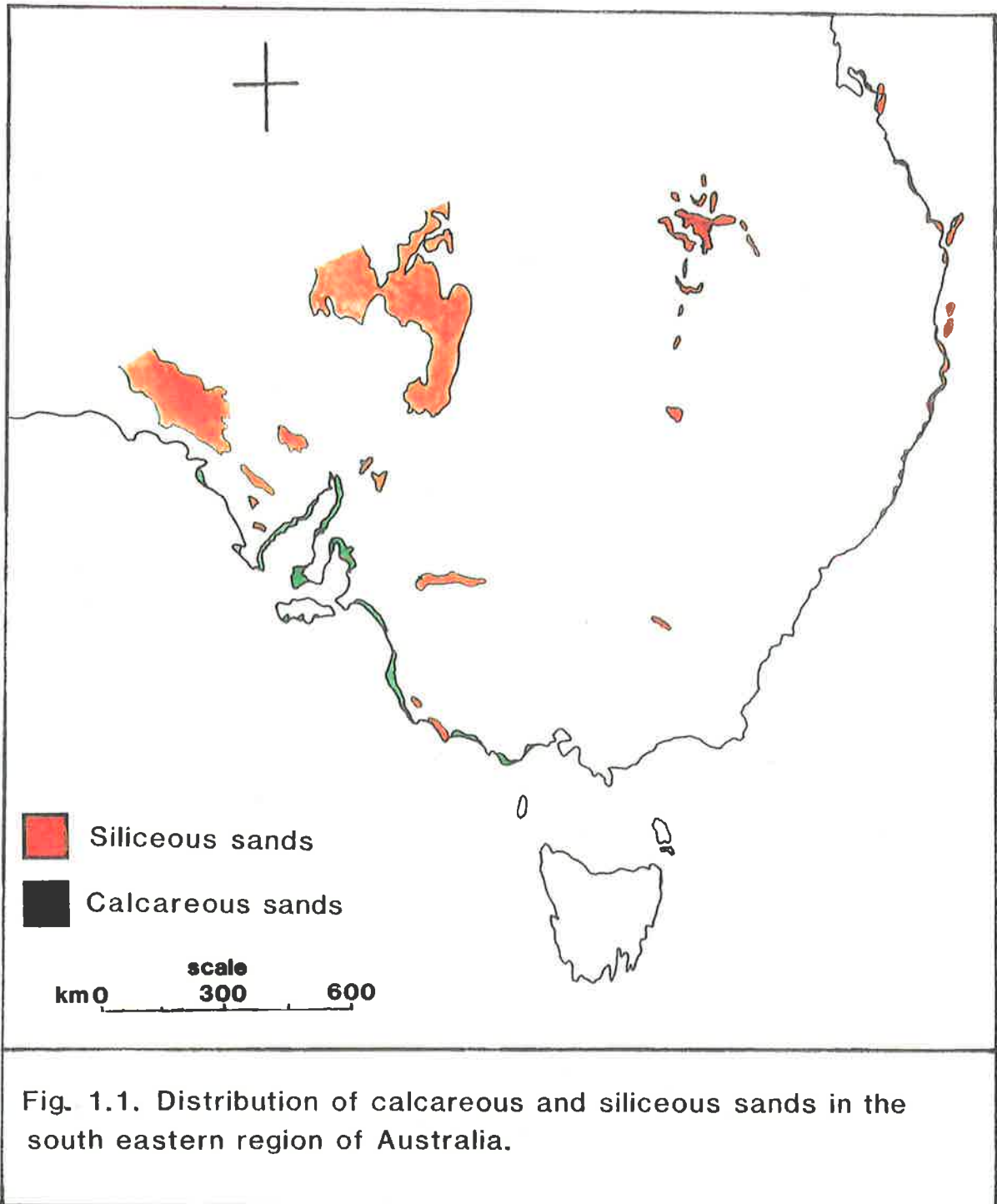


Fig. 1.1. Distribution of calcareous and siliceous sands in the south eastern region of Australia.

illustrates the area covered by calcareous and siliceous sands in the south eastern half of Australia which constitutes parts of the sampling area, and Fig. 1.2 shows the extent of Podzol development in these areas. In practice sands are ideal materials for heavy mineral work because of their larger grain sizes and weak coalescence. This opinion has been very recently re-emphasized by Bateman (1989), who noted that the vigorous physical and/or chemical extraction or cleaning methods of heavy minerals from well coalesced sediments inevitably damages specific minerals. One interesting characteristic of the soils is that, on a regional basis, they often constitute definite age sequences. Also, the parent materials were accumulated due to either marine transgression or aeolian accretion. The study of time, as related to dating absolute geomorphological and climatic events leading to the formation of the various sandmasses is well documented for some of the soils (e.g. Suzuki *et al.*, 1982; Bowman and Harvey, 1986). Inferences drawn from these studies have shown that soil development processes in these soils span an age interval from Holocene to Pleistocene. However, for some of the better preserved sequences no absolute ages have been determined for the time elapsed since the sands started accumulating. Also, the nature of deposition and weathering of the minerals, especially the heavy minerals, has not been investigated.

The objectives of this regional investigation have been to test the applicability of thermoluminescence dating to some of the soils from the coastal Queensland region, and to develop and/or adapt methods to study weathering of heavy minerals and associated pedogenic changes in sandy soils from coastal regions of south east Queensland, central and south east South Australia. Also, attempts were made to explain the pedological (post-depositional) and geological (pre-depositional) factors that were likely contributors to the observed differences.

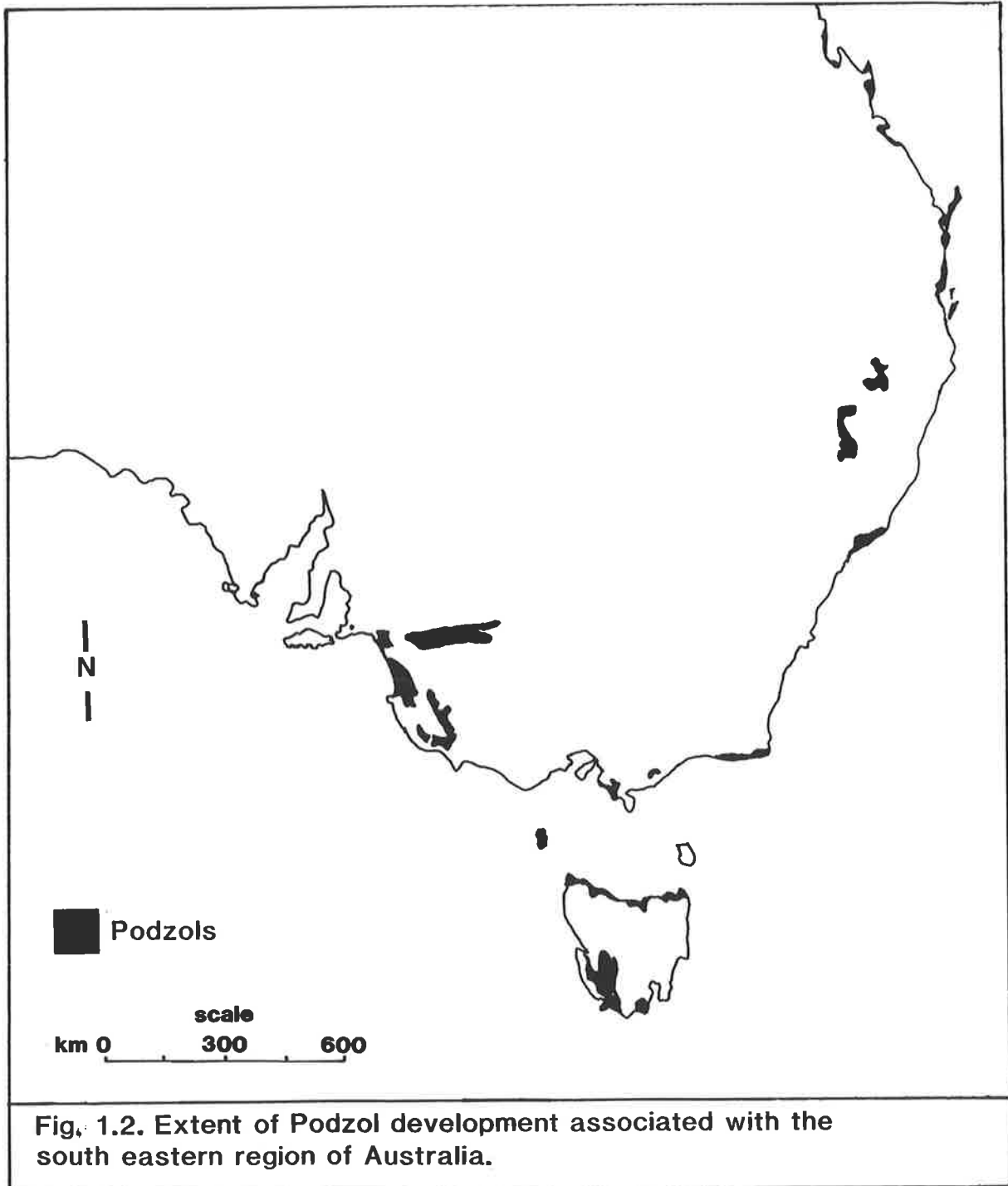


Fig. 1.2. Extent of Podzol development associated with the south eastern region of Australia.

CHAPTER 2

SITE DESCRIPTIONS, SOIL PROPERTIES AND SOIL CLASSIFICATION

2.1. Site descriptions

2.1.1. Introduction.

Soil materials used in this study were selected from three sandy soil age sequences in regions from Queensland and South Australia that cover a wide range of factors which influence soil formation. Climate, time, relief and landscape morphology varied, but generally the mineralogical and particle-size variations in the parent material were restricted. Most of the sites selected have reasonably good records of ages on the soils. Three separate coastal regions in the south eastern half of Australia were selected for study (Fig. 2.1). Two or more sets of soil profiles comprising an age sequence were sampled from two locations within each region. Two of the locations were on the south eastern coast of Queensland (Cooloola and North Stradbroke Island), two were along the central South Australian coast (LeFevre Peninsula and Mount Compass) and two in the south east region of South Australia (Mount Burr and Canunda) (Fig. 2.1). Soils are associated with (i) sand dunes that occur as mainland deposits (Cooloola, Mount Compass and Mount Burr), (ii) sand dunes that occur as island deposits (North Stradbroke Island) and (iii) stranded beach ridges (LeFevre Peninsula and Canunda).

2.1.2. Location and general description.

2.1.2.1. Cooloola and North Stradbroke Island.

The Cooloola sandmass (latitude 26°S) is situated along the coast about 150 km north of Brisbane, Queensland (Fig. 2.1). It consists of six systems of parabolic dunes overlying older strongly degraded dune systems (Thompson and Moore, 1984). The parabolic dunes are aligned with the south east onshore winds and their shapes are

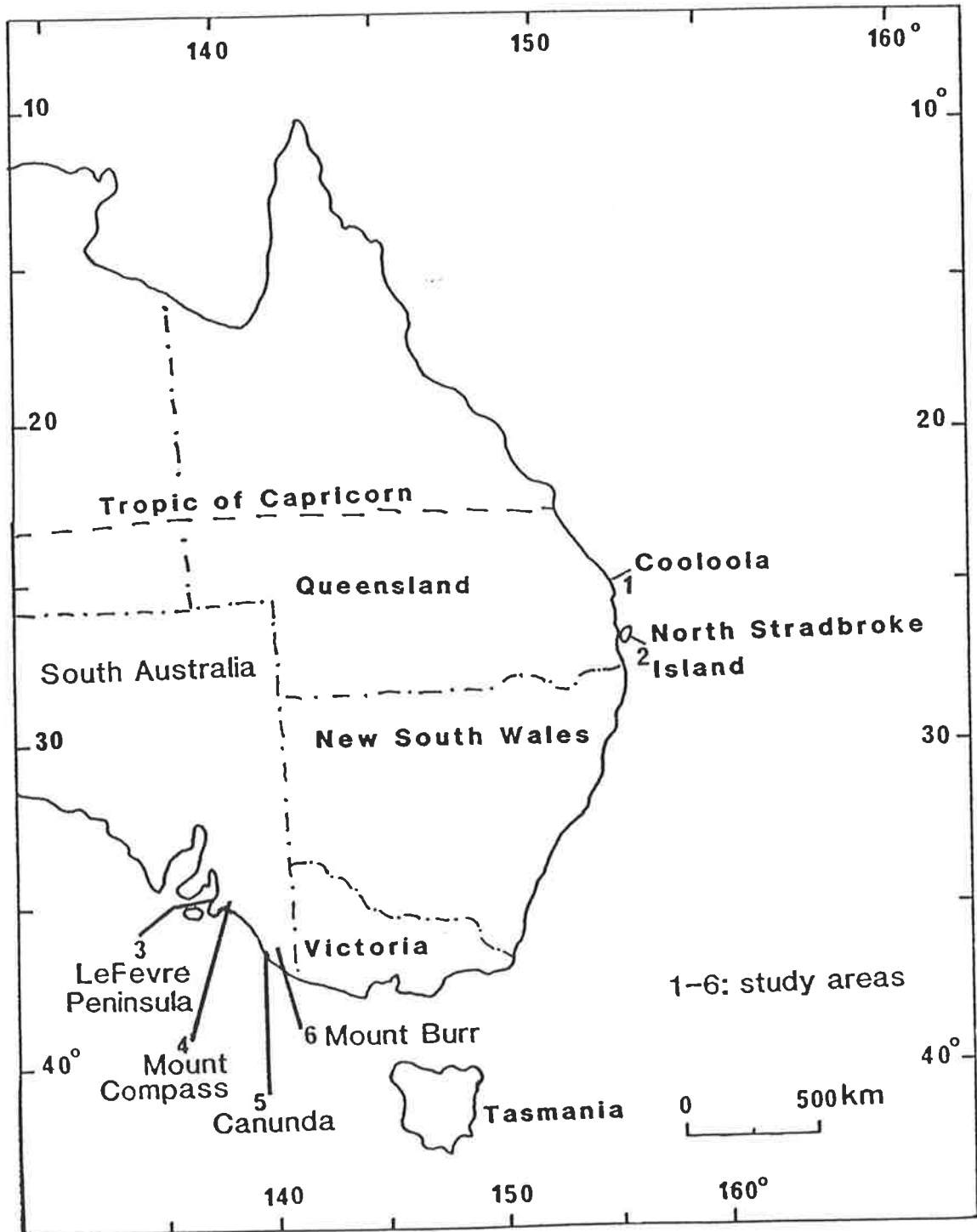


Fig. 2.1. Locality map of sampling areas.

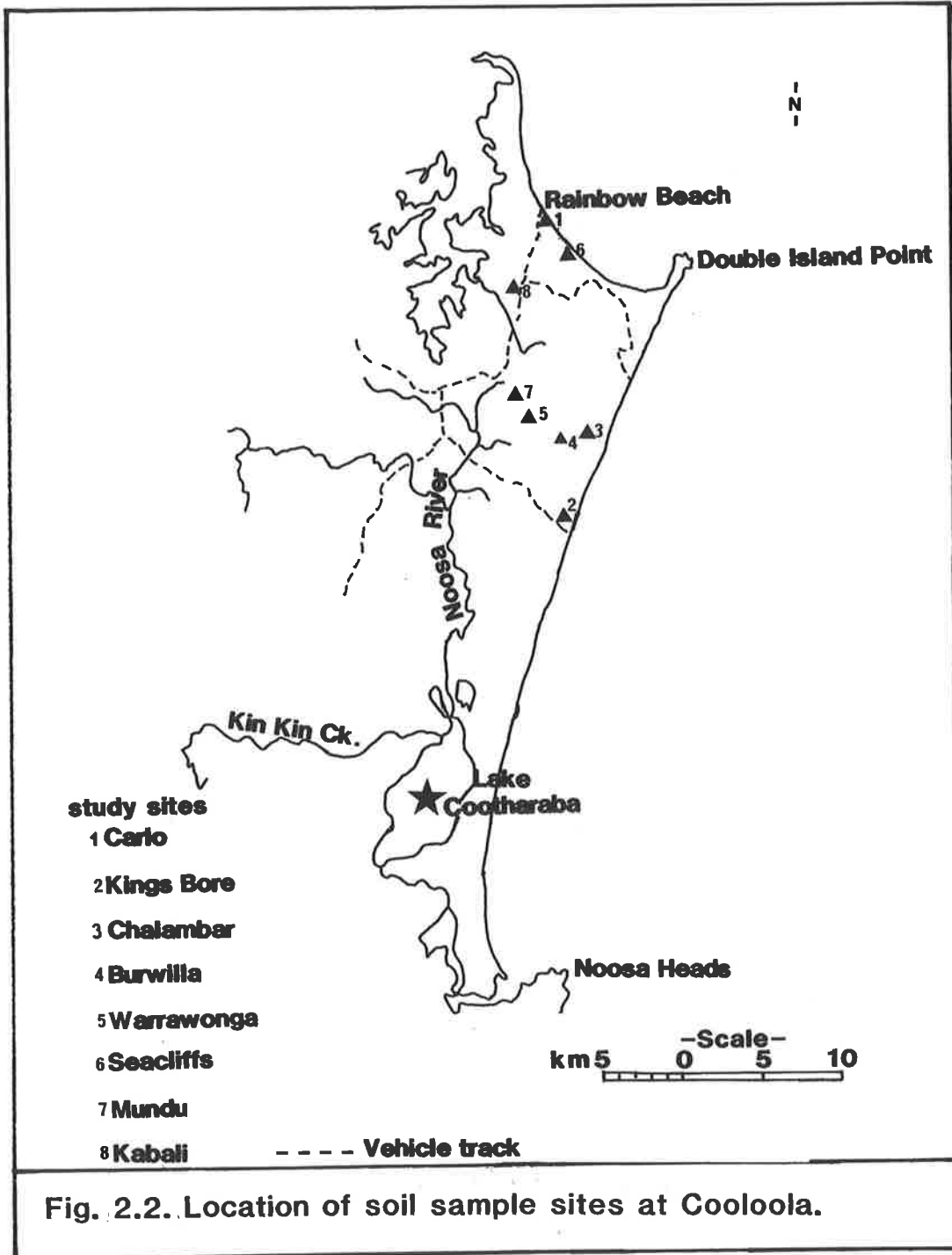
influenced by the underlying topography and the onshore winds at exposed sites. Fig. 2.2 shows the locations of the different sampling sites within the Cooloola sandmass.

At North Stradbroke Island the sandmass is a small island situated approximately 38 km east of Brisbane, Queensland, at about latitude $27^{\circ} 30'S$ (Fig. 2.1) (Durbidge, 1975). Like other sandmasses in the region (Benussi, 1975), it is composed primarily of quartz sands deposited by wind in a series of parabolic dune systems overlying much degraded older systems (Pickett *et al.*, 1984, 1985). The dunes are generally oriented in the north westerly direction indicating that dune building was by onshore winds dominantly from the south east. Fig. 2.3 shows the location of the Amity site within the North Stradbroke Island sandmass.

2.1.2.2. LeFevre Peninsula and Mount Compass.

LeFevre Peninsula constitutes sediments that form part of a regressive coastal dune system along the present northern metropolitan coast of Adelaide (latitude $34^{\circ} 56'S$), South Australia as shown in Fig. 2.1 (Bowman and Harvey, 1986). The area is approximately 18km northwest of the Central Post Office in Adelaide. The sandmass consists of marine and estuarine sediments. The prevalence of northward drift of sand is due to the effects of northwesterly waves. Fig. 2.4 shows the location of LeFevre Peninsula within the sampling sites on the Adelaide coast.

The sand dunes in the Mount Compass region (latitude $35^{\circ} 21'S$), South Australia, are situated approximately 53 km south of Adelaide in South Australia. The dunes are fairly extensive and resulted from aeolian redistribution of Permian sandy sediments. These dunes are referred to as Myponga sands (Maud, 1972) and at the site sampled (Fig. 2.5) have a west-north-west to east-south-east trend. The nature of the dunes and other associated sandy deposits indicate that the wind direction during their formation was from the west.



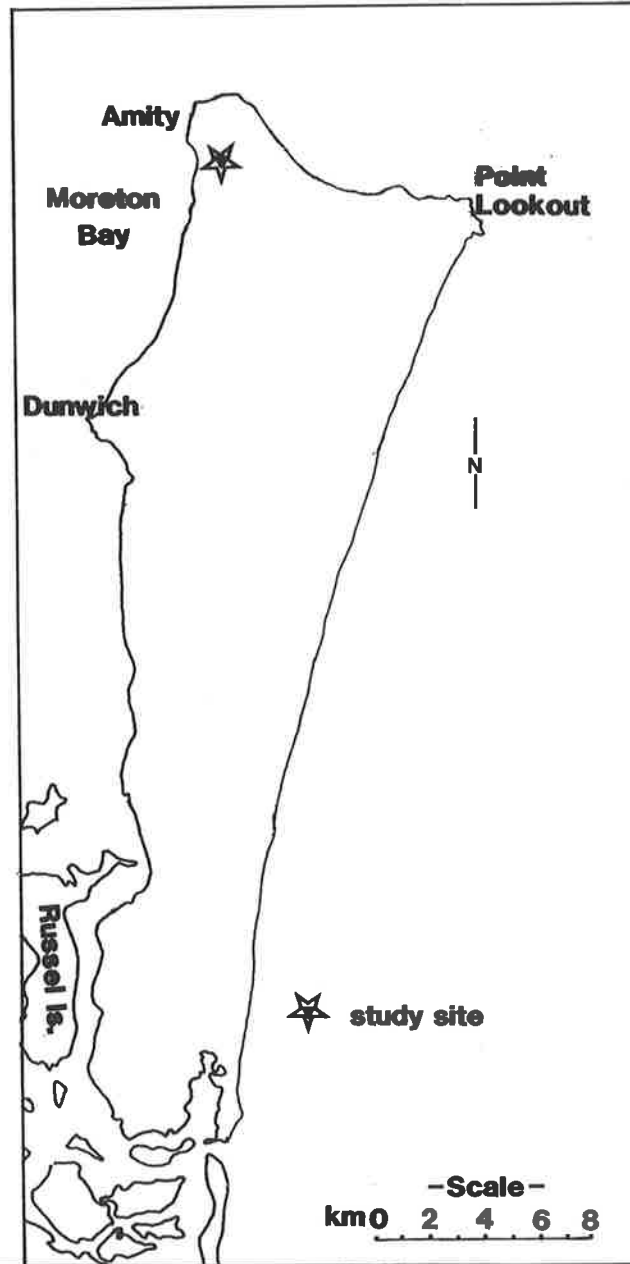
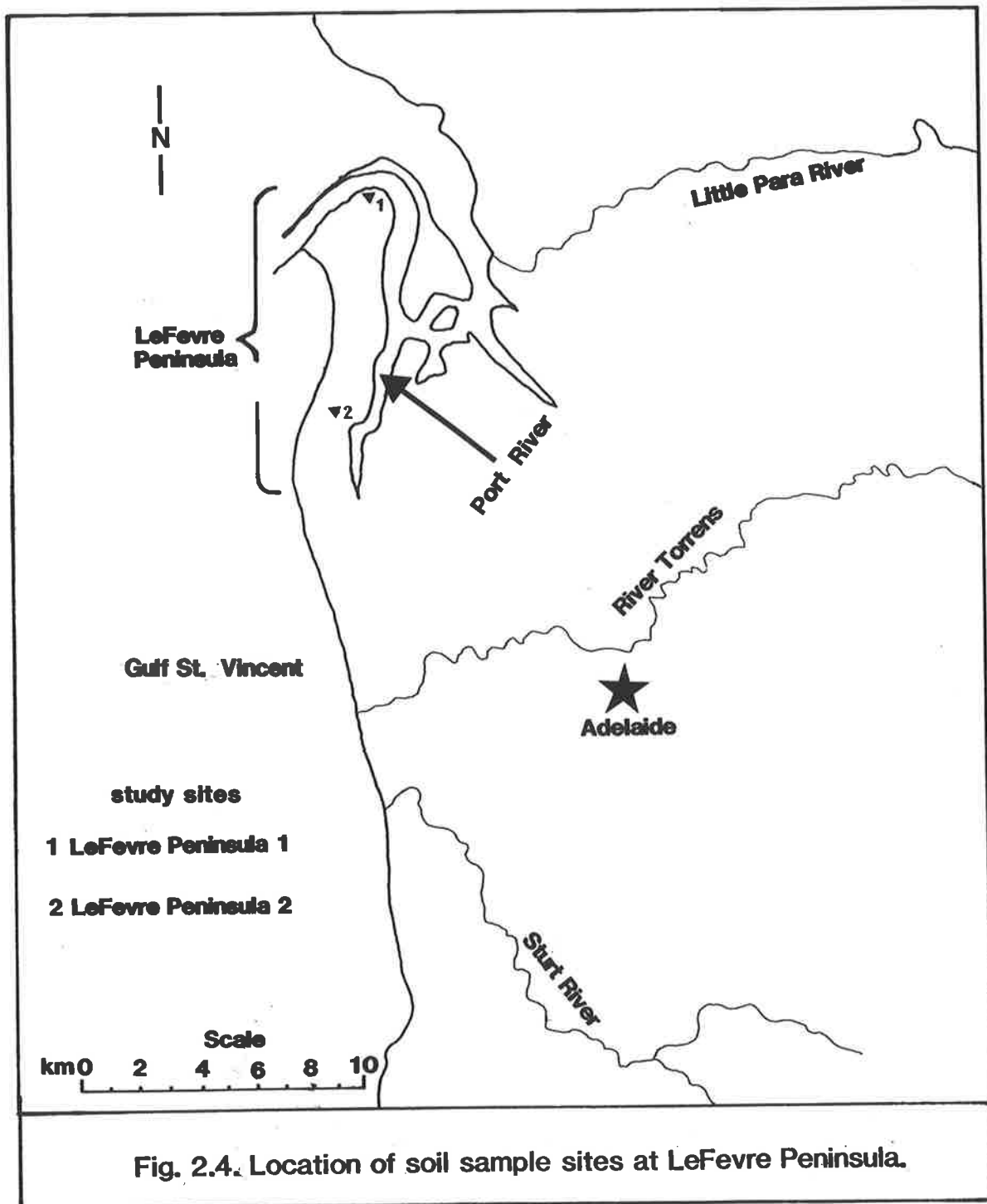


Fig. 2.3. Location of soil sample site North Stradbroke Island.



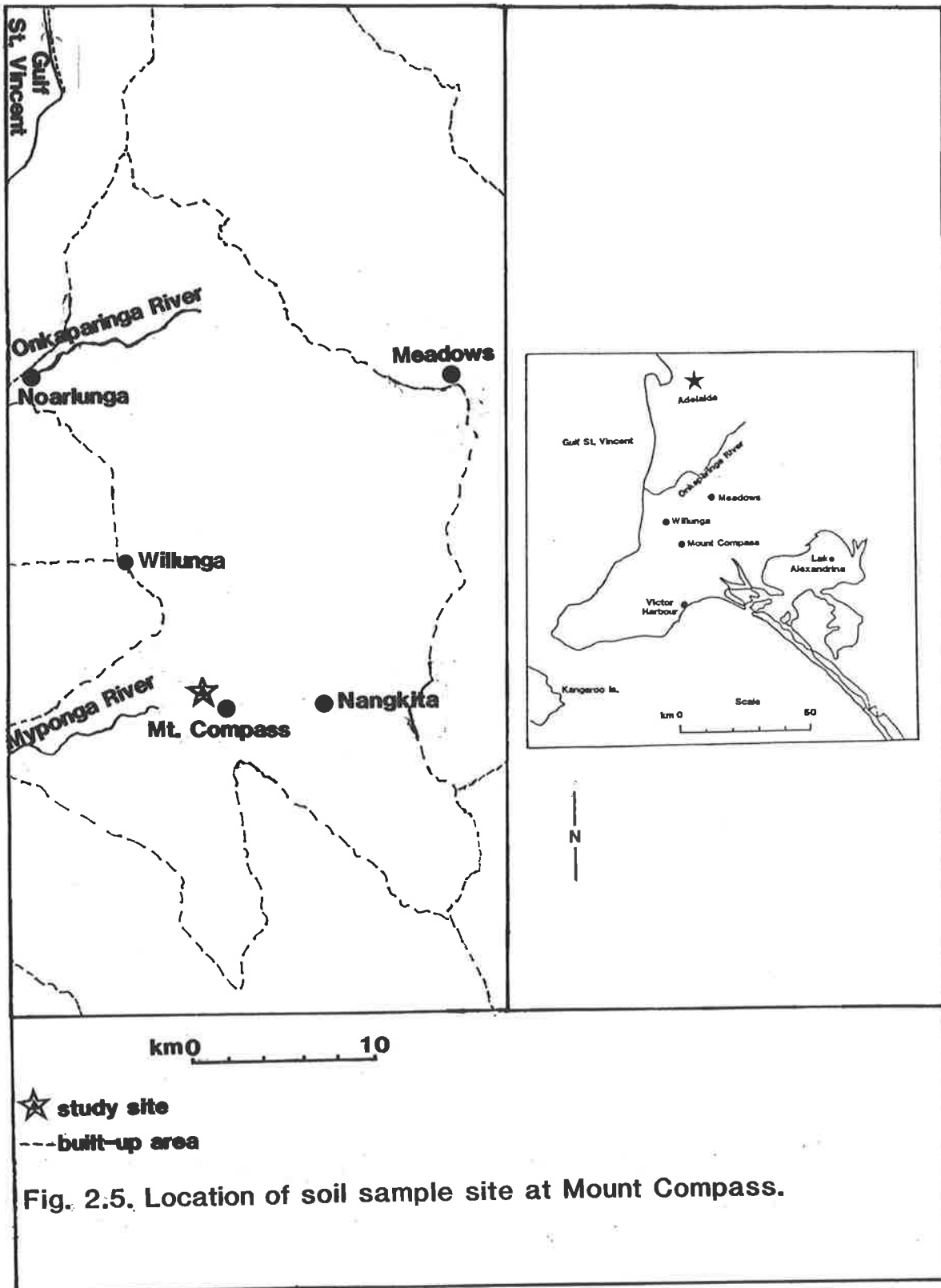


Fig. 2.5. Location of soil sample site at Mount Compass.

2.1.2.3. Canunda and Mount Burr.

Sands from Canunda region (latitude 37° 39'S), occur some 12 km southwest of Millicent in south eastern South Australia and consist of compact, massive and lithified calcareous deposits in the form of stranded beach ridges (Blackburn *et al.*, 1965). The area sampled included the present beach deposit and site number 3 within the Canunda Oil Rig Square (Fig. 2.6) as described in Suzuki *et al.* (1982). Each parabolic dunes is oriented normal or oblique to the present beach. Aeolian transport of the sands has resulted in the accumulation of sand ridges.

Sands from the Mount Burr region (latitude 37° 32'S), occur some 11 km east of Millicent (Fig. 2.6) in south eastern South Australia. The soil material sampled has been referred to as Mount Burr sand (Stephens *et al.*, 1941; Blackburn *et al.*, 1965) and is composed mainly of siliceous dune sand of aeolian origin. These sands are approximately aligned in the east-west direction.

2.1.3. Geology and geomorphology.

2.1.3.1. Introduction.

The geology and geomorphology of the sampling areas represent complex and unique records of geologic events in these parts of Australia that represent different tectonic events, eustatic sea-level changes, erosional and depositional episodes. These aspects are discussed in the sections below for each of the different sampling regions.

2.1.3.2. Cooloola and North Stradbroke Island.

Sand dunes at Cooloola occur as mainland deposits. The overlapping nature of the dunes suggests different successive periods of dune building. The dunes are predominantly quartz sands which at depths are interbedded with clay, shale, coarse sand and water-worn pebble beds that are underlain by Jurassic basement rocks (Ball, 1924). According to Ball (1924), the Cooloola sandhills consist of two different units both deposited since the Tertiary. A similar view was held by Coaldrake (1962) who described the two units as oceanic sands and Teewah sands. Coaldrake (1962) recognised that the oceanic sands

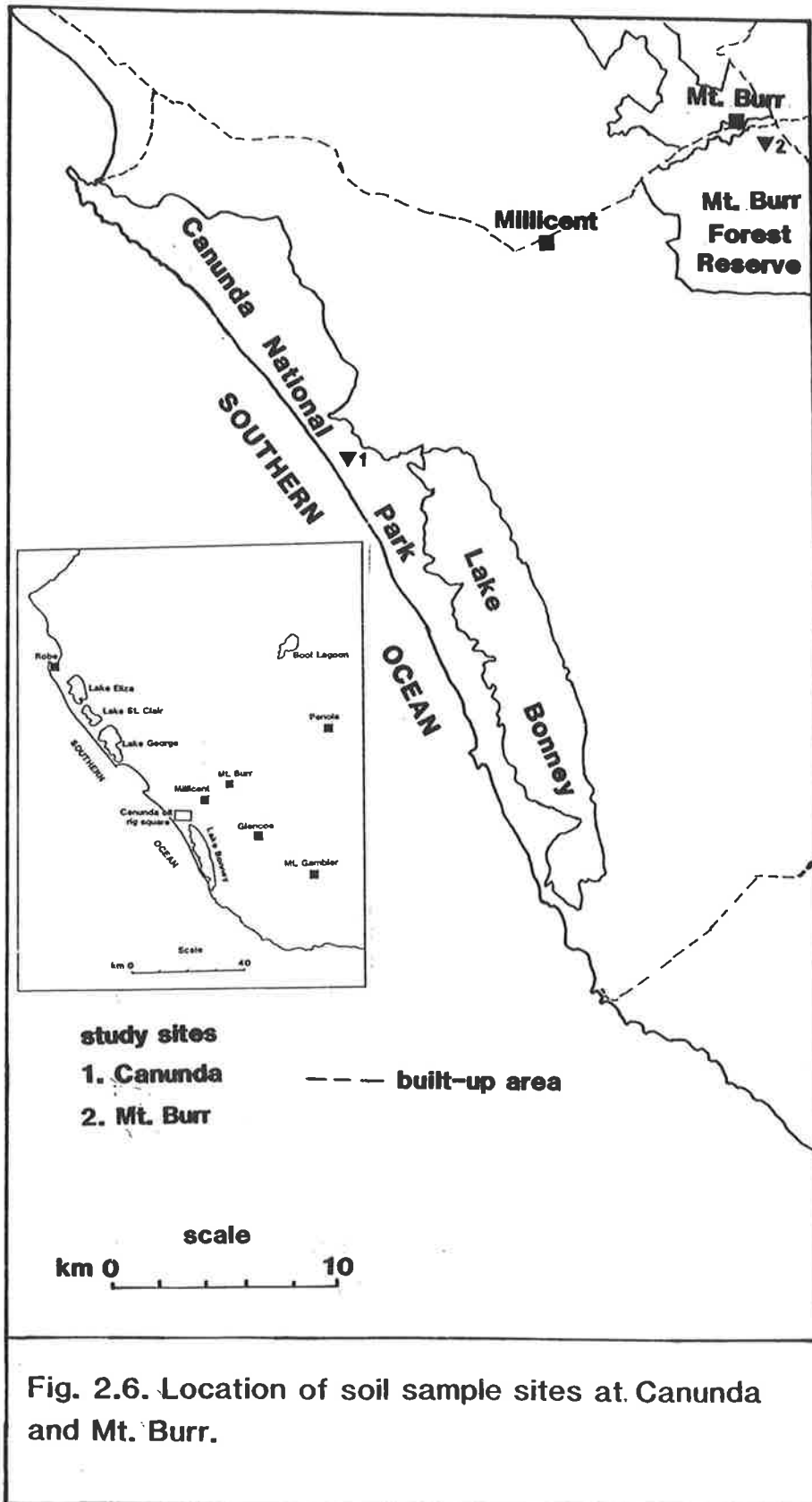


Fig. 2.6. Location of soil sample sites at Canunda and Mt. Burr.

occurred both below and above the Teewah sands, presumably as large lenses within the latter. The two unit theory was rejected in later works by Ward *et al.* (1979) and Thompson and Moore (1984). Thompson and Moore (1984) recognised eight major depositional units, with two underlying the equivalents of the Teewah sands and five overlying them. Their subdivisions were based on stratigraphic evidence, dune geomorphology, erosional features, and depth and intensity of soil profile development.

According to Thompson and Moore (1984) there are four dune units within the Cooloola sandmass with U- and V- shaped parabola that are exposed to the formative south east onshore winds. The parabolic shapes are a function of time with water erosion destroying the shapes of the older units. The parabolic shapes are well preserved in three of the units (Mutyi, Chalambar and Burwilla), the dune floors extensively eroded in the fourth unit (Warrawonga) and the original shape and orientation not evident in the fifth (Mundu) and sixth (Kabali) units. As established by Thompson (1983) each unit in the Cooloola sandmass has a characteristic geomorphic pattern based on the initial size of the dunes, the wind history during deposition and development, the nature and form of the underlying dunes or country rock and the amount of water erosion to which the dune has been exposed. The Cooloola dunes reach elevations of some 260 m and extend 10 km inland.

On North Stradbroke Island the dune systems comprise mainly quartz sands, with most of the island made up of overlapping dune systems reaching elevations of 200 m (Durbidge, 1975). Dunes have a northwesterly trend demonstrating that the winds responsible for dune building occurred mainly from the south east. According to Pickett *et al.* (1984) the dune at Amity consists of an eroded western ridge of a large parabolic dune deposited by prevailing onshore winds. The aeolian form is still maintained, but the dune has been strongly degraded by water erosion. The indications are that the dune was basically of parabolic form representing either a very large single dune or more likely a combination of several parabolic dunes. Ward (1978) suggested that the dunes rest on a prior land surface and are enclosed by a post-glacial strand plain

on most sides, as opposed to the concept of a barrier island (Hails, 1964) or a barrier spit (Bird, 1973). The overlying sediments as shown by Ball (1924) are aeolian and extend to considerable depths below sea level and to basement rock. Relatively high sea levels during the last interglacial period caused partial submergence of the land surface that included several high areas of aeolian sand overlain by beach sand, intertidal sediments, subtidal muds and sandy alluvium (Pickett *et al.*, 1984). During subsequent inter-glacial ages, the sea level has risen enough to encircle the accumulated sands. In addition to the underlying sands and marine muds, hard rocks of Palaeozoic, Mesozoic and Cainozoic ages (sandstones and igneous rocks of rhyolite and greenstone types) occur as basement assemblages (Laycock, 1971).

Heavy mineral composition.

The sands from both Cooloola and North Stradbroke Island contain up to 3 % heavy minerals, 90 % of which constitute zircon, rutile and ilmenite (Gardner, 1955). The sources of these heavy mineral sands have been traced principally to the Mesozoic sandstones of the Clarence and Moreton Basins (Beasley, 1948; Gardner, 1955). A later conclusion arrived at by Whitworth (1956) traced the ultimate source of the zircon and rutile in the sands to pegmatitic and quartzitic veins in the Precambrian shield, and the ilmenite to a relatively recent addition from local basic igneous rocks. Whatever the known source rocks are for the mineral sands, it is clear that prior to their final deposition, the source rocks were exposed to several episodes of diatrophism, erosion, transportation and deposition in different geologic environments along the eastern coast of Australia.

2.1.3.3. *LeFevre Peninsula and Mount Compass.*

LeFevre Peninsula is located on the eastern edge of the Gulf of St. Vincent graben which was formed as a result of a number of northeast to southwest trending faults between which large blocks of mostly Precambrian rocks that have either subsided or been uplifted (Mt. Lofty Ranges). The peninsula is the result of the accumulation of

reworked sediments from the Gulf of St. Vincent floor by marine transgression, forcing a system of subparallel linear dunes, in the form of sand barriers, up to 12 m high and 500 m wide (Wynne *et al.*, 1984). The natural geomorphology of LeFevre Peninsula has been considerably changed and concealed by residential and industrial development in the last forty years. The core structure of the peninsula is largely made up of several beach ridges with a north-south trend (Thom *et al.*, 1978). The ridges are narrower at the southern end but sequentially recurve towards the east. The elevation of the peninsula generally decreases from west to east and from south to north (Bowman and Harvey, 1986). Hails *et al.* (1982) reported sandy sediments from local rivers and cliff erosion as lesser proximate sources contributing to the peninsula sediment build-up. The net accumulation of sand on LeFevre Peninsula is a result of a northward longshore drift due to a predominantly south-westerly wave action since the end of the last post-glacial marine transgression (Bowman and Harvey, 1986). Bowman and Harvey (1986) observed six broad sedimentary facies at sites in the peninsula which included coarse sandy and shelly washover deposits, regressive backbarrier, organic rich muds, well-sorted beach and aeolian sands, transgressive nearshore shell-rich sands, transgressive sands and gravel and a basal limestone crust within the Glanville Formation (Howchin, 1888). In places, the latter are underlain by the Hindmarsh clay (Firman, 1966). These Quaternary sediments are underlain by thick sequences of complex Tertiary strata over the Permian and Precambrian basement rocks (Daily *et al.*, 1976).

In the Mount Compass region the geology and geomorphology is as complex as the LeFevre Peninsula region, since they are both contained within the orogenic belt of the Mount Lofty Ranges or Adelaide region (Daily *et al.*, 1976). The oldest rocks in the region are of Archean age which include a complex suite of metamorphic rocks such as mica schists, gneisses and migmatites (Horwitz, 1960). Following the burial, consolidation, metamorphism and deformation of the basement rocks, a series of Precambrian sedimentary rocks referred to as Adelaidean (800-900 my) were formed, followed by a hiatus of long duration that led to erosion followed by glaciation of the

end of the Permian glaciation with erosion of higher land surfaces to lower reliefs during the Tertiary. There are surface occurrences of lateritic ironstones that reflect various phases of weathering and erosional history dating back to the Mesozoic period (Maud, 1972). The present site is made up of Permian fluvio-glacial sediments from the Tertiary that have been redistributed by aeolian activity in Holocene times. The soil which was sampled in this study is within the sandy materials of partially exhumed Permian valleys (Maud, 1972). The redistribution of the sand by aeolian activity in this area affected the local drainage patterns, as exemplified by the occurrence of a ponded sandy deposit east of the sampling site. The topography of the dune surfaces indicated that wind direction during their formation was from the west, as occurs presently. The dunes have a west-north-west to east-south-east trend at elevations of up to 150 m (Maud, 1972). The geomorphological evidence of the present area has been associated with glacio-eustatic sea level highs in the Quaternary (Ward and Jessup, 1965; Ward, 1966) as established for southern Australia. The comparisons between likely contemporaneous formations from the study area and those of Ward (1966) are discussed by Maud (1972). However, Twidale (1976) suggested that most of the forms and deposits regarded by Ward as evidence of high sea level are either marine or scarp foot features, possibly of pre Pleistocene age, which have been raised to the present positions by faulting. If lower sea levels of about +8, +5 and +3 m are accepted, the evidence of raised beaches, and river terraces graded to raised beaches, is generally in agreement.

In summary, the geology and geomorphology of the region (indeed the entire Adelaide region) from which samples were taken, are complex and span Archean times to Holocene. The series of folding and faulting, erosion, deposition, glaciation and changes in sea levels starting predominantly from the Delamerian Orogeny

Cainozoic broadly account for most of the modern erosion, transport and sedimentation in the Tertiary and Quaternary geologic units and topography found within the region.

Heavy mineral composition.

According to Aitchison *et al.* (1954) and Morris (1978) most investigations of heavy minerals in beach and dune sands from LeFevre Peninsula and Mt. Compass regions are unpublished. However, limited published information does exist for localized adjacent areas such as on Kangaroo Island, Port Noarlunga, Yankalilla Gorge, Christies Beach and River Murray mouth. The heavy mineral contents of sediments from these regions vary considerably, ranging from 1 % in some areas (e.g. Kangaroo Island) to 95 % at Noarlunga (Morris, 1978). Both opaque (ilmenite, leucoxene, magnetite) and non-opaque (e.g. zircon, rutile, Kyanite, sillimanite, garnet, staurolite) mineral types occur in the deposits. The heavy minerals are considered to be derived from a range of different rock types including Precambrian and Cambrian schists, gneisses and migmatites, and Tertiary pegmatites and granitoids.

2.1.3.4. Canunda and Mount Burr.

This region forms part of south east of South Australia which is within the Otway Basin (Wopfner and Douglas, 1971) with the eastern-most portion referred to as the Gambier Embayment (Firman, 1973). Basement rocks in the region include Palaeozoic rocks of the Padthaway ridge group which are predominantly igneous and metamorphic. The Otway Group of rocks of Late Jurassic and Early Cretaceous overly the Padthaway ridge group in subsiding down-faulted valley regions (Harris, 1983). Without any evidence of Permian sediments in the region, the next sequence of sedimentation consisted of sandstones (Pretty Hill Sandstone) and sediments of the Eumeralla Formation of mainly terrestrial origin with minor marine incursions during the Early Cretaceous, followed by uplift and erosion in Middle Cretaceous, subsidence in Late Cretaceous and deposition of a thick sequence of complex deltaic and marine sediments (Sherbrook Group). Finally the Curdies Formation was deposited during a

marine regression. The Cretaceous to Tertiary boundary was marked by a major hiatus, followed by the formation of the terrestrial Wangerrip group of rocks in Middle to Late Paleocene times. During this time global tectonic events resulted in marked changes in rise and fall of sea levels and separation of Australia from Antarctica in the southern hemisphere. This was followed, during the Eocene, by sedimentation of rock units known as Mepunga Formation and Narrawaturk marls consisting of calcareous sandstones, marls and sandstones near the base. Marine transgression through the Oligocene led to deposition of the Gambier Limestone, parts of which are either fossiliferous with corals or siliceous and very compact with shells of fresh water snails. Marine regression in Miocene period caused exposure and erosion of the limestone and other older exposed deposits. At the close of the Tertiary there was uplift and further erosion and deposition of nearshore sands, most of which have been eroded during the Pleistocene. At the time of the uplift widespread volcanoes produced basalt flows and tuffs at several sites, including Mt. Schank, Mt. McIntyre and Mt. Gambier. In Mt. Burr region the volcanic ash is overlain by aeolian quartz sands which form overlapping ridges down slopes. These ridges have developed soil profiles which have been stabilized by vegetation. The sands stand at elevations of some 180 m in the Mt. Burr range and are roughly parallel to the present coast (Blackburn, 1959). At Canunda, changes in the position of the coast line has led to the development of unconsolidated, locally active, stratified, calcareous sand dunes at the beach range. The dunes are parabolic in shape and have heights greater than 50 m (Suzuki *et al.*, 1982).

Erosion of the ranges and subsequent deposition in adjacent areas has modified the topography of large areas of the ranges and plains, with minimum effect around the Mt. Burr range. With very little relief, coupled with the soft nature of the underlying limestone deposits there has been little dissection of the areas to allow the formation of water channels and therefore large streams to serve as outlets to the sea (Stephens *et al.*, 1941). As such natural drainage in the lower sands is poor.

The overall geological events from the Early Palaeozoic to the Quaternary accounted for the present day stratigraphy and topography of the Mt. Burr and Canunda region. The events that led to the formation of the soils at Mt. Burr and Canunda occurred mainly in the Quaternary with changes in climatic condition as the main factor that led to the erosion, transportation and deposition of the dunes in the ranges region (Mt. Burr) and beach range (Canunda).

Heavy mineral composition.

Similar to the central coastal region of South Australia, the south east coast has had a limited amount of exploration conducted for heavy mineral content (Colwell, 1976 and 1979). The latter published work is for the Robe-Naracoorte, Bordertown and Murray Basin regions. These areas lie north of the sites sampled at Canunda and Mt. Burr. Heavy mineral concentrations are generally low. In the Quaternary deposits in this region, the heavy mineral concentration does not exceed 0.5 % by weight and is commonly below 0.1 % (Colwell, 1976). Between 25 and 45 % of the heavy mineral suite is opaque (ilmenite and magnetite), with zircon and rutile accounting for up to 25 % of the non-opaque species. A variety of rock types appear to contribute to the heavy mineral deposits in this region. These include sialic igneous rocks, mafic igneous rocks, metamorphic rocks and pre-existing sedimentary sources (Colwell, 1979).

2.1.4. Climate.

2.1.4.1. Introduction.

Climatic data covering the study areas (regions) are presented here to give a general representation of the contemporary climatic conditions prevailing in the areas. Data is from the nearest station with long term climatic records (Bureau of Meteorology, 1988) namely, Double Island Point Lighthouse for Cooloola, Brisbane Regional Office for North Stradbroke Island, Adelaide (West Terrace) for LeFevre Peninsula, Myponga Post Office for Mount Compass and Mount Burr Forest Reserve

for Mount Burr and Canunda (Appendix 1). For rapid comparison between sites, mean annual data are presented in Table 2.1.

Table 2.1. Mean annual climatic data for stations nearby sampling sites (Bureau of Meteorology, 1988)†.

Station	Rainfall (mm)	Rain days (no.)	Daily max. temp. (°C)	Daily min. temp. (°C)	Humidity (%)	
					9 am	3 pm
REGION - SOUTHEAST QUEENSLAND COAST						
Double Island Point Lighthouse (Coolooloa)	1446	145	23.8	18.5	74	70
Brisbane Regional Office (N. Stradbroke Is.)	1149	123	25.5	15.7	65	52
REGION - CENTRAL SOUTH AUSTRALIAN COAST						
Adelaide (West Terrace) (LeFevre Peninsula)	530	120	21.8	12.0	59	48
Myponga Post Office (Mount Compass)	759	117	19.5	7.7	68	57
REGION - SOUTHEAST SOUTH AUSTRALIAN COAST						
Mt. Burr Forest Reserve (Mount Burr)	789	178	19.1	8.7	75	59

† Detailed monthly and annual climatic data are given in Appendix 1.

The climate of the Coolooloa and North Stradbroke Island areas is characteristically subtropical coastal, with hot, moist summers and mild, drier winters (i.e. Udic moisture regime, Table 2.2).

The climate of the Adelaide region (LeFevre Peninsula and Mount Compass) and the south eastern region (Canunda and Mount Burr) is mediterranean, with uneven seasonal distribution of rainfall in winter and relatively long, dry summers (i.e. Xeric moisture regime, Table 2.2).

Table 2.2. Summary of selected environmental characteristics at each sampling location.

Sampling location	Geology	Geomorphology	Moisture regime†	Temperature regime†	Vegetation	Parent material
Cooloola	Quaternary siliceous sand with heavy mineral concentrate; basement Mesozoic sandstone including Jurassic mudstone and shale	Various shaped parabolic dunes with alluvial fans, gully heads and wet depressions	Udic	Hyperthermic	Coastal shrubs, shrubby and layered woodlands, layered forest	Aeolian quartz sand
North Stradbroke Island	Quaternary siliceous sand with heavy mineral concentrate, marine sands and clay, basement Mesozoic sandstones and rhyolite, Palaeozoic greenstone	Relic parabolic dune with strongly degraded features	Udic	Hyperthermic	Shrubby to very tall layered woodland	Aeolian quartz sand
LeFevre Peninsula	Quaternary shelly coarse sand, organic rich muds, sands and gravel; basement Tertiary, Permian and Precambrian sediments and metasediments including greywackes, sandstones, shales and limestones	Complex beach ridges and spits now very degraded	Xeric	Thermic	Grasses (e.g. <i>Spinifex sp.</i>) samphire, rare shrubs (e.g. salt bush)	Marine transgressive calcareous sand
Mount Compass	Quaternary aeolian siliceous sand, Permian fluvio-glacier sand; basement Tertiary, Permian and Precambrian sediments and metasediments as for LeFevre Peninsula, Archean schists, gneisses and migmatites	Complex range of sand dunes with valley swamps	Xeric	Thermic	Patchy dwarf scrubby woodland, pastures	Aeolian quartz sand
Canunda	Quaternary shelly coarse sand, Pleistocene waterworn flints and pebbles; basement Tertiary limestone, calcareous sandstone, marl; Mesozoic sandstones and sediments, Palaeozoic igneous, metamorphic and sedimentary rocks	Coastal dunes as low level beach barrier deposits	Xeric	Thermic	Grasses and shrubs e.g. <i>Ammophila</i> , <i>Casuarina</i> and <i>Spinifex sp.</i>	Aeolian calcareous sand
Mount Burr	Quaternary aeolian sand, basement units as for Canunda	Low level inter-dune flat on top of pre-existing ridges	Xeric	Thermic	Pine and Sclerophyll forest	Aeolian quartz sand

† According to Soil Survey Staff (1987)

2.1.4.2. *Rainfall.*

Rainfall is higher in the eastern Queensland region with annual mean and median for Double Island Point at 1446 mm and 1388 mm respectively, and for Brisbane at 1149 mm and 1107 mm. In South Australia the figures for Adelaide are 530 and 526 mm, Myponga 759 and 768 mm and Mount Burr 789 and 789 (Appendix 1). The closeness of mean and median values suggests that rainfall distribution is about normal over the record period.

Over 75 % of the annual rainfall in the Adelaide region (LeFevre Peninsula), Myponga (Mount Compass) and Mount Burr Forest (Mount Burr and Canunda) is received between the months of April and October. In the eastern Queensland region, at Double Island Point (Cooloola) and Brisbane (North Stradbroke Island) over 75 % of the annual rainfall on record occurs between November and July, and November and May respectively (Appendix 1). The highest average monthly rainfall over these periods occurs in June (Adelaide), July (Myponga and Mount Burr), March (Double Island Point) and January (Brisbane). On 50 % of the days, there is a certain occurrence of rainfall in the months of June to August (Adelaide), July to August (Myponga), May to October (Mount Burr), February (Double Island Point) and March (Brisbane). A rainday occurs when a daily rainfall of at least 0.2 mm is recorded. Severe droughts in the South Australian region make the rainfall data generally unreliable compared with the eastern Queensland region.

The rainfall varies considerably in the areas of study, and the total amount is no guide to the actual quantity entering the soil and therefore that affecting soil formation. How much rainfall enters the soil is determined by a range of factors which include relief, soil texture, soil porosity, soil shrink-swell potential, rainfall intensity and vegetation cover (FitzPatrick, 1980; Buol *et al.*, 1980). Even though several methods have been developed for measuring the relationships between rainfall and soil characteristics (Jenny, 1941), the complex interplay of the other factors with rainfall largely limits their efficacy.

2.1.4.3. *Evapotranspiration.*

Data on evaporation in the sampling regions is very scarce, and estimates made are based on Class A pans of the U.S. Weather Bureau and are now the standard measurement. Evaporation contours from these measurements have been published by the Australian Bureau of Meteorology (1975 map set 3). Though the quarterly average evaporation in mid seasonal months, i.e. January, April, July and October are given for the period January 1967 to May 1974 the actual evaporation in most cases is higher than these. In January evaporation is high over most regions, South Australia being higher than Queensland. By April the averages are fairly high but less than January. The decrease in Queensland is greater than South Australia; a similar trend is observed for July. In October there is again a general increase, with higher evaporation values for Queensland compared to South Australia. The influence of radiation and temperature may be responsible for the general trends seen in evaporation in the two regions. In general, evaporation exceeds rainfall on yearly basis, and in periods of drought (summer in South Australia and winter in Queensland) there can be serious consequences on vegetative growth due to water stress in the soil. Soil moisture regimes and available soil water for crop growth were calculated by the water balance method of Allison *et al.* (1983), which was based on rainfall distribution, temperature and a calculation of the potential evapotranspiration.

2.1.4.4. *Temperature and relative humidity.*

Average daily maximum and minimum temperatures and relative humidity at 0900 and 1500 hours, on monthly basis, for weather stations nearest sampling sites are shown in Appendix 1. Temperature regimes (based on Soil Management Support Services, 1987) associated with the sampling locations are given in Table 2.2. In general, the highest and lowest maximum and minimum temperatures are in January to February and July respectively. Highest maximum temperatures range from 29.4°C at Brisbane to 25.6°C at Mount Burr, and highest minimum temperature from 20°C at Brisbane to 12.6°C at Myponga. Lowest maximum and minimum temperatures follow

the same trend (Appendix 1). The 14 and 86 percentile values for monthly temperatures represent the temperature which was not reached on 14 % and 86 % of the days respectively in a month for the maximum temperatures. For the minimum temperature the 14 percentile for a month is the value below which the temperature falls on about one night in seven (14 % of days) on average. Likewise the minimum temperature remains above the 86 percentile value on average of one night per week. From Appendix 1, the 14 and 86 percentile values for Brisbane and Double Island Point, Adelaide and Myponga are essentially central from monthly means which may suggest that the temperature values are normally distributed, with identical mean and median.

Relative humidity is higher in July for Mount Burr, Adelaide and Myponga and ranges from 89 % at Mount Burr to 75 % in Adelaide for the highest maximum at 0900 hours. The lowest maximum values in these areas are in January to February, at 0900 hours ranging from 61 % at Burr to 47 % in Adelaide. The situation in the Brisbane and Double Island Point region is different with the highest values at 0900 hours obtained in February to March (78 %) for Double Island Point and February to June (69-70 %) for Brisbane. The lowest values for 0900 hours (68 %) are in August for Double Island Point and 59 % in November for Brisbane.

Temperature affects soils by influencing the rate of reactions. In general for every 10°C rise in temperature the speed of a chemical reaction increases by a factor of two or three. The main source of heat transmitted to the soil is the sun, and the amount of heat received by the soil directly depends on the amount of solar radiation transmitted and therefore the atmospheric temperature for the same soil type and environmental conditions. The rate of chemical (e.g. hydrolysis of minerals), biological (e.g. microbial decomposition of organic matter) and physical (e.g. mechanical breakdown of larger particles) activity varies with temperature, with chemical and biological processes directly related to temperature, and physical processes either directly or indirectly related to temperature (FitzPatrick, 1980). For the soils sampled the temperature would be generally higher in the summer months

with peaks in months of highest and lowest maximum temperatures, that is January to February. In winter with decreasing atmospheric temperature the soil temperature drops to the lowest minimum. This occurs in July and August.

High relative humidity reduces soil temperature by absorbing incoming radiation and the amount reaching the soil during the day, and reduces heat loss at night. Therefore in Adelaide, Mount Burr and Myponga the soil temperature is again expected to decrease in July and increase in January accompanied by high and low relative humidity values respectively. At Double Island Point high relative humidity values in February to March and low values in July to August are expected to decrease and increase soil temperature respectively. Based on the above argument, the soil temperature at Brisbane is expected to be lower in February to June and higher in July to August because of lower relative humidity values.

2.1.4.5. Wind.

Wind direction data are collected by standard wind roses and, like the evaporation data, is limited for the study areas. At Double Island Point, Coaldrake (1961) reported wind data over a 30 year period, and mid season month data for some locations close to sampling areas have been presented by the Australian Bureau of Meteorology (1979, map set 8). The record covers a period of over 15 years up to 1976. In January south to east winds predominate inland during morning hours due to the influence of anticyclones located off the southern coasts, whilst sea breezes dominate the coastal areas in the afternoons. In April the westerlies are dominant in the south during morning hours, whilst sea breezes are again the dominant influence on the coast in the afternoons. In July the westerlies predominate due to the combined influence of anticyclones over the continent and depressions over the southern ocean. The westerlies become stronger in the afternoons. In October the winds from the west are weakened by the southward movement of Intertropical Convergence Zone and anticyclonic belt, and sea breezes become notable again in coastal areas. The pattern of wind movement over the years has strongly influenced the orientation of the wind

blown deposits at Cooloola, North Stradbroke Island (mainly south-easterly), Mount Compass (mainly westerly), Canunda (south-westerly) and Mount Burr (mainly westerly). Besides influencing the systematic pattern of dune orientation, the character of the prevailing winds can influence soil temperature. For example a dry wind implies low relative humidity which increases evaporation leading to heat loss and a fall in soil temperature.

2.1.4.6. Vegetation.

In most of the areas sampled there is no satisfactory guide to the composition of the former vegetative association, because little of the original vegetation is left. There has been extensive modification of the native floral associations due to selective land management by humans, ranging from hunting, gathering and burning (Aboriginal inhabitants) to agriculture, residential and industrial development (white settlement).

Where there has been less extensive disturbances of the natural vegetation there exists an extremely well marked ecological relationship between vegetation, soil and climate. The generalized vegetation map of South Australia (Prescott, 1929) testifies to this. In that map the present South Australian study areas fall into one category of temperate savannah or temperate forest (slightly higher rainfall) association typified by the Stringybark formation and Savannah Woodland formation.

At Cooloola the number of plant species, which exceeds 750, occurs in many structural forms varying from sedgelands and wet heath through various types of woodlands and grassy forests to closed Sclerophyll forests and rainforests (Thompson and Moore, 1984). The vegetation on the different soil landscape units (Thompson and Moore, 1984) include species from the genera *Pultenaea*, *Banksia*, *Acacia*, *Monotoca*, *Casuarina*, *Callitris*, *Lopnostemon*, *Melaleuca*, *Syncarpia*, *Pteridium*, *Leptospermum*, *Angophora*, *Eucalyptus*. Walker *et al.* (1981) and Thompson and Walker (1986) showed floristic groupings of plant species in the different dune systems based on depth of soil weathering. They showed that the depth of soil weathering is related to vegetation succession to the extent that successional changes are reflected in species

composition. There is progressive build-up in vegetation biomass and height to a maximum in the extremely tall open forest of dune system 4 and the subsequent regression to dwarf shrubby open woodlands in dune system 6.

At Amity, open to tall woodland is prominent with *Melaleuca*, *Callitris*, *Casuarina* and *Eucalyptus* species as the common plants (Thompson and Ward, 1975; Walker *et al.*, 1987). Species of other families occur as important components of the understorey, e.g. the heath genera.

LeFevre Peninsula has its vegetation greatly modified by residential and industrial development. At the site close to the coast succulent species of *Samphire*, *Spinifex* and grey Saltbush were common, whilst the more inland site had weed species different from native coastal vegetation.

At Mount Compass the sands had very sparse open woodland (e.g. *Eucalyptus baxteri*) with grasses and herbs (e.g. *Xanthorrhoea sp.*).

Scrub vegetation was unevenly distributed on parts of the Canunda sands. Characteristic plants include *Spinifex* near the beach, sedges, shrubs such as heath (*Lencopogon*) and planted grasses (e.g. *Ammophila sp.*).

The Mount Burr sands in the main are covered by *Pinus radiata* plantation, replacing the original forest cover of *Eucalyptus baxteri* (Blackburn, 1959). There is significant difference in the growth of the pines on the different soil types within the Mount Burr soil association (Blackburn, 1959). The nature and degree of plant cover on the soils accounts for the amount of organic matter in the top soil and subsequently in the subsoil, the amount of precipitation reaching the soil and therefore the amount of water erosion. Plant cover is in turn influenced, amongst other factors, by the nutrient status of the soil and the climatic conditions (rainfall and temperature).

A summary comparison of selected environmental characteristics of the sampling locations is given in Table 2.2. The geology, geomorphology, climate and vegetation of the sampling areas are the most important of the soil-forming factors which determine the state of the soil system, especially physical soil properties such as particle-size distribution, chemical properties such as pH, base saturation and mineral

transformation and mineralogical properties e.g. type and proportion of minerals. The soil patterns mentioned earlier can be mainly attributed to the effects of a changing and variable climate on parent material (siliceous or calcareous sands) which has been exposed by intermittent geologic events such as tectonic uplift, erosion, transformation and deposition. Climatic changes and the accompanying vegetational, erosional, depositional and weathering changes have helped the development of the different soils in more stable areas on one hand (inland soils) and more unstable (active) soils on the other hand (coastal areas).

2.2. Soil properties

2.2.1. Introduction.

The morphology of a soil shows the cumulative alteration of the parent material by soil forming processes. Except for the Cooloola soils, little published information was available on the morphology, physical and chemical properties of the soils from other sites. For this reason, detailed studies of field morphological properties such as colour, texture, structure, consistence, physical characteristics (e.g. particle-size distribution) and chemical characteristics (e.g. pH, exchangeable cations, carbon content, electrical conductivity, etc) were conducted on selected samples. The methods of measurement of the various morphological, physical and chemical properties are given below. The information obtained from the measurements is discussed below and later used to classify these soils and discuss sections on micromorphological and mineralogical studies.

2.2.2. Soil sample collection and profile description.

Nine soil profiles were sampled from Queensland, eight from Cooloola and one from North Stradbroke Island. The eight profiles from Cooloola were from the following soil landscape units: Carlo (CL), Kings Bore (KB), Chalambar (CH), Burwilla 1 (BW), Warrawonga 1 or Seacliffs (SC), Warrawonga 2 (WA), Mundu 4

(MU) and Kabali 2 (KL). These sites are shown in Fig. 2.2. The soil profile from North Stradbroke Island was from the Amity (AM) site as shown in Fig. 2.3. The soil profile at this site has been equated with Dune System 5 (MU) at Cooloola (Thompson, 1983).

The second soil sequence consisted of two profiles sampled from LeFevre Peninsula (Fig. 2.4) and one from Mount Compass (Fig. 2.5) in the central coastal region of South Australia. The two soil profiles from LeFevre Peninsula are designated LeFevre Peninsula 1 (1LP) and LeFevre Peninsula 2 (2LP) and the one profile from the Mount Compass region is referred to as Mount Compass (MC).

The third sequence of soil profiles were from Canunda (CN) and Mount Burr (MB) in the south east of South Australia (Fig. 2.6).

Soil profiles and samples at all sites were described either from fresh exposures of existing vertical pits or fresh auger borings at depths within horizons as shown in Appendix 2. Morphological descriptions were made according to Soil Survey Staff (1951) and Soil Survey Staff (1987), and these are given in Appendix 2. From each profile, representative soil samples were taken and transported to Adelaide in polythene bags and air dried in a glass house. Subsamples were crushed by hand (i.e. not mortar and pestle) in order to minimize the crushing of fragile mineral grains. Samples were then sieved using a 2 mm sieve in order to separate the > 2 mm gravel fraction. These gravel fractions were reduced in size by repeated hand crushing and sieving to obtain representative fine earth subsamples. About 100 g of the representative fine earth subsamples were used for physical and chemical analysis.

2.2.3. Laboratory analyses.

2.2.3.1. Physical analyses.

Air-dry moisture.

10 g of air-dry sample was dried overnight at 105°C in a bench oven and reweighed. The air-dry moisture content was calculated from the loss in weight on

drying expressed as a percentage of the oven-dry weight from the equations:

$$O = A \times M$$

where O = oven-dry weight, A = air-dry weight, M = moisture factor;

$$\text{and } M = 1 + D/100$$

where D = air-dry moisture.

Particle size analysis.

A 25 g air-dry subsample was added to 200 mL water containing 25 mL 10 % (w/v) sodium tripolyphosphate and mechanically shaken end-over-end for 64 hours (Smith and Tiller, 1977). The sample was transferred to a sedimentation cylinder, diluted to 1250 mL with water and thoroughly mixed. A 20 mL subsample was pipetted at the appropriate time for silt + clay (smaller than 20 μm) and a second subsample pipetted for clay (small than 2 μm) determination. These subsamples were dried overnight at 105°C before weighing (USDA Soil Conservation Service, 1972; revised 1982). The sand was washed by decantation to remove the remaining silt and clay. The dried sand was sieved to determine coarse (210-2000 μm) and fine (20-210 μm) sand fractions.

2.2.3.2. Chemical analyses.

pH, Electrical Conductivity (E.C.) and Chloride.

A 1:5 soil:water suspension was prepared by adding 50 mL of air-equilibrated deionised water to 10 g air-dry soil and mechanically shaken end-over-end for one hour at 25°C (Piper, 1942). At least one control soil was included in the batch. After allowing the suspension to settle for 30 minutes, 1 mL of supernatant was removed for chloride analysis. The E.C. of the supernatant was measured using a calibrated conductivity cell and meter; the result was expressed on an air-dry basis, corrected to 25°C, in dS m^{-1} units to 2 decimal places. The pH of the supernatant was measured using a pH meter and combination electrode calibrated at pH 7.0 and 4.0. The pH of the sample was measured while gently stirring the supernatant and is reported

to the nearest 0.1 pH unit. The 1 mL removed earlier was diluted with 2 mL 0.15 M $\text{Ba}(\text{NO}_3)_2$ and analysed colorimetrically for chloride by auto analyser (Fransan, 1976). Chloride values are reported in $\mu\text{g g}^{-1}$.

Total carbon.

Samples were analysed for total carbon by heating approximately 1.5 g air-dry sample in a stream of oxygen at 1200°C on a Leco CR-12 Carbon Determinator previously calibrated using CaCO_3 (12.0 % C). Total carbon was calculated directly from the quantity of CO_2 produced (Merry and Spouncer, 1988).

Extractable phosphorus.

A 1.0 g air-dry subsample and 100 mL 0.5 M NaHCO_3 solution which had previously been adjusted to pH 8.5, were mechanically shaken end-over-end for 16 hours at 25°C . At least one control soil was included in the batch. The extract was filtered into an auto analyser sample tube and analysed colorimetrically for phosphorus (McLeod, 1982).

Exchangeable cations and cation exchange capacity (CEC).

A 2.5 g air-dry subsample was used for these analyses. At least one control sample and one blank was included in each sample batch. The sample was placed in a leaching tube, complete with filter pulp plug, of a mechanical leaching device (Holmgren *et al.*, 1977) or 'automatic extractor' (Concept Engineering Corp., USA). This sample was first leached free of soluble salts using deionized water and then leached overnight with 55 mL of 1 M NH_4Cl to remove exchangeable cations. The leachate was diluted to 100 mL using deionized water and analysed for Ca, Mg, Na and K by atomic absorption spectrophotometry. The residual NH_4Cl was leached out from the sample/filter pulp using deionized water and then leached with 45 mL of solution containing 1.5 M $\text{KNO}_3/0.25$ M $\text{Ca}(\text{NO}_3)_2$. This leachate was diluted to 50 mL with

deionized water and analysed for NH_4^+ and Cl^- on the auto analyser (McLeod and Zarcinas, 1976). The CEC was calculated from the NH_4^+ released from the sample.

2.2.4. Results and discussion.

Soil profile descriptions together with the corresponding analytical data for selected soil samples are given in Appendices 2 and 3.

2.2.4.1. Calcareous soils.

Soils sampled from LeFevre Peninsula 1 site (profile 1LP) are calcareous sands which comprise between 20 to 27 % CaCO_3 and with pH values ranging between 8.6 to 8.9 (1:5 soil:water extract). Very low amounts of clay (≤ 2 %) and organic carbon (i.e. between 0.6 to 1.2 %) were measured. Electrical conductivity ranged between 1.77 to 3.46 dS m^{-1} , chloride concentrations ranged between 2012 to 4924 $\mu\text{g g}^{-1}$ and the NaHCO_3 soluble P ranged between 14 to 17 $\mu\text{g g}^{-1}$ (Appendix 3). At the other site at LeFevre Peninsula (profile 2LP) the samples are also calcareous sands, with much lower CaCO_3 contents (ranging from 0.3 to 3.3 %), pH range of 8.2 to 9.1 (1:5 soil:water extract), low clay content (≤ 5 %) and an organic carbon content between 0.1 to 4.1 %. The electrical conductivity varied from 0.09 to 0.19 dS m^{-1} , chloride concentration ranged between 20 to 179 $\mu\text{g g}^{-1}$ and NaHCO_3 soluble P ranges from 2 to 55 $\mu\text{g g}^{-1}$.

The soil samples from Canunda National Park (CN) are predominantly calcareous (83 to 96 % CaCO_3 depending on the horizon) (Appendix 3). The total sand content ranged between 7 to 14 % and the clay content between 0.0 to 0.3 % for acid treated samples. pH values were ~ 9.3 (1:5 soil:water extract) and base status (7 to 25 $\text{mmol}[+]\text{kg}^{-1}$). Total C ranged between 9.6 to 10.3 % and was predominantly inorganic. Electrical conductivities ranged between 0.09 to 0.12 dS m^{-1} and chloride in soil solution ranged between 6 to 33 $\mu\text{g g}^{-1}$. The available P and exchangeable Ca, Mg & K values are given in Appendix 3. Particle size distribution curves for sand fractions (with and without CO_3) show remarkable similarity between the different

horizons (Figs. 2.71 and 2.72), indicating a similar source material for all the horizons.

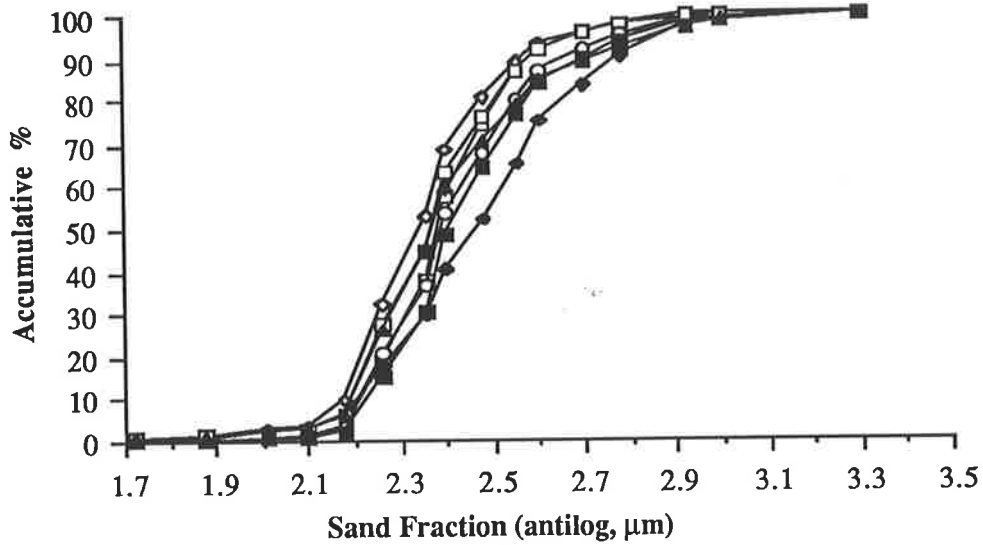


Fig. 2.71. Particle size distributions of horizons within Canunda soil profile (untreated samples).

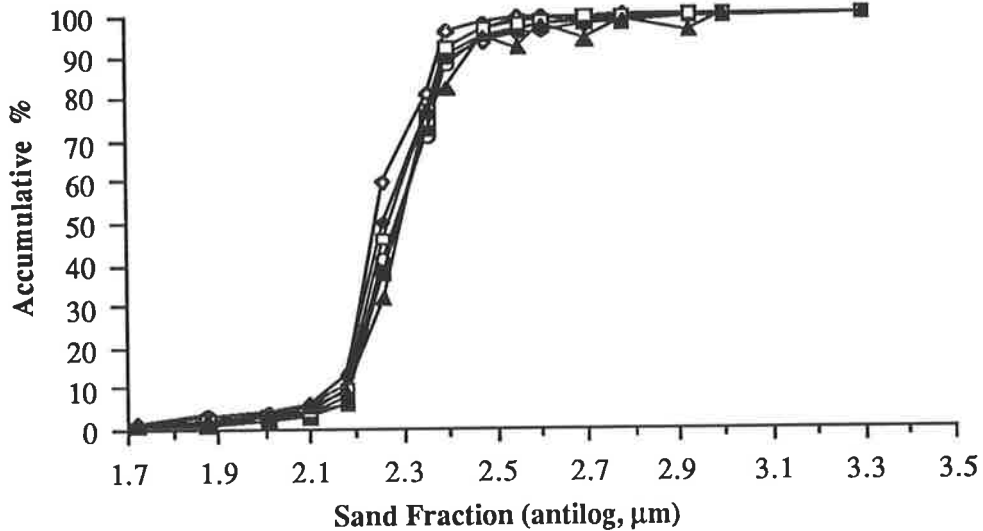
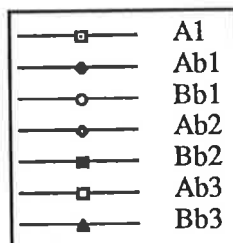


Fig. 2.72. Particle size distributions of horizons within Canunda soil profile (acid treated samples).



2.2.4.2. *Siliceous soils.*

At Amity, the soil profile (AM) is sandy textured with a pH range of 5-5.6 (1:5 soil:water extract). Total exchangeable cations ranged between 1-5 mmol[+] kg⁻¹, clay contents were ≤ 1 %, total carbon (≤ 0.4 %), electrical conductivity (≤ 0.04 dS m⁻¹) and chloride (< 2 µg g⁻¹). Soluble P concentrations were < 4 µg g⁻¹.

The soil material from Mount Compass (MC) is generally of sandy texture, locally becoming sandy loam in the B3 horizon, siliceous (i.e. with no CaCO₃), relatively leached, has pH values ranging between 5.9 to 6.9 (1:5 soil:water extract), base saturation values (0 to 13 mmol[+] kg⁻¹), clay contents (1-12 %), low organic carbon contents (0.2-1.2 %), very low and invariant electrical conductivities (0.03-0.04 dS m⁻¹) and low chloride concentration in soil solution (6-17 µg g⁻¹). Available P values were low (0 to 4 µg g⁻¹) as were extractable cations (Appendix 3).

The Mount Burr soil samples (MB) consist of ≥ 95 % sand and ≤ 3 % clay with a pH of 4.2-5.1 (1:5 soil:water extract). Total exchangeable cations ranged from 1-9 mmol[+] kg⁻¹, total C concentrations (≤ 0.6 %), E.C. (≤ 0.04 dS m⁻¹), Cl⁻ (< 2 µg g⁻¹) and soluble P concentrations (≤ 3 µg g⁻¹).

The profile morphological, physical and chemical data summarized in Appendices 2 and 3 provide a very comprehensive data set for comparing the range of typical calcareous and siliceous sands from the areas under study.

The pH (1:5 soil:water extract) of the calcareous soils (LP and CN) are significantly higher (8.2-9.2) than those for MC soils (5.9-6.9). In general soil pH in calcareous soils rise with increase in the proportion of water to soil, which may in part result from a reduction in soil CO₂ pressure (Whitney and Gardner, 1943). However, for all the soils the relationship can be even more complicated and any dependable measure of soil pH should take into account other soil factors such as soluble salts, nature and amount of electrolytes, type of clay and organic matter (Coleman and Thomas 1967).

Extractable P levels are generally higher in the calcareous soils than in more neutral and acid siliceous soils. These calcareous soils generally contain Ca phosphates

(Norrish and Rosser 1983), and NaHCO_3 extractant tends to decrease the concentration of Ca in solution by precipitating Ca as CaCO_3 . Consequently this increases the P concentration in solution (Olsen *et al.*, 1954). Lindsay and Moreno (1960) showed that, in acid soils containing Al and Fe phosphates, P concentration in solution increases as the pH rises. This could explain the marginally higher concentration of extractable P in the upper horizons of the Mount Compass profile. The behaviour of P in soils is more complex than outlined here, and can be affected by numerous other soil factors including, in particular, the concentration of Ca^{2+} , Mg^{2+} , K^+ , NH_4^+ , H^+ , Fe^{3+} , Al^{3+} , OH^- ions in solution (Norrish and Rosser 1983).

Total extractable chloride levels vary widely from one site to another, with the ILP profile having between 2012-4924 $\mu\text{g g}^{-1} \text{Cl}^-$. Except for the upper Al horizon of the 2LP profile, the chloride concentration of this profile is similar to the CN profile. Overall the MC profile has the lowest concentration of Cl^- , which ranges between 6 to 11 $\mu\text{g g}^{-1}$. The close proximity to the coast suggests that strong oceanic influence may be responsible for the very high Cl^- concentrations in ILP (Hutton, 1976). Though Canunda is also very close to coast, the low Cl^- ion concentrations in the samples may be due to redistribution by the wind and some been returned in the rain. At the other sites (2LP and MC) the Cl^- concentrations are low, due to leaching of the chloride salts from the profiles over a long period of time. The true nature, extent of contribution and dissipation of the Cl^- ion in these environments is more complicated than this.

Soluble Ca, Mg, Na and K salts are higher in CN samples than in MC samples. However, there are variations in soluble Ca and Mg concentrations down profile and with Ca as the dominant cation. The very high carbonate content of the CN profile may affect the relative concentrations of Ca and Mg in this soil. The MC samples contain relatively higher concentrations of Ca and Mg in the Al and Bh2 horizons which may be due to higher organic matter content of the Al horizon and the presence of saprolitic material in Bh2 horizon. The influence of soil factors on the interpretation of exchangeable cations and C.E.C. is more complex than is outlined here (Tucker, 1983).

Total carbon levels in soils 2LP and MC are mainly due to organic matter derived from plant material. However, there is a minor inorganic influence in samples from the 2LP profile. In contrast, in the ILP and CN samples the carbon present is inherited from carbonaceous sedimentary parent material.

The electrical conductivities are generally low throughout the CN, 2LP and MC profiles but high in the ILP profile.

Based on the morphological properties of texture, colour and structure the soils are readily distinguishable in the field. The main difference between the siliceous sands of Cooloola, North Stradbroke Island, Mount Compass and Mount Burr regions and the coastal sands from LeFevre Peninsula and Canunda is the higher pH values for the LeFevre Peninsula and Canunda soils. This is due to the higher carbonate contents of the latter soils and the much greater development (podzolization) in the former siliceous soils.

2.3. Soil classification and pedogenic processes

2.3.1. Introduction.

The concept of soil classification involves naming and classifying horizons and whole soil profiles. To date the topic is still controversial among international soil scientists the world over, as each country often develops a system of soil classification suitable for its own specific requirements. The complex nature of soils and the continually increasing knowledge about their characteristics make soil classification a continuously changing and evolving topic (Simonson, 1959). A summary review of the criteria necessary for the classification and nomenclature of various soils used in this study is outlined here with the object of clarifying and supporting the soil names given to the areas of study.

In the Australian context Stace *et al.* (1968) reviewed some of the principles and historical developments of soil classification. Soil classification has continuously developed in Australia, with Jensen (1914), Prescott (1931) and Stephens (1962) all

having different approaches to the subject. Jensen's (1914) system was based on the geological nature of the parent material, whilst Prescott (1931) introduced the Great Soil Group concept and emphasized the role of climate and vegetation in genetic classifications. Later Stephens (1962) improved on Prescott's (1931) work to include more characteristics of the soil itself in the definition of the soil groups. Stace *et al.* (1968) further modified Stephens' work by attempting to more definitively characterize various soil groups, add to the number by splitting some groups and providing a framework of subdivision above the Great Soil Group. They arranged the Great Soil Group in order of "progressive increase in the degree of profile development and degree of leaching". Nevertheless, their system still failed to distinctly define and suitably distinguish the major characteristics of soil orders and great soil groups used in Soil Taxonomy.

In comparison, Northcote (1979) used a "factual key" approach to include specific soil properties (morphological criteria) to define "Principal Profile Forms". Northcote (1979) developed a key in which one or two properties were used as differentiating criteria at each categorical level. Whilst this has the advantage of ease of use, it has the severe limitation that like soils are often separated at upper levels in the hierarchy and dissimilar soils included. Some soils may only be similar with respect to the differentiating criteria.

In Australia, therefore, the two systems of classification currently in use are the Great Soil Group classification (Stace *et al.*, 1968) and the Factual Key classification (Northcote, 1979). However, there are two other classification systems that are also commonly used by soil scientists in Australia, viz. U.S. Soil Taxonomy (Soil Survey Staff, 1987) and the "World Soil Map" (F.A.O., 1974). In Table 2.3 all soils in this study have been classified according to all four systems.

Table 2.3. Comparison of the approximate classification of soils studied, using different systems.

Coastal region	Location	Soil profile	Northcote (1979)	Stace <i>et al.</i> (1968)		Soil Taxonomy: Sub Group	FAO: UNESCO World Soil Map
			PPF†	Degree of profile development and degree of leaching	Great Soil Group		
South East (Qld.)	Cooloola	Carlo	Uc1.22	No profile differentiation	Siliceous sand	Typic Quartzipsamment	Eutric Regosol
		Kings Bore	Uc 3.21	Mildly to strongly acid and highly differentiated	"Rudimentary" Podzol	Spodic Quartzipsamment	Orthic Podzol
		Chalambar	Uc2.21	"	Podzol	Troporthod	Orthic Podzol
		Burwilla	Uc2.21	"	Podzol	Troporthod	Orthic Podzol
		Sea cliffs	Uc2.22	"	"Giant" Podzol	Spodic Quartzipsamment	Orthic Podzol
		Warrawonga	Uc2.22	"	"Deep" Podzol	Spodic Quartzipsamment	Orthic Podzol
		Mundu	Uc2.22	"	"Giant" Humus Podzol	Spodic Quartzipsamment	Humic Podzol
		Kabali	Uc2.21	"	"Giant" Humus Podzol	Spodic Quartzipsamment	Humic Podzol
	Nth. Stradbroke Is.	Amity	Uc2.22	"	"Giant" Podzol	Spodic Quartzipsamment	Orthic Podzol
South East (S. Aust.)	Canunda	Canunda	Uc1.14	No profile differentiation	Calcareous sand	Typic Xeropsamment	Calcaric Regosol
	Mt. Burr	Mt. Burr	Uc2.21	Mildly to strongly acid and highly differentiated	Podzol	Entic Haplorthod	Orthic Podzol
Central (S. Aust.)	LeFevre Peninsula	LeFevre 1	Uc1.11	No profile differentiation	Calcareous sand	Typic Xeropsamment	Calcaric Regosol
		LeFevre 2	Uc1.14	"	Calcareous sand	Typic Xeropsamment	Calcaric Regosol
	Mt. Compass	Mt. Compass	Uc 2.21	Mildly to strongly acid and highly differentiated	Podzol	Typic Haplorthod	Orthic Podzol

† Principal Profile Form

2.3.2. Uniform textured soils.

Northcote (1979) classified soil profiles with a predominantly mineral fraction and with hardly any textural differences throughout the profile as "uniform" (U), and this is referred to as their "Principal Profile Form" (PPF). The PPF for uniform textured soils is based solely on soil colour. This level of classification has no direct equivalent in the Great Soil Group classification of Stace *et al.* (1968).

All soil profiles sampled in this study were predominantly uniform and of coarse sandy texture. The Factual Key defined these soils as a Uc subdivision at which level again there is no direct equivalent to the system of Stace *et al.* (1968). The degree of profile development and degree of leaching level of Stace *et al.* (1968) is equivalent to the section level of Northcote (1979), whilst the great soil group level (Stace *et al.*, 1968) is analogous to the sub-section level (Northcote, 1979).

2.3.2.1. Calcareous sands.

The name Calcareous sands is used by both Stace *et al.* (1968) and Northcote (1979) for soils with uniform coarse to medium textured sands, with little or no profile development except for some organic matter accumulation in the surface horizon. The LeFevre Peninsula 1 (1LP), LeFevre Peninsula 2 (2LP) and Canunda (CN) profiles all qualified as calcareous sands (see morphological descriptions and selected laboratory data in Appendices 2 and 3). Pedogenetic alteration is minimal in these soils, the parent material is of coastal origin and the calcareous fraction is comprised of mainly marine shells and other skeleton grains (Table 2.2. and 2.3). Pedogenesis is restricted to accumulation of organic matter in the surface horizon (A1 horizons of 1LP and 2LP profiles and Ab1 horizon of CN with slightly more organic carbon), some leaching of carbonate by water or removal by other factors such as wind (compare the carbonate contents of 1LP and 2LP profiles).

2.3.2.2. *Siliceous sands.*

Siliceous sands are texturally and macromorphologically similar to calcareous sands insofar as there is minimal or no profile development, but are mineralogically different (mainly quartz sands) (Stace *et al.*, 1968; Northcote, 1979). The Carlo profile (CL) was the only siliceous sand sampled and has been described and named (Thompson and Moore, 1984) as Mutyi 1. The classification and nomenclature of CL using the four systems of classification is summarized in Table 2.3. The Carlo profile is a presently drifting sand derived from beach deposits and older dunes within the Cooloola landscape. The parent material is aeolian quartz sand (Table 2.2). The soil has an acidic reaction trend. Pedologic development is absent, with no organic matter accumulation on the soil surface and no noticeable accumulation of clay or silt in the subsurface.

2.3.2.3. *Podzols.*

Podzol represents the Great Soil Group level of classification of Stace *et al.* (1968). The degree of profile development and degree of leaching is described as "mildly to strongly leached highly differentiated soils". In comparison, Northcote (1979) described such soils as (i) Uc2 at the section level i.e. "soils showing pedologic organisation including a conspicuous bleached E¹ horizon" and (ii) Uc 2.2 or 2.3 at the class level with no carbonate pan, or any other pan, with different PPF depending on the forms of the soil colour and degree of induration below the E horizon. The fundamental characteristics of podzols are the accumulation of amorphous and/or poorly crystalline iron, aluminium and humus compounds in the B horizon, which underlies either (a) an E horizon above which may be an O and/or A1 horizon or (b) an A1 overlain by an O horizon. Based on the solum depth and thickness of the bleached E, three classes of podzols were sampled viz 'Rudimentary' Podzol (thin and weak E), Podzol (intermediate and well developed E) and 'Giant' or 'Deep' Podzols and Humus Podzols (massive and very well developed E) (Table 2.3). The underlined names are

¹ Note Northcote (1979) uses the term A2 for E horizon. Throughout this thesis "E" horizon is used.

those recognised by Stace *et al.* (1968) and the lengthened names are those given by Thompson (1983) and Thompson and Moore (1984) to emphasize the degree, nature and extent of podzolization. Based on the extended system of Thompson and co-workers the podzols studied were classified as shown in Table 2.3. Even though the horizon patterns are those of Podzols or Spodosols (Soil Survey Staff, 1987) the solum depth and horizon thickness (especially of the E) is much greater than the range recommended for a Spodosol. The observable Bh and placic horizons are at depths in excess of 2 m (Soil Survey Staff, 1987). The relationship between the Podzols, Spodosols and other related soil groups are discussed by Thompson and Hubble (1980).

Podzols are mainly formed through strong leaching, the accumulation of acidic organic matter in the surface horizon, and the downward translocation and deposition of some organic matter, sesquioxides and some clay, to form the dominantly iron-humus B horizons. Podzol genesis and hypotheses to explain the former have been described by many workers (e.g. Stobbe and Wright, 1959; McKeague *et al.*, 1978, 1983). The formation of sesquioxidic-organic matter complexes in the B horizon either does not occur or is a minimal process in soils of high base status. The combined effects of base depletion through leaching, microbial decomposition of organic substances, translocation of water-soluble organic substances and sesquioxides and subsequent precipitation of the insoluble translocated complexes (sesquioxides and organic matter) leads to the formation of the spodic B horizon. The formation of Humus Podzols is similar manner as Podzols except that in the latter deposition of organic matter and sesquioxides to form the B horizon is regulated by the ground water level (Farmer *et al.*, 1983). The formation of a Bh (humus B) horizon in these instances results in the loss of Fe and precipitation of organic compounds, with the Bh horizon forming at the top of the water table.

2.4. Summary.

The macromorphological and soil chemical data support a trend in leaching status of the soils being studied. In the calcareous soils (CN, 1LP and 2 LP) and acid siliceous soils (CL, KB, CH, SC, WA, AM, MC, MB, etc.) the chloride and exchangeable cation levels indicate a progressive increase in the degree of leaching and hence in corresponding soil profile development (Table 2.3). For each location, Table 2.3 lists soil profiles in order of increasing profile development.

CHAPTER 3**AGE SEQUENCES****3.1. Introduction**

The study of soils in relation to landform can provide considerable understanding of processes. Sedimentary records of stable landscapes often provide geomorphic and other palaeo-environmental information which can facilitate regional extrapolation. During soil formation, climate, organisms and relief are dynamic environmental factors which are subject to periodic and/or sequential alteration, either individually or collectively with time (Yaalon and Ganor, 1973). For soils formed in situ from weathering bedrock, the parent material is usually referred to as a passive or time-independent attribute, but for soils developed from materials accumulated by natural geomorphic agencies the process is definitely time-related.

The contemporary landscapes on which soils develop owe many of their natural differences to specific events in prehistoric times. After deposition the parent sediments are exposed to a variety of soil forming processes, e.g. weathering, leaching, plant colonization and horizonation at particular times. The time elapsed from the inception of soil formation to its maturity will vary greatly and is largely dependent on the intensity of the soil forming factors. The integrated effects of these processes over time within a soil profile result in additions, removals, transformations and translocations of the bulk of the organic and inorganic constituents in the soil. In studies related to time-sequence functions, the assumption is that the constituent units were once exposed to similar developmental stages through time.

Since all the soils used in this study were transported sandy sediments, time was thus a significant factor in producing soil differences, particularly in soil landscapes thought to constitute an age sequence or, in some cases, a chronosequence. A chronosequence as defined in the Glossary of Soil Science Terms (1987) is a

sequence of related soils that differ, one from the other, in certain properties primarily as a result of time as a soil-forming factor. Stevens and Walker (1970) defined a chronosequence more specifically as a sequence of soils developed on similar parent materials and relief under the influence of constant or ineffectively varying climatic and biotic factors. Differences between soils in a chronosequence can thus be ascribed to the lapse of differing increments of time since the initiation of soil formation. Differences between soils of different ages in such a sequence are considered to depend upon the progressive increase of time after the start of soil formation. Jenny (1941) stated that the larger the number of horizons and the greater their thickness and intensity the more mature is the soil. The bulk of the knowledge on pedogenesis as revealed by profile formation are deductions, based on the concept of time as a soil forming factor. To study the effect of time on soil development it is vital to establish the soils as constituents of a chronosequence, and if the ages of the soils are known, soil development can be related to time (duration of the development of the soil). However, most of the dating techniques seem to measure time in the historical context (ie the inception and/or completion of geomorphic and/or pedologic processes).

Processes of physical and chemical weathering of sediments are fairly slow, and the intensity of their effects is approximately proportional to the time over which they have operated. Quaternary sediments have been dated using the intensity of weathering of mineral grains or rock samples (Setlow, 1978; Colman, 1981) by detailed observations of the sediment characteristics such as grain colour, thickness of weathering rind and the extent of preservation of diagnostic surface features on mineral grains. From these studies, the relationships between mineral weathering and time have been established. In soils, pedogenic effects (observations of profile characteristics) and rates of heavy mineral weathering are similarly related to time.

Given this background concerning the importance of time in soil development studies, the purpose of this chapter is to examine specifically the efficacy of the thermoluminescence dating technique on selected samples from the Queensland region, where the concept of a chronosequence has long been established, but without absolute

ages for any of the soil landscape units and to review the available published ages of the other soils studied. The ages obtained or given for the different soils are used to examine or explain the relationship between heavy mineral weathering and time in Chapters 5, 6 and 7.

3.2. Cooloola - North Stradbroke Island sequence

3.2.1. Introduction.

The geology and geomorphology of the Cooloola and North Stradbroke Island sandmasses have been described in Chapter 2. These larger sandmasses lie mainly along the subtropical coast with a maximum concentration as sand islands and mainland deposits to the east and north of Brisbane i.e. Fraser, Moreton, and North Stradbroke Islands and the Cooloola and Peregian sandhills. As mentioned in Chapter 2, at least eight dune systems can be recognised in the deposits at Cooloola (Ward, 1977; Thompson, 1981; Thompson and Moore, 1984) and this implies a longer or better-preserved record of Quaternary events than reported for similar sandmasses in New South Wales to the south (Thom, 1978) or to the north (Pye, 1983).

The dune systems at Fraser Island (Ward, 1977) and Cooloola (Thompson 1981, 1983) can be placed in an inferred age sequence according to their stratigraphic, geomorphic and denudational relationships and correlated with similar dunes in the adjacent sandmasses such as North Stradbroke Island (Ward, 1978; Pickett *et al.*, 1984). The inferred age sequence is also supported by soil evidence that shows progressive advances in the depth of podzol development resulting from increasing periods of leaching (Thompson, 1983). Few absolute age determinations have been made because of the paucity of suitable material for dating, and what ages are available provide only some indication of maximum ages rather than direct evidence of the ages of dune deposition.

In New South Wales, many radiocarbon dates have been obtained from shell fragments in the marine deposits at the base of the Holocene beach-ridge plains (Thom *et al.*, 1981), and in some instances these have provided a maximum age for the overlying parabolic dunes. In southern Queensland, the parabolic dunes of the sandmasses overlie older aeolian quartz sands and both lack shell fragments. Wood, charcoal and other organic fragments have been recovered from some beds but in the older dunes these are beyond the limits of radiocarbon dating and serve only to indicate a Pleistocene age, such as at Cooloola (Coaldrake, 1962). In the younger dunes, radiocarbon dating at Triangular Cliff, Fraser Island, indicates that the large parabolic dune there is of Holocene age (Grimes, 1979; Ward and Grimes, 1987), although it had previously been regarded as a Pleistocene feature (Ward, 1977).

At Cooloola, recognition of Holocene and Pleistocene dunes has been based on the marked differences in geomorphology and denudation which indicate a sizeable time gap and extensive fluvial erosion between the older dune systems and the three youngest. This time gap is also supported by accompanying differences in the depth and degree of podzol development (Thompson, 1983).

On North Stradbroke Island, uranium series dates for three coral species recovered by dredging during sandmining, from beneath a large degraded parabolic dune yielded $^{230}\text{Th}/^{234}\text{U}$ isotope ages of 101-108 ka BP (Pickett *et al.*, 1985), since revised to 119-132 ka BP (Pickett *et al.*, 1989). The stratigraphic relationships imply that the coral was buried by a prograding shore as the dune advanced into the ancestral Moreton Bay and that the dune sands and corals are therefore contemporaneous.

None of the radiometric dates so far obtained provides an absolute age for the period of dune formation. Thermoluminescence (TL) dating of the quartz sand offers a method whereby the actual age of dune deposition may be determined, providing the quartz sands were bleached or "zeroed" of TL energy by sunlight during the aeolian deposition. Several studies including Aitken

(1985), Wintle and Huntley (1982), Gardner *et al.* (1987), Berger (1988) and Readhead (1988) have discussed the theoretical bases and practical problems associated with TL dating and its application in a geological context.

The method is used to date sediments based on their last exposure to sunlight.

The age of the deposition is given by the so-called "age equation" :

$$\text{age} = \frac{\text{TL}}{(\text{TL per unit dose}) \times (\text{annual dose})}$$

where "TL" indicates the TL light from the sample as measured in the laboratory, "annual dose" is the dose rate delivered to the sample since deposition by radiation in the environment and "TL per unit dose" is a measure of the sensitivity of the sample, also a laboratory measurement. In the "coarse grain" or "inclusion" technique used in the present study, 100 μm quartz grains are extracted from the sample. Before TL measurements are made, the grains are etched with HF to remove the outer layer, of about 10 μm , which has been exposed to alpha radiation from its surroundings. This procedure greatly simplifies the calculation of dose rate. Bell and Zimmerman (1978) have discussed such questions as the uniformity of etching, and the rather small amount of subsequent work has been listed by Aitken (1985) in his Appendix C, where he points out that there is need for more work on the response to etching. For example, the pretreatment has not been investigated to determine the continued presence or otherwise of coatings on the surfaces and/or in cracks in quartz grains. For this reason, the effects of various pretreatments used in TL dating were evaluated.

The objectives of this section of the chapter are: (i) to apply a TL dating technique using quartz grains isolated from a selected number of horizons from three of the dune systems at Cooloola spanning youngest to oldest, and from the dune overlying the dated coral on North Stradbroke Island: dates so obtained are discussed in relation to the inferred age sequence deduced from field data; (ii) to use thermogravimetric analysis (TGA), differential thermal analysis (DTA) and scanning electron microscope (SEM) methods to investigate possible differences in the nature of the quartz (i.e. α - β inversion at 571-573°C and water content) and

to monitor the various pre-treatment methods (size fraction, magnetic separation and acid pre-treatments) used in TL dating.

3.2.2. Materials and methods.

3.2.2.1. Site description.

The locations of Cooloola and North Stradbroke Island are shown in Fig.2.1.

Cooloola

See Chapter 2 for detailed description. Three samples, from Kings Bore, Warrawonga and Kabali were studied (Figs. 2.2 & 3.1).

North Stradbroke Island

The location (Fig. 2.1) and general site description of North Stradbroke Island are given in Chapter 2. One sample near Amity (Fig. 2.3) was used as a reference to cross-check the TL results. This dune has been equated with the Yankee Jack Dune sand (Ward 1978) and Dune System 5 at Cooloola (Thompson, 1983), and has been described and dated by Pickett *et al.*, (1985, 1989) using isotopic ratios $^{230}\text{Th}/^{234}\text{U}$.

3.2.2.2. Sampling.

Considering the nature of transport and development of the dunes it is presumed that the sands were exposed to sunlight for a sufficient period to fulfil the TL clock resetting by daylight to a low (though not necessarily zero level), I_0 . For example Lu *et al.* (1987) showed that the natural aeolian transport of loess is enough to reset the TL clock and that I_0 can be estimated by a laboratory bleach of about 15 hour. Similar conclusions are drawn by Readhead (1988) for aeolian quartz in south east Australia, and in the review by Berger (1988).

To minimize the uncertainty of the effect on the annual dose rate of variable content of water, which absorbs some of the energy which would

Soil landscape	Kabali	Amity	Warrawonga	Mutyi (Kings Bore)
Dune system	6	5	4	1
TL ages (ka)	730±70	120±11	90±10	19±2
Sampling depth (m)	1.8-2.0	3.8-4.0	1.8-2.0	1.2-1.4

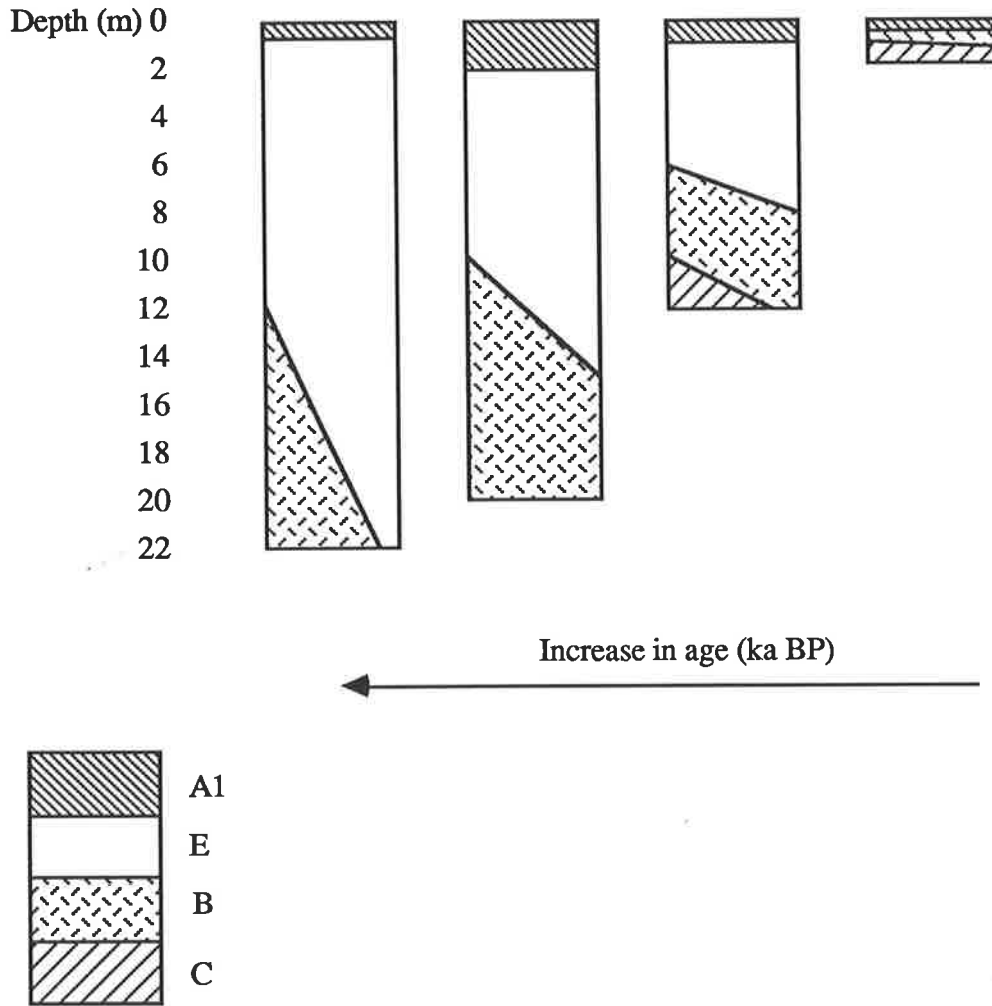


Fig. 3.1. Schematic cross-section of the soil profiles sampled showing the increase in development with age (modified from Thompson, 1983).

otherwise be absorbed by the quartz grains, samples were taken only from freely-drained dunes where the sands are unaffected by the water table.

The three samples from Cooloola: Kings Bore, Warrawonga and Kabali and one from North Stradbroke Island: Amity were taken at depths of 1.2-1.4 m, 1.8-2.0 m, 1.8-2.0 m and 3.8-4.0 m respectively (Fig. 3.1). These depths correspond to the soil C horizon of Kings Bore and E horizons of the remaining samples. Care was taken not to expose the samples to direct sunlight during collection by using a method modified after Smith and Prescott (1987).

Subsequently, *in situ* radiation measurements were taken at the sampling sites using a γ -scintillometer placed in auger holes bored to the depth of sampling for the purpose of checking the background radiation.

3.2.2.3. *Laboratory analysis.*

The quartz inclusion technique (Aitken, 1985) was adopted. The 90-125 μm grain fraction was separated by dry sieving. Further separation with a heavy liquid (sodium polytungstate of density 2.96 Mg m^{-3}) was used to sort the light fraction (mainly quartz) from the heavy mineral grains. The separated quartz fraction was passed through a Frantz Isodynamic Separator to remove magnetically sensitive grains from the fraction before etching the residual grains in a 40 % HF solution for 40 minutes so as to remove the outer alpha-irradiated layers (Aitken, 1985). Final washing of the etched grains in 10 % HCl and subsequently with deionized water to neutral pH removed any fluoride compounds formed.

Stainless steel discs were sprayed with silicone, then coated with a single layer of grains, and either kept in darkness (yellow light) or exposed to sunlight for bleaching over a 48 hour period. The natural and bleached samples were placed in a chamber containing an inert atmosphere, given different levels of artificial irradiation and heated to generate TL glow curves using a Risø automatic TL reader (Bøtter-Jensen *et al.*, 1983). The temperature was increased to 550°C using a constant heating rate of 5 K s^{-1} and a ^{90}Sr - ^{90}Y plaque β -source was used for irradiating the samples.

After determination of the moisture content, the untreated bulk samples were analysed for their U and Th content using a thick source alpha counting (TSAC) technique (Aitken 1985) and X-ray fluorescence spectrometry (XRF) (Norrish and Chappell, 1977). The K₂O and other major element compositions of similar subsamples were determined by wavelength dispersive XRF, using fused glass discs and a Philips PW 1400 instrument (Norrish and Hutton, 1969). Zircon grains were separated quantitatively from the samples by density and magnetic properties, crushed and their α particle activity measured by TSAC.

Differential thermal analysis (DTA) and thermogravimetric analysis (TGA) were conducted simultaneously on four sets of samples using a Rigaku TG-DTA infrared heating apparatus (Thermoflex 8100 series) as described by Eggleton and Fitzpatrick (1988). The following four pre-treatments were applied to the quartz samples; after density separation (except for treatment d):

treatment (a) - the non-magnetic quartz fraction was sieved to give a 90-125 μm fraction.

treatment (b) - a portion of the fraction from (a) was acid etched and washed.

treatment (c) - a portion of the entire sample was sieved to give a 53-125 μm fraction.

treatment (d) - a portion of the entire sample was left untreated, with a full range of grain sizes.

Weight loss was determined on 40 mg samples at temperatures ranging from ambient to 800°C.

3.2.3. Results and Discussion

A general schematic cross-section of the soil profiles examined is summarized in Fig. 3.1, showing that the degree of profile development is a function of increasing age based on the field morphological data and TL results.

3.2.3.1. TL measurements.

The measurements on the natural samples resulted in glow curves as illustrated in Fig. 3.2 for the natural sample from Amity. Glow curves were also obtained on bleached samples after receiving laboratory radiation.

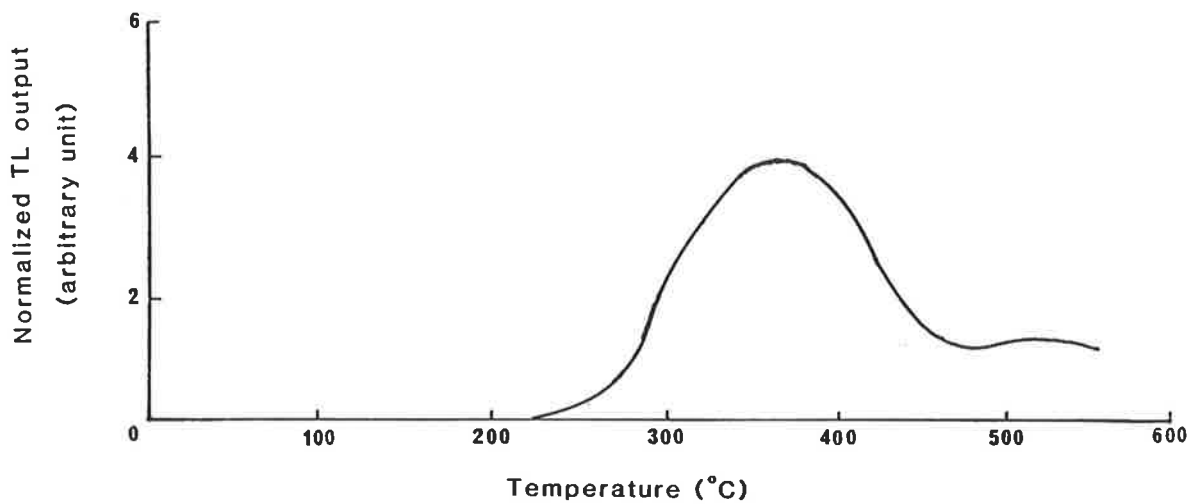


Fig. 3.2. Glow curve for Amity sample which has received only the natural dose.

The long term stability of the stored TL at temperatures above 300°C, which is critical to dating sediments with ages in the order of tens of thousands of years or more, was tested by finding the Equivalent Dose (ED) temperature plateau. This extended from about 320 to 420°C (Fig. 3.3).

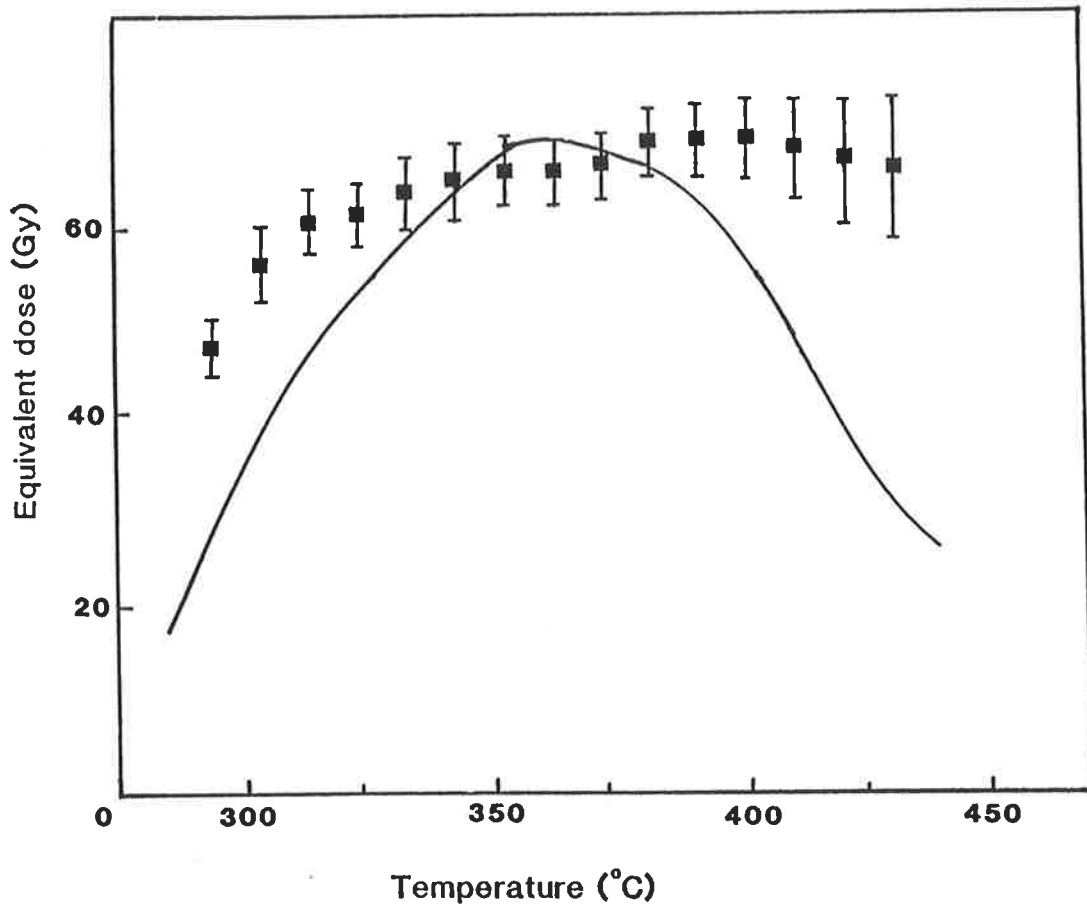


Fig. 3.3. Dose plateau for Amity sample with natural glow curve superimposed. The error bars are assigned by the curve fitting programme.

ED values were calculated based on method C discussed in Lu *et al.* (1987) where the TL growth is regenerated by bleaching out the natural TL to some arbitrary minimum level (I_0), followed by addition of a series of artificial doses. Regenerated curves for both the artificially dosed, bleached and natural samples are matched to obtain the ED values. An example, for the Amity dune sample, is shown in Fig. 3.4. In this figure the circles indicate the natural samples without and with radiation doses. All the data points are shown. The squares are bleached samples. The latter curve is used as a model for the shape of the dose growth curve under the assumption that the addition of dose after bleaching reproduces the growth of the TL after the original bleaching. The ED is found by fitting the two curves. The fitting was done by a

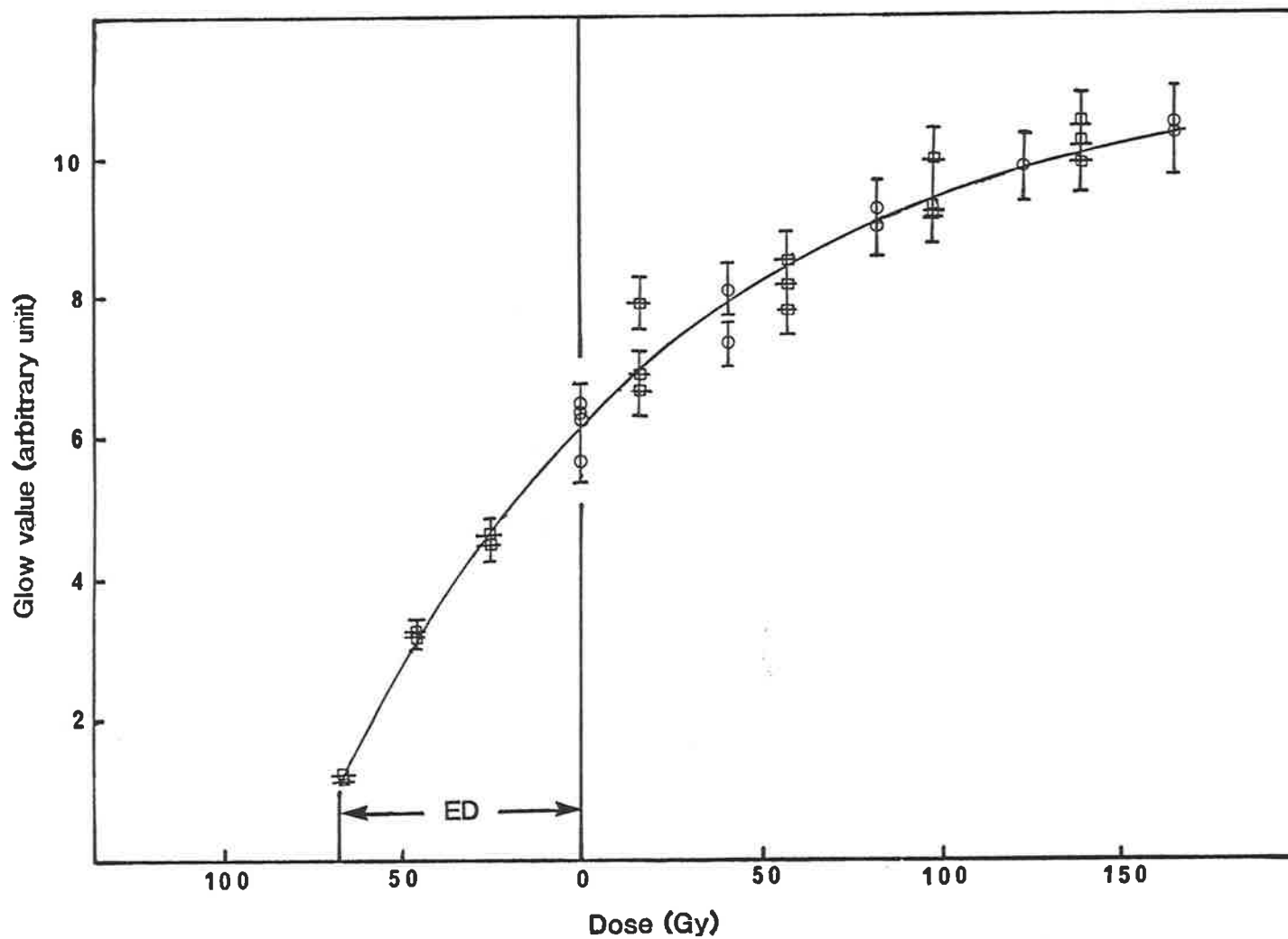


Fig. 3.4. Regenerative TL data for Amity sample used for calculating ED at peak temperature (\circ , natural sample; \square , bleached sample).

statistical least squares procedure which first uses the bleached curve as a model for fitting the natural curve and then optimises the fit of the entire data set to an exponential function of the form $g = A\{1 - \exp[-b(d+x)]\}$. The ED (Fig. 3.4) follows from the fitted parameters. This is done for all plateau temperatures. The ED used in dating is for the 20° interval at the peak of the glow curve. This lies well within the plateau.

For applied doses of radiation, differences and similarities among the samples were observed, with the Warrawonga and Kabali samples having identical TL response curves within the statistical uncertainties; these were different from Amity and from Kings Bore. The latter two also differed in absolute sensitivity to radiation.

3.2.3.2. *DTA-TGA and SEM analysis.*

DTA has been used successfully to differentiate between the origin of quartz samples from different rock types, based on the inversion temperatures for the quartz (Nagasawa, 1953; Symkatz-Kloss, 1974). Generally speaking, quartz from high temperature deposits shows simple and sharp curves, and that from low-temperature deposits shows broad or flat curves. Symkatz-Kloss (1974) found higher inversion temperatures in igneous quartz crystals than sedimentary rocks formed by weathering or diagenesis. DTA measures the difference in temperature (ΔT) between the sample and an inert reference material (ignited α Al_2O_3) as a function of temperature (T). DTA curves for selected samples are given in Figs. 3.5 and 3.6 (solid lines) where the ΔT factor is plotted on the ordinate, and T on the abscissa.

The narrow endothermic peak near 573°C (plotted downwards) represents the α to β transition of quartz, and the broad exothermic (plotted upwards) and endothermic peaks between 100 to 500°C may represent the recrystallization and dehydroxylation of poorly crystalline alumino-silicate and iron oxide mineral coatings. In all samples, the narrow peaks representing the quartz endotherm (Figs. 3.5 and 3.6) do not show any

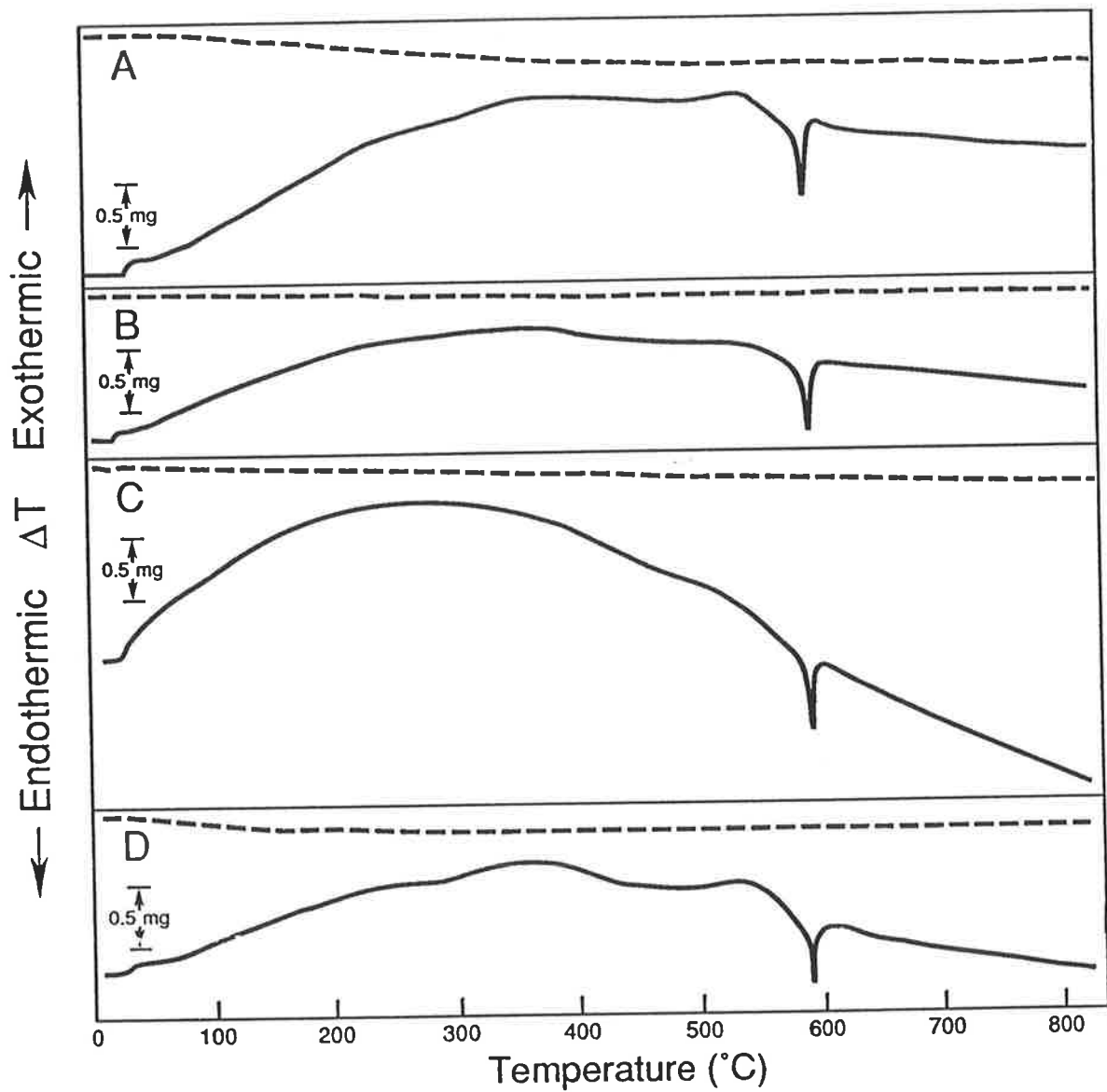


Fig. 3.5. DTA (—) and TGA (---) traces for (A) Kings Bore, (B) Warrawonga, (C) Amity and (D) Kabali samples for pre-treatment (b): the 90-125 μm non-magnetic fraction, HF and HCl treated, used in TL dating.

marked differences in shape and peak position which might correspond to the observed dissimilarities in the TL outputs. Furthermore, the DTA curves of the different pre-treatments (listed in Table 3.1) also showed only small differences in their respective endothermic and exothermic broad peak shapes between temperatures of 0 to 500°C [compare Figs. 3.5 and 3.6 for pretreatments (b) and (a) respectively]. However, the

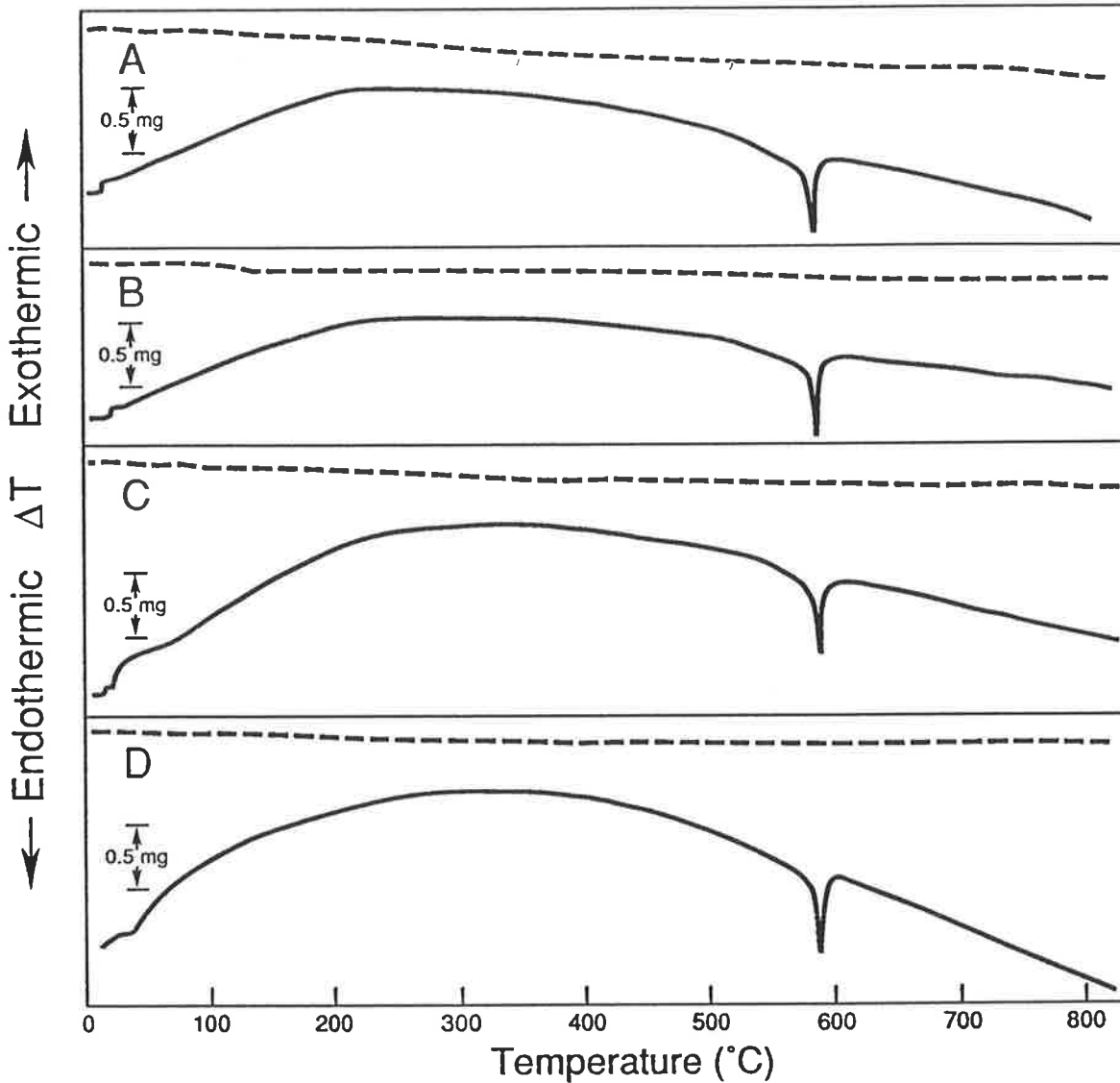


Fig. 3.6. DTA (—) and TGA (- - -) traces for (A) Kings Bore, (B) Warrawonga, (C) Amity and (D) Kabali samples for pre-treatment (a): the 90-125 μm non-magnetic fraction, untreated.

TGA data (dashed lines), which measure the weight loss of a sample as a function of temperature, do show slight differences between samples and pre-treatments. The main differences between pre-treatments are shown by the weight losses which correspond with the broad exothermic DTA peaks between 230°C and 550°C. In Table 3.1 the TGA data for the four pre-treatments at temperatures of up to 800°C are shown. Weight loss in the samples ranged from 0.13 % for Warrawonga sample, pre-treatment

(b) to 2.19 % for Kings Bore, pre-treatment (c). Generally, the weight loss for the different pre-treatments is in the order $d > c > a > b$ (Table 3.1).

Table 3.1. Percent weight losses for 40 mg air dried samples subjected to four different pre-treatments, based on TGA curves.

Pre-treatment [†]	Site Horizon	Kings Bore C	Warrawonga E	Amity E	Kabali E
(a)		1.00	0.50	0.50	0.25
(b)		0.75	0.13	0.44	0.25
(c)		2.19	0.75	1.19	1.00
(d)		1.56	1.06	1.94	0.88

[†] (a) 90-125 μm non magnetic fraction.

(b) 90-125 μm non magnetic fraction, HF and HCl treated.

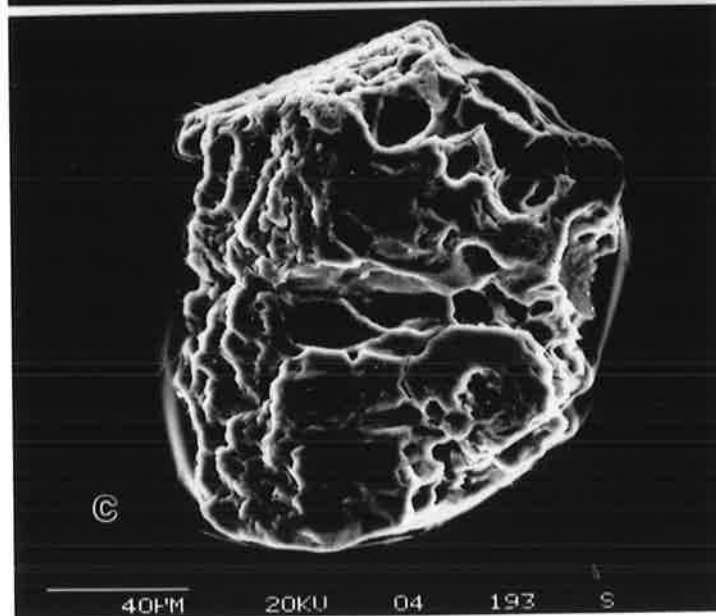
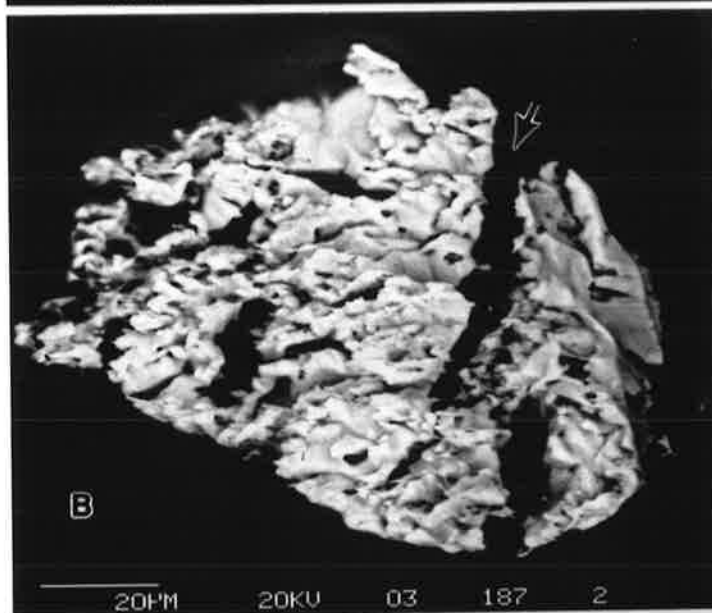
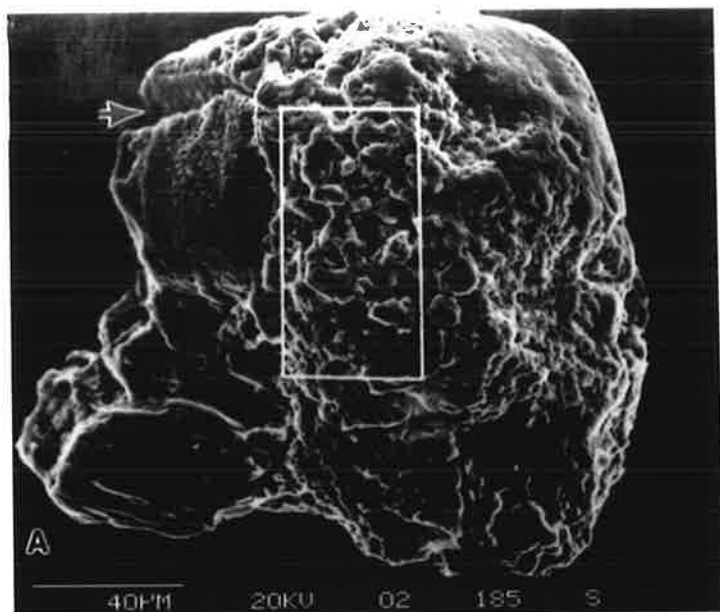
(c) 53-125 μm , untreated.

(d) bulk sample, untreated.

This dehydration trend is possibly caused by the decrease in water sorbing substances (e.g. clay and other amorphous and cryptocrystalline materials) present as coatings on grain surfaces and/or in cracks.

The presence of grain coatings (pre-treatment d) and absence of grain coatings (pre-treatment b) resulted in substantial and reduced water loss respectively (Table 3.1). The thin coatings on quartz grains from the Kings Bore and Amity samples are shown in the SEM micrographs in Plate 3.1 A and B. Using energy dispersive X-ray analysis (EDAX) these coatings were found to consist mainly of Si and some small

Plate 3.1. Scanning electron micrographs of quartz grains after different pre-treatments (A) 90-125 μm , non-magnetic fraction (pre-treatment a) for Kings Bore, (B) 90-125 μm , non-magnetic fraction (pre-treatment a) for Amity and (C) 90-125 μm , non-magnetic fraction (pre-treatment b) for Kings Bore. Note, in (A) arrow indicates natural crack in quartz grain and boxed area indicates a portion of the surface coatings, and in (B) arrow indicates accentuated crack after HF etching.



3.1.

amounts of Al and Fe. The small cracks which can be observed on untreated grains (see arrow in Plate 3.1 A) are accentuated following HF treatment (see arrow in Plate 3.1 C). After HF treatment there is evidence (row (b) in Table 3.1) for some coatings persisting on quartz grains from all samples, with more on the Kings Bore sample than on the Warrawonga, Amity and Kabali samples. However, it is possible that some of the moisture retained by the quartz grains (Table 3.1) can also be explained by the presence of surface cracks (suitable for the retention of atmospheric moisture) as enhanced by HF etching (Plate 3.1 C). The SEM results on the removal of grain coatings and the preferential etching of cracks are similar to those of Bell and Zimmerman (1978). The DTA and TGA studies, which are believed to be new, are consistent with the other observations. However, it appears that the additional information that these techniques provide is not sufficient to justify their regular use in TL dating.

3.2.3.3. *Annual dose rate measurements.*

The XRF, TSAC and γ -spectroscopy data together with the TL age data for all samples are given in Tables 3.2, 3.3 and 3.4. The geochemical data (Table 3.2) show the youngest, unleached unit, Kings Bore, to have the highest concentrations of all the elements analysed except for SiO_2 . The high $\text{K}_2\text{O}/\text{SiO}_2$ ratio of Kings Bore relative to the other profiles is evidence of less weathering. The Amity sample contains more Fe and Ti reflecting the greater concentration of heavy minerals than the samples from Warrawonga and Kabali, but is otherwise geochemically similar. The very low K_2O and high SiO_2 values for all the samples confirm the findings of other workers (e.g. Little *et al.*, 1978; Thompson, 1981) which show these coastal dunes comprise ~98 % quartz, some heavy minerals and very few feldspars.

The XRF, TSAC and γ -spectroscopy results (Table 3.3) show highest concentrations of U and Th are from Kings Bore, with lower and decreasing concentrations for Amity, Warrawonga and Kabali. XRF measures the parent isotopes of the uranium and thorium chains. Gamma-spectroscopy records a single γ -ray late in

Table 3.2. Major element composition of ignited samples.

Dune System	Site	Max sampling depth (m)	% Oxide composition								
			SiO ₂	Al ₂ O ₃	Fe ₂ O ₃	TiO ₂	CaO	MgO	Na ₂ O	K ₂ O	MnO
1	Kings Bore	1.4	94.1	0.96	1.2	1.2	0.02	0.05	n.d.	0.14	0.02
4	Warrawonga	2.0	97.9	0.20	0.43	0.28	n.d.	n.d.	n.d.	0.01	n.d.
5	Amity	4.0	96.7	0.23	0.66	0.79	n.d.	0.01	n.d.	n.d.	0.01
6	Kabali	2.0	97.8	0.18	0.46	0.30	n.d.	n.d.	n.d.	n.d.	n.d.

n.d. = not detected, i.e. below the limit of detection using Norrish and Hutton (1969) method.

Table 3.3. Comparison of U and Th concentrations ($\mu\text{g g}^{-1}$) using XRF, TSAC and γ -spectroscopy.

Dune System	Site	XRF		Bulk sample		TSAC		γ -spectroscopy	
		Th	U	Th	U	Zircon grains Zircon content	U†	Th	U
1	Kings Bore CA2S/1	9.2±0.5	2.7±0.3	6.7±1.3	2.3±0.2	15000	3	7.5±0.2	2.7±0.2
4	Warrawonga CA7S/2	-	-	0.8±0.2	0.4±0.1	1600	0.4	0.70±0.05	0.57±0.1
5	Amity SK11S/4	1.8±1.0	1.3±0.4	1.1±0.3	1.3±0.1	4400	1	1.3±0.08‡	1.1±0.07‡
6	Kabali CA9S/2	-	-	0.2±0.1	0.50±0.04	1200	0.2	0.48±0.03	0.48±0.03

Note: U and Th concentrations for Warrawonga and Kabali samples are based on α counting of 2 subsamples; for Kings Bore and Amity samples they are based on the average of α counts of 4 subsamples and XRF results of 2 subsamples.

† Calculated from separated zircons containing 200-220 $\mu\text{g g}^{-1}$ U.

‡ Measurements taken 40m from the original site which has been cleared for mining.

Table 3.4. Comparison of TL, inferred and isotope dates for samples.

Dune system	Site	Sampling depth (m)	Dose rate (Gy ka^{-1})	ED (Gy)	TL age (ka BP)	TL laboratory identifier	Inferred age† (ka BP)	Isotope age‡ (ka BP)
1	Kings Bore CA2S/1	1.2-1.4	1.53±0.10	29±2	19±2 (11±2)§	AdTL88014	0.5	-
4	Warrawonga CA7S/2	1.8-2.0	0.35±0.02	31±3	90±10	AdTL88015	~ 40	-
5	Amity SK11S/4	3.8-4.0	0.57±0.03	67±5	120±11	AdTL88016	120-135	119-132
6	Kabali CA9S/2	1.8-2.0	0.33±0.02	240±15	730±70	AdTL88017	>> 135	-
Samples not analysed ¶								
2	Chalambar	-	-	-	-	-	<<3.88	-
3	Burwilla	-	-	-	-	-	< 3.88	-
4	Seacliffs #	-	-	-	-	-	~ 40	-
5	Mundu ††	-	-	-	-	-	120-135	-

Note † Based on extrapolation of dates determined by radiocarbon and uranium series analysis of profiles of similar morphology from other geographic locations (Thompson, 1981; Thompson and Moore, 1984).

‡ Pickett *et al.* (1989).

§ See text.

¶ Samples included for complete comparison of soils from the Queensland region.

In the same soil landscape unit as Warrawonga (Thompson and Moore 1984).

†† Equivalent to Amity sample (Thompson, 1983).

the chain, whereas TSAC records all the alpha particles in the chain. The agreement among the differing methods of analysis indicates that radioactive disequilibrium is insignificant.

It should be noted that the γ -spectroscopy was carried out in the field some time after the collection of the original samples. The measurements were made at the same sites and at the same depth, except for Amity where the original site has been destroyed by mining. The data in the Table are for a similar site close by. They are for comparison purposes and are not actually used in age analysis.

The total U concentration of all samples was closely related to the zircon content of the samples (Table 3.3) as the U concentration in the separated zircon grains as measured by TSAC was uniform, ranging from 200-220 $\mu\text{g g}^{-1}$. This close agreement between U concentration calculated from zircons and that obtained by other methods indicates that all the U in these coastal sands is in the zircon grains and essentially none in the quartz. Th concentrations were not obtained because TSAC is not suitable for measuring Th in the presence of 200 $\mu\text{g g}^{-1}$ of U.

The K, U and Th analyses are used to find the annual dose rates, using the conversion factors of Bell (1979). Gamma-spectroscopy gives an independent, calibrated gamma dose rate directly (Prescott and Hutton, 1988). To these must be added a contribution from cosmic rays, which depends only slightly on depth (Prescott and Hutton, 1988), ranging from $0.18 \pm 0.02 \text{ Gy ka}^{-1}$ at Kings Bore to $0.14 \pm 0.02 \text{ Gy ka}^{-1}$ at Kabali. The heterogeneous distribution of U (and probably also of Th) will have a lowering effect on the calculated β dose rate received by the quartz. The magnitude of the effect has not been calculated but it is doubted if the resulting increase in age will be significant. All the analysis data in Table 3.3 are for dry samples. In the field the samples will be wet. As collected, the samples varied from 3-5 % H_2O . In calculating an annual dose, allowance must be made for water which attenuates the dose to the quartz. As indicated above, samples were collected from well drained sites. In calculating the dose rates a water content of 5 % was taken, as representing an average water content over the round of the seasons.

3.2.3.4. Age determination.

In Table 3.4 the TL data for all the samples are summarized. The ages are determined by dividing the ED by the annual environmental dose rate. The TL results show that the shallowest profile at Kings Bore is the youngest, followed by Warrawonga, Amity and Kabali, consistent with the geomorphological expectation. The TL ages are compared with other dating methods. As shown in Table 3.4, except for Kings Bore, the inferred ages based on the stratigraphic and geomorphic relationships and differences in degradation (Thompson, 1981; 1983), do not disagree with the TL ages obtained for the Cooloola samples. The TL age on the Amity dune is in good agreement with the radioisotope age (119-132 ka BP) on corals obtained by Pickett *et al.*, (1989) and inferred age. Climatic conditions and sea levels during this period of dune-building are discussed by Pickett *et al.* (1985) and he showed the dune-building was not associated with low sea levels or arid conditions. A similar interpretation might be advanced for the Warrawonga sample with a TL age of 90 ± 10 ka BP.

The TL age of 19 ± 2 ka BP for the Kings Bore sample is greatly at variance with the geomorphological evidence. The age of this C horizon sample is based on the time elapsed since the TL clock was reset, and is not consistent with the minimal development of the overlying soil horizons. Also, an absolute age of 19 ka BP for the sample from Kings Bore is markedly out of keeping with its geomorphic relationships, minimal evidence of water degradation and rudimentary podzol features. All of these suggest a very young dune probably less than 500 years old. Podzol development is in keeping with that recorded on young beach-ridge plains in New South Wales (Thompson and Bowman, 1984) and far less than in the parabolic dune at Triangle Cliff, Fraser Island (Ward and Grimes, 1987). This suggests that either the truncated roots of an older dune mantled by younger sands is involved (although there is no field evidence for this), or that the dune sands were not completely bleached or "zeroed" during aeolian redistribution. The latter situation could have arisen on a small dune, such as this, adjacent to the seacliffs during a high energy event under cloudy

conditions such as occur during some tropical cyclones. Under these conditions sands can be rapidly and successively stripped from the bare dune floor and deposited under vegetation along the trailing arms, which is where the sample came from. Also, this sample had by far the highest weight loss during pre-treatments due to water-sorbing grain coatings, perhaps these coatings had contributed to incomplete sunlight "zeroing" of the grains during aeolian transport and deposition (although laboratory bleaching showed no evidence of this). It is also possible that *in situ* bleaching does not reduce the TL as effectively as laboratory bleaching and that the TL intensity recorded for Kings Bore is close to the natural level for the material.

This possibility was checked by measurements on a sample from the Carlo blowout a few km north of Kings Bore, where a dune of similar parentage is currently mobile. Samples were taken from the advancing apex of the dune which is obviously mobile because it is encroaching on living vegetation. Samples CA20S/1 and CA20S/1.5 were taken from about the same depth as at Kings Bore. Their TL level was about 60 % of the natural level of Kings Bore, and could be further reduced by one half by exposure to sunlight. After bleaching, the Carlo and Kings Bore samples were indistinguishable both in their residual TL, in their response to radiation and in their glow curve shapes. A sample from the top mm of the dune surface (CA20S/00) was found to be fully bleached.

The time since last exposure to daylight at Carlo could scarcely exceed a decade. It follows that under present day conditions, sand is not completely reset while being transported. This effect has been noted before (Prescott, 1983) and discussed by Readhead (1988). If it is assumed that the level of bleaching at Carlo (effectively zero age) also represents the zero age at Kings Bore, at a comparable depth, then the age for that site is reduced to 11 ka. It is clear that either the C horizon material sampled at Kings Bore is considerably older than the apparent pedological/geomorphological age, or that there was insufficient exposure time for the TL to be reset before it was deposited where it is now.

If the same argument is applied to Warrawonga, Amity and Kabali, each of those ages should be reduced. However, because of the marked non-linearity in the dose response curves the effect is negligible for the latter two and within the stated uncertainty for Warrawonga.

The sample from Kabali provides the TL measurement probably representing the longest record of dune-building so far dated in Australia, and the TL age of 730 ± 70 ka BP is consistent with other evidence. Based on the field evidence indicating a very long period of water erosion, greater depths of weathering and profile development in the Australian context, it is reasonable to suggest that the deposition occurred during the Early Pleistocene period. The deep sea oxygen isotope record (Shackleton and Opdyke, 1976) shows a high $\delta^{18}\text{O}$ occurring shortly before the Matuyama-Brunhes magnetic reversal which is dated as ~ 700 ka BP. Thus at 730 ka BP there could have been conditions suitable for the Kabali coastal dune to be deposited. An *et al.* (1986) have shown that dune accumulation in parts of Australia spans 0-700 ka BP, and Idnurm and Cook (1980) using palaeomagnetic studies showed that sand dunes older than 700 ka occur in the south east of South Australia.

In considering the TL ages (Table 3.4) it is important to note that the calculated ages are based on samples from single points within a complex range of dune components. The dune apices, trailing arms and floors have modest differences in geomorphic, stratigraphic, erosional and pedologic histories (Thompson, 1983; Thompson and Moore, 1984).

A word needs to be added about the uncertainties assigned in Table 3.4. They are based on internal consistency of the data, and include an allowance for possible systematic errors in the calibration of the dose rates. The data are based on measurements under current conditions. For environments spanning such a large time-span, changes in moisture content, weathering, distribution and deposition of the radioactive minerals and cosmic rays all increase the uncertainty of the dates obtained by TL measurements, the more so for older deposits. The choice of 5 % for average water content represents a reasonable average for field condition in sand of this type.

The apparent age is increased about 0.5 % for each 1 % increase in water content. The data in Table 3.3 also show that the uranium is in zircon grains and since these are relatively very resistant to weathering, transport of U and Th in the profile by weathering would be minimal.

3.2.4. Conclusions

The TL dates are in the same chronological order as indicated by field relationships, and the individual TL, isotope and inferred ages give reasonable and agreeable comparison amongst them for the Amity sample, and probably for Warrawonga which is older than the 40 ka limit of radiocarbon. Nevertheless, the TL and inferred dates for the youngest sample are discrepant and fail to give a clear indication of the absolute age of the episodic period of dune-building and its podzolization. Given the large time span, the already low K content of the Kings Bore sample would be reduced further by weathering. However, the K contribution to the dose rate is small. The age of 730 ka for the Kabali sample is consistent with the inferred age and with coastal dune formation associated with a high $\delta^{18}\text{O}$ before about 700 ka BP. Palaeomagnetic studies might show an age greater than 700 ka BP. A more detailed study to include each of the the Dune Systems and perhaps more of the soils within them is now needed.

3.3. LeFevre Peninsula-Mount Compass sequence

3.3.1. Introduction.

The name LeFevre Peninsula - Mount Compass sequence is proposed for the profiles sampled from LeFevre Peninsula and Mt. Compass locations (Fig. 2.1, and Figs. 2.4 and 2.5). The site descriptions, soil properties and soil classification aspects of this sequence have been discussed in Chapter 2.

Geological and geomorphic investigations in relation to the history of sedimentation and to soil development in these areas have shown that the varied

landforms are related to a sequence of sea-level and climatic fluctuations which have given rise to stranded shorelines extending from modern sea-level up to a height of several hundred metres (Ward and Jessup, 1965; Ward 1966). The general area is within the Adelaide region, the geology and geomorphology of which is categorized under the orogenic belt of the Mt. Lofty ranges (Daily *et al.*, 1976; Twidale, 1976).

3.3.2. Inferred ages

At LeFevre Peninsula, which is within the Gulf St. Vincent basin, no detailed studies of the stranded beach ridges were undertaken prior to the work of Bowman and Harvey (1985, 1986) and Keller (1986). The bulk of the preliminary dating was reported for the Spencer Gulf region (e.g. Gostin *et al.*, 1981; Burne, 1982 and Hails *et al.*, 1983) which lies on the opposing side of the St. Vincent Gulf tectonic graben. From these studies it was established that the base strata of the degraded seacliffs supported rise in Quaternary sea level, and that the overlying sediments were of Holocene age. Gostin *et al.* (1987) concluded that the Quaternary sea level was no higher than about 3 m above local mean sea level, and that since about 5.0-6.0 ka BP, Holocene sea level has been within about 1 m of its present level and has reworked older sediments. Also von der Borch (1979) reported that in St. Vincent Gulf, during the maximum of the last glaciation (about 18 ka BP), the recorded sea level was well over one hundred metres below the present level. This led to a drying up of the Gulf and location of the coastline south of Kangaroo Island. Rapid flooding of the St. Vincent and Spencer Gulfs subsequently occurred as a result of sea level rise, to attain its present level nearly 7.5 ka BP. The present location of LeFevre Peninsula at that time was covered by about 8 m of seawater (Bowman and Harvey, 1986) with the shoreline positioned some kilometres to the east (Fig. 2.4).

At Mt. Compass the sedimentary events are not recorded in absolute terms. Whatever dates are suggested, are extrapolations from dates on similar sediments to the west (Ward 1966; Ward and Jessup, 1965) which were correlated with European interglacial high sea levels (Zeuner, 1959). According to Maud (1972), the sand dunes at

Mt. Compass are analogues to the Ngankipari Sand (Ward, 1966) which is of Holocene age (Table 3.5).

Table 3.5. Summary comparison of ages for samples from LeFevre Peninsula-Mount Compass and Canunda-Mount Burr sequences.

Location	Sample symbol	Inferred geologic age	Absolute ages (ka BP)		Climatic changes
			¹⁴ C	TL	
Le Fevre Peninsula	1 LP	-	0.5-1.0 (Bowman & Harvey, 1986)	6.0? (Keller, 1986)	Post marine transgression, marginally higher temp. and drier conditions.
	2LP	-	6.5-7.0 (Bowman & Harvey, 1986)	2.4? (Keller, 1986)	Post marine transgression, marginally higher temp. and rainfall.
Mount Compass	MC	Holocene (Flandrian transgression at 8ft. level) (Ward, 1966; Maud, 1972)	-	-	Post glacial marine transgression. Perhaps more humid but becoming dry, windy and stormy.
Canunda	CN	Holocene (Blackburn <i>et al.</i> , 1965; Blackburn 1966)	< 0.1-7.6 (Suzuki <i>et al.</i> , 1982)	-	Post glacial marine transgression, marginally warmer and becoming drier.
Mount Burr	MB	>> Holocene/ Pleistocene (Blackburn <i>et al.</i> , 1965; Blackburn 1966)	-	-	Late Pleistocene high sea levels, relatively more arid and hot.

During this time the sea level was approximately 2.5 m above present level. This period was shown (Ward and Jessup, 1965) to have been one of extensive dune formation.

3.3.3. Absolute radiocarbon ages

Detailed dating of Holocene sequences using radiocarbon techniques is available only for LeFevre Peninsula. Bowan and Harvey (1986) dated shell and seagrass materials and showed that sedimentation in this beach-ridge complex commenced at the end of the post-glacial marine transgression around 7.5 ka BP. The two soil samples, LeFevre Peninsula 1 and 2 represent the youngest (< 1 ka BP) and oldest (≥ 7 ka BP) units respectively (Table 3.5). These two samples lie within the complex which constitutes a post incisive chronosequence (Fig.3.7) similar to the chronosequence at Cooloola (Fig. 3.1).

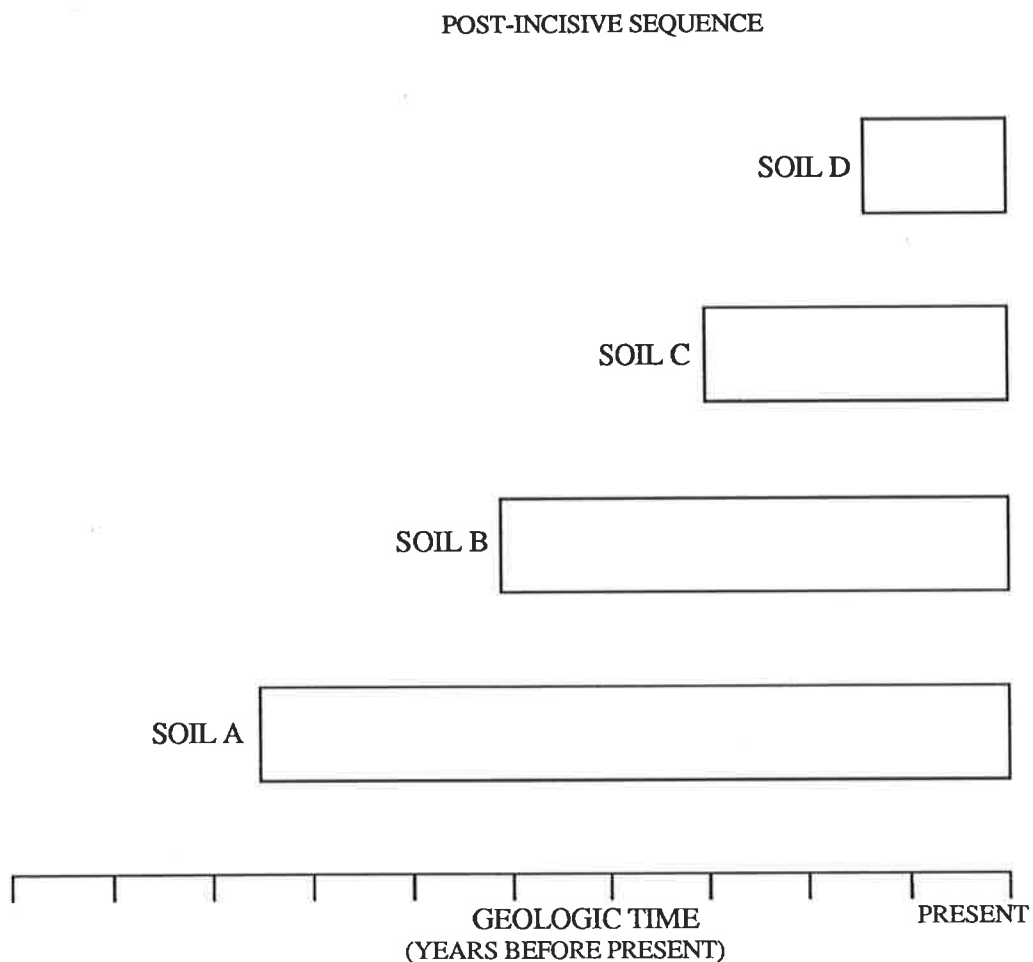


Fig. 3.7. Schematic time diagram for a post-incisive chronosequence. The bars represent time intervals of soil development (after Vreeken, 1975).

The age of ~7 ka BP corresponds to the period of northward progradation with the major influx of sediment between 7 and 5.5 ka BP. Subsequently there was a decrease in sediment supply which led to the contrast between the series of low ridges in the north and the single barrier further to the south. The sediment influx around the < 1 ka BP towards the south was comparatively very low. Bowman and Harvey (1986) also concluded that there was a major pulse of sediment following the last post-glacial marine transgression which was similar to that which occurred in many localities in eastern Australia, with the possibility that there were subsequent smaller sediment pulses.

3.3.4. Absolute thermoluminescence ages.

Keller (1986) attempted to apply TL dating techniques to the already dated sediments at LeFevre Peninsula (Bowman and Harvey 1985; 1986). The quartz inclusion method plus two additional techniques were adopted, and a study of TL characteristics was done by calibrating the TL dates against ^{14}C dates. The age comparisons were shown to be poorly correlated. The ^{14}C dates for the youngest and oldest samples were 0.61 ± 0.09 and 6.12 ± 0.27 ka BP respectively. The TL determined dates for these samples were 6.03 ± 0.76 and 0.39 ± 0.21 ka BP for the youngest and oldest ^{14}C dates respectively, i.e. the older sample was considered much younger and vice versa (Table 3.5). Keller (1986) attributed the lack of correlation between the two dates to a number of causes, including the possibility of impurities in the quartz samples. Keller concluded that the samples from LeFevre Peninsula may be too young for successful and accurate dating by the TL techniques used.

3.4. Canunda-Mount Burr sequence

The Canunda and Mt. Burr soils are grouped as an age sequence from the south east of South Australia. Soils from both locations form part of a broad coastal plain in which has been preserved a unique record of Quaternary geologic and climatic events.

Slow tectonic uplift, low coastal plain gradient and eustatic sea-level oscillations have combined to produce a series of subparallel depositional shorelines (Schwebel, 1984). The Canunda - Mount Burr sequence constitutes a beach-dune unit (Cook *et al.*, 1977) which has been maintained as apparent topographic ranges on what could have once been a flat coastal plain. The Mt. Burr profile may be regarded as an unconformity within the beach-dune unit, which has been stabilized and exposed to weathering for a longer period of time.

3.4.1. Inferred ages

Earlier work (e.g. Crocker and Cotton 1946; Hossfeld, 1950; Sprigg, 1952) suggested the correlation of stranded beach ridges with Pleistocene inter-glacial high sea levels such as those recognized by Zeuner (1959). Controversy surrounded the suggested age limit because of lack of agreement on the contribution from the effect of tectonism and glacial-eustatic sea-level changes to the development of the beach ridges and the fact that only one transect of the ridges (Robe to Naracoorte) was used in most previous correlation attempts. Later Blackburn *et al.* (1965) concluded that none of the ridges are known to be older than Pleistocene (Table 3.5) and that the influence of tectonic activity and glacial-eustatic sea level fluctuations contributed to the development of the ridge systems.

The bulk of absolute age determinations have been carried out on samples from the northwest (e.g. Robe and Woakwine, Salt Creek, Konetta) and south east (e.g. Mt. Gambier and Mt. Shank) of sites sampled for this study. Blackburn (1966) determined radiocarbon ages on marine shells from a range of soils in the Robe, Salt Creek, Konetta and Mount Gambier areas. The youngest material which was a calcareous shelly sand, that may be similar to the Canunda sands, was dated as 4.33 ± 0.1 ka BP. It can be estimated from this result that the Canunda sediments had been either (i) deposited since sea level peaked after the last transgression or (ii) resulted from crustal movement which did not involve tilting parallel to the beach ridges. Much older samples of siliceous sands, Rendzina and Terra Rosa soils gave radiocarbon ages of

approximately 25 - > 45 ka BP (Blackburn, 1966) in which range radiocarbon dating is critical (Radtke, 1988). In terms of soil development the Mt. Burr podzol is well developed compared with the podzol at Salt Creek dated as 30.6 ± 0.45 ka BP (Blackburn, 1966). Therefore, the Mt. Burr podzol has an age range that may be greater than 30 ka BP. According to Blackburn (1966) differences in elevations between these soils could be due to either (i) the apparent down-tilting of the region over distance or (ii) Pleistocene high sea levels.

The TL dates obtained for samples from Mt. Schank yielded an average age of 4.9 ± 0.5 ka BP which corresponds with the volcanic eruption, that was consistent with palaeomagnetic measurements (Smith and Prescott, 1987). However, the history of the volcanism in the area is much complex. This is exemplified by the occurrence of aeolian sands in the Mt. Burr range and Mt. Schank where the volcanic ash underlies and overlies the aeolian sands respectively. Stephens *et al.* (1941) reported that the volcanic activity in the Mt. Burr region occurred before the final uplift and the aeolian sands were deposited during the eustatic sea level changes associated with the various ice ages. In summary the TL date confirms that the volcanic ash deposit at Mt. Schank is recent (Holocene), and has buried the original soils (e.g. Mt. Burr sand equivalents) which are much older.

To the north and northwest (between Naracoorte and Robe) of the study areas, Cook *et al.* (1977) concluded that the entire sequence of dunal-interdunal sediments was deposited during the Pleistocene (during the last 690 ka BP). Furthermore, they reported that during this period there were at least 20 high sea-level stands in the region. The age of 690 ka BP represent limestone deposits in the Naracoorte ranges which are about 100 km inland. Closer to the coast Schwebel (1983) gave age estimates of 4.3 ± 0.1 ka BP (from Blackburn, 1966) for Robe beach-dune unit, and between 100-125 ka BP for the Woakwine barrier deposits (slightly inland). The ages of 100-125 ka BP suggest a last inter-glacial age. The stratigraphic relationship between Woakwine barriers and the soil profile at Mt. Burr is marked by several

unconformities of different ages. Nevertheless, it can be contended that the Mt. Burr profile is of Pleistocene age (i.e. much younger than 690 ka BP).

3.4.2. Absolute radiocarbon ages.

^{14}C data acquired through the study of land snails and charcoal (Suzuki *et al.*, 1982) from the active dune sands at Canunda, near Millicent gave ages that ranged from 7.6 to 2.0 ka BP for the Bb (Do) and Ab (Ho) horizons. From this study it was confirmed that the dunes in this region were active between 4.0 and 3.0 ka BP. At Canunda the A1 (PD) horizon gave ^{14}C dates of 0.1 ± 0.07 ka BP (Suzuki *et al.*, 1982). ^{14}C age of charcoal from buried B horizons (DO IV and DO V), that were not sampled for this study, above the Bb1, gave a date of 3.0 ± 0.015 ka BP (Suzuki *et al.*, 1982). This could mean that the underlying Ab1 horizon and all subsequent buried horizons are older than 3 ka BP at Canunda. During most of this period, the climate was slightly warmer in the southern Australian region, which led to reduction in lake levels with minor reversion to more arid conditions (Bowler *et al.*, 1976).

3.5. Summary

All the soils sampled were formed during the Quaternary period. This period was marked by the accumulation of a complex succession of sedimentary deposits in the south east coastal regions of Queensland and South Australia, and the central coastal region of South Australia.

At Cooloola and North Stradbroke Island the TL, isotope and inferred ages are in the same chronological order as indicated by field relationships (increasing profile development with age, Fig. 3.1). In this region the dune building process was not associated with low sea levels or arid conditions, but was attributed to periods of wind-blown activities from the coast.

The combined effects of predominantly climatic and eustatic sea-level changes, and to some extent tectonic activity led to the accumulation of the sediments (e.g.

LeFevre Peninsula), which were later redistributed by aeolian activity in (i) areas further inland from the coast (Mt. Compass and Mt. Burr) and (ii) locally active coastal dunes (present drift) at Canunda. The aeolian activity in the different stages of deposition were attributed to relatively increasing aridity.

Bird (1976) discussed the controversial issue of Holocene sea-level changes, tracing the picture from about 20 ka BP (Flandrian transgression in Europe). A summary diagram (Fig. 3.8) outlines the main views held on the question of Holocene sea level changes. There is a general consensus on rapid marine transgression between 17 ka BP and 7 ka BP, but different views on changes since the last 7 ka BP. One school of thought considers a stillstand sea level to the present since between 3 and 5 ka BP (dashed line in Fig. 3.8). The alternate consideration is that there have been sea-level rises during the past 6 ka with oscillating stillstands above the present level (solid line in Fig. 3.8). As conceded by Bird (1976) much more detailed work is needed to resolve this contention.

The total period involved spans from about 0.1 ka BP for the presently drifting sand at Canunda to Pleistocene at Mt. Compass and Mt. Burr. A comparative summary of the ages for the different soils and the climatic changes associated with the different periods is given in Table 3.5.

From the above summary section, it is clear that the contemporary climatic conditions in these regions are not necessarily likely to represent the conditions prevailing during the long period of formation of many of the soils, particularly the older samples. Some of the soils (e.g. Amity, Kabali, Mt. Compass and Mt. Burr), perhaps represent the effects of long periods of weathering and soil formation, while others (e.g. Carlo, Kings Bore, LeFevre Peninsula 1 and Canunda) represent a relatively shorter period of soil formation. These younger soils can be regarded as influenced by climatic conditions similar to those of the present period. For the older soils the effects of minor climatic variations may be much less than the effects of prolonged weathering and soil formation. Thus some weathering effects on the heavy minerals in these soils may be attributable to conditions different from the present.

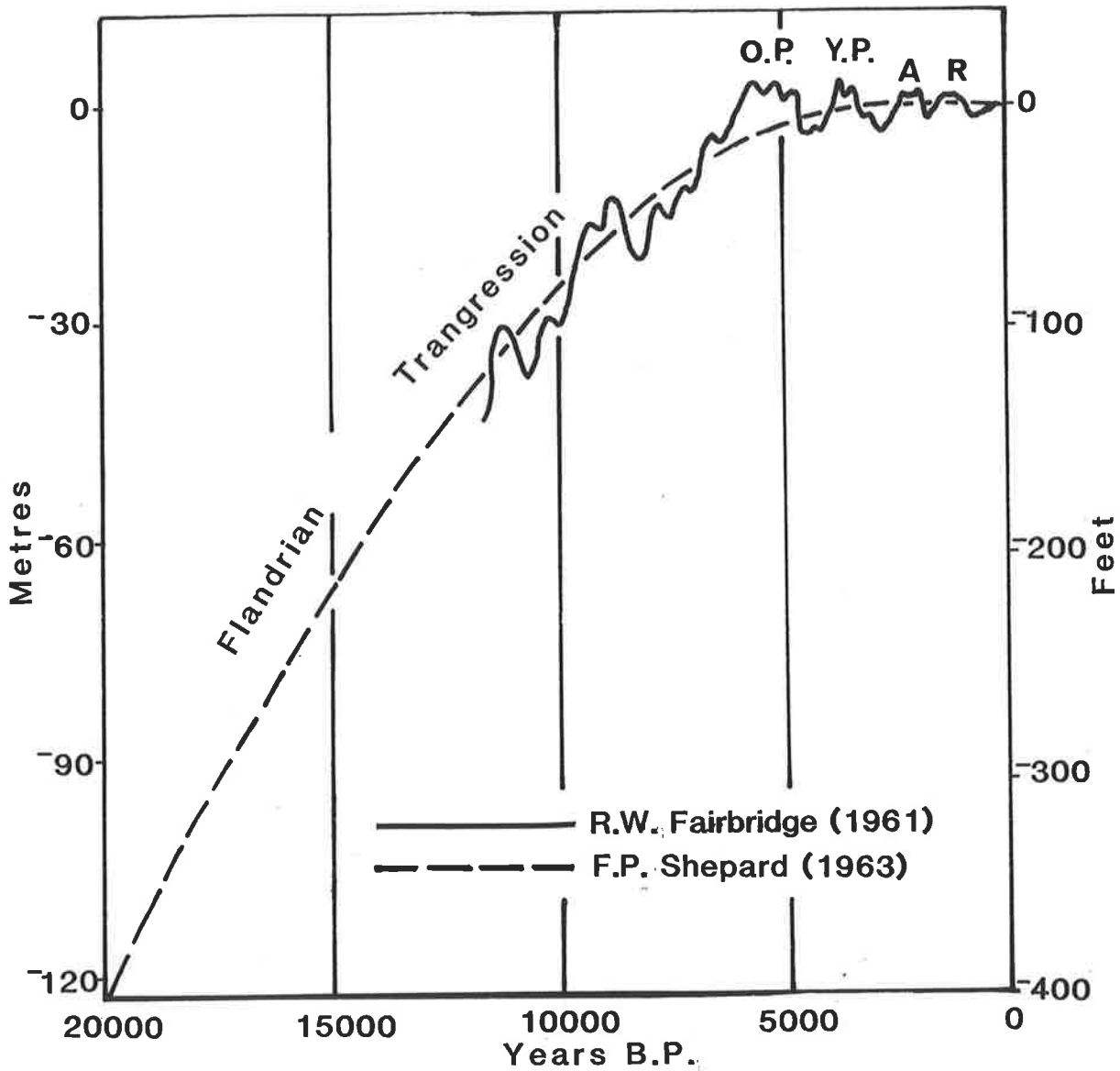


Fig. 3.8. The Holocene marine transgression. Alternative interpretations of sea level changes during the past 6000 years are indicated. Fairbridge considers that the sea rose to higher levels (O.P. = Older Peron, Y.P. = Younger Peron, A = Abroihos, and R = Rottnest stages); Shepard thinks it attained present level without exceeding it during Recent times (after Bird, 1976).

CHAPTER 4

MICROMORPHOLOGY

4.1. Introduction

In mineral weathering studies, characterization of parent material is a prerequisite for distinguishing pedogenic features from inherited ones. This is particularly important in soil derived from transported sediments. Thin section studies provide useful clues on micro-morphological properties which can be attributed to soil development and/or inheritance prior to transportation and deposition (Brewer and Sleeman, 1960; Churchward, 1963; Sleeman, 1964). Sleeman (1964), for example, studied the characteristics and variations of the structure and fabric of two Red-brown earth profiles from which he suggested that the presence of certain grain cutans, papules, soil nodules and voids interpreted as inherited features from the parent sediment were different from other forms of these features which were interpreted as due to soil forming processes. In this, and most similar studies, the interpretations were tentative, owing to lack of precise information on the processes involved; as some processes leave virtually no trace of their operation within the profile or different processes leave a similar trace.

Brewer (1972) reported on the complications of using micromorphological data in interpretations of soil processes, and suggested two distinct levels at which interpretations could be attempted. The first level involves interpretation based on generalized processes, such as concentration of specific constituents, illuviation of clay-sized material, etc. At the second level of interpretation, mechanisms responsible for these generalized processes of concentration, illuviation, etc are explained in terms of specific chemical and physical conditions. Pedogenetic processes are better explained when micromorphological data are integrated with other physical, chemical, biological and mineralogical data. Apart from the work of (Brewer and Thompson,

1980; Farmer *et al.*, 1983) there is little published work on the micromorphology of the podzols at Cooloola and none on either North Stradbroke Island or the other profiles in regions from South Australia. Recently, more detailed micromorphological, chemical and mineralogical analysis have been used to explain the processes of podzolization in a podzol from Jervis Bay (Farmer, 1987; Milnes and Farmer, 1987).

In the light of the paucity of any detailed micromorphological data on the soils used in this study, the objectives of this chapter are (i) to present micromorphological data on selected horizons for selected soil profiles to account for the generalized processes of soil formation and (ii) to demonstrate differences between horizons within profiles and more particularly between similar horizons from different sites or location. The usefulness of the observed micromorphological properties, of the different soils examined, in relation to heavy mineral weathering studies is considered in later chapters.

4.2. Materials and methods

4.2.1. Soils.

Selected soil samples from profiles already discussed in Chapter 2 were sampled for thin section preparation. See section below on detailed descriptions for the soils studied.

4.2.2. Sampling.

Large undisturbed soil blocks were taken using a tin (15.5 x 9.5 x 5 cm) from selected soil profiles as near as practicable to the sites sampled for the physical, chemical and mineralogical analysis and where field descriptions were carried out. Samples were collected using methods described by FitzPatrick (1984) for soft coherent non-stony and hard materials, using cotton wool as a packing material.

4.2.3. Impregnation.

Sample impregnation was carried out using the following mixture: 3:1 parts of polyester resin (Escon 4527) and methyl methacrylate monomer, Cumene hydroperoxide as a catalyst at the rate of 0.4 g per 100 g of polyester mixture and a drop of promoter per 100 g of polyester mixture. Samples were impregnated in a vacuum chamber at a pressure of about 30 mm Hg for approximately three hours, after which they were placed in a fume cupboard to cure for three weeks.

4.2.4. Sawing, mounting and lapping.

The large soil blocks were cut horizontally into size 4 x 6 cm using a diamond saw. One side of each block was ground flat on a surface grinder (Struers Discoplan - TS) to within approximately 5 μm variation and finished by hand grinding on a ribbed glass plate with 600 grit silicon carbide powder. Kerosine was used as a lubricant in both sawing and grinding procedures.

The ground face of each block was cleaned of any grinding residue and rinsed in Freon (carbon tetrafluoride). The blocks were fixed onto slides using 4:1 parts of an epoxy resin (araldite M and LC 234) and fixed into position (approximately 20 hours) using a spring-loaded press.

The mounted blocks were sawed to a thickness of approximately 1 mm using a 25 mm diamond saw and ground on a surface grinder until about 40-50 μm thick. The sections were reduced to a thickness of approximately 30 μm by hand grinding on a ribbed glass plate, using 600 grit silicon carbide paste. Final polishing of the sections was done using a Kent 3 automatic lapping and polishing machine.

4.2.5. Descriptive methods and terminology.

The method of description and terminologies used in this chapter closely follows those of Stoops and Jongerius (1975), Bullock *et al.* (1985) and Murphy *et al.* (1985). An illustration from Murphy *et al.* (1985) of the coarse to fine components is given in Fig. 4.1. Based on these types of coarse to fine arrangements, a comparison







FORM	SIMPLE DESCRIPTION	REMARKS
	UNCOATED GRAIN	<ul style="list-style-type: none"> - single grains may be silt, sand or gravel. - are further described using sorting, packing criteria.
	INTERGRAIN MICROAGGREGATE	<ul style="list-style-type: none"> - microaggregate may be organic, clay or silty clay.
	COATED GRAIN	<ul style="list-style-type: none"> - coats may be organic, clay or silty clay. - may be fully coated or partially coated.
	BRIDGED GRAIN	<ul style="list-style-type: none"> - all grains are coated and most are linked by bridges.
	BRIDGED AND COATED	<ul style="list-style-type: none"> - coated grains are occasionally linked by bridges.
	EMBEDDED GRAIN	<ul style="list-style-type: none"> - is 'single spaced' when grains are touching, or nearly so, and 'double spaced, etc.' when grains are further apart. - embedded medium may be 'porous' or 'dense.'

Fig. 4.1. The simple arrangements of coarse to fine components observed in soil thin sections (after Murphy *et al.*, 1985).

of related distribution patterns in soils is given in Table 4.1 using different terminologies developed by different researchers.

4.3. Results

In Table 4.2 a summary comparison is given of selected field macromorphological and micromorphological data for all the horizons examined. The field consistence of the different samples was well correlated with the related distribution pattern. As the field consistence became stronger the amount and arrangement of the fine material between the skeletal grains increased in degree.

In the section below the micromorphological organisation of soil constituents is described and possible interpretations of observed features are given.

4.3.1. Micromorphology of the Cooloola-North Stradbroke Island sequence.

Kingsbore, B2hs2/B3, 58-75 cm.

Microstructure

Apedal soil material, without clods or fragments, having a predominantly single grain microstructure. Dominantly simple packing voids, with a wide size range (80-500 μm long). The voids have smooth walls, with subangular and subrounded faces. Estimated total void space is 40 %. The voids are unoriented and have a random basic distribution pattern.

Basic mineral components

c/f limit at 10 μm , c/f ratio of 99:1

Coarse fraction: mainly single grains, size range between 50-350 μm in diameter, randomly distributed. Composition: single grains-dominantly quartz (~ 98 %) and some heavy minerals (rutile, zircon and opaques) (Plate 4.1). Perfectly sorted material; shapes are equant to elongate, predominantly subangular and subrounded grains. Most mineral grains are fresh to slightly altered.

Table 4.1. Classifications of related distribution patterns of soils[†] (modified from Murphy *et al.*, 1985).

Type	Stoops and Jongerijs (1975) [‡] :	Kubiens (1938):	Brewer (1964/1976):	Eswaran and Banos (1976):	Brewer (1979):
	c/f related distribution	Elementary fabric	Plasma-skeleton grains related distribution	Normal or specific related distribution	Plasma and framework members related distribution
Uncoated single grain	monic [§]	bleached sand	granular	granic	orthogranic
Intergrain microaggregate	enaulic	agglomeratic	agglomeroplastic [¶]	congelic	mullgranic (in part) matigranic (in part)
Coated grain	chitonic	chlamydomorphic	granular or intertextic ^{¶,#}	dermatic	chlamydic
Bridged grain	gefuric	intertextic magmoidic	intertextic [¶]	intertextic	iuntic
Bridge and coated grain	chitonic-gefuric	plectoamictic		intertextic-dermatic	plectic
Embedded grain	porphyric	porphyropectic porphyropeptic	porphyroskelic	porphyric	porphyric

[†] Comparisons can only be made if components are basic units.

[‡] System used in this description.

[§] Can also be pure clay.

[¶] When this coating is considered to be a pedological feature, these related distributions should be described as granular (Brewer, 1964).

[#] Usually some coated grains are touching.

Table 4.2. Comparison of selected soil and micromorphological data for the different sections.

Region	Profile	Horizon	Depth (cm)	Texture†	Structure†	Consistence†	Boundary†	RDP‡	b-fabric	Other features
South east Queensland	Kings Bore	Bhs2	58-65	s	0sg	mvfr	cs	monic	undifferentiated	rare fragments of root tissue
		B3	65-75	s	0sg	mvfr		monic	undifferentiated	very thin grain coatings
	Chalambar	Al	30-40	s	0sg	mvfr	dw	monic, minor gefuric	undifferentiated	rare fragments of plant tissues (charcoal?) coatings, organic infillings
		E	40-50	s	0sg	ml		monic, minor chitonic	undifferentiated	organo-mineral coatings
		Bhs2	90-105	s	0sg	mvfr	-	chitonic	undifferentiated	rare highly altered plant fragments, coatings, organic-mineral infillings
	Seacliffs	E	270-278	s	0sg	ml	di	monic	undifferentiated	very rare fine fraction
		B1	278-285	s	0sg	ml		monic	undifferentiated	
	Amity	E	420-428	s	0sg	ml	di	monic	undifferentiated	rare fragments of highly altered plant tissues, very rare coatings
		B1	428-435	s	0sg	ml		monic	undifferentiated	
		E§	650-665	s	0sg	ml	ci	monic	undifferentiated	very rare coatings
		Bhs2	650-665	s	0sg	mfr		gefuric to minor enaulic	undifferentiated	patchy grain coatings, loose continuous infillings
		Bhs2	670-685	s	0sg	mfi	-	enaulic	undifferentiated	abundant crypto-crystalline and amorphous loose continuous infillings
	Bhs2	750-765	s	0sg	mfr	dw	chitonic	undifferentiated	highly fragmented organic rich coatings	

Table 4.2 contd.

Region	Profile	Horizon	Depth (cm)	Texture†	Structure†	Consistence†	Boundary†	RDP‡	b-fabric	Other features
South east Queensland	Amity	Bs2	750-765	s	Osg	mfr		chitonic	undifferentiated	thin sesquioxidic rich coatings
		B3	1500-1515	s	Osg	mfr	-	monic, minor chitonic	undifferentiated	few amorphous impregnative monomorphic coatings
Central South Aust- ralian coast.	LeFevre Peninsula	A2	90-110	s	Osg	ml	-	monic, minor enaulic	undifferentiated	abundant coarse plant and shell fragments, organic fine fragments, very few faunal excrements ?
		Mount Compass	E§	90-98	s	Osg	ml	aw	monic	undifferentiated
		B1	98-105	s	Osg	mfr		chitonic-gefuric	undifferentiated	rare dense complete & incomplete infillings, nodules
		E	95-115	s	Osg	ml	aw	monic	undifferentiated	rare, thin grain coatings
		B1	95-115	s	Osg	mfr		chitonic	undifferentiated	very few nodules
		Bhsb2	95-115	s	Osg	mfr	gw	monic-gefuric	undifferentiated	thin, irregular, patchy coatings
		Bhsb2	120-128	s	Osg	mfr	di	chitonic-gefuric	undifferentiated	rare plant tissues
		Bhsb3	128-135	s	Osg	mfr		complex chitonic-gefuric-porphyric	undifferentiated, stipple speckled & crescent striated	nodules and dense complete infillings
	Bhsb3	140-150	s,g	Osg	mfr	ds	chitonic, minor porphyric	complex combination of undifferentiated, stipple speckled and striated fabric	few nodules, dense complete infillings	

Table 4.2 contd.

Region	Profile	Horizon	Depth (cm)	Texture†	Structure†	Consistence†	Boundary†	RDP‡	b-fabric	Other features
Central South Australian coast	Mount Compass	Bsb3	165-175	ls	Osg	mvfr	ds	monic-chitonic, minor prophyric	combination of undifferentiated, stipple speckled and striated fabrics	laminated dense complete infillings, dense incomplete infillings
		Bb4	180-200	s	Osg	mvfr	ds	chitonic	combination of undifferentiated, stipple speckled and striated fabrics	dense incomplete amorphous infillings
South east South Australian coast	Canunda	Bb1	160-168	s	Osg	ml	as	monic-gefuric	undifferentiated	porous microaggregates of organic rich excrements as coatings, some organic pigmentation.
		Ab2	168-176	s	Osg	mvfr		monic-gefuric	undifferentiated, very locally crystallitic	
		Ab2	192-200	s	Osg	mvfr	as	monic	undifferentiated locally crystallitic	rare, highly altered excrements, some organic pigmentation
		Bb2	200-208	s	Osg	ml		monic	undifferentiated locally crystallitic	minor microcrystalline carbonate aggregates
		Bb3	310-326	s	Osg	ml	as	monic	undifferentiated locally crystallitic	rare, highly altered excrements, minor infillings of microcrystalline carbonate rich material, some organic pigmentation
	Mount Burr	E§	220-235	s	Osg	ml	aw	monic	undifferentiated	highly decomposed plant tissues
		Bhs2	220-235	s	Osg	mfr		chitonic-gefuric	undifferentiated, rare stipple speckled	few ferruginous nodules

Table 4.2 contd.

Region	Profile	Horizon	Depth (cm)	Texture†	Structure†	Consistence†	Boundary†	RDP‡	b-fabric	Other features
South east South Aust- ralian coast	Mount Burr	Bs2	230-245	s	0sg	mfr	di	chitonic- gefuric	undifferentiated stipple speckled minor crescent striated	occasional dense complete and incomplete infilling of organo-mineral material

† Abbreviations are those assigned to texture, structure, consistence and boundary in Soil Survey Staff Manual (1951), where s = sand; 0 = structureless; sg = single grain; ml = loose; mvfr = very friable; mfr = friable; a = abrupt; c = clear; g = gradual; d = diffuse; s = smooth; w = wavy; i = irregular.

‡ Related distribution pattern.

§ Material associated with a pipe.

Fine fraction: rare organo-mineral material, with a mixture of reddish brown, yellowish brown and black components; containing optically isotropic poorly crystalline sesquioxidic and organic materials; moderately impregnated; speckled appearance; some fine material present as pale brownish pigment on grains.

Basic organic components

c/f limit at 10 μm .

Coarse fraction: fragments of plant tissues, up to 5 mm long (Plate 4.2); weakly to moderately altered; small fragments ($\sim 250 \mu\text{m}$ in diameter) of black and reddish brown cell structures; rare.

Groundmass

The c/f related distribution is monic. The micromass has an undifferentiated b-fabric.

Pedofeatures

Textural: clay and silt size coatings in the form of cappings and pendants; non-laminated; irregular and elongate; low variability; unoriented, randomly distributed; 5-20 μm thick; shades of yellow and brown with black patches; rare.

Chalambar, A1/E, 30-50 cm.

Microstructure

Similar to Kings Bore Bhs2/B3 horizon, but with predominantly single grain (95 %) and intergrain micro-aggregate (5 %) microstructure. Very dominantly simple packing voids (95 %) and few complex packing voids (5 %), with a wide size range between 100-400 μm long. The larger and smaller voids have smooth and undulating walls respectively, with irregular faces.

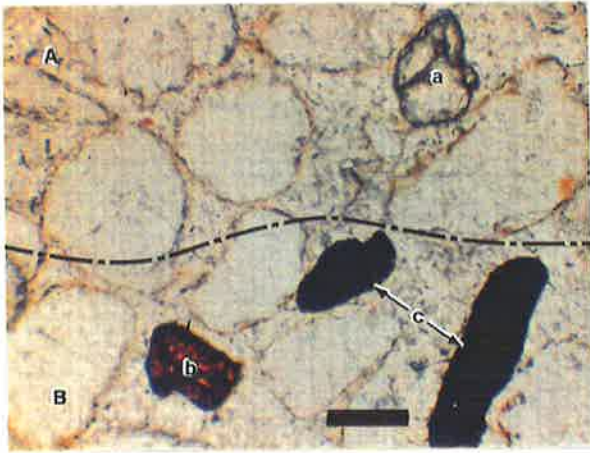
Basic mineral components

c/f limit at 10 μm , c/f ratio of 98:2

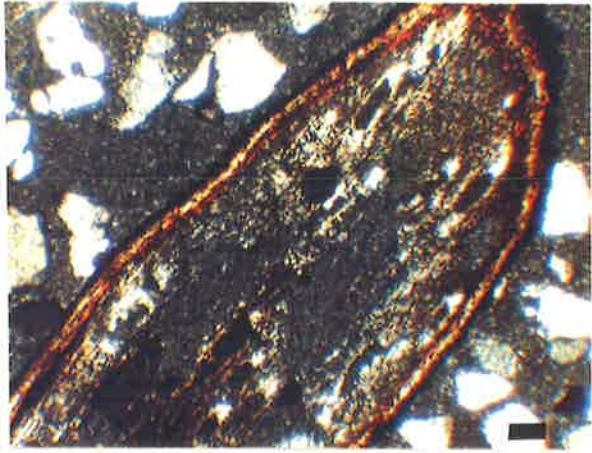
Coarse fraction: same as for Kings Bore Bhs2/B3 horizon (Plate 4.3).

Fine fraction: Similar to Kings Bore Bhs2/B3 horizon, but slightly more in frequency and abundance.

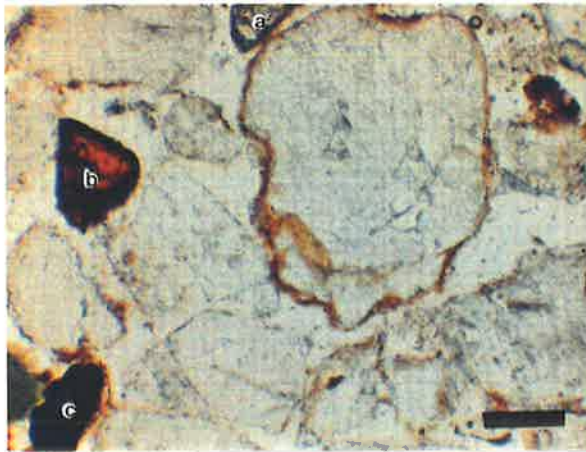
- Plate 4.1. Photomicrograph showing single grain structure in section from Bhs2 (A)/B3 (B) horizon of Kings Bore. Quartz and heavy mineral grains (a = zircon, b = rutile, c = ilmenite) loosely arranged with little or no fine material around grains. *PPL*. Bar scale 100 μm .
- Plate 4.2. Photomicrograph of monic related distribution pattern in section from Bhs2/B3 horizon of Kings Bore with a large fragment of weakly to moderately altered plant tissue. *PPL*. Bar scale 100 μm .
- Plate 4.3. Photomicrograph of monic related distribution pattern in section from A1/E horizon of Chalambar. Locally a tendency to chitonic with quartz and heavy mineral grains (a = zircon, b = rutile, c = ilmenite) partly or wholly surrounded by dark yellow brown fine material. *PPL*. Bar scale 100 μm .
- Plate 4.4. Photomicrograph of monic related distribution pattern in section from A1/E horizon of Chalambar. Note, highly altered plant fragments and moderately coalesced excrements. *PPL*. Bar scale 100 μm .
- Plate 4.5. Photomicrograph of chitonic related distribution pattern in section from Bhs2 horizon of Chalambar. Coarse quartz grain wholly or partly coated with dark yellowish brown fine material. *PPL*. Bar scale 100 μm .
- Plate 4.6. Photomicrograph of dense incomplete and loose infillings in the Bhs2 horizon of Chalambar. Dense strongly coalesced excrements (arrow) masked by organic rich fine material. *XPL*. Bar scale 100 μm .



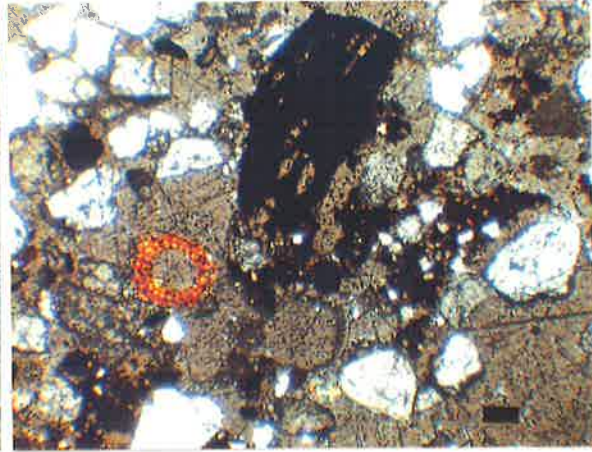
4.1.



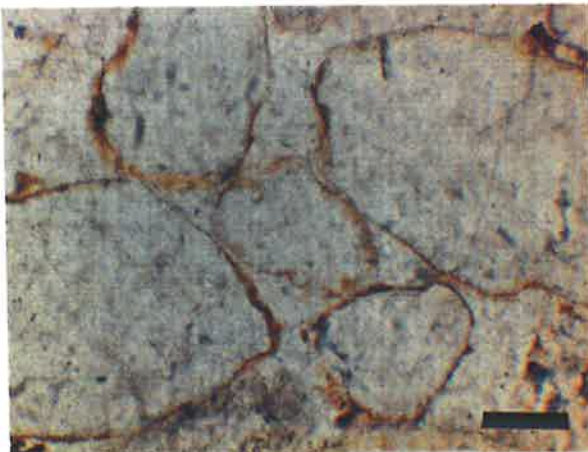
4.2.



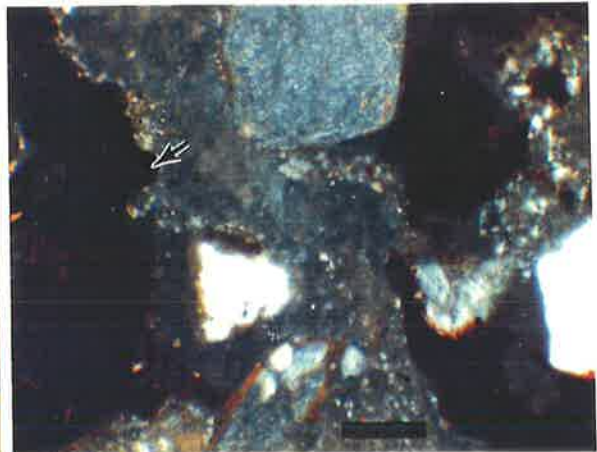
4.3.



4.4.



4.5.



4.6.

Basic organic components

c/f limit at 10 μm

Coarse fraction: plant residues mainly as root tissues, ranging from 0.4 mm to 2 mm in length (Plate 4.4); mostly highly altered, showing dark brown to black cell walls and cell contents, some clear voids; largely isotropic with some birefringence; irregular black fragments (charcoal ?), up to 500 μm long are rarely seen.

Fine fraction: dark brown to black, occurring in patches, isotropic, rough walled with irregular patchy internal fabric (Plate 4.4).

Groundmass:

The c/f related distribution is monic, with very minor gefuric-chitonic. The b-fabric is undifferentiated.

Pedofeatures

Textural: clay and silt size coatings same as for Kings Bore Bhs2/B3 horizon, thicker (Plate 4.3).

Amorphous: few impregnative, loose continuous and discontinuous infillings in voids (Plate 4.4).

Excrement: frequent excrements, with a variety of shapes (mainly ellipsoids and spheres), sizes up to 500 μm thick (thin meso medium); smooth to rough walls; organic; dark brown to black; random basic distribution pattern; moderately coalesced, dense microaggregates.

Chalambar, Bhs2, 90-105 cm.*Microstructure*

Similar to Kings Bore Bhs2/B3 horizon, but with a mixture of single grain (60 %) and pellicular (40 %) microstructure. Void size range between 100-300 μm long. Voids have smooth walls with irregular, elongate and rounded faces. Estimated total void space is 35 %.

Basic mineral components

c/f limit at 10 μm , c/f ratio of 97:3

Coarse fraction: same as for Kings Bore Bhs2/B3 horizon.

Fine fraction: similar to Chalambar A1/E horizon but slightly more in abundance and frequency (few) (Plate 4.5).

Basic organic components

c/f limit at 10 μm

Coarse fraction: rare tissue fragments, ranging from 300-700 μm in length, mainly highly altered, showing dark brown to black cell walls and cell contents, some clear voids, largely isotropic, some black fragments (charcoal ?) up to 300 μm long were observed.

Groundmass

The c/f related distribution is chitonic (Plate 4.5). The b-fabric is undifferentiated.

Pedofeatures

Textural: similar to Chalambar A1/E horizon; 5-30 μm thick; yellowish brown to dark brown in colour; occasional (Plate 4.5).

Amorphous and Cryptocrystalline: very few impregnative dense incomplete and loose infillings in voids (Plate 4.6), up to 800 μm in length; with various shades of brown with darker colours; irregular and subrounded; clear external boundaries; distinct contrast; low variability; randomly distributed; moderately to strongly impregnated; complete pseudomorphosis.

Excrement: frequent excrements, spherical shape, sizes up to 50 μm wide (very thin), mainly smooth walls, organic, dark brown to black, randomly distributed, strongly coalesced, dense.

Seacliffs, E/B1, 270-285 cm.

Microstructure

Similar to Kings Bore Bhs2/B3 horizon, with void size between 80-200 μm long, smooth to slightly undulating walls, with irregular, elongate and subrounded faces.

Basic mineral components

c/f limit at 10 µm, c/f ratio of 100:0

Coarse fraction: same as for Kings Bore Bhs2/B3 horizon (Plate 4.7), with grain exhibiting higher degree of alteration (irregular linear and dotted patterns).

Fine fraction: none

Basic organic components

c/f limit at 10 µm

Coarse fraction: none

Fine fraction: none

Groundmass

The c/f related distribution is monic. The b-fabric is undifferentiated.

Pedofeatures : none

Amity, E/B1, 420-435 cm.*Microstructure*

Similar to Kings Bore Bhs2/B3 horizon with void size range between 100-500 µm long, smooth to undulating walls, irregular, mainly elongate but sometimes equant in shape.

Basic mineral components

c/f limit at 10 µm, c/f ratio of >99:<1

Coarse fraction: similar to Kings Bore Bhs/B3 horizon but with notable alteration patterns (irregular linear) on mineral grains (Plate 4.8).

Fine fraction: same as for Kings Bore Bhs/B3 horizon.

Basic organic components

Coarse fraction: rare fragments of slightly to moderately altered root tissues, sizes up to 9 mm long, with outer yellowish red and inner red cell contents, cell walls are black, voids are clear.

Fine fraction: rare dark brown to black organic pigments in patchy pedofeatures.

Groundmass

The c/f related distribution is monic. The b-fabric is undifferentiated.

Pedofeatures

Textural: same as for Kings Bore Bhs2/B3 horizon (Plate 4.8).

Amity, E(pipe)/Bhs2, 650-665 cm.1) *Microstructure*

Apedal soil material without clods or fragments with single grain (50 %), pellicular (30 %) and intergrain micro-aggregate (20 %) microstructure. Very dominantly simple packing voids (90 %) and complex packing voids (10 %) with a wide size range (40-300 μm long), smooth to rough walls, irregular, mainly elongate but equant in shape. Estimated total void space is 20 %. The voids are unoriented and randomly distributed.

Basic mineral components

c/f limit at 10 μm , c/f ratio of 98:2

Coarse fraction: same as for Kings Bore Bhs2/B3 horizon.

Fine fraction: very few yellowish brown to dark brown fine material, mainly of dusty clay texture, containing optically isotropic, poorly crystalline sesquioxidic material; moderately to strongly impregnated; speckled to cloudy aspect.

Basic organic components

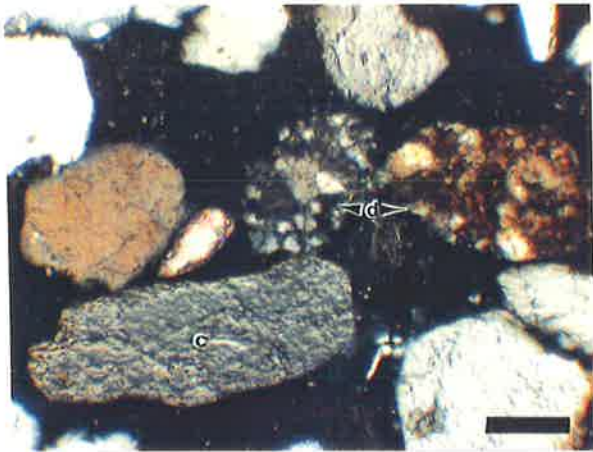
Coarse fraction: none

Fine fraction: very few dark brown to black amorphous fine material, mainly as patchy grain coatings, minor pigments, with undulating to rough walls.

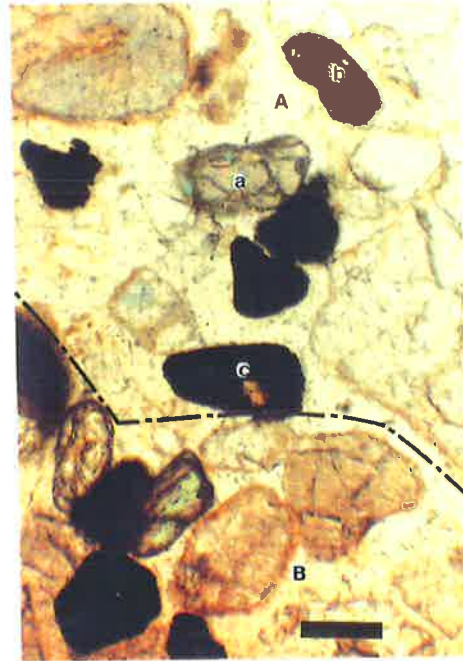
Groundmass

The c/f related distribution is monic-gefuric to minor enaulic (Bhs2 portion, Plate 4.9). The b-fabric is undifferentiated.

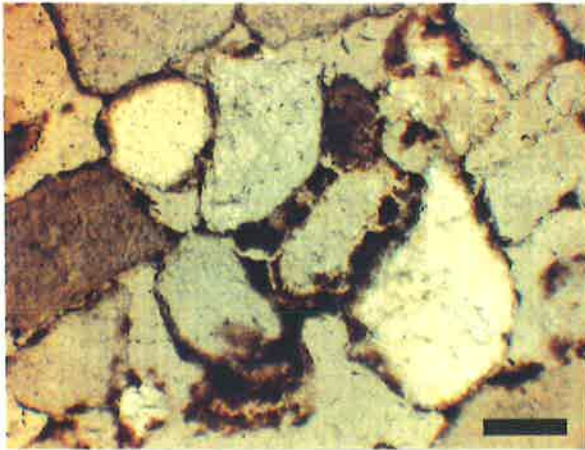
- Plate 4.7. Photomicrograph of monic related distribution pattern in section from E/B1 horizon of Seacliffs. Mineral grains show high degree of alteration (c = irregular linear, d = dotted) patterns. *XPL*. Bar scale 100 μm .
- Plate 4.8. Photomicrograph of monic related distribution pattern in section from E/B1 horizon of Amity. In section A = E horizon and B = B1 horizon. Quartz and heavy mineral (e.g. a = zircon, b = rutile, c = ilmenite with rutile inclusion) grains show irregular linear alteration patterns. *XPL*. Bar scale 100 μm .
- Plate 4.9. Photomicrograph of gefuric related distribution in section from Bhs2 portion of E(pipe)/Bhs2 horizon of Amity. The bridging fine material comprises mainly opaque organic components. *XPL*. Bar scale 100 μm .
- Plate 4.10. Photomicrograph of a combination of monic, gefuric and enaulic related distribution in section from E(pipe)/Bhs2 horizon of Amity. Note, A part of section is E horizon (monic) and B part is Bhs2 (gefuric and enaulic). Pigmentation of quartz grains with dark brown coloured organic fine material. *PPL*. Bar scale 100 μm .
- Plate 4.11. Photomicrograph of enaulic related distribution in section from central Bhs2 horizon of Amity. Note, irregularly shaped aggregates of dark stained fine material in inter-granular spaces of quartz grains. *XPL*. Bar scale 100 μm .
- Plate 4.12. Photomicrograph of coarse mineral grains wholly or partly surrounded by fragmented dark fine material. Section of lower Bhs2 horizon of Amity. Note, z = zircon grain. *XPL*. Bar scale 100 μm .



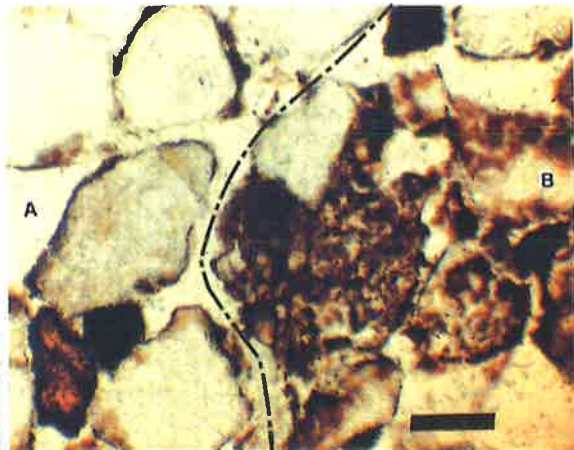
4.7.



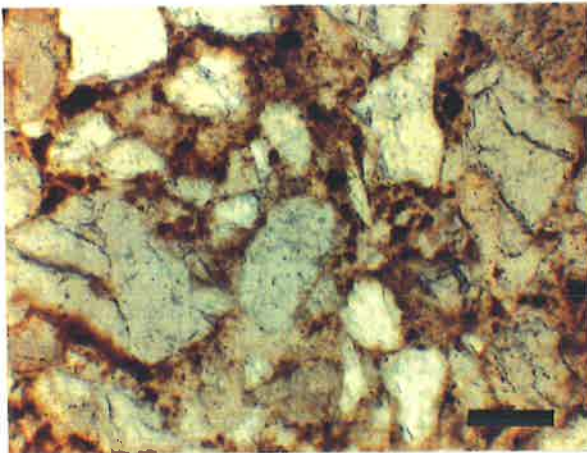
4.8.



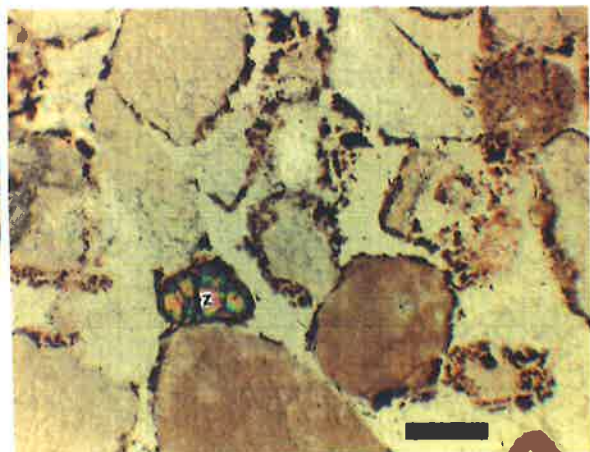
4.9.



4.10.



4.11.



4.12.

Pedofeatures

Depletion: rare coatings and infillings depleted in sesquioxidic and/or organic minerals; irregular; distinct contrast; clear boundaries with adjacent groundmass; low variability.

Amorphous and Cryptocrystalline: occasional monomorphic organo-mineral coatings (up to 30 μm thick) and minor infillings (up to 400 μm wide) (Plate 4.10), with various shades of brown and darker colours; clear boundaries; with distinct contrast; randomly distributed; moderately to purely impregnated; complete pseudomorphosis.

Amity, Bhs2, 670-685 cm.

Microstructure

Similar to Bhs2 portion above, with inter-grain (80 %), pellicular (15 %) and single grain (5 %) microstructure. Void size range (30-450 μm long). Estimated total void space is 20 %.

Basic mineral components

c/f limit at 10 μm , c/f ratio of 98:2

Coarse fraction: same as for Kings Bore Bhs2/B3 horizon

Fine fraction: same as above for Bhs2 portion

Basic organic components

Coarse fraction: none

Fine fraction: very few dark brown to black amorphous material, smooth to rough walls, occurring mainly as coatings on grains.

Groundmass

The c/f related distribution is enaulic. The b-fabric is undifferentiated.

Pedofeatures

Depletion: frequent coatings and minor infillings depleted in sesquioxidic and/or organic minerals; distinct contrast; clear boundaries; low variability.

Amorphous and Cryptocrystalline: organo-mineral coatings in the form of cappings and pendants; impregnative monomorphic coatings (up to 50 μm thick) and minor infillings (up to 80 μm thick); various shades of brown and red with darker colours with minor black or opaque portions; distinct contrast; medium variability; randomly distributed; moderately to strongly impregnated; complete pseudomorphosis (Plate 4.11).

Amity, Bhs2/Bs2, 750-765 cm.

Microstructure

Similar to Bhs2 portion above, but with intergrain micro-aggregates (50 %; Bhs2 portion, Plate 4.12) and pellicular (50 %; Bs2 portion, Plate 4.13) microstructure. Estimated total void space is 25 %.

Basic mineral components

c/f limit at 10 μm , c/f ratio of 97:3

Coarse fraction: same as for Kings Bore Bhs/B3 horizon with rare compound grains (rutilated-quartz, Plate 4.13).

Fine fraction: very few yellowish brown to dark brown, limpid clay (Bs2) and impure clay (Bhs2) consisting of optically isotropic, poorly crystalline sesquioxidic material; weakly to moderately impregnated with mainly limpid to speckled aspect.

Basic organic components

Coarse fraction: none

Fine fraction: very few dark brown to black amorphous fine material, mainly as highly fragmented coatings, rough walled.

Groundmass

Chitonic. Undifferentiated b-fabric.

Pedofeatures

Textural: grains coated as cappings, pendants, external quasi-and hypo-coatings; mainly of impure to limpid clay texture; non-laminated; irregular, elongate; medium variability; unoriented; up to 20 μm thick; yellowish brown; rare.

Depletion: few coatings and minor infillings depleted in sesquioxides and/or organic minerals; irregular; distinct contrast; diffuse to clear boundaries; low variability.

Amorphous and Cryptocrystalline: occasional monomorphic highly fragmented coatings (up to 50 μm thick); mainly black or opaque; sharp to diffuse boundaries; prominent to faint contrast; medium variability; randomly distributed; strongly to purely impregnated; complete pseudomorphosis (Plate 4.12).

Amity, B3, 1500-1515 cm.

Microstructure

Similar to Kings Bore Bhs2/B3 horizon with void size range between 100-300 μm long, smooth to undulating walls, irregular, mainly elongate in shape. Estimated total void space is 25 %.

Basic mineral components

c/f limit at 10 μm , c/f ratio of >99:<1.

Coarse fraction: similar to Kings Bore Bhs2/B3 horizon, with void size range between 50-250 μm in diameter; complex alteration patterns (Plate 4.14).

Fine fraction: similar to Kings Bore Bhs2/B3 horizon.

Basic organic components

Coarse fraction: none

Fine fraction: none

Groundmass

The c/f related distribution is monic with very minor chitonic. Undifferentiated b-fabric.

Pedofeatures

Textural: similar to Kings Bore Bhs2/B3 horizon.

Depletion: none

Amorphous: none

4.3.2. Micromorphology of the LeFevre Peninsula-Mount Compass sequence.

LeFevre Peninsula 1, A2, 90-110 cm.

Microstructure

Complex apedal microstructure with a mixture of single grain (70 %) and intergrain micro-aggregate (30 %) microstructure. Mainly simple and complex packing voids of a wide size range, often inter-connected. The voids have generally undulating walls that are irregular, elongated and subangular. Estimated total void space is 40 %. The voids are unoriented and have a random basic distribution pattern.

Basic mineral components

c/f limit at 10 μm , c/f ratio of 95:5

Coarse fraction: mostly single mineral grains, sizes range from 80 μm -400 μm in diameter, randomly distributed. Composition: single grains- calcite (80 %), quartz (17 %), feldspars (plagioclase) (Plate 4.15) and heavy minerals (2 %). Moderately sorted material; shapes are equant to elongate, mainly subangular to subrounded. Quartz grains are fresh to slightly altered; carbonate mineral grains exhibit complex alteration patterns.

Fine fraction: organo-mineral material, grey to dark brown, in places showing highly birefringent carbonate rich material; moderately impregnated, with a speckled to dotted aspect.

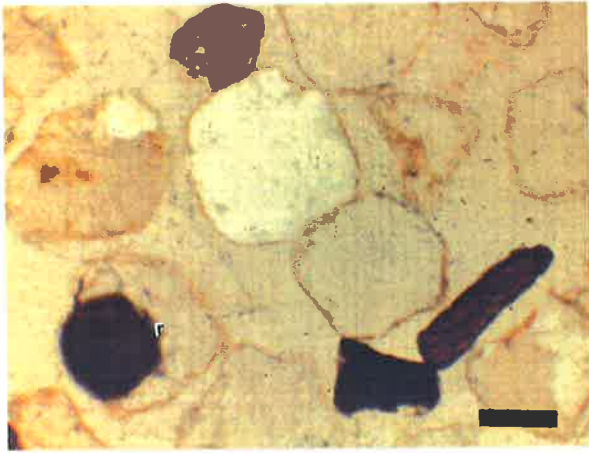
Basic organic components

c/f limit at 10 μm

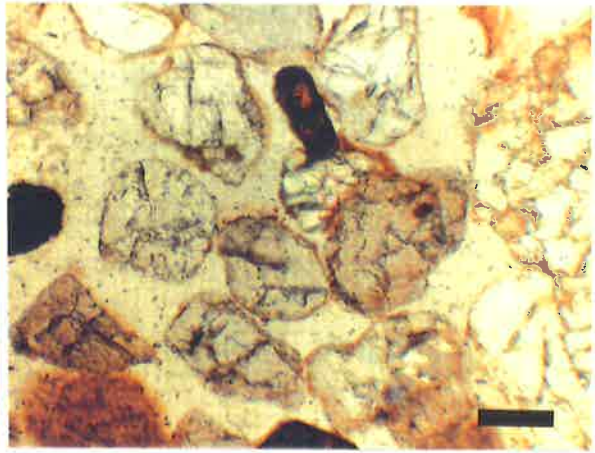
Coarse fraction: frequent plant residues embedded between mineral and shell fragments; moderately to strongly altered, with various size fragments of brown and black coloured cell structures (Plate 4.16).

Fine fraction: dark brown to black organic fine fragments, impregnated in places by carbonate material, small areas of fine aggregation, sometimes locally pigmented coarse components; rough walled with irregular patchy internal fabric.

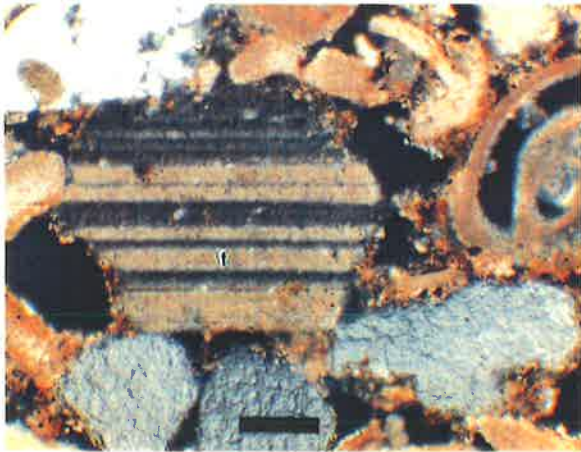
- Plate 4.13. Photomicrograph of coarse mineral grains from section of the lower Bs horizon of Amity showing chitonic related distribution and pellicular microstructure. The grains are surrounded by thin sesquioxidic coatings. Note, r = rutilated-quartz grain. *XPL*. Bar scale 100 μm .
- Plate 4.14. Photomicrograph showing monic related distribution, locally tending to chitonic. The fine material surrounding and pigmenting the coarse grains is yellowish brown organo-mineral complex. Coarse grains exhibit complex alteration patterns. Section from B3 horizon of Amity. *XPL*. Bar scale 100 μm .
- Plate 4.15. Photomicrograph showing inter-grain micro-aggregate structure from section of A2 horizon of LeFevre Peninsula 1. Generally uncoated mineral grains (e.g. f = plagioclase feldspar) and inorganic residues of gastropods with numerous organic micro-aggregates in the inter-granular spaces. *XPL*. Bar scale 100 μm .
- Plate 4.16. Photomicrograph showing single grain structure from section of A2 horizon of LeFevre Peninsula 1. Quartz grains, gastropods and plant remains loosely arranged with little or no fine material to provide aggregation. *XPL*. Bar scale 100 μm .
- Plate 4.17. Photomicrograph of open porphyric related distribution in section from E(pipe)/B1 horizon of Mount Compass. The coarse grains are embedded in a dense ferruginous matrix. *XPL*. Bar scale 100 μm .
- Plate 4.18. Photomicrograph of gefuric and chitonic related distribution in section from Bhsb2/Bhsb3 horizon of Mount Compass. The coatings and infillings comprise dark organo-mineral fine material in places pigmenting coarse grains. *XPL*. Bar scale 100 μm .



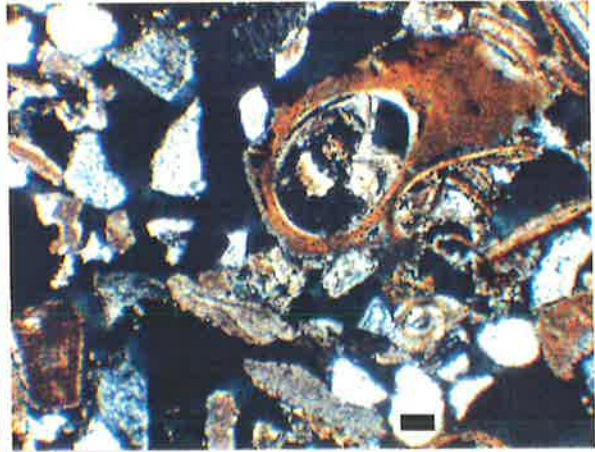
4.13.



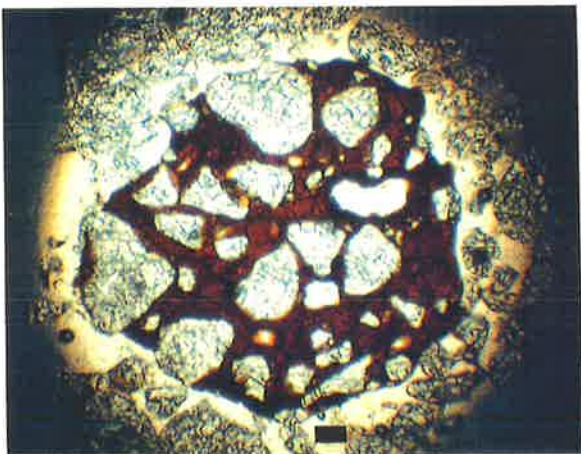
4.14.



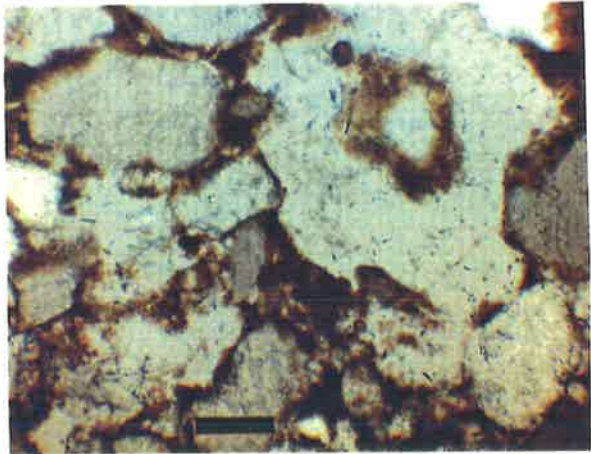
4.15.



4.16.



4.17.



4.18.

Inorganic residues

Abundant remains of molluscs, e.g. gastropods, brachiopods and cephalopods, some other marine fauna and micro-fossils, ranging in length from 100 μm -5 mm, parts are impregnated with organic fine material.

Groundmass

Mainly monic, tending locally towards enaulic related distribution. Undifferentiated b-fabric.

Pedofeatures

Amorphous and Cryptocrystalline: a) occasional polymorphic organo-mineral coatings (10-50 μm thick) as cappings and pendants; various shades of brown and darker colours; clear boundaries; distinct contrast; randomly oriented; moderately impregnated; moderate pseudomorphosis.

b) loose infillings of voids with aggregates, mainly organic fragments and some micro-crystalline carbonate minerals; irregular and subrounded; low variability; unoriented, randomly distributed; 50-200 μm thick; greyish, brown to black; occasional.

Excrement: few, different shapes, sizes up to 50 μm (extremely thin micro-coarse); rough surfaces; organic; random to clustered basic distribution pattern; weakly coalesced, porous microaggregates. Very rarely, very thin meso-fine (\sim 200 μm diameter), dark brown and slightly rough excrements occur.

Mount Compass, E(pipe)/B1, 90-105 cm.*Microstructure*

Apedal soil material without clods or fragments, with a mixture of single grain (80 %) and pellicular (20 %) microstructure. Very dominantly simple packing voids (100 %) with size between 50-400 μm in length; mainly smooth to undulating walls with irregular, elongate and subrounded faces occurring between mineral grains. Estimated total void space is 40 %. The voids are not oriented and have a random basic distribution pattern.

Basic mineral components

c/f limit at 10 μm , c/f ratio of 99:1

Coarse fraction: mainly single grains with size range between 50-500 μm in diameter, randomly distributed. Composition: dominantly quartz (98 %), some iron oxides and heavy minerals (zircon, rutile, and opaques). Perfectly sorted, dominantly rounded to subangular, equant to elongate. Complex mineral alteration.

Fine fraction: organo-mineral fine material, yellowish brown to dark brown, containing isotropic amorphous iron oxides with some organic rich component; moderately to strongly impregnated, with a speckled to cloudy aspect.

Basic organic component : none

Groundmass

mainly monic tending locally to chitonic and porphyric (Plate 4.17) related distribution. The b-fabric is mainly undifferentiated.

Pedofeatures

Textural: a) clay and silt size coatings on mineral grains, coatings occur as cappings, pendants and external hypo-coatings; non-laminated; irregular and elongate; low variability; unoriented, randomly distributed; 5-30 μm thick; yellowish brown to dark brown; occasional.

b) silty clay, loose continuous, dense incomplete and complete infillings (latter shown in Plate 4.17); irregular and subrounded; low variability; unoriented, randomly distributed; 50-100 μm in length; yellowish brown to dark brown; occasional.

Depletion: very few yellowish brown to brown nodules of varying sizes depleted in Fe oxides and/or organic minerals; faint to distinct contrast between constituent materials; commonly sharp to diffuse external boundaries; medium variability between depleted components.

Amorphous and Cryptocrystalline: very few monomorphic nodules of iron oxides, composed of fine mineral and organic particles and mineral aggregates; up to

1.3 mm in diameter; reddish brown to dark brown; shapes are rounded, slightly elongated and irregular; sharp external boundaries; randomly distributed; strongly to purely impregnated, anorthic, porphyritic in places; complete pseudomorphosis.

Mount Compass, E(pipe)/B1/Bhsb2, 95-115 cm.

Microstructure

Similar to E(pipe)/B1 horizon, with a mixture of pellicular (60 %), bridged (30 %) and single grain (10 %) microstructure. Void size range between 80-500 μm in length. Estimated total voids space is 30 %.

Basic mineral components

c/f limit at 10 μm , c/f ratio of 98:2

Coarse fraction: same as for E(pipe)/B1 horizon.

Fine fraction: same as for E(pipe)/B1 horizon.

Basic organic components

Coarse fraction: none

Groundmass

The c/f related distribution is predominantly chitonic, locally becoming gefuric-monic. The b-fabric is undifferentiated.

Pedofeatures

Textural: a) clay and silt size coatings in the form of cappings, pendants, external hypo- and sometimes typic-coatings; non-laminated; irregular and elongate; low variability; unoriented, randomly distributed; 10-80 μm thick; reddish brown; occasional.

Depletion: very few nodules of varying sizes depleted in iron oxides and/or organic minerals; faint to distinct contrast between constituent materials; commonly sharp to diffuse external boundaries; high variability between depleted components.

Amorphous and Cryptocrystalline: very few pure nodules of Fe oxides; up to 300 μm in diameter; nodules are reddish and black; rounded and elongate; diffuse to

sharp boundaries; with prominent to weak contrast; randomly distributed; strongly to purely impregnated, anorthic; complete pseudomorphosis.

Mount Compass, Bhsb2/Bhsb3, 120-135 cm.

Microstructure

Apedal soil material without clods or fragments, with a mixture of pellicular (60 %), intergrain micro-aggregate (40 %) and bridge (10 %) microstructure (Plate 4.18). Very dominantly simple packing voids (60 %) and complex packing voids (40 %) with size range between 80-400 μm in length; complex packing voids have rough and irregular walls, with much inter-connection, angular to subangular and elongate, sometimes equant in shape; simple packing voids have irregular shapes with smooth to rough walls. Estimated total voids space is 40 %. Voids are unoriented and have a random basic distribution pattern.

Basic mineral components

c/f limit at 10 μm , c/f ratio of 97:3

Coarse fraction: similar to E(pipe)/B1 horizon, void size range between 40-800 μm in diameter; moderately sorted. Most grains are slightly altered with rarely any complex alteration patterns.

Fine fraction: similar to E(pipe)/B1 horizon, with poorly crystalline sesquioxidic and/or organic minerals, moderately to strongly impregnated with a dotted to cloudy aspect.

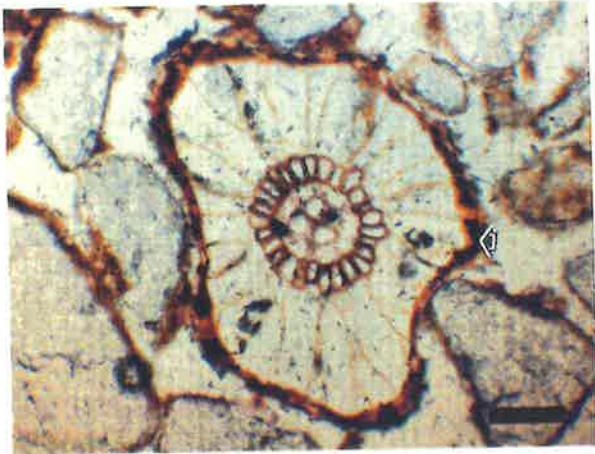
Basic organic components

Coarse fraction: very few embedded fragments of moderately to strongly altered root tissues, sizes up to 6 mm long (Plate 4.19).

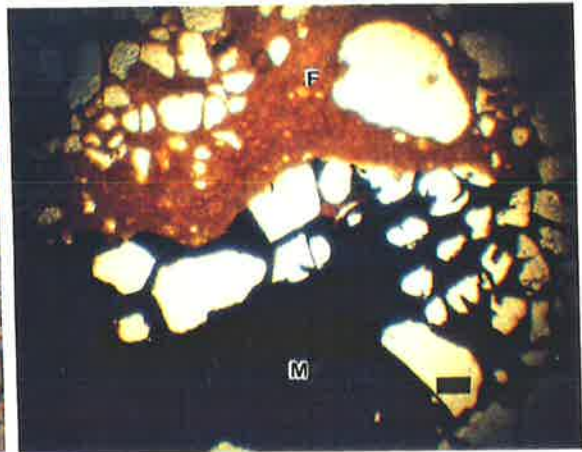
Groundmass

The c/f related distribution is complex with distribution patterns of chitonic-gefuric (Plate 4.18) with minor open porphyric (Plate 4.20). A combination of complex undifferentiated, weakly stipple speckled and crescent (Plate 4.21) partial b-fabric.

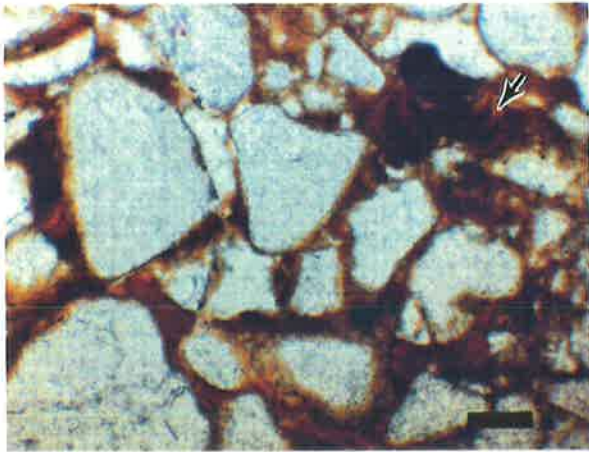
- Plate 4.19. Photomicrograph showing chitonic related distribution in section from Bhsb2/Bhsb3 horizon of Mount Compass. Note, altered plant tissue (organic residue) with deposits of dark coloured organic matter occupying the outer layer (arrow) of the organ fragment. Organic pigments also stain grains. *XPL*. Bar scale 100 μm .
- Plate 4.20. Photomicrograph showing open porphyric related distribution in section from Bhsb2/Bhsb3 horizon of Mount Compass. Note, the quartz grains are embedded in a dense ferruginous (F) and manganiferous (M) matrix forming a large impregnative nodule. *XPL*. Bar scale 100 μm .
- Plate 4.21. Photomicrograph showing dense complete void infillings with bow-like distribution pattern (arrow) in section from Bhsb2/Bhsb3 horizon of Mount Compass. The microlaminated infillings consist of deposits of dark coloured organic matter plus clay. *PPL*. Bar scale 100 μm .
- Plate 4.22. Photomicrograph of compound manganiferous and ferruginous strong impregnative nodule in a section from Bhsb2/Bhsb3 horizon of Mount Compass. Note, the ferruginous outer component diffuses into the manganiferous inner member. *XPL*. Bar scale 100 μm .
- Plate 4.23. Photomicrograph showing chitonic related distribution in section from Bhsb3 horizon of Mount Compass. The strong orientation of the fine material around the coarse grains (a = zircon) causes micro-channel formation in voids (arrow). *XPL*. Bar scale 100 μm .
- Plate 4.24. Photomicrograph showing vughy microstructure in section from Bhsb3 horizon of Mount Compass. The continuity of the organic rich fine mass is broken by irregularly shaped vughs (e.g. v). Note, large channel (c) with walls coated with organic rich fine material. *PPL*. Bar scale 100 μm .



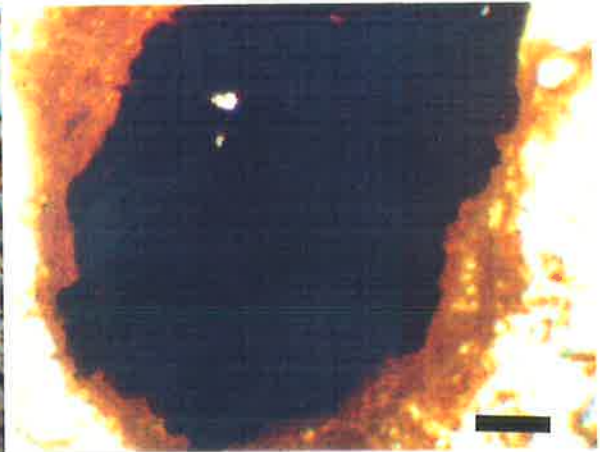
4.19.



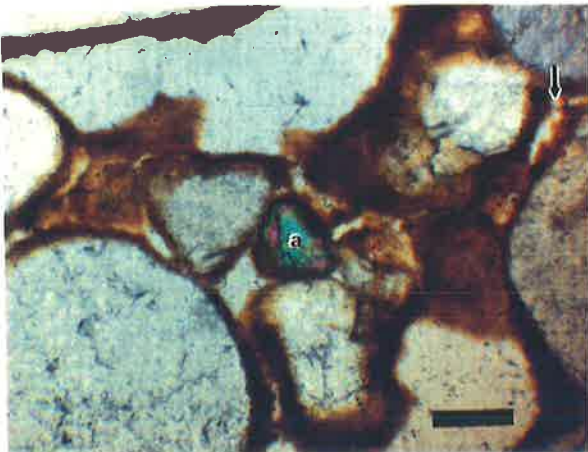
4.20.



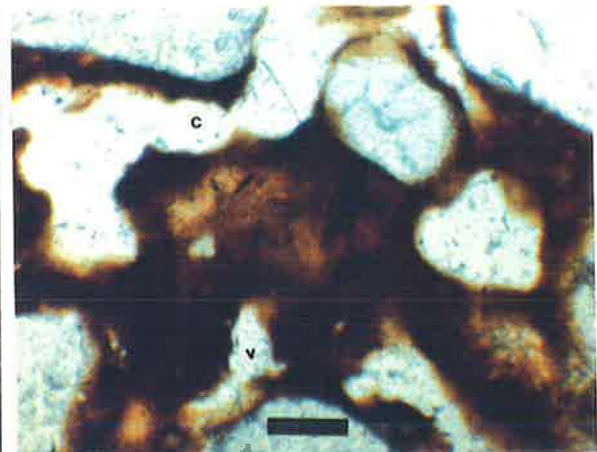
4.21.



4.22.



4.23.



4.24.

Pedofeatures

Textural: a) mainly silty clay textured coatings in the form of cappings, pendants and hypo-coatings; non-laminated; irregular and elongate; low variability; unoriented, randomly distributed; 5-60 μm thick; yellowish brown to dark brown; occasional

b) loose infillings of silty clay size; irregular and mainly subrounded; low variability; unoriented, randomly distributed; 50-100 μm in diameter; yellowish brown, dark brown with some black fragments; many. Rare dense complete infillings with microlaminations (Plate 4.21).

Depletion: very few nodules, 50 μm -5 mm thick depleted in Fe oxides; prominent contrast between constituent components; sharp boundaries with adjacent groundmass; high variability between depleted components.

Amorphous and Cryptocrystalline: few pure and impregnative anorthic nodules of predominantly Fe oxides with minor sesquioxidic and/or organic minerals (?); 50 μm -5 mm thick; components have a mixture of pale yellow, yellowish brown, reddish brown, brown and black colours (Plate 4.22); shapes are irregular and rounded; often sharp external boundaries; distinct to prominent contrast; medium to high variability; randomly distributed, strong impregnation; complete pseudomorphosis. Units of the groundmass with very different allophanic material impregnation create a strongly mottled appearance.

Mount Compass, Bhsb3, 140-150 cm.*Microstructure*

Apedal soil material without clods or fragments with predominantly pellicular grain (100 %) microstructure. Very dominantly vughs and channels (90 %) with some simple packing voids (8 %) and complex packing voids (2 %) (Plates 4.23 and 4.24), size range between 50-700 μm in length; channels and vughs have undulating to rough walls, sometimes inter-connected, irregular, round to elongate, sometimes equant in shape, some channels partly filled with silty to clayey material; simple packing voids

have irregular shapes with smooth to rough walls. Estimated total void space is 25 %. Voids are unoriented and have a random basic distribution pattern.

Basic mineral components

c/f limit at 10 μm , c/f ratio of 90:10

Coarse fraction: similar to E(pipe)/B1 horizon. Moderately sorted; rounded to subrounded, equant to elongate grains. Most grains are slightly altered, and rarely any complex pattern of alteration.

Fine fraction: similar to Bhsb2/Bhsb3 horizon; composed of isotropic amorphous combinations of Fe oxides and poorly crystalline sesquioxidic material; moderately to purely impregnated, with a speckled to cloudy aspect.

Basic organic components

Coarse fraction: none

Fine fraction: organic fine material is present as micro-contrasted particles up to 30 μm thick and organic pigment (dark to black) in unsorted pedofeatures (coatings and infillings); moderately to strongly impregnated, mainly with dotted appearance (Plate 4.24).

Groundmass:

Mainly chitonic with locally close porphyric c/f related distribution. A combination of complex undifferentiated partial, stipple speckled partial, and some weakly developed striated b-fabric as grano-, mono-, random- and poro- striated partial fabrics; thin and medium continuous, 40-100 μm long.

Pedofeatures

Textural: a) mainly silty clay size coatings in the form of typic-, hypo- and external quasi-coatings covering grain and void surfaces; microlaminated; irregular and elongate; medium variability; mainly unoriented with parallel weak orientation in places; 20-100 μm thick; reddish brown, yellowish brown and dark brown; abundant

b) dusty clay and silt size dense infillings; irregular and subrounded; medium variability; unoriented, randomly distributed; 100-500 μm in diameter; various shades of brown with very few small embedded fragments of black materials; many.

Depletion: few nodules, 20-1000 μm thick depleted in Fe oxides; distinct contrast between constituent components; sharp boundaries with adjacent groundmass; medium variability between depleted components.

Amorphous and Cryptocrystalline: very few pure and impregnative, anorthic, monomorphic and polymorphic nodules, composed of Fe oxides; up to 1000 μm thick; black and brown components; irregular and rounded; sharp external boundaries; prominent contrast; medium to high variability; randomly distributed; strongly to purely impregnated; complete pseudomorphosis.

Mount Compass, Bsb3, 165-175 cm.

Microstructure

Apedal soil material without clods or fragments, with a mixture of pellicular (75 %) and single grain (25 %) microstructure. Dominantly vughs and channels (60 %) with simple packing voids (38 %) and very minor zig zag planes (2 %), size range between 30-600 μm in length; channels and vughs have undulating to rough walls, without much inter-connection, irregular mainly elongate and sometimes equant in shape; simple packing voids have irregular shapes with smooth to rough walls. Estimated total void space is 25 %. Voids are unoriented and have a random basic distribution pattern.

Basic mineral components

c/f limit at 10 μm , c/f ratio of 95:5

Coarse fraction: same as for E(pipe)/B1 horizon.

Fine fraction: organo-mineral fine material, with a mixture of colours ranging from yellowish brown, brown, dark brown to black, containing poorly crystalline sesquioxides with some organic rich pigments, moderately to strongly impregnated, with mainly a speckled to cloudy and localized dotted to opaque aspect. Some anisotropic fine fraction on void and grain surfaces with common interference colours is present (Plates 4.25 and 4.26).

*Basic organic components*Coarse fraction: none*Groundmass*

The c/f related distribution is a complex combination of chitonic to monic with minor porphyric. A combination of undifferentiated partial b-fabric, weakly stipple speckled partial b-fabric and a complex well developed striated b-fabric with mono-, random-, grano- and crescent- striated partial fabrics, continuous and medium, 30-300 μm long (Plates 4.25 and 4.26).

Pedofeatures

Textural: a) grains covered with coatings in the form of typic-, external hypo- and quasi- coatings, with frequent cappings and pendants; silty clay textured; mainly micro-laminated; irregular, compact to elongate; medium variability; moderately to strongly oriented; banded basic distribution pattern, parallel to inclined to grain surfaces; 10-200 μm thick; yellowish brown to brown; very abundant

b) dense and loose infillings of silty clay size; commonly laminated; irregular and mainly subrounded; medium variability; moderately to strongly oriented; banded basic distribution pattern, parallel to bow-like referred orientation patterns; 50-300 μm thick; yellowish brown to brown; very abundant (Plates 4.25 and 4.26).

Depletion: commonly coatings, infillings and nodules, 10-300 μm thick depleted in Fe oxides and/or organic minerals; with distinct contrast; sharp boundaries with adjacent components; medium variability.

Amorphous and Crystalline: common impregnative, anorthic coatings and infillings; up to 400 μm thick; yellow brown to black, with sesquioxidic and allophanic material of different forms creating mottling appearance; diffuse to sharp boundaries; prominent to faint contrast; medium variability; randomly distributed; moderately to strongly impregnated; complete pseudomorphosis.

Mount Compass, Bb4, 180-200 cm.*Microstructure*

Apedal soil material without clods or fragments, with pelicular (100 %) microstructure. Dominantly vughs and channels (100 %) with very much inter-connection between voids; size range between 60 μm -2 mm in length; commonly undulating to rough walls, irregular, mainly elongate and sometimes equant in shape. Estimated total void space is 30 %. Voids are unoriented and have a random basic distribution pattern.

Basic mineral components

c/f limit at 10 μm , ratio of 96:4

Coarse fraction: same as for Bsb3.

Fine fraction: same as for Bsb3.

Basic organic components

Coarse fraction: none

Groundmass

The c/f related distribution is predominantly chitonic (Plate 4.27). A combination of mainly undifferentiated partial b-fabric with minor grano- and poro-striated partial b-fabric and stipple speckled partial b- fabric.

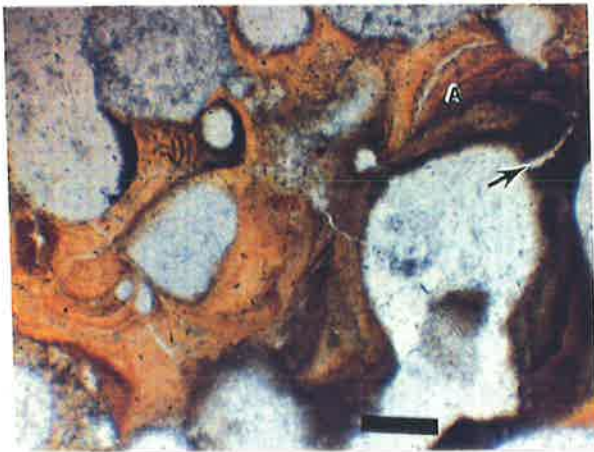
Pedofeatures

Textural: a) mainly clayey silty textured coatings in the form of typic- and external hypo-coatings, in places fragmented to form external quasi-coatings; laminated; irregular and elongate; low variability; unoriented; banded basic distribution pattern; 10-70 μm thick; yellow brown to brown; occasional

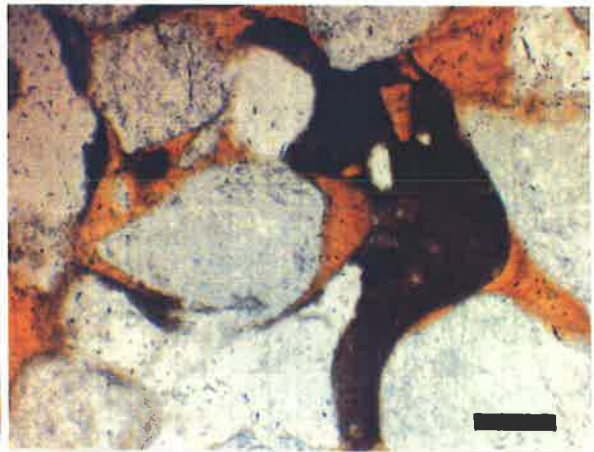
b) dense incomplete infillings of clayey silty size; irregular, patchy internal fabric, subrounded; low variability; unoriented; randomly distributed; 50-200 μm thick; yellow brown to brown; occasional (Plate 4.28).

Depletion: frequently coatings and infillings 10-200 μm thick depleted in Fe oxides and/or allophanic material; distinct contrast between constituent components;

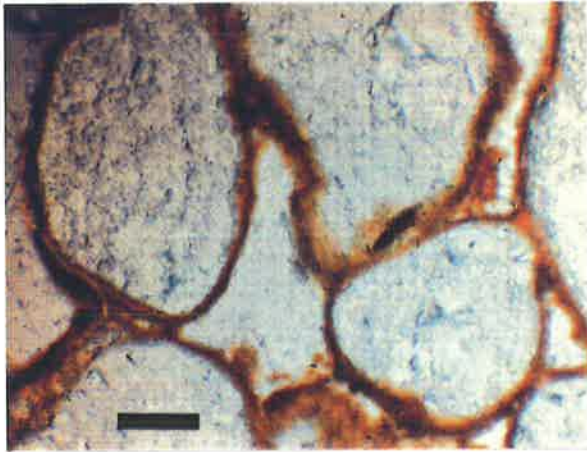
- Plate 4.25. Photomicrograph of microlaminated organic and clay rich infilling in section from Bsb3 horizon of Mount Compass. The layered infillings around grains and walls of voids (v) show complex replicated zones of dark and bright coloured organic and clay rich deposits respectively (A) Note, dessication cracks (arrow). *PPL*. Bar scale 100 μm .
- Plate 4.26. Organic-clay rich void infillings and coatings similar to that in Plate 4.25, but with more distinct zones of accumulation of organic and clay rich fine material. Replicated boundary layers between organic and clay rich fine material. *XPL*. Bar scale 100 μm .
- Plate 4.27. Photomicrograph of pellicular microstructure in section from Bb4 horizon of Mount Compass. The quartz grains are completely surrounded by organo-mineral fine material which bridges and welds the grains together. *PPL*. Bar scale 100 μm .
- Plate 4.28. Photomicrograph of vughy microstructure in section from Bb4 horizon of Mount Compass. The continuity of the organic fine material is broken up by irregular shaped vughs as in Plate 4.24. Note, the dark coloured organic deposit has condensed earlier deposits of yellow coloured clayey fine material (e.g. arrow). *XPL*. Bar scale 100 μm .
- Plate 4.29. Photomicrograph of gefuric related distribution in section from Ab2 horizon of Canunda. Organic and carbonate rich fine material forms bridges between coarse grain carbonate inorganic residues. Distinctive carbonate deposit (a) in void space. Coarse grains are stained by organic pigments. *XPL*. Bar scale 100 μm .
- Plate 4.30. Photomicrograph of inter-grain micro-aggregate structure in section from Bb1 horizon of Canunda. The mostly uncoated grains have numerous organic micro-aggregates (possibly soil animal excrements) in the inter-grain spaces. Organic pigmentation of coarse grains. *XPL*. Bar scale 100 μm .



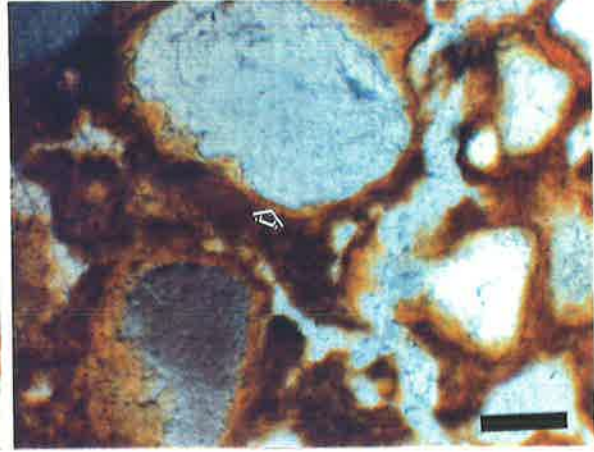
4.25.



4.26.



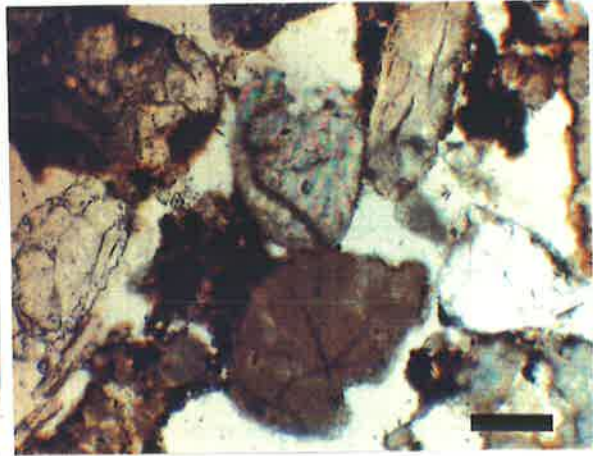
4.27.



4.28.



4.29.



4.30.

diffuse boundaries with adjacent groundmass; low variability between depleted components.

Amorphous and Cryptocrystalline : common impregnative, anorthic coatings and infillings; up to 400 µm thick; yellow brown to black, with allophanic and organic material of different forms; sharp to diffuse boundaries; prominent to faint contrast; medium variability; randomly distributed; moderately to strongly impregnated; complete pseudomorphosis.

4.3.3. Micromorphology of the Canunda-Mount Burr sequence.

Canunda, Bb1/Ab2, 160-176 cm.

Microstructure:

Apedal soil material without clods or fragments with very dominantly single grain microstructure. Mainly simple packing voids (100 %) of a wide size range, up to 800 µm long, smooth walls, irregular, elongate, subangular to subrounded. Estimated total void space is 40 %. The voids are unoriented and have a random basic distribution pattern.

Basic mineral components

c/f limit at 10 µm, c/f ratio of 99:1

Coarse fraction: very dominantly single grains with a size range between 60-500 µm wide, randomly distributed. Composition: calcite grains (99 %), very few quartz grains (1 %), rarely any heavy minerals. Perfectly sorted; dominantly rounded, equant to elongate; calcite grains have complex alteration pattern and quartz grains are slightly to moderately altered.

Fine fraction: rare cryptocrystalline grains of fine silt size dispersed in the fine mass as greyish green high birefringence carbonate rich material; weakly to moderately impregnated; generally limpid, with some speckled aspect where there is organic fine material present.

Basic organic components

Coarse fraction: none

Fine fraction: black organic fine micro-aggregates of fine silt size sometimes dispersed in cryptocrystalline calcite, with finer fraction as brownish organic punctuations and pigments, highly transformed (Plate 4.29).

Inorganic residues

Abundant embedded remains of molluscs and some other marine fauna and micro-fossils, length range between 120-800 µm; parts impregnated with organo-mineral fine material.

Groundmass

The c/f related distribution is monic to gefuric. The b-fabric is undifferentiated.

Pedofeatures

Depletion: very few greyish brown and dark brown to black cryptocrystalline and amorphous infillings and coatings of variable sizes and thicknesses, depleted in carbonate and organic material; prominent and distinct contrasts in organic and carbonate depleted components respectively; clear to sharp boundaries with adjacent groundmass; medium variability (Plate 4.30).

Amorphous and Cryptocrystalline: very few brownish coatings, orthic and anorthic impregnative, composed of a mixture of microcrystalline carbonate and organic fine material with few silt size excrete fragments; weakly to moderately impregnated; prominent contrast with adjacent material; low variability; randomly distributed.

Excrement: few very thin meso fine excrements with different shapes; rough ; organic fine material; randomly distributed; densely to very densely coalesced micro-aggregates; dark brown to black.

Canunda, Ab2/Bb2, 192-208 cm.

Similar to Bb1/Ab2 horizon, but with rarely any fine material as coatings and/or other amorphous pedofeatures (e.g. depletion or excrement) at the boundary, and the following differences:

Microstructure: (i) void size range up to 600 μm long, (ii) void walls are commonly smooth or undulating to rough, (iii) estimated voids space is 50 %.

Basic mineral components: Coarse fraction has a grain size range of 50-450 μm in diameter.

Groundmass: monic. Undifferentiated to very locally crystallitic b-fabric.

Amorphous and Cryptocrystalline: very few anorthic impregnative microcrystalline carbonate aggregate; weak contrast with adjacent material; low variability; randomly distributed, slightly at depth in Bb2 portion.

Canunda, Bb3, 310-326 cm.

Similar to Bb2 portion above (Plate 4.31), but with the following differences:

Microstructure

void sizes up to >800 μm long. Estimated total void space is 60 %.

Basic mineral components

c/f limit at 10 μm , c/f ratio of 98:2

Coarse fraction: grain size range between 50-450 μm wide; calcite and quartz grains show complex alteration patterns (cross linear).

Fine fraction: very few cryptocrystalline grains of fine silt size calcite dispersed in the micromass as greyish green, high birefringent carbonate rich material.

Coarse fraction: none

Fine fraction: black opaque organic fine silt size grains and aggregates, sometimes dispersed in cryptocrystalline calcite, with finer particles as brownish organic punctuations and pigments, highly transformed.

Inorganic residues

Length range between 150-700 μm .

Pedofeatures

Excrement: very few with a variety of shapes and sizes up to 120 μm long, rough, organic fine material; randomly distributed; densely to very densely coalesced; dark brown to black.

Mount Burr, E(pipe)/Bhs2, 220-235 cm.*Microstructure*

Apedal soil material without clods or fragments, with a mixture of single grain (60 %), bridged (30 %) and pellicular (10 %) microstructure. Very dominantly simple packing voids (90 %) with some vughs (10 %), size range between 80-400 μm in length, mainly smooth walls, with irregular, elongate and subangular faces. Estimated total void space is 30 %. The voids are unoriented and randomly distributed.

Basic mineral components

c/f limit at 10 μm , c/f ratio of 97:3

Coarse fraction: mainly single grains, size range between 50-250 μm in diameter, randomly distributed. Composition: quartz (98 %), some biotite and heavy minerals (~ 2%). Moderately sorted, subangular to subrounded, equant to elongate; complex alteration patterns.

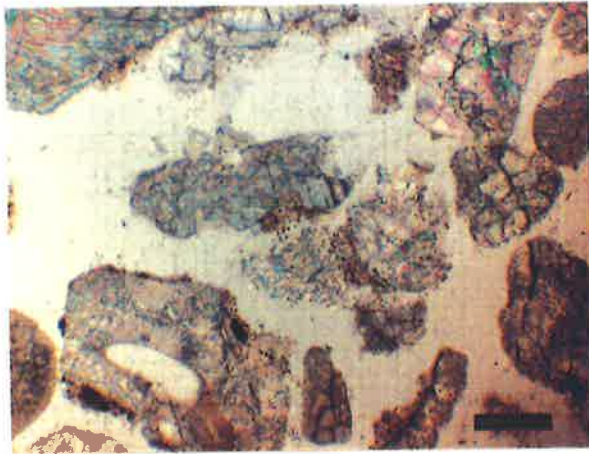
Fine fraction: reddish brown to dark brown, mainly silty clay size with allophanic material including particles up to 20 μm thick; moderately to strongly impregnated; speckled aspect.

Basic organic components

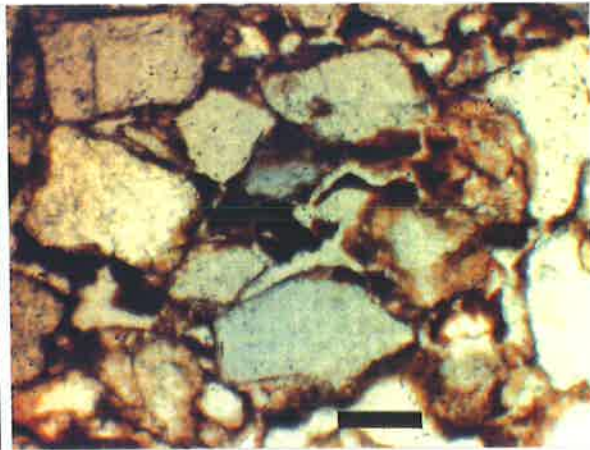
Coarse fraction: rare embedded fragments of moderately to strongly altered root tissues, sizes up to 3.5 mm long, with yellowish red stained cell walls and contents, interior (voids) mainly colourless and greyish (cell structures).

Fine fraction: very few brown to black amorphous fine material and organic pigment in unsorted pedofeatures, irregular with cloudy to dusty aspect (Plate 4.32).

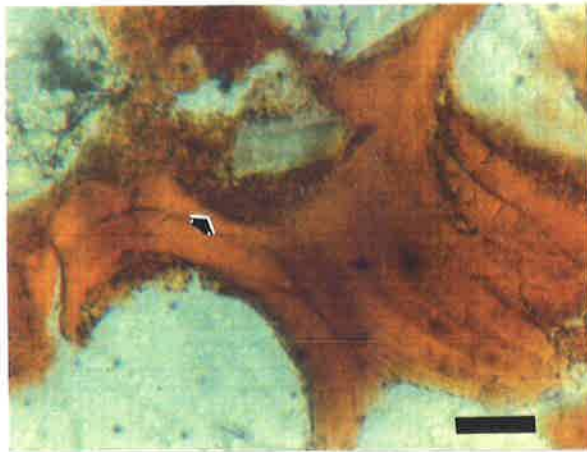
- 4.31. Photomicrograph of monic related distribution in section from Bb3 horizon of Canunda. The inorganic residues are highly altered, with distinctive carbonate rich deposits in inter-granular spaces. Organic pigmentation of coarse grains. *XPL*. Bar scale 100 μm .
- 4.32. Photomicrograph showing chitonic related distribution in section from Bhs2 horizon of Mount Burr. The quartz grains are partly or wholly surrounded by dark organic rich fine material. Locally tending to gefuric, with organic pigmentation of coarser grains. *XPL*. Bar scale 100 μm .
- 4.33. Photomicrograph of microlaminated clay rich infilling of void in section from Bs horizon of Mount Burr. Note, complete infilling of inter-granular spaces, and alternating layers of impure clay and silt (arrow). *XPL*. Bar scale 100 μm .



4.31.



4.32.



4.33.

Groundmass

The c/f related distribution is monic-gefuric-chitonic. The b-fabric is dominantly undifferentiated with rare stipple speckled partial fabric.

Pedofeatures

Textural: a) silty clay coatings on mineral grains, occurring as cappings and pendants; non-laminated; irregular and elongate; low variability; unoriented, randomly distributed; 10-20 μm thick; reddish brown; occasional

b) silty clay loose infillings of irregular shape, mainly subrounded; low variability; unoriented, randomly distributed; up to 150 μm wide; various shades of brown with darker colours.

Depletion: frequent coatings, infillings and nodules of various sizes depleted in Fe oxides, allophanic and/or organic material; faint to distinct contrast between constituent materials; commonly diffuse to sharp external boundaries; high variability between depleted components.

Amorphous and Cryptocrystalline: very few impregnative monomorphic nodules of variable sizes (up to 600 μm long); with various shades of red with darker colours; rounded and elongate; diffuse to sharp boundaries; distinct to prominent contrast; randomly distributed; moderately to strongly impregnated; anorthic; complete pseudomorphosis.

Mount Burr, Bs2, 230-245 cm.

Microstructure

Apedal soil material without clods or fragments, with a mixture of pellicular (85 %), intergrain micro-aggregate (10 %) and bridged (5 %) microstructure. Dominantly vughs and channels (85 %), complex packing voids (10 %) and simple packing voids (5 %), with size range between 30-1300 μm long; vughs and channels have undulating to smooth walls without much interconnection, they are irregular, mainly elongate but sometimes equant in shape, some channels are filled with fine material causing zig zag planar voids in places; simple and complex packing voids have

irregular shapes with smooth to rough walls. Estimated total void space is 35 %. Voids are unoriented and randomly distributed.

Basic mineral components

c/f limit at 10 μm , c/f ratio of 95:5

Coarse fraction: similar to E(pipe)/Bhs2 horizon with the following differences: poorly sorted; moderate to complex mineral alteration.

Fine fraction: yellowish brown to reddish brown, mainly clay and silt size particles with isotropic amorphous Fe oxides; strongly impregnated; speckled to dotted aspect.

Basic organic components

Coarse fraction: none

Fine fraction: few brown and black amorphous fine material and organic pigments in unsorted pedofeatures; rough walled with irregular patchy internal fabric.

Groundmass

The c/f related distribution is chitonic to minor geric. The b-fabric is a complex mixture of undifferentiated (80 %), stipple speckled (15 %) and crescent striated (5 %) types.

Pedofeatures

Textural: a) grains and voids occasionally covered with coatings in the form of typic- and external hypo-coatings, as well as cappings and pendants; non-laminated; irregular and elongate; medium variability; largely unoriented with some parallel orientation; random distribution; up to 60 μm thick; yellowish red

b) occasionally dense incomplete and loose continuous infillings composed of Fe oxides, allophanic and/or organic material, silty clay textured; locally micro-laminated; irregular and mainly subrounded; medium variability; unoriented, randomly distributed; up to 300 μm wide; yellowish red, brown and dark brown (Plate 4.33).

Depletion: frequent coatings and infillings depleted in Fe and/or organic components; prominent contrast between constituent components; clear boundaries with adjacent groundmass; medium variability between depleted components.

4.4. Discussion

4.4.1. Cooloola-North Stradbroke Island sequence.

In the Bhs/B3 horizon of Kings Bore there is little or no indication of pedogenesis apart from the occurrence of very thin and incomplete Al-rich sesquioxide coatings on the surfaces of some of the loosely packed skeleton grains (Plate 4.1, Bhs2 portion). Organic matter occurs as plant parts in various stages of decomposition (Plate 4.2), not associated with grain surfaces (Brewer and Thompson, 1980).

In Chalambar profile, the A1/E horizon has mixed complex of monic-chitonic-gefuric type of related distribution pattern (Plates 4.3 and 4.4). The monic pattern dominates and the gefuric pattern is due to accumulation of comminuted amorphous organic fine material (Plate 4.3). There is also a minor chitonic component (Plate 4.3), in which the coatings are thicker and much more developed than in the Bhs/B3 horizon of Kings Bore probably because the latter is younger and deeper. The presence of few strongly coalesced excrement pedofeatures (Plate 4.3) indicate some macrofaunal activity in this horizon. In the Bhs horizon (Plates 4.5 and 4.6) the chitonic distribution pattern predominates. The coatings are a mixture of organic and sesquioxidic minerals (Plate 4.5). There are complexes in small areas with dense infillings of predominantly amorphous fine organic rich material (Plate 4.6). The polymorphic characteristics of this section of the horizon suggests vertical migration of organo-mineral complexes (illuviation) from upper horizons and decomposition of organic fragments brought down by fauna (recognizable strongly coalesced spherical excrement pedofeatures do occur). Although very few, the decomposed faunal transported organic fragments would have contributed substantially to the total infilled organic component given a long period of time.

In E/B1 horizon of Seacliffs the related distribution pattern is monic. The section of the horizon sampled is devoid of coatings and intergranular organic fragments. The individual mineral grains show more internal weathering patterns compared to the previous sections where grain surfaces were covered with coatings to different degrees.

At Amity the grains in the E/B1 horizon are loosely packed and have predominantly monic related distribution patterns. Few grains have very thin and mostly incomplete coatings rich in sesquioxidic materials (Plate 4.8). There is rare organic matter, present as organic residue in various stages of decomposition. The mineral grains show irregular linear alteration patterns displaying slight organic pigmentation in restricted areas.

In the B1 portion and E(pipe)/Bhs horizon the grains have strong dark brown to black organic coatings (mainly incomplete), giving rise to a complex monic-gerufic to minor enaulic related distribution patterns (Plates 4.9 and 4.10). The concentration of organic fine material in localized areas causes a gerufic-enauleic related distribution pattern. Some grains have strongly developed organic pigmentation probably resulting from dispersion and movement of the soluble component of the organic matter. The concentration of unevenly thick organo-sesquioxidic fine material on grain surfaces and inter-granular voids may suggest that they formed by slight gravitational movement under the influence of wetting and drying, causing the packing of the organic fine material between the grains and around their points of contact (Brewer *et al.*, 1983). In the Bhs2 horizon below the E(pipe)/Bhs2, the degree of grain pigmentation is higher than in the latter horizon, and the amount of coalesced organic fine component is reduced (Plate 4.11). At this depth in the profile there is either less coalescing of organic fine material or greater dispersion of previously higher concentration of organic fine components due to wetting and drying processes. The reddish colours in the fine mass may be due to finely divided poorly crystalline sesquioxides intermixed with allophanic material (Farmer *et al.*, 1983, Milnes and Farmer, 1987), a part of which is illuviated as a result of podzolisation, as well as from minerals during weathering. The

degree of cementation is stronger than in the E(pipe/Bhs2) horizon above. Further down the profile there is a clear boundary between the Bhs/Bs transitional horizons. The Bhs portion comprises small comminuted aggregates of organic rich grain coatings (Plate 4.12), whereas the Bs portion has grains very thinly coated with sesquioxide rich material (Plate 4.13) combining to form a chitonic related distribution pattern. There is also less pigmentation of grains in the Bs portion than the Bhs of transition horizon. The fine mass around the grains is oriented parallel to their surfaces, except where the fine mass is unusually coarse. Wetting and drying, with slight movement of the material, may produce such a distribution pattern (Brewer *et al.*, 1983). Brewer and Thompson (1980) discussed possible interpretations of the opaque comminuted material as either faecal pellets or breakdown products of fractured coatings, based on the works of other researchers. The latter theory may seem more appropriate because of (i) the overlying sections of the Bhs horizon (Plates 4.9 to 4.11) are considered to have formed by wetting and drying phenomena (ii) there is no evidence of biological activity in the form of excrement pedofeatures, which may cause a relatively homogenous fine material (compared with Plate 4.6). The B3 horizon shows evidence of thin, irregular sesquioxide dominated coatings on grain surfaces similar to the Bs horizon above. The grains have an irregular linear alteration pattern and pigmentation by sesquioxidic rich fine material.

4.4.2. LeFevre Peninsula-Mount Compass sequence.

The LeFevre Peninsula 1 is clearly a recent calcareous sand deposit in which the A2 horizon shows no evidence of profile development. The section has a monic to minor enaulic related distribution pattern with predominantly organic fine (Plate 4.15) and rare carbonate crystallites (portions of Plate 4.16) mixed to form coatings and inter-grain microaggregates. The coarse fraction includes many shell fragments. The relatively homogeneous nature of the organic fine material may suggest mixing by biological agents as there is evidence of excrement pedofeatures in the form of weakly coalesced porous microaggregates. The random nature of the coatings and

microaggregates is indicative of wetting and drying phenomena with gravitational movement involved.

At Mount Compass, the E(pipe)/B1 horizon has a predominantly monic and locally chitonic and porphyric related distribution pattern (Plate 4.17). There is also grain pigmentation in restricted areas. The coatings and pigmentation are rich in sesquioxides. The dispersion and subsequent accumulation of soluble sesquioxides due to wetting and drying could cause the fine material to either form pigments on grains or coat the coarse particles with an indeterminate orientation. The porphyric distribution pattern is highly localised and appears to be inherited from the parent sediment, due to its sharp boundary, distinct form and separation from the rest of the coarse fraction and rounded shape. This pedofeature was sufficiently resistant to survive the processes of erosion and sedimentation. In the E/B1/Bhsb2 horizon the coatings and pigmentation become thicker, with the segregation of the iron rich material into typical pure to moderately impregnated nodules. The sharp internal boundaries and coatings around them suggest they are transported inherited features, and where moderately impregnated iron depletion could be responsible for the degree of purity. The Bhsb2/Bhsb3 horizon has a relatively complex micromorphology. The fine material is a complex of coatings and infillings, composed of organo-mineral components, with evidence of wetting and drying and illuviation phenomena. The occurrence of cracks (e.g. Plate 4.18) in grain coatings parallel to the grain surfaces could be due to modification of the fine material as a result of shrinking and swelling. There is also some evidence of local illuviation of clay rich fine fraction (Plate 4.21) due to microlaminated infilling of voids. Usually in Spodosols developed from simple (untruncated) profiles the coatings and infillings in the B2 horizon become thinner and less complete with increasing depth. The presence of plant fragments (Plate 4.19) and comparatively thicker infillings and coatings in this transitional horizon suggest the possibility of a truncated and buried horizon. These pedofeatures could be part of a relict component of a much shallower profile to which illuviated fine material from overlying horizons has been incorporated. Also complex porphyric distribution (Plate

4.20) and a thickly coated typical pure impregnated nodule (Plate 4.22) suggests a complex sequence of events. The compound nodule, for instance, suggests subsequent accumulation of fine yellow fraction (iron rich?) around previously formed enclosed black nodule (relatively iron deficient?). The diffuse boundary with the outer iron component suggests in situ formation of this pedofeature. The very large composite porphyric related distribution (Plate 4.20) appears to be an inherited feature from previous soil profile. The boundary between the yellow and black fractions is quite distinct and sharp. In the Bhsb3 horizon the wetting and drying processes cause the fine material with slightly more clay to coat grain surfaces with stronger orientation within the fine material (Plates 4.23 and 4.24). That is, there is a stronger degree of preferred orientation parallel to the grain surfaces, causing the formation of channels in the voids. The organic matter content is higher (see Appendix 3). This is evident in the section by finely dispersed organic matter masking the inorganic (relatively clay rich) fine material. The coatings are irregular in thickness and conform to the outer boundary. Illuviation is the primary process of deposition of organic matter removed from the surface horizon to the lower horizon (in this case Bhsb3 and Bsb3). However, in parts of the Bhsb3 examined the orientation of the fine material around the coarse grains was dominated by wetting and drying phenomenon. In the Bsb3 horizon the distribution of the fine material components becomes segregated, with distinct boundaries between organic and clay rich portions (Plates 4.25 and 4.26). There is evidence for both wetting and drying (occurrence of cracks; Plate 4.25) and illuviation (dense complete microlaminated non laminated infillings of dense complete infilling of voids; Plates 4.25 and 4.26). In the Bb4 horizon below, the influence of wetting and drying becomes the main process in the distribution pattern of the fine material with strong preferred orientation of the organo-mineral component parallel to the surfaces of the coarse grains it coats. The channels are wider and longer indicating considerable shrinking and swelling in this horizon (Plates 4.27 and 4.28).

4.4.3. Canunda-Mount Burr sequence.

At Canunda the Bb1/Ab2 transitional horizon is clearly a young soil in which the coarse material is predominantly shell fragments. In the Bb1 section the fine material occurs as mainly organic coatings in the form of densely coalesced

microaggregates (Plate 4.29). There is also organic pigmentation of coarse grains. The coalesced microaggregates are evidence of biological activity in the form of excrements. The Ab2 horizon is similar to Bb1, but with fewer organic rich fine material and the occurrence of very few microcrystalline calcite accumulations in the groundmass (Plate 4.30). With depth, the amount and distribution of the fine material around coarse grains diminish as evident in the Ab2/Bb2 and Bb3 (Plate 4.31) horizons. In the Bb2 and Bb3 horizons there is evidence of microcrystalline calcite accumulation (Plate 4.31). The morphological form of carbonate accumulation in the horizons is restricted to very few discontinuous, extremely thin flakes in voids and on grain surfaces. Such accumulations are similar to stage 1 in the sequence described by Gile *et al.* (1966) for non-gravelly materials. The calcitic formations seem to be of secondary origin, a result of *in situ* formation during pedogenesis (Sehgal and Stoops, 1972).

The development of the podzol profile at Mount Burr is similar to the processes already discussed for similar podzols at Cooloola, North Stradbroke Island and Mount Compass. In the E(pipe)/Bhs2 horizon the coatings are dominantly organic with distribution patterns similar to the E(pipe)/Bhs2 horizon of Amity (compare Plates 4.32 and 4.10) or the Bhs2 portion to the Bhsb2 horizon of Mount Compass (compare Plates 4.32 and 4.18). The presence of very few moderately impregnated mainly typic monomorphic amorphous nodules with diffuse boundary could suggest *in situ* formation of this pedofeature. In the Bs2 horizon there is strong evidence of illuviation of fine material, occurring as non-laminated and microlaminated dense infilling (Plate 4.33), similar to Bsb3 horizon of Mount Compass (Plate 4.25). The main soil forming process in Bs2 is illuviation of fine organo-mineral complexes.

4.4.4. General discussion.

In all the three soil sequences studied there was a close relationship between age of profile and the degree of soil development. Two general groups of soil development were observed with subdivisions within each group.

Group one is represented by the calcareous sands (LeFevre Peninsula 1 and Canunda) which were the youngest profiles studied. There is hardly any pedogenesis in these profiles apart from (i) segregation of faunal excrements as one subdivision (LeFevre Peninsula 1 and shallower horizons of Canunda Bb1 and Ab2) and (ii) very minor crystalline (microcrystalline calcite) formation in deeper horizons of Canunda (Bb2 and Bb3).

In group two the podzol profiles developed from siliceous sands represent the different stages of podzolisation in profiles from south east coast of Queensland (Cooloola and North Stradbroke Island), central coast of South Australia (Mount Compass) and south east coast of South Australia (Mount Burr). In the absence of substantial clay in many of the horizons (A, E and B horizons, except for B2 and B3 of Mount Burr and Mount Compass respectively), the first subdivision of profile development is marked by the presence of various fragments of plant material in various stages of decomposition and faunal excrements in voids or coating grain surfaces in surface horizons (A or B, depending on the depth). This occurs more commonly in the younger profiles of Kings Bore and Chalambar. This is followed by the formation of thin sesquioxide grain coatings mainly in Bhs horizons of these younger profiles, with the thickness and completeness depending on age (Chalambar > Kings Bore). In older profiles with less clay in the subsurface horizons the Bs2 and B3 horizons have thin, complete sesquioxide coatings of more or less uniform thickness, such as in Bs2 and B3 horizons of Amity. Such coatings are proposed to form by diffusion processes where the material forming the coating (sesquioxide), forms either solution or suspension. The soil concentrates at the surface of the grains due to diffusion, equivalent to diffusion cutans of Brewer (1960). At this second sub-level there are isolated cases of faunal activity in the sub-surface horizons, leading to the homogeneous formation of organic dense complete infillings of voids. In the third subdivision the fine material (predominantly organic in origin) forms coatings of irregular thickness on grain surfaces (as in the Bhs2 horizon of the older profiles - Amity, Mount Compass and Mount Burr). Sometimes the coatings are highly

fractured. Parts of the horizon with more concentration of the organic dominated fine material form either loose continuous or dense incomplete void infillings. These stages of coating and infilling formation are ascribed to processes of wetting and drying causing gravitational movements, reaching maximum development around points of contact of the coarse fragments (e.g. Bhs2 horizon of Amity). In the fourth and final subdivision, which occurs in horizons or portions of it with appreciable amount of fine material, the coatings are much thicker and most of the voids are densely filled with organic and/or sesquioxidic rich fine material (e.g. B2 and B3 horizons of Mount Compass and B2 horizon of Mount Burr profiles). Such distribution patterns (chitonic-gefuric-porphyric) are governed by both wetting and drying activities (causing cracks, channel and planar voids) and illuviation (marked by micro-laminated and non-laminated dense infillings). The development of the deposits (coatings and infillings) in sections of the podzol profiles is quite simplified here. However, as shown by Farmer (1987) and Milnes and Farmer (1987), the formation of allophanic deposits in the B horizon of podzols is highly complex and involves alternating episodes of the influx of organic matter and the deposition of allophanic material. Layering of deposits as found in some B horizons (e.g. Bhs2 of Chalambar; Bhsb2/Bhsb3, Bsb3 and Bb4 of Mount Compass) suggests separate deposition episodes for the inorganic (allophane ?) and organic components in these podzols. This study shows that at least in Mount Compass profile the total clay maximum occurs in the Bsb3 horizon where illuviated clay maximum is also evident. The tentative conclusion is thus that all the clay in the B3 horizon is illuvial, and the acquired orientation around grains or voids is enhanced by stress forces due to wetting and drying. The concept of *in situ* clay formation could be inconsiderable because of the minimal evidence of mineral grain weathering in this horizon. The amount of clay is relatively higher and one would think if it was formed *in situ* many grains would show weathering features such as pellicular or linear alteration patterns (Bullock *et al.*, 1985). However, this was not so obvious in this horizon, but was in the horizons above, particularly the E. Alteration patterns on minerals in all the soils seemed to be

positively correlated with the amount of coating on the grains. In E, B2 and B3 horizons where grains are thinly coated (e.g. Kings Bore Bhs/B3, Chalambar A1/E, Seacliffs E/B1, Amity E/B1, Amity B3 and Mount CompassE(pipe)/B1) the alteration patterns on the grains are much more, with increase in and variable birefringence.

It is hypothesized that the degree of development, nature and distribution of material coating grain surfaces would affect the degree and extent of heavy mineral weathering. It is likely that in a porous medium with less coatings on the grains (e.g. A horizon) heavy mineral weathering will be different from those in a medium (e.g. Bhs and/or B3) in which grain surfaces are protected by coatings. This hypothesis will be more closely tested in Chapter 6 where surfaces of heavy mineral grains will be examined with the scanning electron microscope.

4.5. Conclusions.

Changes in the field morphological properties (e.g. consistence) of the soil mass seemed to be intimately related to the changes in the related distribution patterns of the fine fraction. These were most apparent in the zones of substantial accumulation of organic and sesquioxide rich fine materials.

Similar processes appear to have been involved in the formation of the profiles at LeFevre Peninsula and Canunda on one hand, and Cooloola, North Stradbroke Island, Mount Compass and Mount Burr on the other. The major differences in the LeFevre Peninsula and Canunda profiles are reflected in the nature and distribution of the coarse and fine material, both of which tend to be randomly distributed in each profile. In the Canunda profile there are more carbonate containing coarse and fine material and the organic fine material^{is} more highly developed (more coalesced and homogeneous) at shallower depths. In profiles from Cooloola, North Stradbroke Island, Mount Compass and Mount Burr the major differences are reflected in the distribution of illuvial clay rich coatings and infillings which tend to show up substantially in the Mount Compass profile.

CHAPTER 5

WEATHERING ASSESSMENT USING SCANNING ELECTRON MICROSCOPY

5.1. Introduction

Heavy minerals have been widely used in pedological and sedimentological studies because of their supposed resistance to chemical and physical breakdown and because they are indicators of the provenance of a sediment. On the assumption that they have remained relatively immobile and unweathered, many workers have attempted to estimate the degree of chemical weathering of other minerals (e.g. Beavers *et al.*, 1963; Chittleborough *et al.*, 1984), the loss or gain of particular constituents (e.g. Barshad, 1965; Evans and Adams, 1975 b) and the volume, thickness and weight changes of the parent material in forming a particular horizon (Brewer, 1964). In view of the central role which heavy minerals play in soil studies, it is surprising that there have been few attempts to test the assumption of relative resistance to weathering and further, to define the conditions under which various "resistant" minerals may weather (e.g. Bateman and Catt, 1985; Milnes and Fitzpatrick, 1989).

In most soils, heavy minerals (density $> 2.96 \text{ Mgm}^{-3}$) occur in very low concentrations, typically $< 2 \%$ of the fine sand fraction. Studies involving the nature and properties of heavy minerals in soils are restricted because of (a) the low concentration and the difficulty in counting under the optical microscope sufficient grains to be statistically significant and (b) the lack of high resolution analytical electron microscopes which facilitate the identification of minerals and chemical alteration products on the surfaces of grains.

Descriptive surface microtextural features of mineral grains as revealed by scanning electron microscopy (SEM) has been used to infer mineral weathering mechanisms (e.g. Rahmani, 1973; Berner and Schott, 1982). Most of the descriptions of the degree of surface microtextural alteration have been qualitative, with adjectives

or integers used to qualify the nature and type of surface feature (Creemeens *et al.*, 1987). Also different quantitative approaches have been used to analyse heavy mineral data in relation to environmental parameters (e.g. Bateman and Catt, 1985). Setlow and Karpovich (1972) reported a semiquantitative method of analysing the abundance of microtextural features on grains and used the result to evaluate environmental conditions and processes to which the grains were once subjected. More recently Baker (1976) and Darmody (1985) devised semiquantitative methods of assessing environmental sensitivity and weathering of quartz grains based on a binary scoring system. Multivariate statistical techniques have also been used to analyse SEM data with the purpose of determining the relationship between grain surface microtextures and origin of sand grains (e.g. Bull, 1978). In all such quantitative analysis it has been shown that the techniques are invaluable for evaluating trends which require the simultaneous assessment of several grain surface features. The conventional descriptive analysis *per se* cannot achieve this, in particular it cannot show trends in mineral weathering or readily summarize the combined effects of different variables. The study reported in this chapter describes the development of an ordinal weathering scale, based on the nominal scale methods of Setlow and Karpovich (1972) and Darmody (1985), and the application of the scale to the assessment of the relative weathering of heavy minerals.

The objectives of this chapter are therefore: (i) to describe a semiquantitative method, based on grain surface microtextures, for assessing the degree of heavy mineral alteration and (ii) to demonstrate its efficacy in weathering studies of six Australian sandy soil age sequences.

5.2. Materials and methods

5.2.1. Soil samples.

The samples were collected from sites within the regions discussed in Chapter 2. Two or more sets of soil profiles comprising an age sequence (see Chapter 3) were sampled from two locations within each region. Two of the locations were on the

south eastern coast of Queensland (Coolooloa and North Stradbroke Island), two were along the central South Australian coast (LeFevre Peninsula and Mount Compass) and two in the south east region of South Australia (Mount Burr and Canunda) (Fig. 2.1).

At Coolooloa all eight soils constituting the chronosequence, namely Carlo (CL), Kings Bore (KB); Chalambar 1 (CH); Burwilla 1 (BW); Warrawonga 1 or Seacliffs (SC); Warrawonga 2 (WA), Mundu 4 (MU) and Kabali 2 (KL) were sampled (Fig. 2.2). At North Stradbroke Island, one soil profile (AM) was sampled at a site near Amity (Fig. 2.3).

The two soils sampled from the Le Fevre Peninsula (Fig. 2.4) are part of an age sequence (see Chapter 3), with the two soil profiles from the youngest (1LP) and the oldest (2LP) sedimentary units within this sequence.

In the south east of South Australia the Canunda and Mount Burr (Fig. 2.6) soil profiles were studied. These soils also constitute an age sequence (see Chapter 3).

The depths at which all samples were taken are given in Appendix 2.

5.2.2. Laboratory analysis.

Twenty x 25 g subsamples of soil from each horizon were pretreated by an ultrasonic probe using 10 ml 10 % calgon, 5 ml 1 M NaOH, and 100 ml deionized water, and passed through 125 μm and 53 μm sieves. The 53-125 μm fractions were combined for each horizon and heavy minerals isolated by gravitation in a sodium polytungstate, $\text{Na}_3\text{WO}_4 \cdot 9\text{WO}_3 \cdot \text{H}_2\text{O}$ (Sometu, Falkenried 4, D-100 Berlin, FRG), solution of density 2.96 Mgm^{-3} . Each fraction was washed, dried and weighed. The 53-125 μm fraction was chosen for the various reasons: (i) to limit the variations in mineral proportions with grain size (Cogen, 1935) and (ii) there are relatively higher concentrations of heavy minerals in this fraction based on previous studies (Beasley, 1950; Golding, 1955 and Colwell, 1979). Each fraction was washed, dried and weighed. The heavy mineral fractions were further separated magnetically using a very strong hand magnet to collect the strongly magnetic fraction, and a Frantz Isodynamic Separator to isolate the non- and slightly-magnetic fractions. The following settings

(Flinter, 1959) were used: forward slope 20° , side slope 15° , 1 amp current (for the non-magnetic fraction) and 0.5 amp current (for the slightly magnetic fraction).

Subsamples of the non-magnetic and slightly magnetic fractions were ground to fine powders in a McCrone micronising mill and analysed using a Philips x-ray diffractometer with $\text{CoK}\alpha$ radiation and graphite monochromator, a step interval of $0.01^\circ 2\theta$ and a 0.2 second count per step. Where the amount of sample was insufficient for powder x-ray diffraction (XRD) analysis, the Gandolfi camera was used to obtain diffraction patterns for 6 replicates of individual grains of the dominant heavy minerals (Gandolfi, 1967). The camera was mounted on a Philips x-ray diffractometer with $\text{CoK}\alpha$ radiation, a current of 60 mA and accelerating voltage of 40 kV. Subsamples of the non- and the slightly-magnetic fractions were mounted on stubs and coated with either Au-Pd or C. Thirty grains of each mineral were identified and photographed on either a Cambridge 250 or a Philips 505 scanning electron microscope equipped with energy dispersive X-ray analysers (EDAX). Each grain was analysed for 10 surface features (Table 5.1) according to a modified procedure of Darmody (1985). Fig. 5.1 shows a flow chart of the techniques used in the heavy mineral investigations. Zircon and rutile were analysed for all horizons in all the soil sequences. Sillimanite was analysed for all soil age sequences except those from Cooloola and North Stradbroke Island. Garnet, monazite, spinel and epidote were studied in selected horizons within the Cooloola age sequence. The A1, B3 and C horizons of the Kings Bore and Chalambar profiles and the E and Bhs2 horizons of Kings Bore, Chalambar and Seacliffs, were studied for all four mineral types. Monazite, spinel and epidote were studied in the B2 horizon of Chalambar and Seacliffs.

5.2.3. Weathering assessment.

The degree of weathering of heavy mineral types was assessed by measuring electronoptically (SEM) microtextural features using two modified methods, that of Darmody (1985), and Setlow and Karpovich (1972). The stubs were coded and the

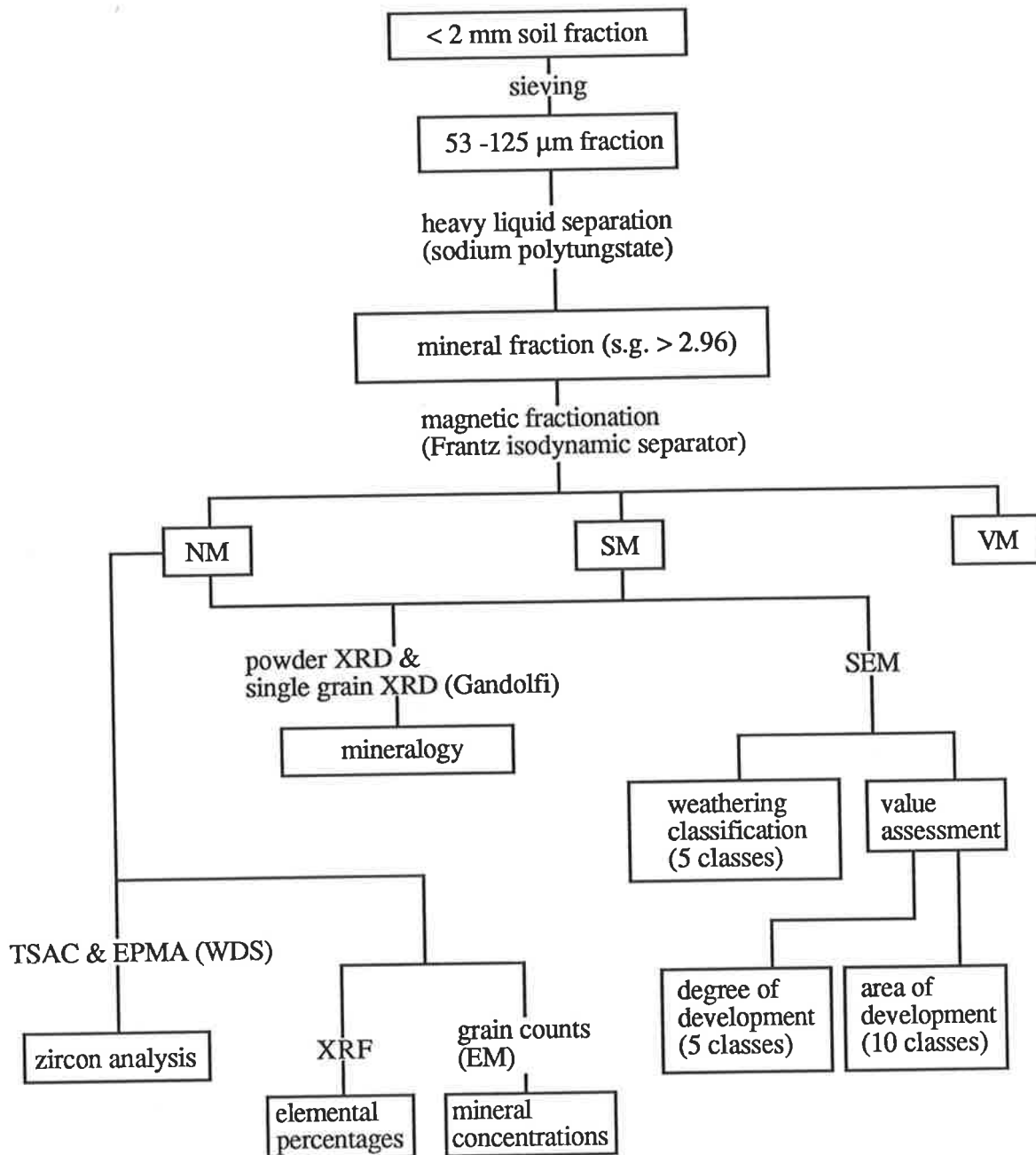


Fig. 5.1. Flow chart of laboratory methods.

Table 5.1. Surface microtextural features of heavy mineral grains used in assessing weathering class.

Surface feature no.	Assigned feature†	Point value‡	Max. value assessment§
1	High relief	+ 1	+ 50¶
2	Clean/smooth fracture or cleavage faces	+ 1	+ 50
3	Arc-shaped/parallel/semi-parallel steps	+1	+ 50
4	Sharp edges and angular grains	+ 1	+ 50
5	Conchoidal fractures/breakage blocks/v-shaped pits	+ 1	+ 50
6	Solution	- 1	- 50
7	Scaling or surface roughness	- 1	- 50
8	Oriented or random etch pits	- 1	- 50
9	Subdued edges and rounded grains	- 1	- 50
10	Hairline cracks	- 1	- 50

† and ‡ Modified from and based on Darmody (1985) respectively.

§ Based on Setlow and Karpovich (1972).

¶ Value based on the product of the maximum degree of development and the maximum area of development.

ratings given in Sections 5.2.3.1 and 5.2.3.2 below were assigned in a blind manner. That is, the source of the sample was unknown during observations.

5.2.3.1. *Point value score (PVS) method.*

A binary scoring system was used to denote the presence or absence of the different surface features on the grains (Table 5.1), with a positive point and a negative point assigned to grains with surface features indicative of "freshness" and weathering respectively (Darmody, 1985). A point value of zero indicated absence of a surface feature. The point value score (PVS) for a grain was derived from the summation of the point values for that grain (Table 5.1). The mean of thirty point value scores for each mineral type was called the mean point value score (MPVS). Based on the MPVS, minerals were assigned to one of five weathering classes (Table 5.2).

Table 5.2. Weathering classification of heavy mineral grains.

Class no. †	Weathering classification †	Mean point value score (MPVS) †	Mean value assessment score (MVAS) range
1	Highly weathered	- 4, - 5	- 150 to - 250
2	Weathered	- 2, - 3	- 50 to - 149
3	Somewhat weathered	1, 0, - 1	49 to - 49
4	Slightly weathered	3, 2	149 to 50
5	Essentially unweathered	5, 4	250 to 150

† Based on Darmody (1985).

5.2.3.2. *Value assessment score (VAS) method.*

Assessment of weathering of individual mineral types based only on presence or

absence of surface features using PVS implies nothing about the extent and magnitude of the different surface features on grains. A transformation of the point value to a value assessment was needed to take into account both the *degree* of development (i.e. intensity) and the *area* of development (i.e. magnitude) of the individual surface features. The value assessment criteria of Setlow and Karpovich (1972) were adopted (Table 5.3).

Table 5.3. Value assessment of heavy mineral grain micro-textures (after Setlow and Karpovich, 1972).

Degree of Development	Value	Area of Development	Value
Dominant	5	Widespread over entire grain	9-10
Abundant	4	Widespread over major portion of grain	6-8
Common	3	Present over regional portion of grain	3-5
Present (few)	2	Local	1-2
Rare	1		
Absent	0	Absent	0

In their scheme the area and degree of development of surface features are categorized and assigned numerical coefficients. The positive and negative point values are transformed to positive and negative value assessments respectively (Table 5.1), after multiplying the value of the degree of development by the value of the area of development. The maximum value assessment was 50 (Table 5.1), based on a degree of development value of 5 and an area of development value of 10. Minimum value assessment was 0, based on a degree of development value of 0 and an area of development value of 0; in other words the feature was absent. The value assessment

score (VAS) was derived from the summation of individual value assessments. A maximum VAS of +250 was given for maximum occurrence of all five features indicative of freshness, and a maximum value assessment of -250 for maximum occurrence of the five surface features indicative of weathering. The mean value of individual value assessments scores (MVAS) for the ten classes of surface features on thirty grains was used to define the degree of weathering. Based on the MVAS, minerals were assigned to one of five weathering classes (Table 5.2).

5.2.3.3. *Statistical analysis.*

The individual point value scores and value assessment scores were statistically analysed using the Kruskal-Wallis test (Kruskal and Wallis, 1952). This nonparametric test was adopted for three reasons. The data was nominal (grains were assigned a particular score), the nature of the frequency distribution of surface features on mineral grains was unknown and there was little control over sample randomization. Nonparametric statistics are more flexible given these constraints (Siegel, 1956). The Kruskal-Wallis H statistics were evaluated against the χ^2 distribution with the corresponding degree(s) of freedom as tabulated in statistics texts.

Three null hypotheses (H_0) were tested. First, that different minerals within the same horizon of a soil profile have identical weathering patterns. Secondly; that the same mineral types in different horizons within the same soil profile have identical weathering patterns. Thirdly; that the same mineral types in similar horizons within different soil profiles of a regional soil age sequence have similar weathering patterns. The criterion for the rejection of a null hypothesis was a value of H greater than, or equal to, the probability under H_0 at 0.05 level of significance (α).

5.3. Results

5.3.1. X-ray diffraction and SEM-EDAX.

Powder XRD patterns for the non-magnetic fraction show that zircon and rutile are the dominant components in all the samples, as shown in Figs. 5.21 and 5.22 for the A2 horizons of Kings Bore and Chalambar respectively. Relative to rutile, zircon reflection intensities are higher in the younger profile (Kings Bore) than in the older profile (Chalambar). In quantitative terms this does not necessarily imply that zircon dominates the non-magnetic heavy mineral suite of Kings Bore, as there are a number of factors other than the concentration of the species (e.g variations in sample packing and crystal orientation) that influence the diffraction intensities of mineral species within a sample. The quartz peaks in the diffractograms are mainly due to a rutilated-quartz phase (Plate 5.1) in these assemblages and minor contamination from the heavy mineral separation. Gandolfi camera photos were taken of single grains to confirm the presence of rutilated-quartz grain (Plate 5.2). Single grains examined using the Gandolfi camera showed that the accessory heavy minerals were predominantly sillimanite, garnet (grossularite), spinel (Cr-spinel) and epidote (zoisite) (Plate 5.2). The minerals were identified using a combination of the ASTM index and direct comparison with standard mineral photographs. Monazite was identified by SEM-EDAX on the basis of high concentrations of Ce, La, Th and P (Fig. 5.3).

5.3.2. Relative weathering assessment.

SEM investigation of the different heavy minerals in the soils studied showed the presence of the full range of surface microtextures mentioned in Table 5.1. Minerals from different soil horizons (Plate 5.3) were used as an example to develop the weathering classification using the PVS and VAS methods (Table 5.4). Both zircon and rutile were classified as weathered and somewhat weathered by the PVS and VAS methods respectively. Epidote on the other hand was classified as highly weathered and weathered (Table 5.4). The weathering classification of the other minerals based

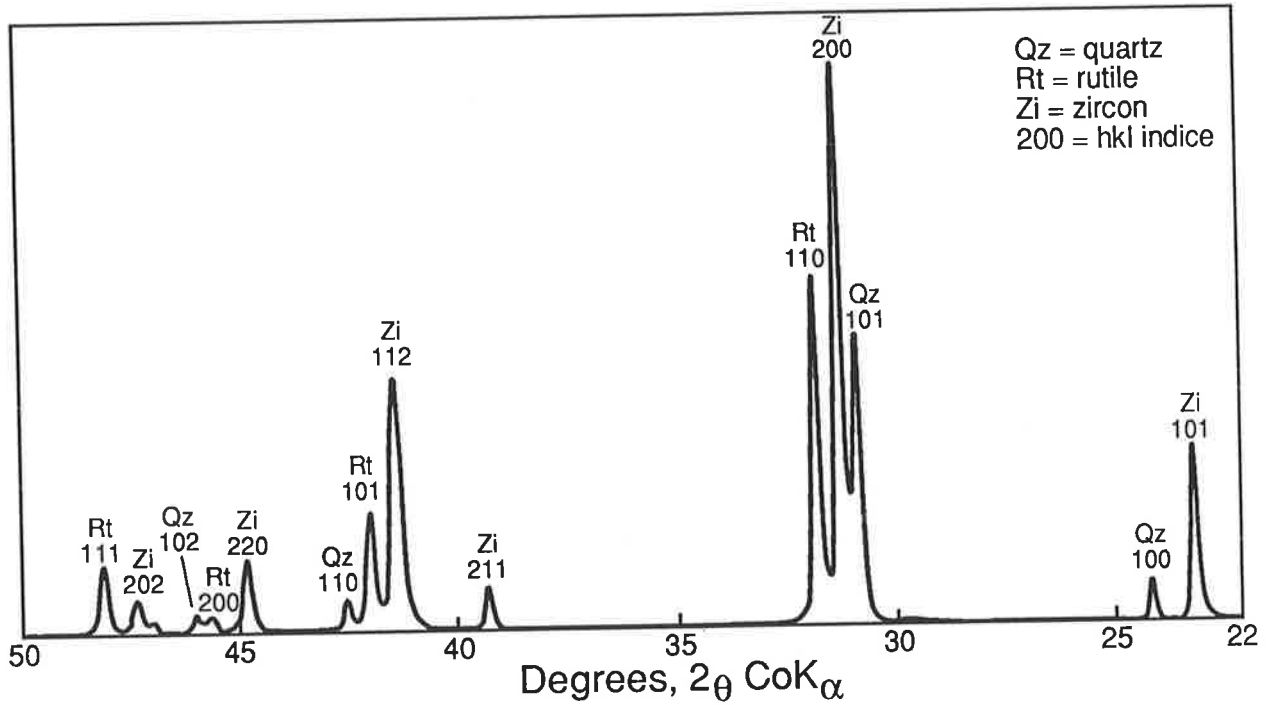


Fig. 5.21. Powder X-ray diffraction pattern of non-magnetic heavy mineral fraction in the E horizon of Kings Bore profile.

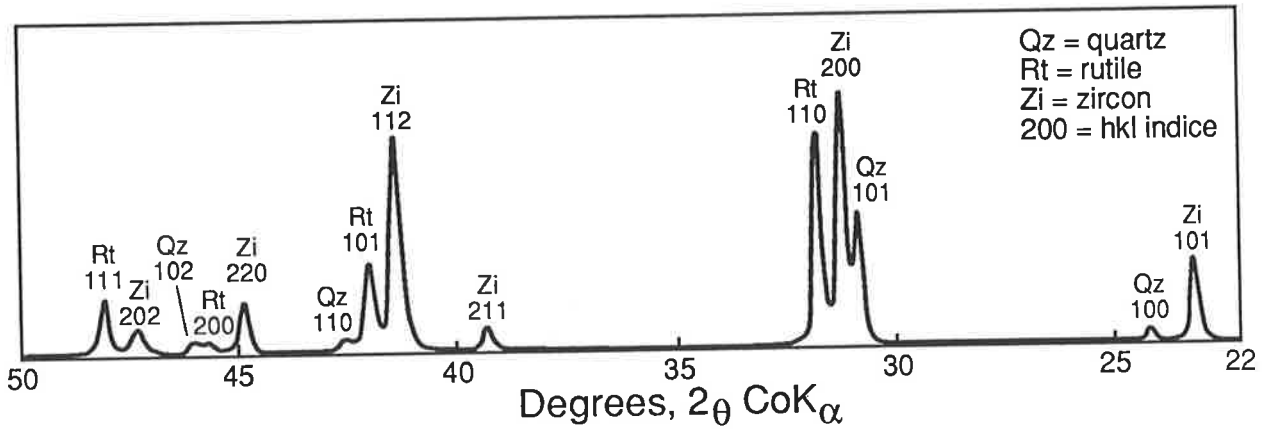
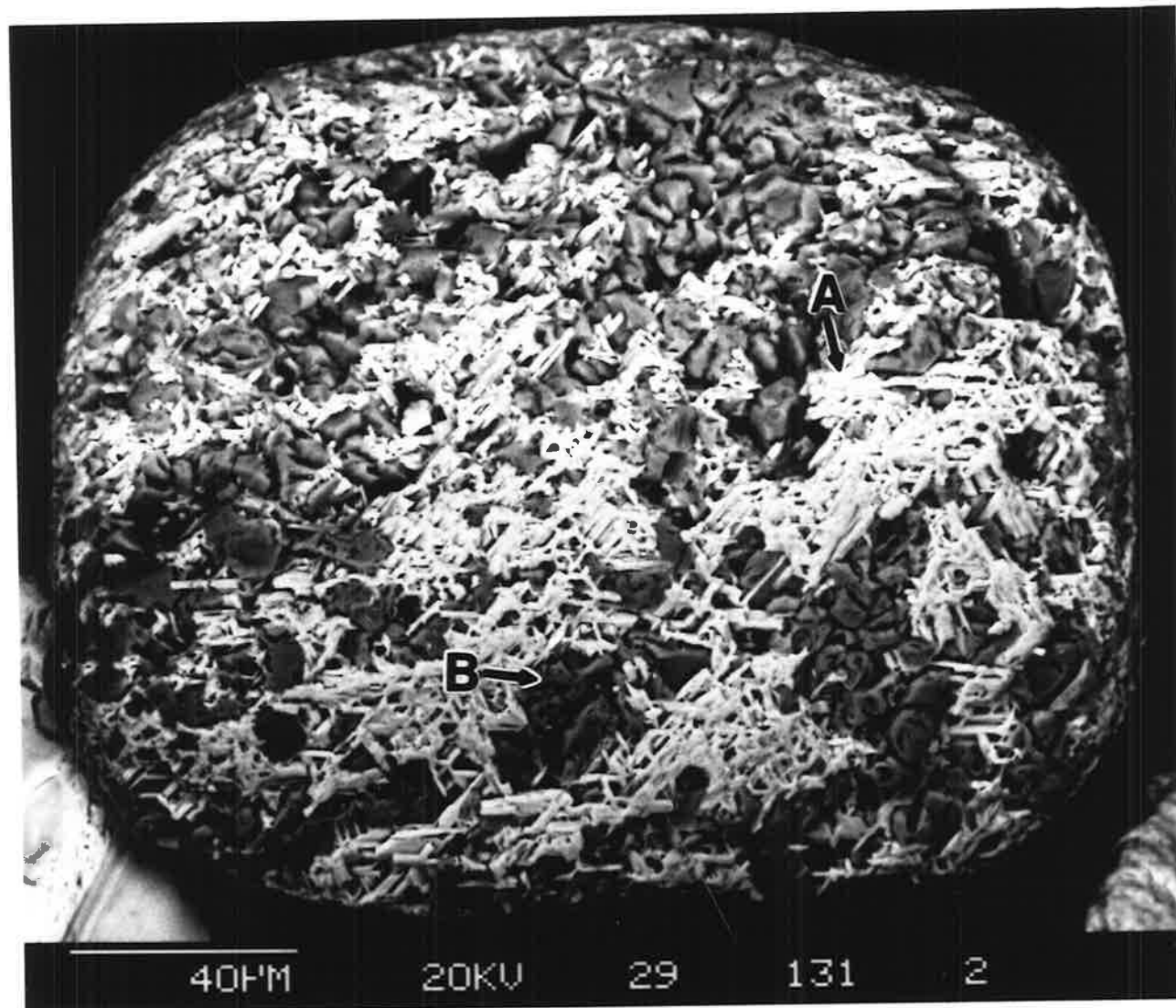


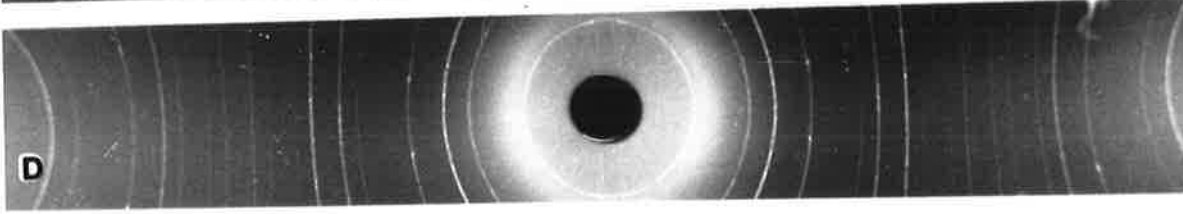
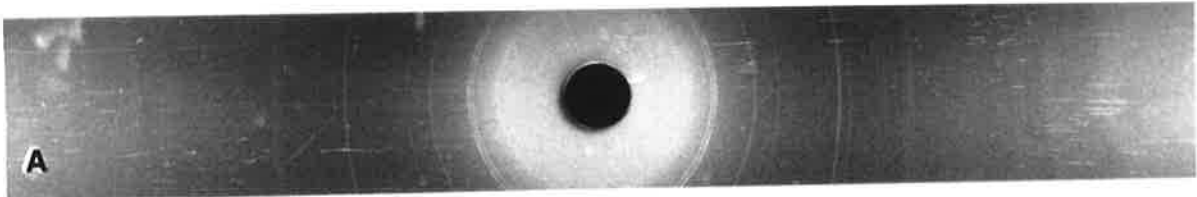
Fig. 5.22. Powder X-ray diffraction pattern of non-magnetic heavy mineral fraction in the E horizon of Chalambar profile.

Plate 5.1. Scanning electron micrograph of rutiled-quartz grain from E horizon of Kings Bore. Note, (A) and (B) indicate portions of rutile and quartz respectively.



5.1.

Plate 5.2. X-ray diffraction patterns of rutilated-quartz and heavy minerals:
(A) rutilated quartz from E horizon of Kings Bore, (B) sillimanite from
A1 horizon of LeFevre Peninsula 2, (C) garnet (grossularite) from Bhs2
horizon of Kings Bore, (D) spinel (Cr-spinel) from E horizon of
Chalambar and (E) epidote (zoisite) from C horizon of Chalambar.
Note, all patterns taken using a Gandolfi single-grain camera and
CoK α radiation.



5.2.

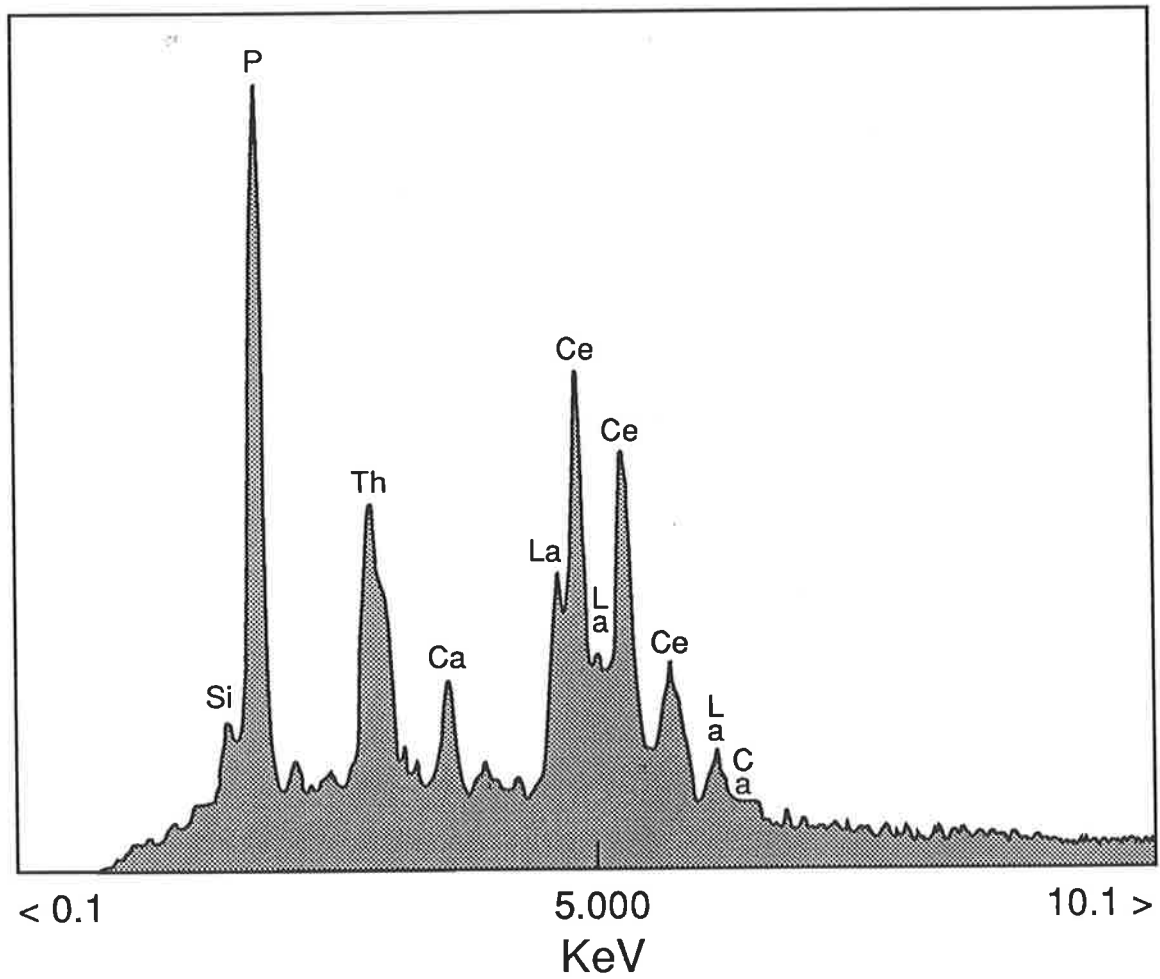


Fig. 5.3. EDAX spectrum for monazite from E horizon of Seacliffs profile.

Plate 5.3. Scanning electron micrographs of selected heavy mineral grains:
(A) zircon, (B) rutile, (C) sillimanite, (D) garnet, (E) monazite,
(F) spinel and (G) epidote used for weathering classification
system outlined in Table 5.5.

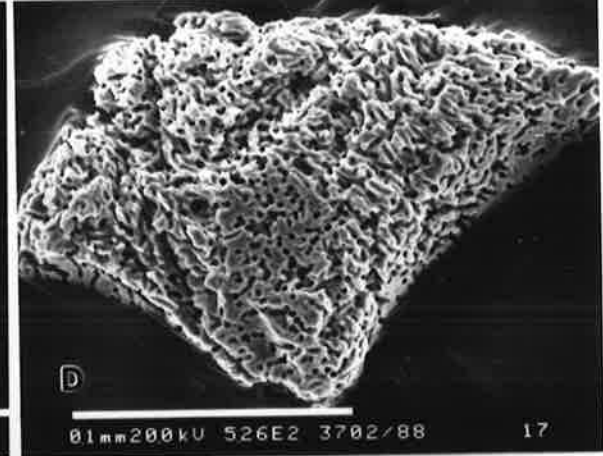
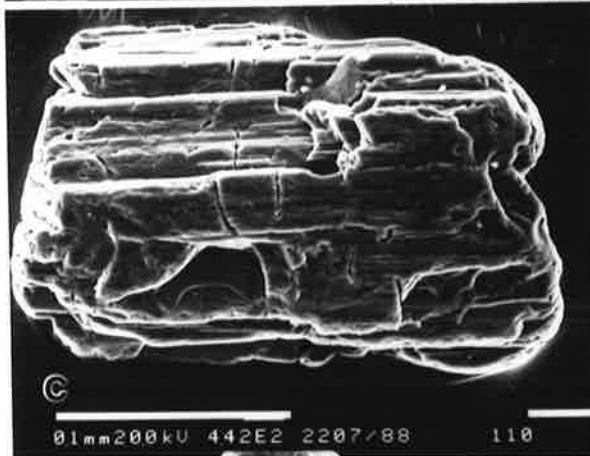


Table 5.4 Weathering classification of minerals based on mean point value score (MPVS) and mean value assessment score (MVAS).

Surface [†] feature	Zircon		Rutile		Sillimanite		Garnet		Monazite		Spinel		Epidote	
	PV	VA	PV	VA	PV	VA	PV	VA	PV	VA	PV	VA	PV	VA
High relief	+1	2,2	+1	3,4	+1	3,4	0		0		+1	2,5	+1	2,2
Clean faces	+1	3,4	+1	1,2	+1	2,2	0		0		+1	1	0	
Arc-shaped steps	0		+1	1,1	0		0		0		0		0	
Angular grains	+1	2,3	0		0		0		0		0		0	
Conchoidal fracture	0		0		+1	3,5	0		0		0		0	
Solution	-1	3,4	-1	2,3	-1	2,3	-1	4,9	0		0		-1	4,9
Scaling	-1	2,3	-1	3,5	0		-1	4,10	0		-1	2,2	-1	3,3
Etch pits	-1	2,2	-1	4,7	-1	2,3	-1	5,10	-1	5,10	-1	3,4	-1	2,2
Subdued edges	-1	1,1	-1	3,6	-1	3,4	-1	4,8	-1	5,9	-1	3,4	-1	4,8
Hairline cracks	-1	2,2	-1	1,1	-1	3,4	0		0		0		-1	1,1
<u>Score and Classification</u>														
MPVS	-2¶		-2¶		-1		-4		-2		-1		-4‡	
MVAS	-5#		-43#		1		-158		-95		-17		-78§	
Classification	¶weathered #somewhat weathered		¶weathered #somewhat weathered		somewhat weathered		highly weathered		weathered		somewhat weathered		‡highly weathered §weathered	

PV and VA = point value and value assessment respectively from Table 5.1.

† Full description given in Table 5.1.

on both the PVS and VAS methods showed that sillimanite and spinel were somewhat weathered and monazite was weathered (Table 5.4). Although it is stated that the mineral with the highest negative PVS and VAS value is the most highly weathered, there are possible causes of misinterpretation. First, the PVS method tends to exaggerate the weathering class to which a mineral belongs. The minor presence of a surface microtexture indicative of freshness, for example, will offset the major presence of another surface microtexture indicative of weathering. As an example, in Table 5.4 zircon, rutile and epidote are classed as weathered and highly weathered using the PVS method and slightly weathered and weathered using the VAS method. Fortunately such situations were rare in the entire study and were mainly a problem for highly weathered mineral grains. Secondly, for the assessment of the VAS, minerals, particularly the highly weathered grains dominated by only one surface feature, may be underestimated where the feature is dominant over the entire grain. Counting large numbers of grains (30 grains in the present study) improved confidence in the results and, although the methods are subjective to some extent, they nevertheless provide a framework for studying weathering of minerals in soils formed in stratified materials.

5.3.2.1. Weathering trends between minerals.

Soil profiles from Cooloola for which zircon, rutile, garnet, monazite, spinel and epidote were analysed showed a general weathering sequence (with the least weathered mineral first) viz zircon > spinel > rutile > garnet > monazite > epidote (Figs. 5.401 to 5.406). In the Cooloola-North Stradbroke Island sequence soils for which only zircon and rutile were examined gave the sequence zircon > rutile (Figs. 5.407 to 5.410).

The experimental data given in Figs. 5.412 to 5.414 and 5.421 to 5.424 represent zircon, rutile and sillimanite analysis in soils from central and south east coastal regions of South Australia. The results show a somewhat consistent weathering trend with a decreasing order of resistance from zircon > sillimanite > rutile. In the B3 horizons of Mount Compass profile (Figs. 5.412 and 5.414)

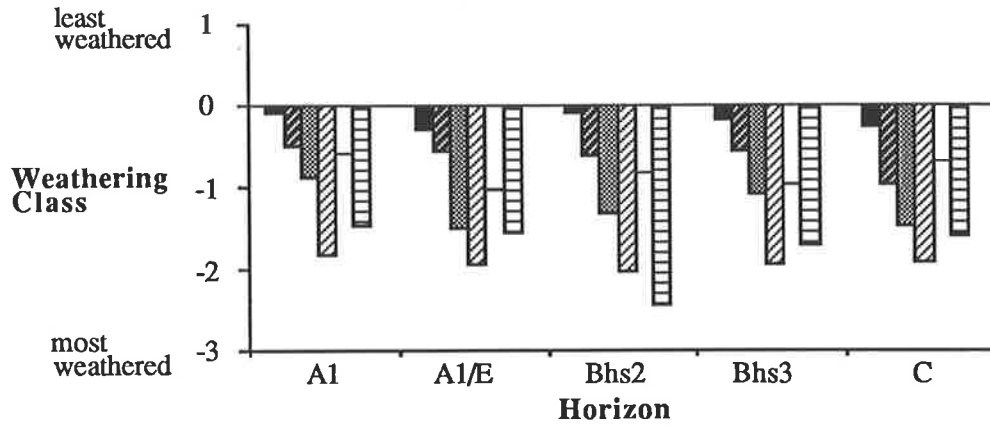


Fig. 5.401. Kings Bore profile, mean point value scores.

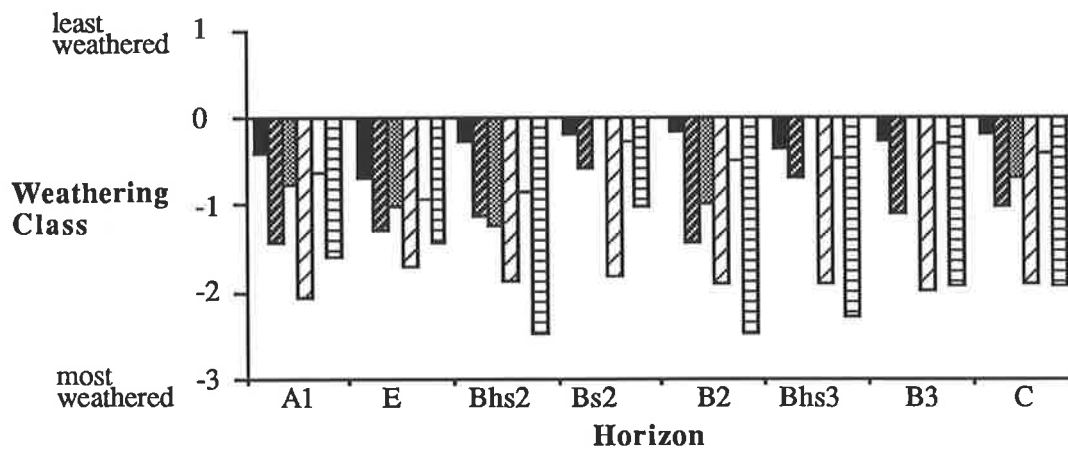


Fig. 5.402. Chalambar profile, mean point value scores.

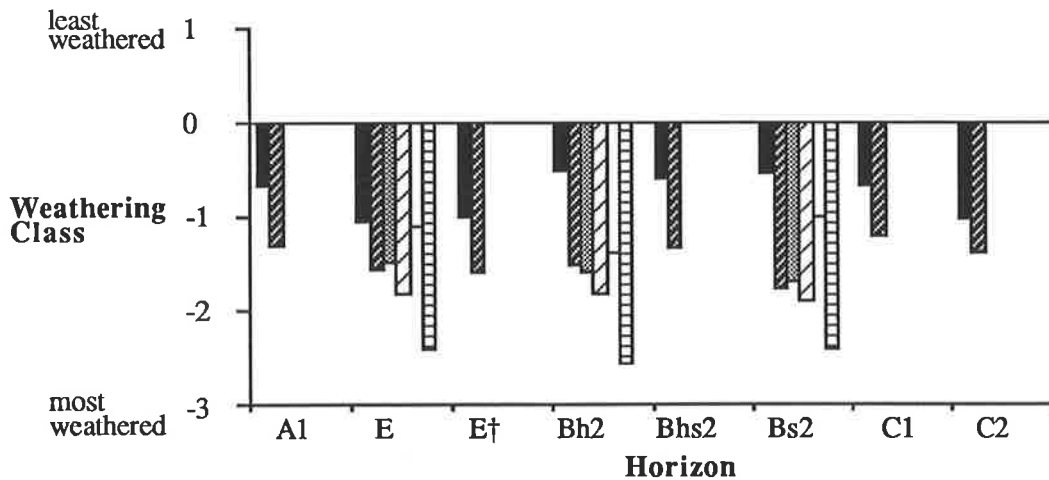
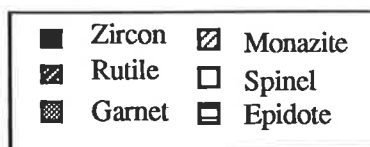


Fig. 5.403. Seacliffs profile, mean point value scores. † = pipe.

Fig. 5.40. Weathering of different minerals in soils from the south east coast of Queensland based on mean point value and value assessment scores of 30 grains.



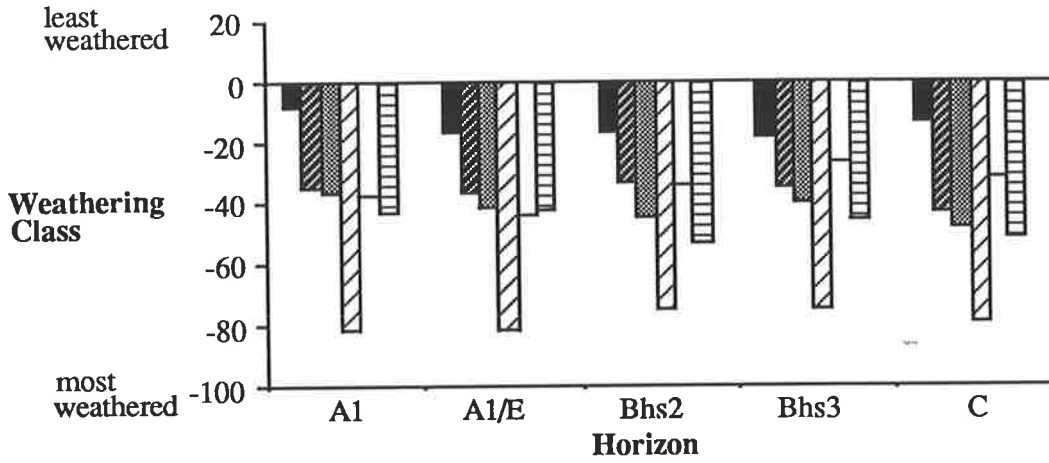


Fig. 5.404. Kings Bore profile, mean value assessment scores.

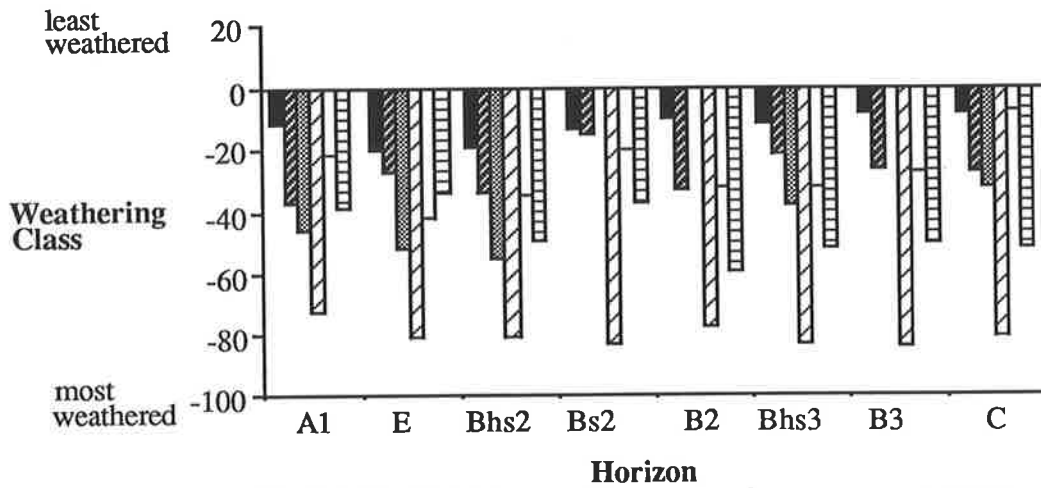


Fig. 5.405. Chalambar profile, mean value assessment scores.

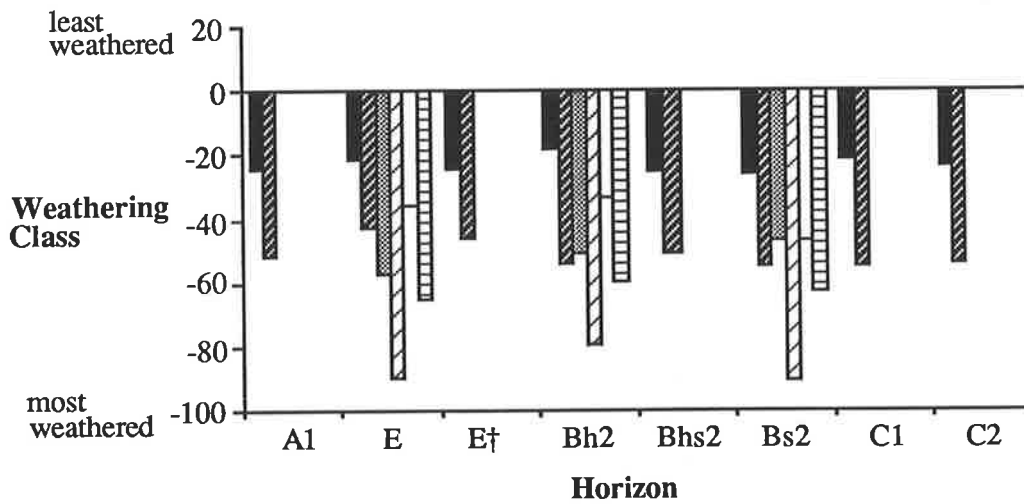
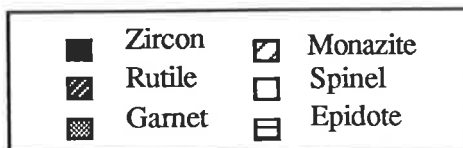


Fig. 5.406. Seacliffs profile, mean value assessment scores.
† = pipe.

Fig. 5.40. contd.



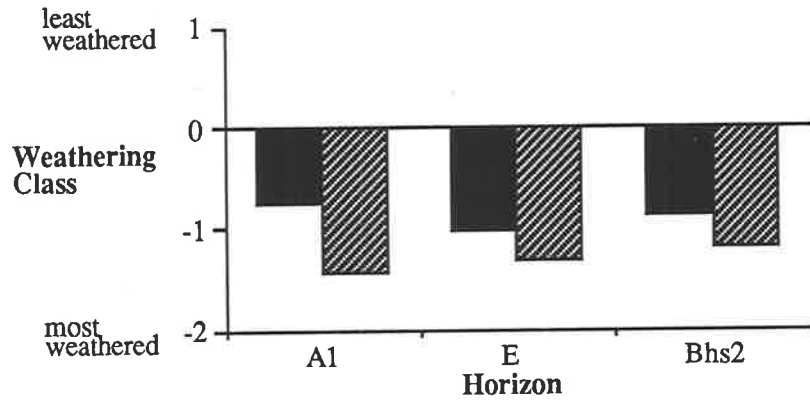


Fig. 5.407. Warrawonga profile, mean point value scores.

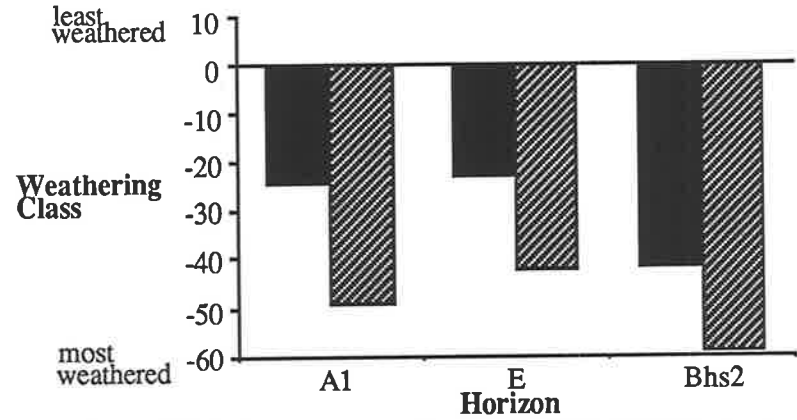


Fig. 5.409. Warrawonga profile, mean value assessment scores.

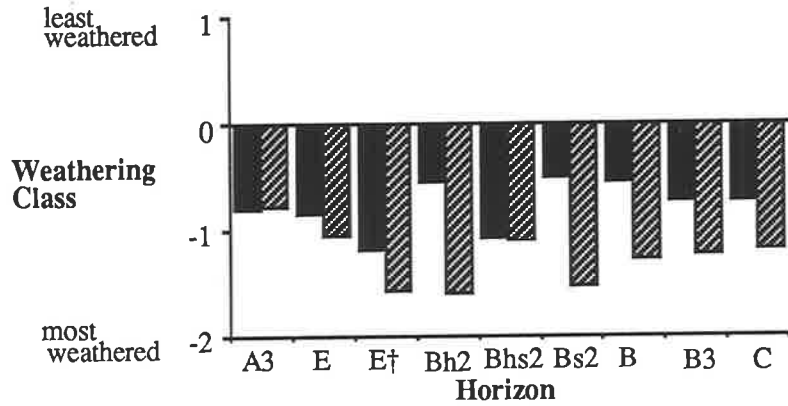


Fig. 5.408. Amity profile, mean point value scores. † = pipe.

Fig. 5.40. contd.

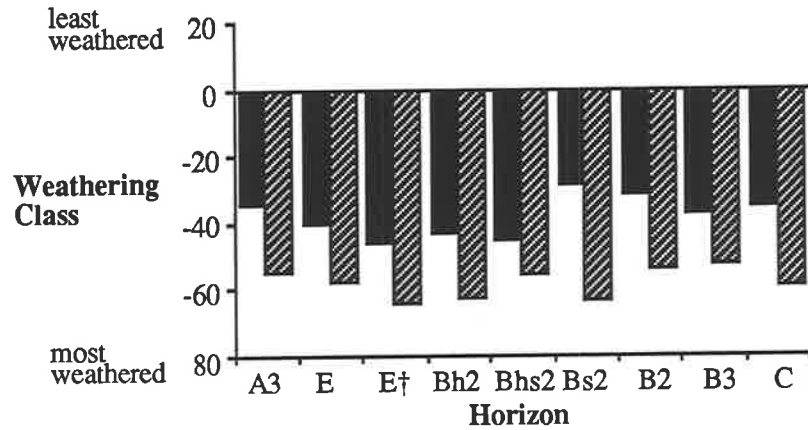


Fig. 5.410. Amity profile, value assessment scores. † = pipe.



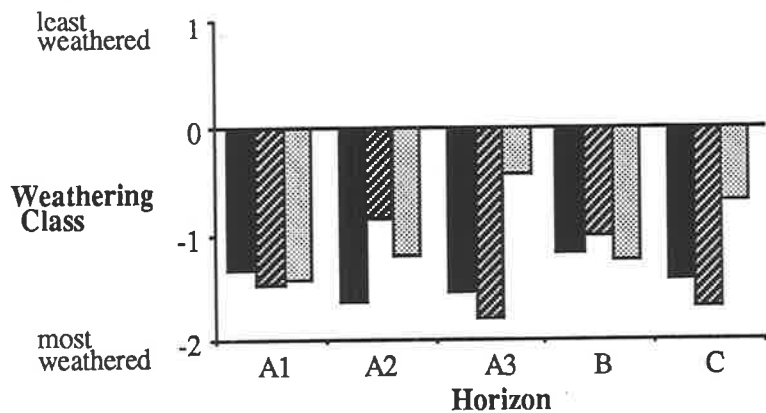


Fig. 5.411. LeFevre Peninsula 2 profile, mean point value scores.

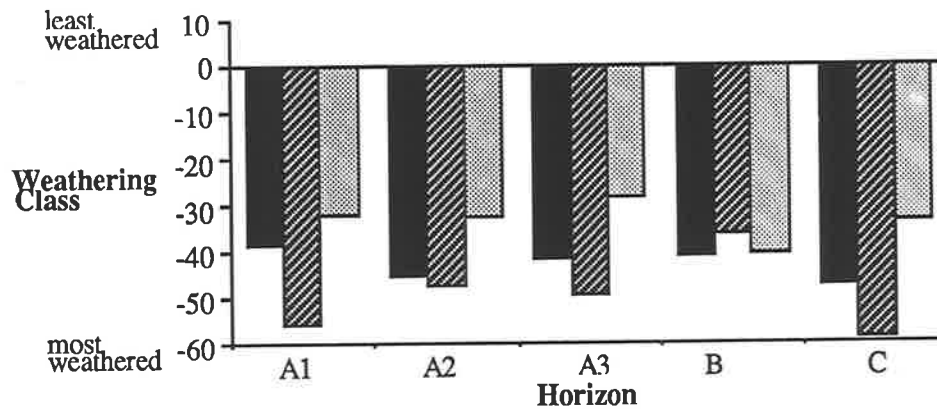


Fig. 5.413. LeFevre Peninsula 2 profile, mean value assessment scores.

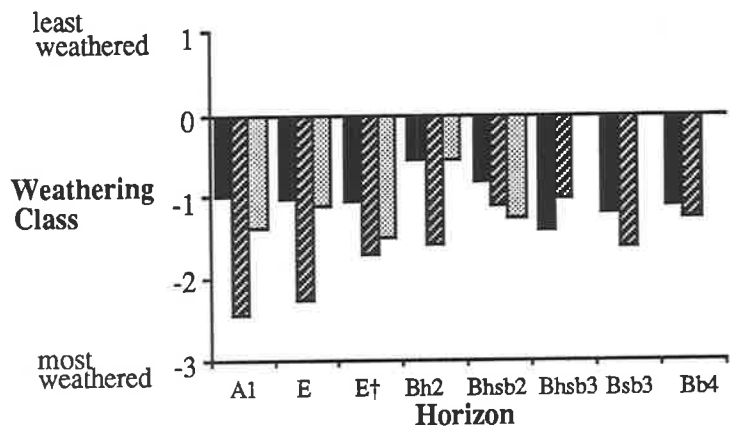


Fig. 5.412. Mount Compass profile, mean point value scores.

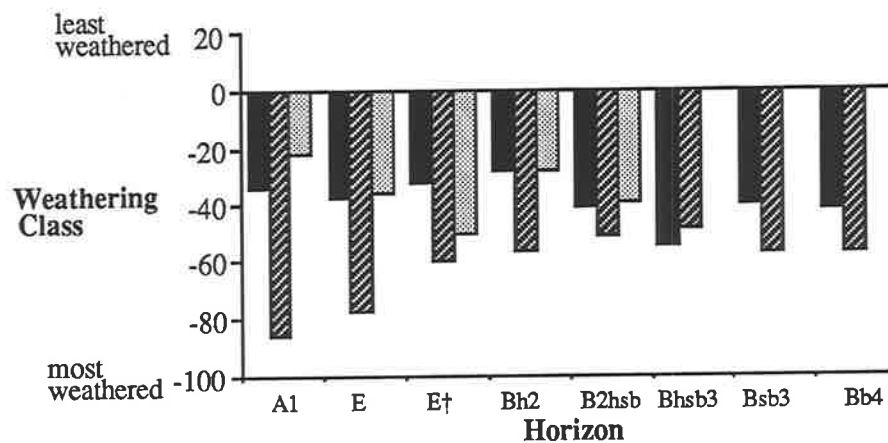


Fig. 5.414. Mount Compass profile, mean value assessment scores.

Fig. 5.41. Weathering of different minerals in soils from the central South Australian coast based on mean point value and value assessment scores of 30 grains.



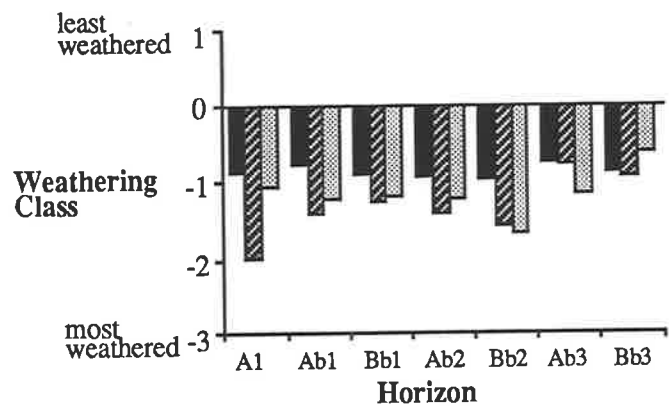


Fig. 5.421. Canunda profile, mean point value scores.

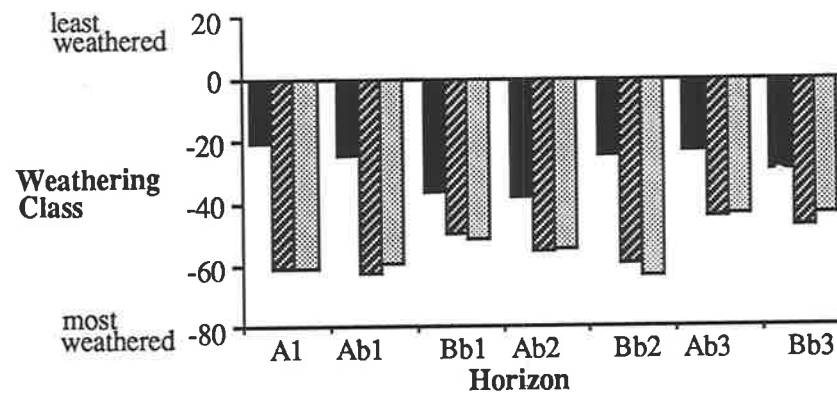


Fig. 5.423. Canunda profile, mean value assessment scores.

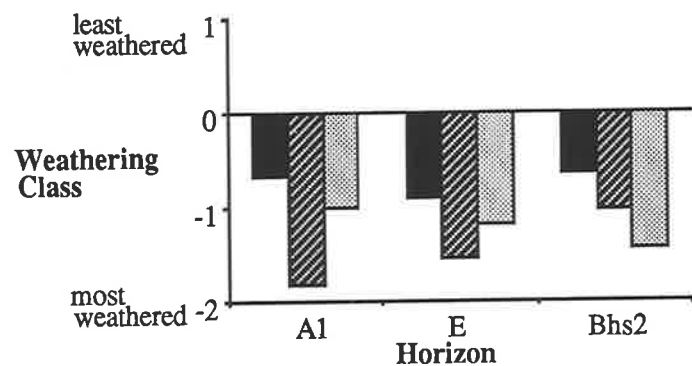


Fig. 5.422. Mount Burr profile, mean point value scores.

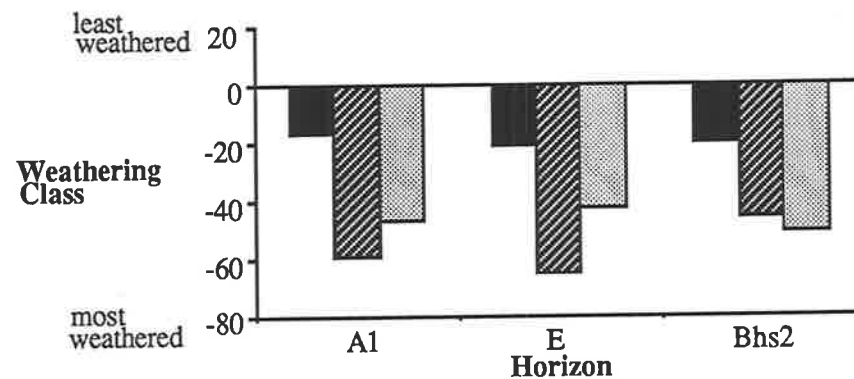


Fig. 5.424. Mount Burr profile, mean value assessment scores.

Fig. 5.42. Weathering of different minerals in soils from the south east South Australian coast based on mean point and value assessment scores of 30 grains.



sillimanite did not occur, although it was present in the overlying horizons.

The general trends in mineral resistance to weathering were similar for both PVS and VAS methods in all soils studied. However, there were deviations from these general trends in some horizons, particularly the younger, less developed soils from LeFevre Peninsula and to some extent Canunda (Figs. 5.411, 5.413 and 5.421, 5.423). This indicated that the effects of pedogenesis on the relative weathering trends of minerals were not as important in these very young soils compared with the older profiles.

5.3.2.2. Weathering trends within profiles.

Figures 5.401 to 5.424 show the relationship between mineral weathering patterns in different horizons within profiles. The patterns show a weaker and less consistent relationship with horizon type. Specific weathering trends were shown for some profiles (e.g. Chalambar and Seacliffs; Figs. 5.402, 5.403 and 5.405, 5.406) in which the order was generally $E \geq A1 \approx E \text{ (pipe)} \geq B2/Bs2 > Bhs > B3/C$. However, the overall differences in all the profiles could not be related to the types of horizons. This indicated that the weathering of these minerals were not only related to the *in situ* soil environmental factors, but to other extrinsic factors.

5.3.2.3. Weathering trends between profiles.

The PVS and VAS weathering patterns of minerals in the A, E, B2hs, other B2, B3, C and AC horizons of soils from different profiles in the three regions are given in Figs. 5.431 to 5.472. There were no overall general trends in the resistance to weathering of minerals with respect to comparable horizons from the different profiles. However, on a regional basis there were weak trends in mineral weathering, with a general tendency for increasing weathering with increasing age (Figs. 5.431 to 5.464). Profiles from the different coastal regions arranged in order of increasing age are : south east Queensland sequence (KB, CH, BW, WA \approx SC, MU \approx AM and KL),

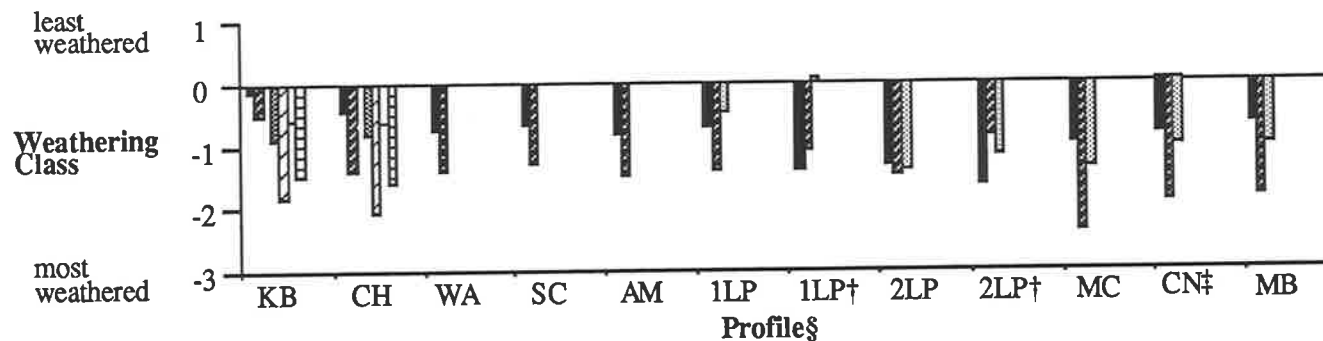


Fig. 5.431. A horizons of different profiles, mean point value scores.

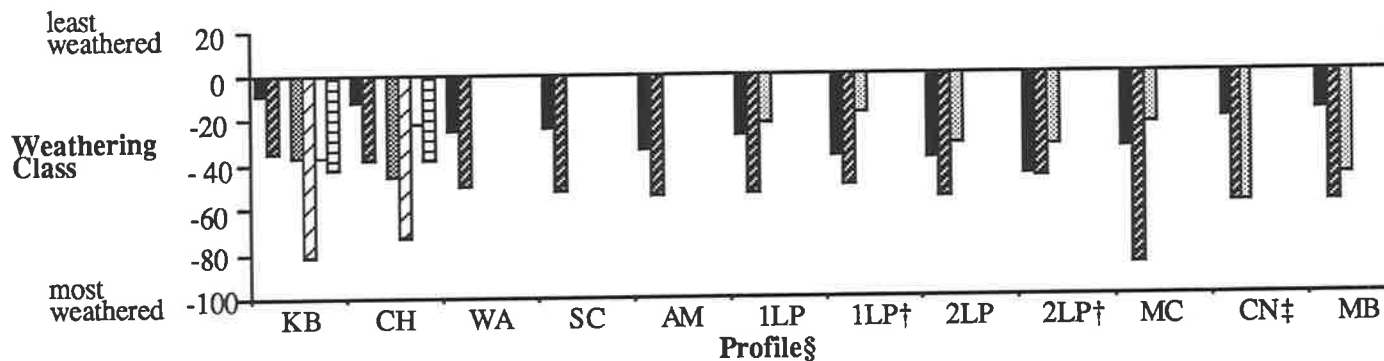
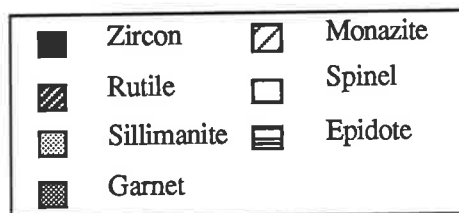


Fig. 5.432. A horizons of different profiles, value assessment scores.

Fig. 5.43. Weathering of different minerals in soils from A horizons of different profiles based on mean point value and value assessment scores of 30 grains.

† = A2. ‡ = Ab1. § KB = Kings Bore, CH = Chalambar, WA = Warrawonga, SC = Seacliffs, AM = Amity, 1LP = LeFevre Peninsula 1, 2LP = LeFevre Peninsula 2, MC = Mount Compass, CN = Canunda and MB = Mount Burr soil profiles.



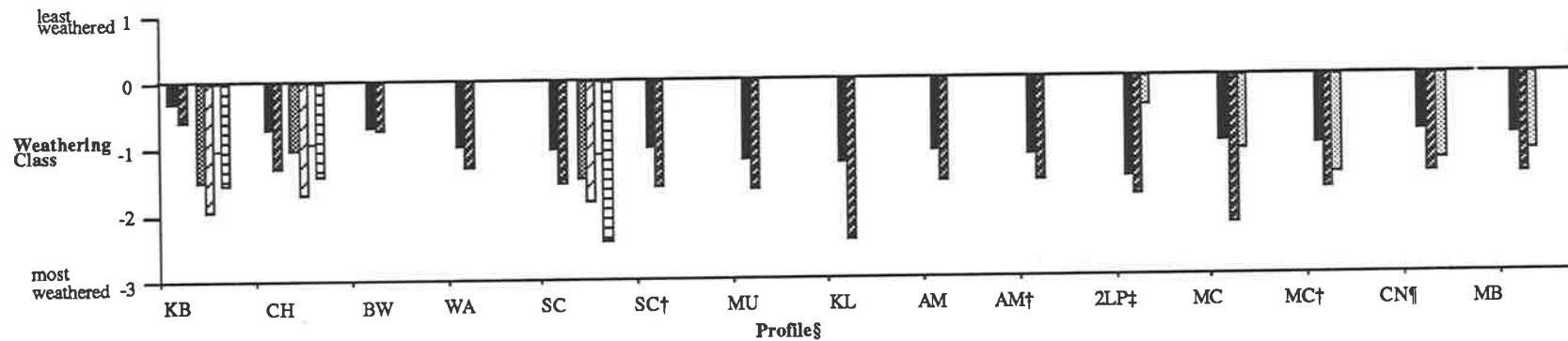


Fig. 5.441. E horizons of different profiles, mean point value scores.

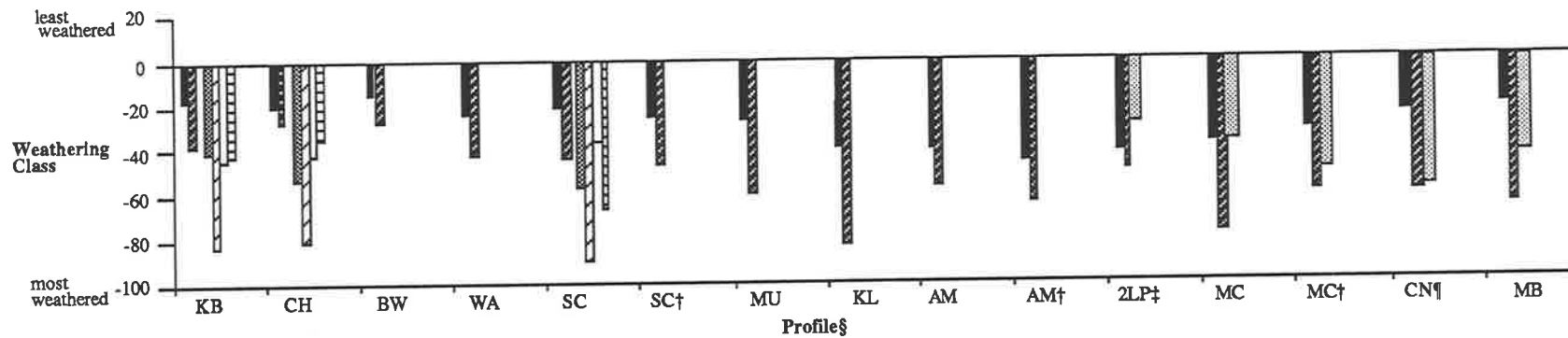
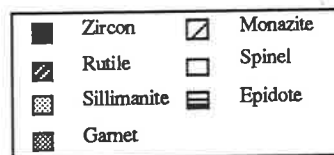


Fig. 5.442. E horizons of different profiles, mean value assessment scores.

Fig. 5.44. Weathering of different minerals in soils from E horizons of different profiles based on mean value and value assessment scores of 30 grains.

† = pipe. ‡ = A3. ¶ = Ab1. § KB = Kings Bore, CH = Chalambar, BW = Burwilla, WA = Warrawonga, SC = Seacliffs, MU = Mundu, KL = Kabali, AM = Amity, 2LP = Le Fevre Peninsula 2, MC = Mount Compass, CN = Canunda and MB = Mount Burr soil profiles.



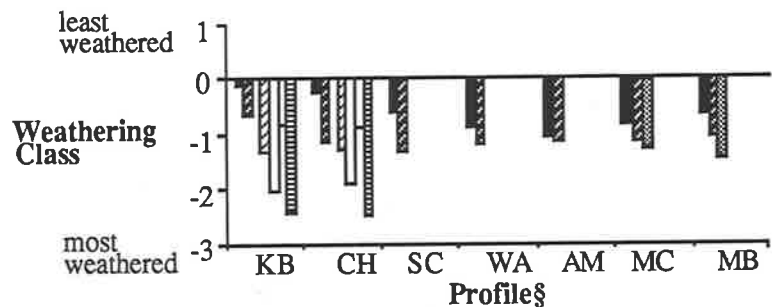


Fig. 5.451. Bhs2 horizons of different profiles, mean point value scores.

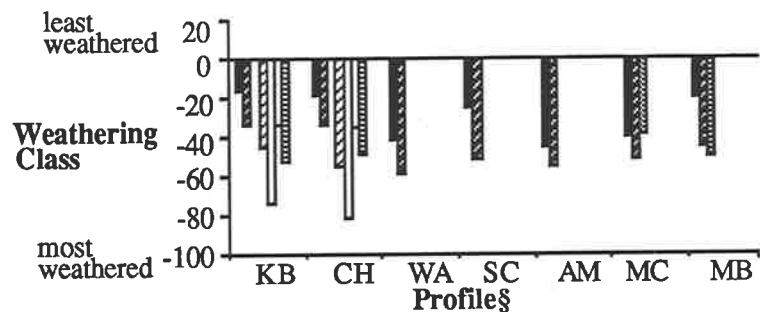


Fig. 5.453. Bhs2 horizons of different profiles, mean value assessment scores.

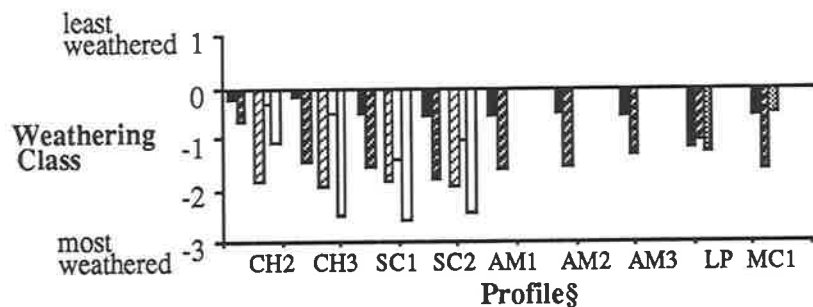


Fig. 5.452. B2 horizons† of different profiles, mean point value scores.

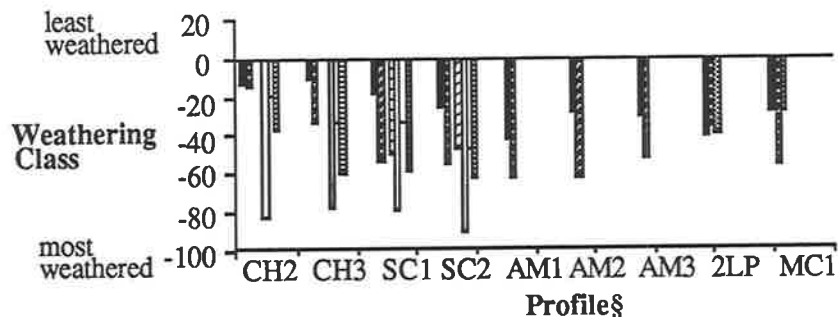
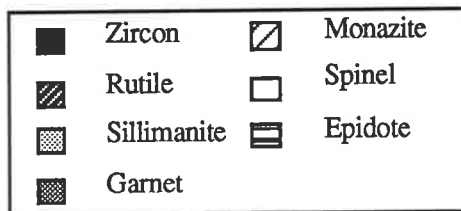


Fig. 5.454. B2 horizons† of different profiles, mean value assessment scores.

Fig. 5.45. Weathering of different minerals in soils from B horizons of different profiles based on point value and value assessment scores of 30 grains.

§ KB = Kings Bore, CH = Chalambar, WA = Warrawonga, SC = Seacliffs, AM = Amity,
 2LP = LeFevre Peninsula 2, MB = Mount Burr and MC = Mount Compass soil profiles. † = 1, Bh; 2, Bs and 3, B



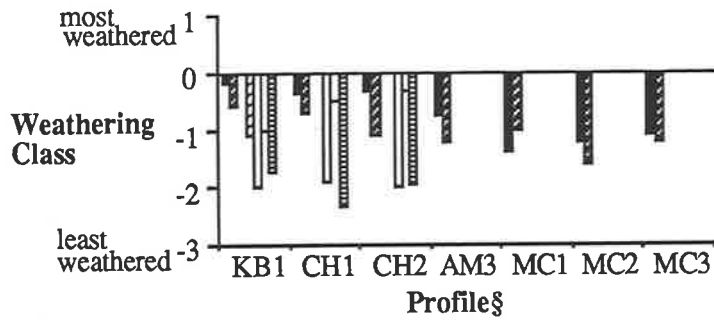


Fig. 5.461. B3 horizons† of different profiles, mean point value scores.

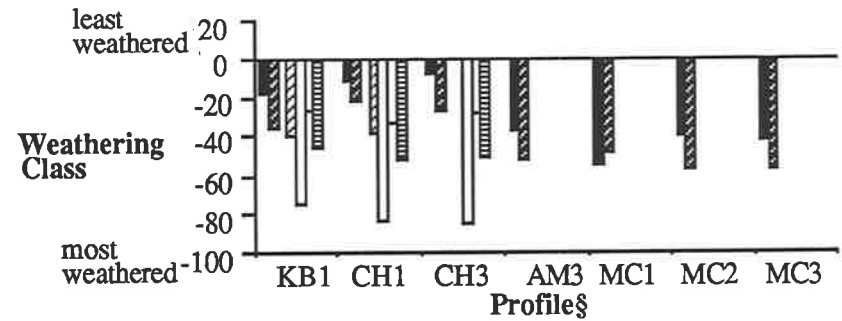


Fig. 5.463. B3 horizons† of different profiles, mean value assessment scores.

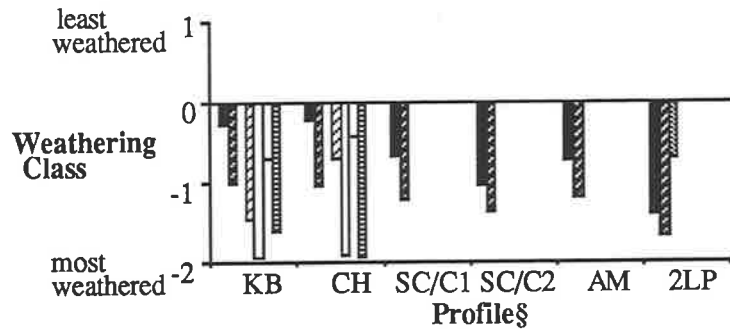


Fig. 5.462. C horizons of different profiles, mean point value scores.

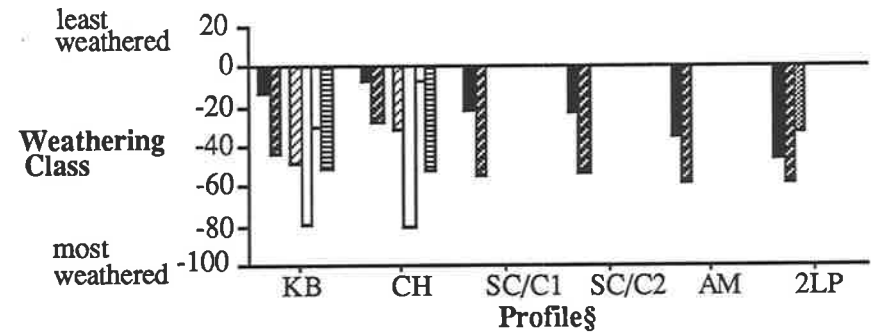
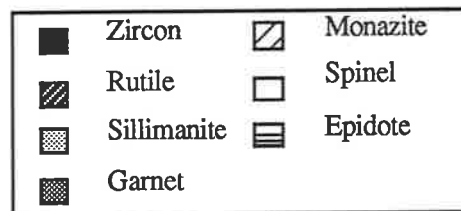


Fig. 5.464. C horizons of different profiles, mean value assessment scores.

Fig. 5.46. Weathering of different minerals in soils from B3 and C horizons of different profiles based on mean point value and value assessment scores of 30 grains.

§ KB = Kings Bore, CH = Chalambar, WA = Warrawonga, SC = Seacliffs, AM = Amity, 2LP = LeFevre Peninsula 2, MB = Mount Burr and MC = Mount Compass soil profiles. † = 1, Bhs; 2, Bs and 3, B



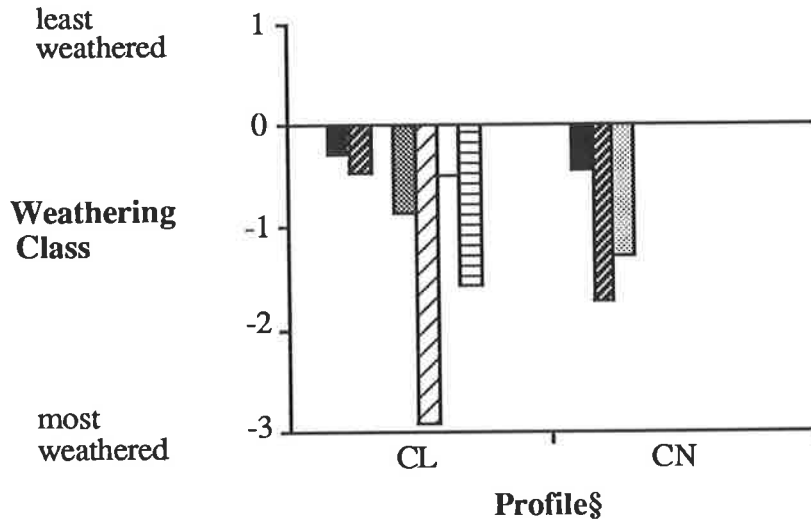


Fig. 5.471. AC horizons of different profiles, mean point value scores.

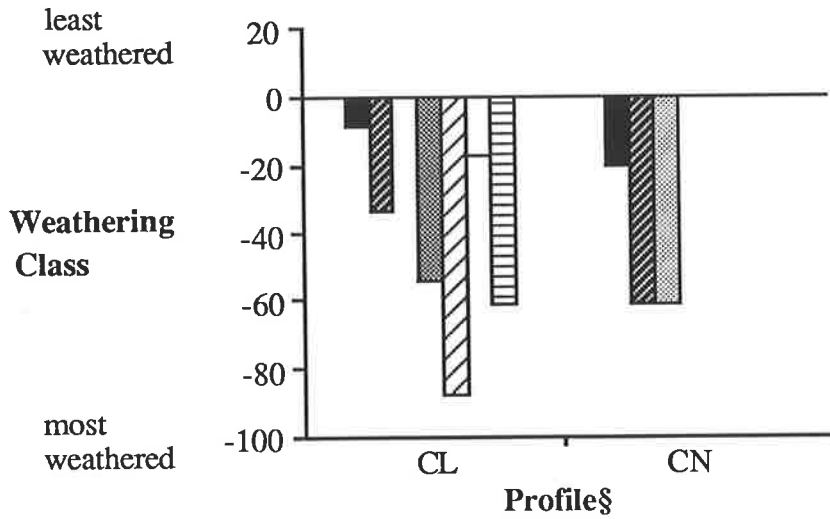
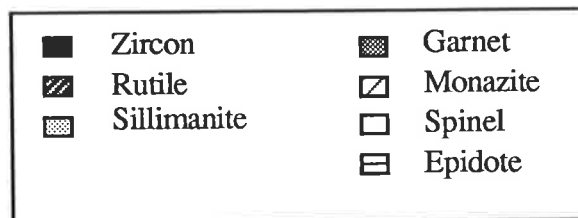


Fig. 5.472. AC horizons of different profiles, mean value assessment scores.

Fig. 5.47. Weathering of different minerals in AC horizons of soils from Carlo and Canunda sites based on mean point value and value assessment scores of 30 grains.

§ CL = Carlo mobile dune, CN = Canunda beach deposit



central South Australia sequence (1LP, 2LP and MC) and south east South Australia sequence (CN and MB). See Chapter 3 for more discussion on the ages of these profiles. This result suggests that with increasing soil development within an age sequence, as interpreted from both field and laboratory properties (see Chapters 2 and 4) there is a tendency for cumulative mineral weathering.

5.3.3. Assessment of weathering patterns from statistical analysis of PVS and VAS data.

Statistical analysis of the point value score (PVS) and value assessment score (VAS) was carried out in order to differentiate samples. The Kruskal-Wallis nonparametric H statistic was computed to determine the differences between minerals within the same horizon in respect of the degree of weathering (Table 5.5). In the Cooloola sequence, there were significant differences between minerals in the degree of weathering: the general order (starting with the least weathered): zircon > spinel ≥ rutile > garnet > epidote > monazite. The order was consistent with the weathering patterns shown in Figs. 5.401 to 5.406. For horizons in which only zircon and rutile were analysed and tested the PVS data showed differences to be non significant in all the horizons except the E of Kabali which showed more severe weathering of rutile grains. In the soils from South Australia, the three minerals zircon, rutile and sillimanite showed irregular trends in weathering patterns, particularly for some horizons within 2LP and CN soil profiles. There was little difference in weathering patterns based on PVS data for the three minerals, but significant differences of greater magnitude were observed using the VAS data (Table 5.5).

The results for differences between weathering of the same mineral types in different horizons within the same soil profile are presented in Table 5.6. In general there are non significant differences between the horizons. The significant differences between PVS scores of zircon for SC; AM; 1LP and MC profile were due to the high weathering scores in the E, E(pipe) and C2 horizons of SC; the E(pipe) and Bhs2 horizons of AM; the A1 horizon of 1LP and the Bhs3 and Bs3 horizons of MC.

Table 5.5. Results of the Kruskal-Wallis non-parametric test based on the hypothesis that no significant difference existed in the degree of weathering between different mineral types within the same horizon of a soil profile.

Soil profile	Horizon	df	Point value score †	Value assessment score †
Carlo	AC	5	***	***
Kings Bore	A1	5	***	***
	E	5	***	***
	Bhs2	5	***	***
	Bhs3	5	***	***
	C	5	***	***
Chalambar	A1	5	***	***
	E	5	*	***
	B2‡	9	***	***
	Bhs2	5	***	***
	B3	10	***	***
	C	5	***	***
Burwilla	E	1	NS	**
Warrawonga	A1	1	NS	***
	E	1	NS	***
	Bhs2	1	NS	*
Seacliffs	A1	1	NS	***
	E	7	***	***
	B2‡	7	***	***
	Bhs2	5	***	***
	C	3	NS	***
Mundu	E	1	NS	*
Kabali	E	1	***	***
Amity	A3	1	NS	NS
	E	3	NS	*
	B2‡	3	**	***
	Bhs2	3	NS	*
	B3	1	*	*
	C	1	NS	***

Table 5.5. continued.

Soil profile	Horizon	df	Point value score [†]	Value assessment score [†]
LeFevre Peninsula 1	A1	5	**	***
LeFevre Peninsula 2	A1	5	NS	*
	A2	2	*	NS
	B	2	NS	NS
	C	2	*	**
Mount Compass	A1	2	***	***
	E	5	***	***
	B2‡	2	**	*
	Bhs2	2	NS	NS
	B3	5	NS	NS
Canunda	AC§	2	***	***
	A1	2	***	***
	Ab1	2	NS	***
	Bb1	2	NS	NS
	Ab2	2	NS	*
	Bb2	2	*	***
	Ab3	2	NS	*
	Bb3	2	NS	NS
Mount Burr	A1	2	***	***
	E	2	NS	***
	Bhs2	2	*	*

*, ** and *** indicate significance at $P \leq 0.05$, $P \leq 0.01$ and $P \leq 0.001$ respectively; NS = non significant.

† Kruskal-Wallis H statistic values.

‡ Includes all B2 horizons, except Bhs2.

§ Beach deposit.

Table 5.6. Results of the Kruskal-Wallis test based on the hypothesis that no significant difference existed between weathering of different mineral types within the different horizons of a soil profile.

Horizon	df	Point value score†	Value assessment score†
<u>Mineral type Zircon</u>			
Kings Bore	4	NS	NS
Chalambar	7	NS	NS
Warrawonga	2	NS	NS
Seacliffs	7	*	NS
Amity	8	*	NS
LeFevre Peninsula 1	1	*	NS
LeFevre Peninsula 2	4	NS	NS
Mount Compass	7	*	NS
Canunda	7	NS	NS
Mount Burr	2	NS	NS
<u>Mineral Type Rutile</u>			
Kings Bore	4	NS	NS
Chalambar	7	NS	NS
Warrawonga	2	NS	NS
Seacliffs	7	***	*
Amity	8	**	*
LeFevre Peninsula 1	1	NS	NS
LeFevre Peninsula 2	4	NS	NS
Mount Compass	7	***	***
Canunda	7	*	*
Mount Burr	2	NS	NS
<u>Mineral type Sillimanite</u>			
LeFevre Peninsula 1	1	NS	NS
LeFevre Peninsula 2	4	NS	NS
Mount Compass	4	NS	*
Ganunda	7	NS	NS
Mount Burr	2	NS	NS
<u>Mineral type Garnet</u>			
Kings Bore	4	NS	NS
Chalambar	4	NS	NS
Seacliffs	2	NS	*
<u>Mineral type Monazite</u>			
Kings Bore	4	NS	NS
Chalambar	7	NS	NS
Seacliffs	2	NS	**
<u>Mineral type Spinel</u>			
Kings Bore	4	NS	NS
Chalambar	7	NS	**
Seacliffs	2	NS	**
<u>Mineral type Epidote</u>			
Kings Bore	4	NS	NS
Chalambar	7	NS	NS
Seacliffs	2	NS	NS

*, ** and *** indicate significance at $P \leq 0.05$, $P \leq 0.01$ and $P \leq 0.001$ respectively; NS = non significant.

† Kruskal-Wallis H statistic values.

Significant differences in rutile weathering for SC; AM; MC and CN soil profiles were attributed to the severe weathering of this mineral in the E(pipe), Bh2 and Bs2 horizons of SC; the E(pipe), Bh2 and Bs2 horizons of AM; A1 and E horizons of MC and A1 and Bb2 horizons of CN. In MC profile greater weathering was observed for sillimanite in the A1 and E(pipe) horizons. Garnet weathering was more severe in the E than Bhs2 and Bs2 horizons of Seacliffs. Additionally, monazite showed more weathering characteristics in the E and Bs2 horizons of Seacliffs profile. The weathering of spinel in Chalambar and Seacliffs profiles was significant because of intense weathering in E, Bhs2, B2 and Bhs3 horizons of Chalambar and Bs2 horizon of Seacliffs.

Differences in the intensity of mineral weathering for the same mineral type in similar horizons within different soil profiles in regional soil age sequences are shown in Table 5.7. In the A horizon of soils from the Cooloola-North Stradbroke Island sequence, the significant difference in zircon and rutile weathering was ascribed to intense weathering of both minerals in the Warrawonga, Seacliffs and Amity soil profiles. Similar observations were made for zircon and rutile in the E horizon of these profiles, where the older profiles were more intensely weathered (Figs. 5.431 to 5.442). Epidote in the E horizon showed more weathering in SC profile, followed by KB and CH. The B2 horizons of SC and AM showed severe zircon weathering resulting in the significant difference shown in Table 5.7. The soils differed in epidote weathering with relatively higher levels of weathered grains recorded for SC than CH. Rutile in the B2 horizon showed a complex pattern of weathering. As an example, Fig. 5.452 shows the severity of weathering increasing in the order SC Bs2 > AM Bh2 > CH B2. Differences shown for zircon and rutile in the Bhs2 horizon resulted from higher degrees of weathering of both minerals in the WA, SC and AM profiles compared with KB and CH (Figs. 5.451 and 5.453). In the B3 horizon, AM and KB profiles showed more weathering of zircon and rutile than CH (Fig. 5.463).

The soils from LeFevre Peninsula and Mount Compass which recorded significant differences in mineral weathering in horizons between profiles were due to

Table 5.7. Results of the Kruskal-Wallis test based on the hypothesis that there were no significant differences between weathering of the same mineral type in similar horizons between different soil profiles in regionalised sequences.

Soil horizon	Mineral type	df	Cooloola-North Stradbroke Island		LeFevre Peninsula - Mt. Compass	
			Point value score†	Value assessment score†	Point value score†	Value assessment score†
A1	Zircon	4	NS	*	*	NS
	Rutile	4	NS	**	**	NS
	Sillimanite	4	-	-	**	
	Garnet	1	NS	NS		
	Monazite	1	NS	NS		
	Spinel	1	NS	NS		
	Epidote	1	NS	NS		
E	Zircon	14	*	***	NS	NS
	Rutile	14	***	***	NS	NS
	Sillimanite	2	-	-	NS	*
	Garnet	2	NS	NS		
	Monazite	2	NS	NS		
	Spinel	2	NS	NS		
	Epidote	2	*	**		
B2‡	Zircon	5	*	NS	*	NS
	Rutile	5	**	NS	NS	NS
	Sillimanite	1	-	-	NS	NS
	Monazite	2	NS	NS		
	Spinel	2	NS	NS		
Bhs2	Zircon	5	*	***	-	-
	Rutile	5	NS	***	-	-
	Garnet	2	NS	NS	-	-
	Monazite	2	NS	NS	-	-
	Spinel	2	NS	NS	-	-
	Epidote	2	NS	NS	-	-
B3	Zircon	3	NS	***	-	-
	Rutile	3	NS	***	-	-
	Garnet	1	NS	NS	-	-
	Monazite	1	NS	NS	-	-
	Spinel	1	NS	NS	-	-
	Epidote	1	NS	NS	-	-
C	Zircon	5	NS	NS	-	-
	Rutile	5	NS	NS	-	-
	Garnet	1	NS	NS	-	-
	Monazite	1	NS	NS	-	-
	Spinel	1	NS	NS	-	-
	Epidote	1	NS	NS	-	-

*, ** and *** indicate significance at $P \leq 0.05$, $P \leq 0.01$ and $P \leq 0.001$ respectively;

NS = non significant.

† Kruskal-Wallis H statistic values.

‡ Includes all B2 horizons, except Bhs2.

- Not analysed.

the following: zircon weathering was highest in the A2 horizon of the 2LP and least in the A1 horizon of 1LP followed by MC (Fig. 5.431). Rutile in the sequence was most weathered in E and A2 horizons of MC and 2LP profiles respectively. Sillimanite weathering intensity followed the order 2LP A1 > MC A1 > 2LP A2 > 1LP A1 > 1LP A2 (for the A horizons) and MC E(pipe) > MC E (for the E horizons). Zircon was more weathered in the B horizon of 2LP than in the B horizon of MC.

5.4. Discussion

5.4.1. Mineral identification.

Mineral identification using x-ray powder diffraction techniques showed the presence of quartz which was ascribed to a rutilated quartz phase in the samples, as well as minor contamination during the heavy mineral separation. Gandolfi camera photos were taken of single grains to confirm the presence of rutile-quartz grains. Gandolfi camera x-ray photos on single grains of sillimanite, garnet (grossularite), spinel (Cr-spinel) and epidote (zoisite) served to demonstrate the value of this technique in identifying these minerals especially where (i) insufficient amount of the bulk sample was available for powder XRD, (ii) where sufficient sample was available but the concentration of specific heavy minerals was too low to be detected by powder XRD, (iii) mineralogy could not be unequivocally inferred from elemental chemistry as determined by EDAX. In Plate 5.2 the discontinuous x-ray line patterns are indicative of these minerals having single crystal component and large crystallite size (in this case particle diameter > 100 μm).

5.4.2. Numerical and statistical weathering assessment.

The susceptibility of minerals to weathering differs considerably and depends on a range of factors including the nature of the minerals (physical and chemical properties), weathering conditions and source material. The general order of resistance to weathering viz zircon > garnet > epidote agrees with the sequences given in Nickel

(1973) Table 1 and Bateman and Catt (1985) Table 5.

5.4.2.1. *Physical characteristics of minerals.*

The physical characteristics of the source material can have an effect on the stability of the constituent minerals. In samples from Cooloola, large zircon grains were more rounded than the smaller types which tended to be euhedral. Even though the sources may have been the same, the smaller crystals would be less prone to abrasion by wave action (Whitworth, 1956). The rutile grains were mostly rounded with few clean cleavage faces due to recent fractures along cleavage directions. Spinel grains usually had rounded edges with traces of the octahedral habit seen in some grains (Plate 5.41) as reported earlier by Beasley (1950) for beach deposits of southern Queensland. Garnet and epidote grains showed rough surfaces with little sign of rounding in most of the grains. Because of the crystal habits of these minerals (e.g. Hemingway and Tamar-Agha, 1975; Morton, 1979; Gravenor, 1979, 1980), weathering proceeded by the formation of small pits leading to a decrease in volume and increase in surface area of the mineral (Plates 5.42 to 5.45). Monazite is well rounded and its soft nature facilitates grinding to a finer size. Monazite was considered to be less stable than epidote because most monazite grains were well rounded and severely etched (Plate 5.46) giving them higher PVS and VAS ratings.

Zircon and rutile samples from the Quaternary sediments in the central and south east coastal region of South Australia were moderately to well rounded, with few well formed crystals (e.g. Plates 5.47 and 5.48 for zircon, and 5.49 and 5.410 for rutile). The sillimanite grains have a subangular to angular forms, often becoming ragged (Plates 5.411 and 5.412). Colwell (1979) made similar observations on heavy mineral grains in the late Cainozoic sediments of South Australia. The differences in physical properties and morphology of grains for the source sediments may therefore have influenced the ultimate weathering behaviour of these minerals after deposition.

Plate 5.41. Scanning electron micrograph of spinel grain from Bs2 horizon of Seacliffs, minor etch pits and slightly rounded edges showing traces of octahedral habit.

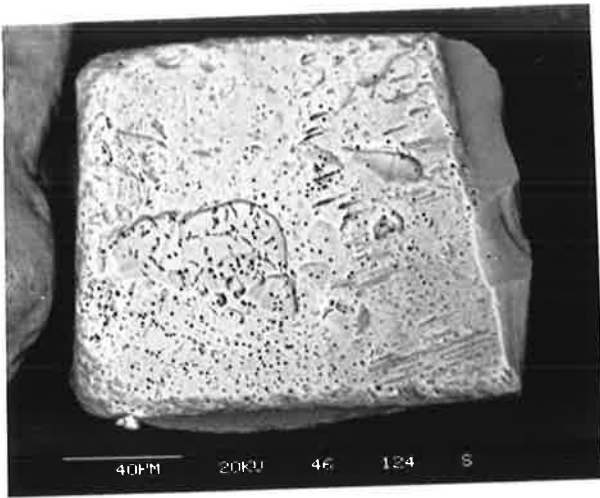
Plate 5.42. Scanning electron micrograph of garnet grain from C horizon of Kings Bore showing rounded edges and slightly more severe etch pits.

Plate 5.43. Scanning electron micrograph of garnet grain from E horizon of Kings Bore showing the development of well defined etch and delicate needle-like terminations during dissolution.

Plate 5.44. Scanning electron micrograph of epidote grain from E horizon of Kings Bore showing mamillatory and virtually unetched features.

Plate 5.45. Scanning electron micrograph of epidote grain from Bhs2 horizon of Seacliffs showing severely etched and rounded features.

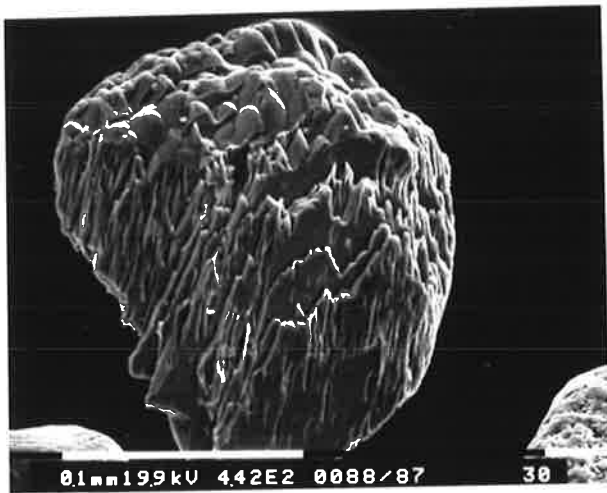
Plate 5.46. Scanning electron micrograph of monazite grain from E horizon of Chalambar showing well rounded and etched features.



5.41.



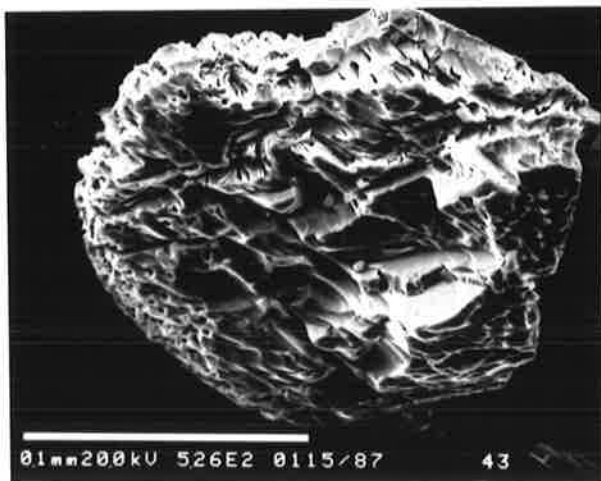
5.42.



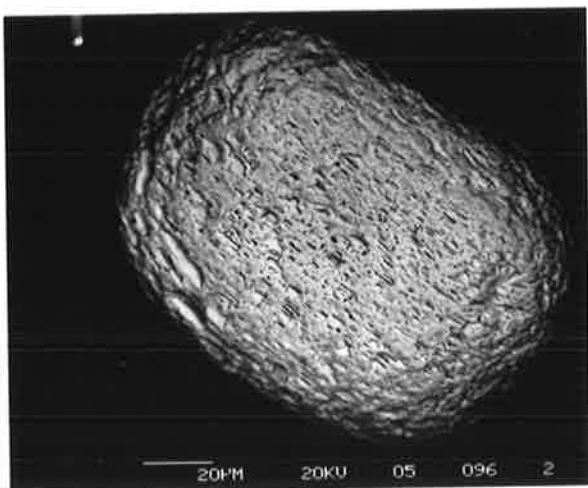
5.43.



5.44.

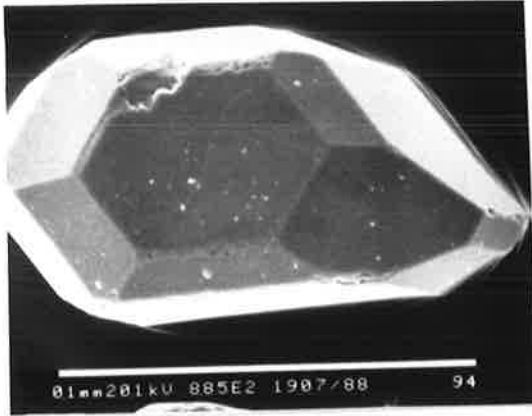


5.45.

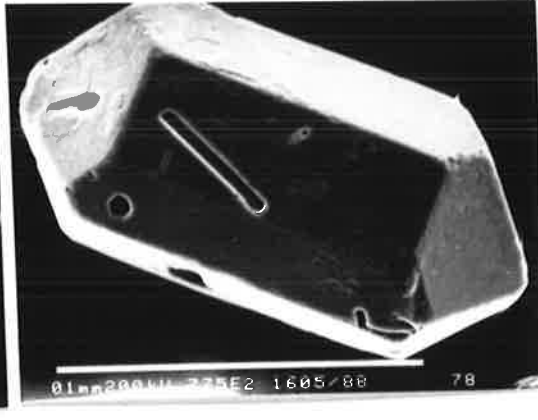


5.46.

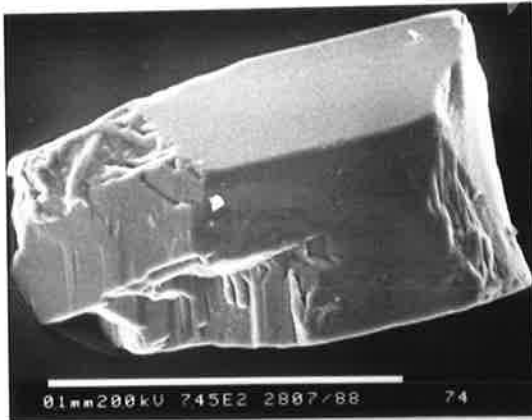
- Plate 5.47. Scanning electron micrograph of zircon grain from A1 horizon of Canunda showing rare etch pits and euhedral surface features and crystal form respectively.
- Plate 5.48. Scanning electron micrograph of zircon grain from E horizon of Mount Compass showing unetched and euhedral surface features and crystal form respectively.
- Plate 5.49. Scanning electron micrograph of rutile grain from C horizon of LeFevre Peninsula 2 showing slight etching at fractured surfaces.
- Plate 5.410. Scanning electron micrograph of rutile grain from E(pipe) horizon of Mount Compass showing angular form and rarely any etch pits.
- Plate 5.411. Scanning electron micrograph of sillimanite grain from A1 horizon of Mount Compass showing fresh unetched crystal faces.
- Plate 5.412. Scanning electron micrograph of sillimanite grain from A1 horizon of LeFevre Peninsula 2 showing etching and dissolution at grain terminations.
- Plate 5.413. Scanning electron micrograph of rutile grain from E horizon of Kabali showing intense dissolution of silicon rich portions, leaving skeletal titanium rich grain.



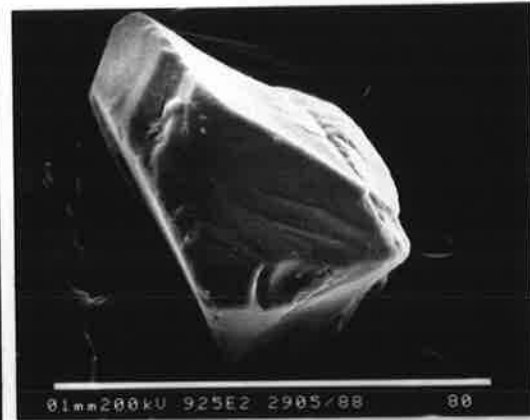
5.47.



5.48.



5.49.



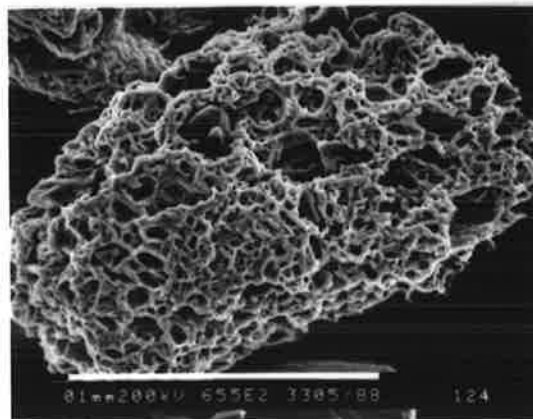
5.410.



5.411.



5.412.



5.413.

5.4.2.2. *Chemical characteristics of minerals.*

The chemical composition of the mineral affects its stability to weathering. Epidote, garnet (almandine type) and some rutile contain Fe which was readily oxidized (Schott and Berner 1983; Bateman and Catt, 1985). The amount of Fe²⁺ present in the mineral determines the severity of weathering in that mineral. In addition, some other varieties of these minerals, without a chemically unstable constituent such as Fe (e.g. zoisite, grossularite and rutile), still showed evidence of considerable weathering. This means that there were other chemical constituents such as mineral inclusions which affected mineral stability. Some zircons from Cooloola were shown to contain apatite and rutile as minor inclusions. In rutiles containing some quartz (rutilated-quartz), selective dissolution of the quartz relative to rutile eventually leaves rutile grains with severe dissolution features (e.g. Plate 5.413).

5.4.2.3. *Geologic history of sediment.*

The degree of mineral weathering and hence its persistence is also affected by the geologic history of the sediment (Pettijohn, 1941). The heavy mineral assemblage becomes impoverished with increasing age of the sediment. In Chapter 2 the geology and geomorphology of the sediments were discussed. In the samples from Cooloola and North Stradbroke Island, zircon, rutile, garnet, monazite and epidote have their origin in Mesozoic freshwater sandstones which were derived from Permian granitic rocks (Beasley, 1950) and Precambrian rocks (Whitworth, 1956). Chrome spinel is known to be derived from the Tertiary basalts on the east coast and adjacent highlands. This could explain why Cr-spinel is relatively fresher than rutile and the other minerals in the weathering sequence. In soils from South Australia the sediments have a much more complex history. Samples from LeFevre Peninsula and Canunda are derived from marine and estuarine Quaternary sediments (Daily *et al.*, 1976). From Mount Burr the sediments are of Quaternary age and have an aeolian origin, whereas the Mount Compass soil consists of Recent aeolian sediments, of Permian origin, that were earlier redistributed during the Tertiary. The provenance of the mineral suites in

sediments from Canunda and Mount Burr is complex. There appear to have been contributions from sialic igneous, reworked sedimentary and metamorphic sources (Colwell, 1979), with little input from mafic igneous rocks and pegmatites. The source rocks vary in age from Pliocene to Lower Palaeozoic. Belperio and Bluck (1988) have also shown that heavy mineral deposits in the western Murray Basin of South Australia (which lies between the the two sampled sequences in South Australia) have a variety of sources throughout the Cainozoic. The indication is that similar source rocks contributed to the soils at LeFevre Peninsula, Mount Compass, Canunda and Mount Burr. Whatever the provenance of the source materials now, it is suggested that the ultimate source of the heavy minerals in all samples may be the Precambrian rocks (schists and gneisses) which make up the core of the Australian continent (Whitworth, 1956), with minor inputs from granitic rocks of younger age. The Precambrian core is now covered by younger sediments of Palaeozoic, Mesozoic and Cainozoic age derived from the core via one or more cycles of weathering, erosion, diastrophism and deposition.

5.4.2.4. *Soil weathering.*

The influence of pedochemical weathering within profiles showed very weak trends, with the upper A and E horizons showing marginally higher weathering patterns compared with horizons lower in the profiles. This trend was more so for the highly resistant minerals (zircon and rutile) and was better expressed for comparable horizons of different profiles from the same region. With increasing profile age weathering intensity increased, a fact which suggests that zircon and rutile are better pedogenic indicators than the other minerals. The trend in weathering pattern with depth within the profiles (A and E closer to the surface) may be due to the combination of several different soil processes. Given that all the soils are sands and therefore relatively permeable to percolating fluids, hydration and oxidation reactions can be important processes in mineral weathering. Within profile, the B3 horizons of Mount Compass (which may be older than all the other horizons sampled as suggested in

Chapters 3 and 4) has more fine sediments (particle size data in Appendix 3 and micromorphology in Chapter 4), higher cohesion and poor sorting characteristics than the other podzols at Cooloola, North Stradbroke Island and Mount Burr. These properties have reduced the permeability of percolating fluids and led to a reduction in the rate of mineral weathering in the B3 horizons of Mount Compass profile, which is under low rainfall conditions (annual average of 759 mm). Between profiles, comparison of the E horizons of soils from the wettest regions (Cooloola/North Stradbroke Island; with an average annual rainfall in the range 1100 - 1446 mm) showed that minerals were less weathered in the younger groups viz KB, BW, CH, WA and SC. Also, the overall pattern in the B3 horizons of the Mount Compass soil indicated that zircon and rutile had much higher weathering intensities than comparatively younger profiles in Queensland region viz KB and CH. However, in the B3 and other horizons of older soil profiles from Queensland viz AM, MU and KL the weathering patterns were comparable with the B3 of MC. Sillimanite in profiles from South Australia was the next most stable mineral to zircon and in this respect followed the order of Dryden and Dryden (1946). In some of the profiles, sillimanite appeared to be more stable than zircon in some horizons, e.g. the A1 horizon of 1LP, A3 horizon of 2LP and Bb3 horizon of CN. This may point to the main source of sillimanite in these soils as being of younger age. Alternatively, the sillimanite may be derived from fresh rock material of older origin. In soils on old reworked (Permian) sediments, sillimanite was more weathered than zircon in the E horizon and may have been completely weathered in the B3, provided the sources of both sediments were the same. The micromorphological data in Chapter 4 suggest that the B3 at Mount Compass is the truncated part of an older soil system. The effect of pedochemical weathering was also substantiated by the occurrence, in the B horizon of the older profiles, of iron rich fine material of secondary origin which has probably been derived from Fe bearing minerals in the sediments. Evidence for mobilization and segregation of iron can be seen in thin sections of these profiles (particularly MC and MB) as shown in Chapter 4.

In natural and artificial weathering environments the effects of pH on relative mineral stability are well documented (Nickel, 1973). The stability sequence established in this work generally agreed with other workers quoted in Nickel (1973; e.g. Lemcke and Fuchtbauer). The main differences were in the positions of garnet and epidote. Except for Fuchtbauer, all the other workers have concluded that epidote is more stable than garnet. Under alkaline conditions (pH = 7.3), Fuchtbauer showed that garnet was more stable than epidote. It is possible that the source rocks for these minerals were basic, the acidic weathering conditions in the present environment having been insufficient to revert the sequence. In general, the degree of weathering of zircon and rutile in the A3 horizon of the young alkaline soil from LeFevre Peninsula 2 was higher than in the older and more acidic soils from Cooloola and North Stradbroke Island, except for the E horizon of KL and AM profiles. Also, the AC horizons from Cooloola and Canunda showed similar trends for zircon and rutile. The possible reason for this is that the source material of the LeFevre Peninsula soil is mostly older reworked Palaeozoic sediments whereas at Cooloola and North Stradbroke Island, the soils are from relatively younger (Mesozoic and Cainozoic) source materials. Because of the small differences in pH between horizons within profiles, and between horizons for profiles with comparable soil reaction (either acidic or alkaline) no relationship was found between severity of weathering and soil pH. This finding was consistent with earlier work by Nickel (1973) and Bateman and Catt (1985).

A major contributing factor to decreased weathering was the reduction of porosity in these soil profiles through translocation and redeposition of Fe and organic minerals. Field and laboratory evidence (Chapters 2 and 4) showed that there was little reduction in porosity in 1LP, 2LP and CL (no grain coatings), was slight in KB, BW and CH (thin coatings around grains) and was considerable in the remaining soils wherein Fe-organic matter rich Bhs horizons have formed. Both within and between profile comparisons showed that the degree of weathering seemed to be slightly higher for minerals in Bs and Bhs horizons. In regions of higher rainfall, the reduction in porosity leads to a greater retention of moisture in the B horizon and hence hydrolytic

reactions can proceed for longer during the year than in other horizons. Within profile, deep in the C horizon heavy minerals, with a few exceptions, were relatively less weathered. In those cases where this was not so, i.e. there was greater weathering in the C horizon than in the horizons above, there may be two explanations. The C horizon may be a remnant of an older dune system, as could be the case for Kings Bore, or, in deeper profiles (e.g. SC), groundwater fluctuation may have influenced the weathering of the minerals.

5.5. Conclusions

The weathering classification and assessment of heavy minerals using point value score (PVS) and value assessment score (VAS) methods were adopted and tested on a wide variety of sandy soils in Australia. The VAS method was considerably more effective in discriminating more weathered minerals from less weathered types both between profiles and between horizons within profiles. The weathering of the minerals in the different soils were complex and dependent on a wide range of factors that contributed to soil forming processes. The weathering sequence viz zircon > sillimanite \geq spinel \geq rutile > garnet > epidote > monazite agreed with those suggested, on qualitative grounds, by other workers. Soil age and profile development in the A and E horizons of the chronosequence at Cooloola showed increasing severity of weathering with time and proximity to the surface. In the lower horizons weathering patterns became complex due to the combined effects of podzolization, fluctuating water table processes and other factors. Minerals in South Australian soils with alkaline pH, even though much less developed and younger than soils from the south east coast of Queensland with acidic soil pH, were found to be more weathered.

The separation of pedogenetic and inherited lithological features proved difficult even in the chronosequence at Cooloola. It was hoped that in a relatively homogeneous sandy parent material, the influence of pedogenesis on heavy mineral weathering could be separated from inherited characteristics. This ideal was confounded by mineralogical varieties in the present sediments. In all soils, inherited

microtextural features on the heavy mineral grains influenced the rate and extent of subsequent weathering. A more thorough investigation of provenance, and therefore the nature and distribution of different surface features on these minerals, coupled with accurate age determination, would be necessary to distinguish between the two influences.

In spite of the constraints, it was concluded that the semiquantitative method of analysing microtextural features on grains was a valuable technique for assessing the extent of pedogenetic weathering between profiles from various regions as well as trends within profiles.

CHAPTER 6

PRE- AND POST-DEPOSITIONAL WEATHERING CHARACTERISTICS OF ZIRCON AND RUTILE

6.1. Introduction

Since access to the scanning electron microscope (SEM) became readily available 25 years ago, numerous workers have attempted to define the transportational, depositional and diagenetic record of soils and sediments by the occurrence of particular grain surface features. By far the bulk of work has been on quartz grains, the surfaces of which have been examined by electron microscopy to distinguish the environmental influences of weathering and erosion, and extent and nature of transformation during transportation, deposition and post-deposition (Margolis, 1968; Krinsley and Donahue, 1968; Krinsley and Doornkamp, 1973; Bull *et al.*, 1987; Krinsley and McCoy, 1978; Eswaran and Stoops, 1979; Manickam and Barbaroux, 1987). Of the factors which have been shown to be responsible for the development of individual surface microtextures, the most important are: (i) the interaction between mechanical and chemical processes and, (ii) the crystallographic, mineralogical, physical and chemical properties of the minerals.

In recent years there have been several attempts to explore the relationship between surface texture and age. For example, Andrews and Miller (1972) and Douglas and Platt (1977) have suggested that particular surface features of quartz grains can be used as indicators for the length of time that different geological and soil development processes have operated. Although most of the environmental discrimination work using SEM studies of surface microtextures has been on quartz grains, there are a few studies where heavy mineral grains have been used. Such investigations have been mostly confined to rock or sedimentary environments (Raeside, 1959; Steiglitz, 1969; Setlow and Karpovich, 1972; Lin *et al.*, 1974, Setlow,

1978; Gravenor and Gostin, 1979; Morton, 1979,1984) with very few studies involving soil environments. Regardless of the mineral, the underlying assumption in all such environmental discrimination work using SEM is that grain surface textural features are diagnostic of a specific set of energy conditions and therefore of particular environments. Several workers (Margolis and Krinsley, 1973; Whalley and Krinsley, 1974; Bull, 1981 and Whalley, 1985) have specifically reported on the problems associated with data interpretation relating to grain surface microtexture and environmental discrimination. These workers have noted that features identified from quartz and other mineral grains can hardly be shown to have only one source of development. That is, similar features can form by either as a combination of other features or through different energy conditions.

The few soil studies which have been reported have been confined primarily to podzols (e.g. Bateman and Catt, 1985) with emphasis on petrographic techniques to identify, quantify and provide weathering indices for the various mineral species (Matelski and Turk, 1947; Marel, 1949; Pawluk, 1960; Alias, 1961). As pedogenic indices, zircon, rutile and to a lesser extent xenotime, monazite and tourmaline have often been assumed to be resistant to weathering. However, these assumptions have not been critically tested, although several workers (Carroll, 1953; Erlank *et al.*, 1978 a; Correns, 1978; Berrow *et al.*, 1978) have observed features which appear to be evidence of weathering of zircon and rutile as well as Zr and Ti mobility (see also Chapter 5 of this thesis). In view of the paucity of studies on the nature and extent of weathering of zircon and rutile in soil environments, the objectives of this chapter are: (i) to apply the SEM method described in Chapter 5 for characterizing microtextural features of zircon and rutile from a series of soils (predominantly podzols; Spodic Quartzipsamments) within a chronosequence, (ii) to examine the relationship between the type and abundance of particular surface features associated with zircon and rutile to horizon type and profile age, and (iii) to interpret, by surface texture analysis, the palaeoenvironmental conditions to which zircon and rutile have been subjected .

6.2. Materials and Methods

6.2.1. Study area and Materials.

Four soils from the Cooloola podzol chronosequence, ranging in age from Holocene for the Carlo to mid-Pleistocene for the Seacliffs soil were studied (Table 6.1).

Table 6.1. Soils associated with the different profiles in the dunes studied.

Age of association	Dune system†	Soil landscape unit	Profile	Classification ‡	Horizon§
Holocene	1	Mutyi	Carlo	Typic Quartzipsamment	AC
Pleistocene (11±2 ka BP¶)	1	Mutyi	Kings Bore	Spodic Quartzipsamment	A1 E Bhs2 Bhs3 C
Pleistocene	2	Chalambar	Chalambar 1	Troporthod	A1 E Bhs2 Bhs3 C
Pleistocene (90±10 ka BP¶)	4	Warrawonga	Seacliffs	Spodic Quartzipsamment	A1 E Bhs2 C2

† Based on Thompson (1983).

‡ Soil Management Support Service (1987), Keys to Soil Taxonomy.

§ For morphological descriptions, see Thompson and Moore (1984) and Appendix 2.

¶ Based on Thermoluminescence dates given in Chapter 3.

See Fig. 2.1 for the location of sites along the south eastern Queensland coast. Details of field morphological descriptions and selected laboratory data for each profile are provided in Appendix 1. As well, the geology and geomorphology are discussed in Chapter 2. Fourteen samples representative of the A, B and C horizons were collected from each of four selected soils. Samples were air dried and passed through a 2 mm

sieve.

6.2.2. Methods

See Chapter 5, Section 5.2.2.

6.3. Results

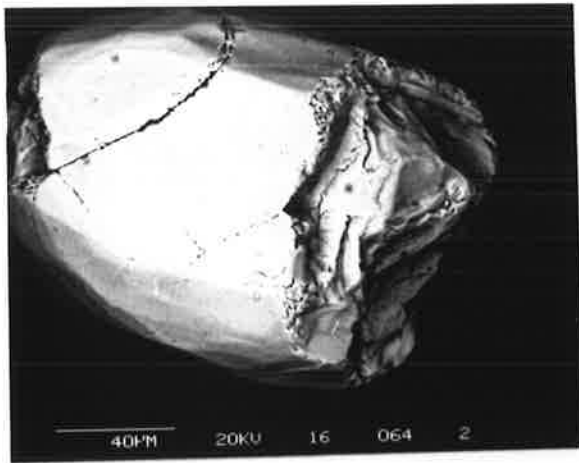
6.3.1. Scanning electron microscopy

The deduction of the environmental conditions responsible for the ten classes of surface features (Table 5.1) observed on the grains was carried out. In addition, the ten classes of surface features identified on the grains were analysed by a semi-quantitative method (based on frequency of occurrence of the different features), using a χ^2 distribution test.

6.3.1.1. Qualitative analysis of surface microtextures.

Photomicrographs of representative zircon and rutile grains illustrating the 10 classes used to describe the surface textural features are presented in Plates 6.1 to 6.6 for zircon and Plates 6.7 to 6.12 for rutile. Fig. 6.1 presents nominal scale data for the frequency of occurrence of the 10 microtextural features on 30 grains for each mineral in a selected number of horizon(s) within the different soil profiles. The dominant surface microtextural features present on the grains of both minerals are in the following order of frequency: etched grain > subdued/rounded grain > clean/smooth fractured or cleavage faces (featureless faces) \approx high relief > conchoidal fractures/breakage blocks > sharp edges and angular grains > solution \approx scaling or surface roughness > hairline cracks \approx arc-shaped/parallel or semi-parallel steps. There are inconsistent but observable trends in the frequency of occurrence of some surface features in horizons within and between profiles. Some of these trends are the disappearance of sharp edge and angular grains with increasing age in comparable

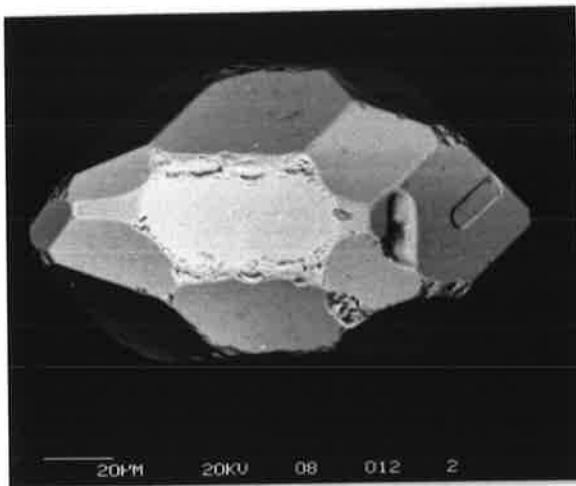
- Plate 6.1. Zircon grain from B3 horizon of Chalambar soil profile with high relief, clean/smooth surfaces, conchoidal fracture/breakage blocks, etch pits, subdued/rounded edges and hairline cracks.
- Plate 6.2. Zircon grain from Carlo soil with high relief, clean/smooth surfaces, conchoidal fractures, etch pits and subdued edges.
- Plate 6.3. Zircon grain from A1 horizon of Chalambar soil profile with clean/smooth surfaces, angular/sharp edges and etch pits.
- Plate 6.4. Zircon grains from A1 horizon of Chalambar soil profile with clean/smooth surfaces, angular/sharp edges and some adhered particles (left grain); clean/smooth surfaces, subdued/rounded edges and hairline cracks (right grain).
- Plate 6.5. Zircon grain from A1 horizon of Chalambar soil profile with scaled surfaces, etch pits, subdued/rounded edges and hairline cracks.
- Plate 6.6. Zircon grain from C horizon of Chalambar soil profile with clean/smooth surfaces, breakage blocks, scaled/rough surfaces, etch pits, subdued/rounded edges and hairline cracks.



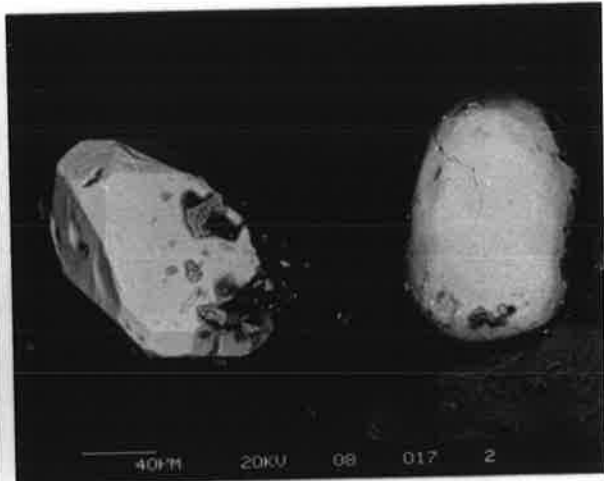
6.1.



6.2.



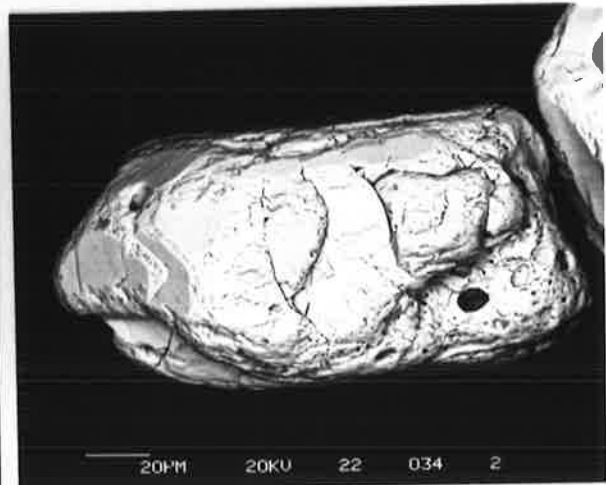
6.3.



6.4.

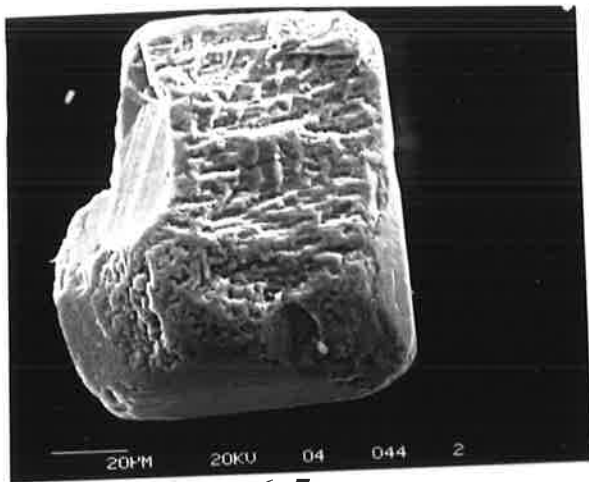


6.5.



6.6.

- Plate 6.7. Rutile grain from E horizon of Chalambar soil profile with breakage block, precipitation surfaces, rough surfaces, etch pits and subdued edges.
- Plate 6.8. Rutile grain from E horizon of Kings Bore soil profile with solution/precipitation surfaces, scaled surfaces and subdued/rounded edges.
- Plate 6.9. Rutile grain from C horizon of Kings Bore soil profile with solution/precipitation surfaces, scaled surfaces and subdued/rounded edges.
- Plate 6.10. Rutile grain from Bhs2 horizon of Seacliffs soil profile with etch pits, subdued/rounded edges and coated surfaces.
- Plate 6.11. Rutile grain from A1 horizon of Kings Bore soil profile with high relief, clean surfaces, solution/precipitation surfaces, scaled surfaces and subdued/rounded edges.
- Plate 6.12. Rutile grain from E horizon of Chalambar soil profile with clean surfaces, breakage block, scaled surfaces, etch pits, subdued/rounded edges and hairline cracks.



20µM 20KV 04 044 2

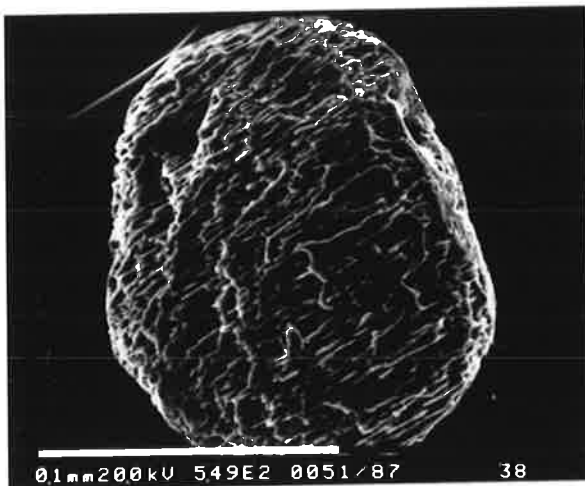
6.7.



0.1mm200kV 549E2 0048/87

26

6.8.



0.1mm200kV 549E2 0051/87

38

6.9.



0.1mm200kV 625E2 0100/87

42

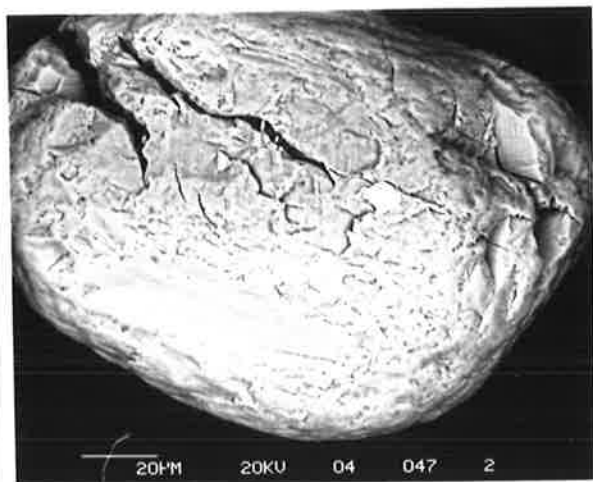
6.10.



0.1mm200kV 573E2 0043/87

26

6.11.



20µM 20KV 04 047 2

6.12.

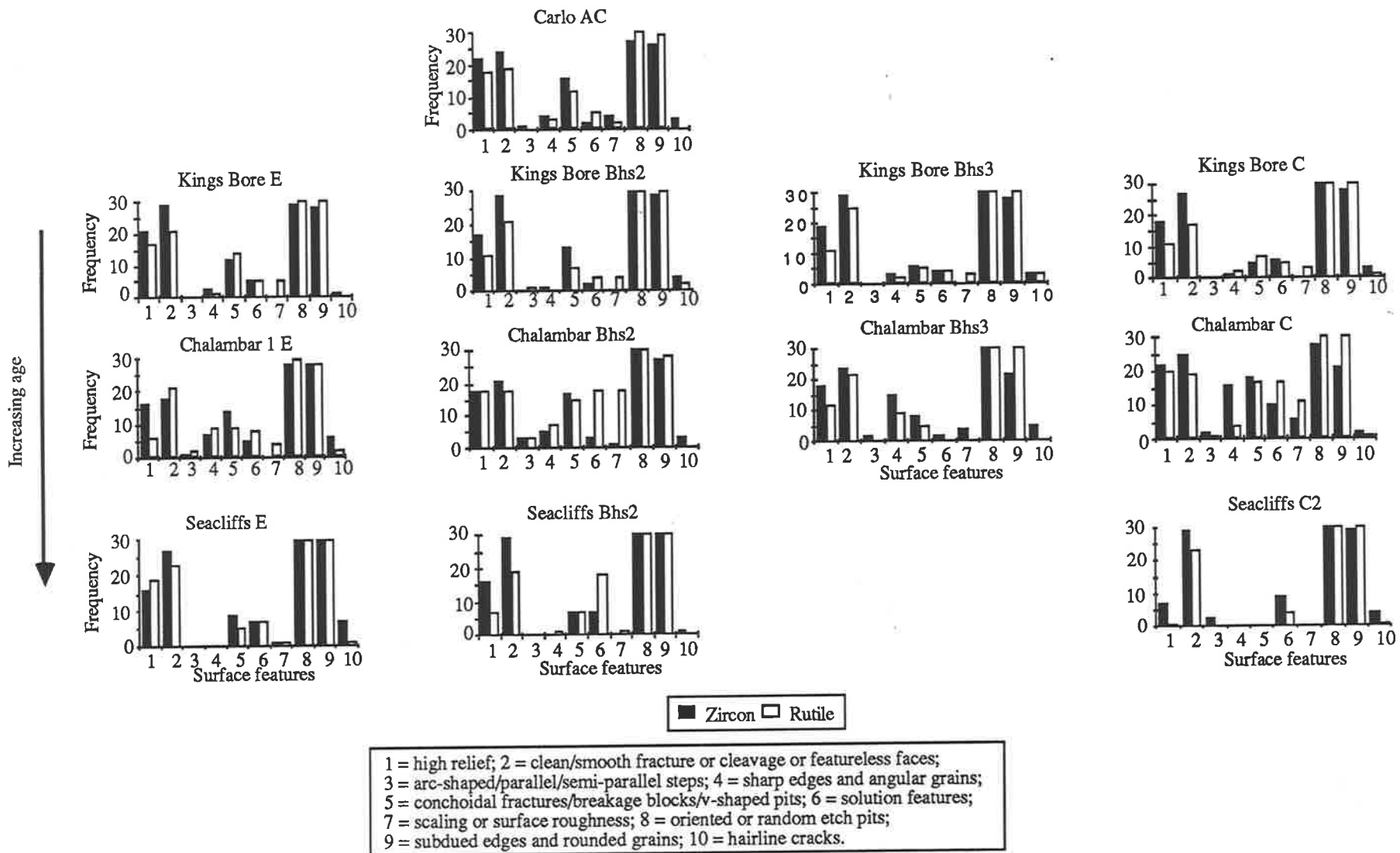


Fig. 6.1. Occurrence of microtextural features on grain surfaces from selected horizons.

horizons of different profiles (e.g. E and Bhs2 horizons). Between minerals, rutile exhibits more of the surface features associated with chemical weathering (features 6 to 10), except for feature 10 which is predominantly present on zircon. Conversely, surface features linked with mechanical weathering (features 1 to 5) occur more on zircon than rutile (Fig. 6.1). The features observed and described here are remarkably similar to those reported by many researchers (Krinsley and Donahue, 1968; Krinsley and Doornkamp, 1973; Setlow, 1978; Eswaran and Stoops, 1979; Bull *et al.*, 1987) albeit on different mineral species (mainly quartz) from those considered in this study.

Figures 6.21 and 6.22 show the energy dispersive x-ray (EDAX) spectra of zircon and rutile grains respectively, based on a part of the grain surface, for the E horizon of Seacliffs. As expected, the spectrum for zircon shows primarily the presence of Zr and Si. However, for rutile, Ti as well as minor amounts of Fe were observed. The very small Ca, Al and Cl peaks associated with the spectrum for rutile are possibly due to the presence of layer-silicates and/or allophanic materials.

6.3.1.2. Quantitative analysis of surface microtextures.

The qualitative differences in the frequency of occurrence of the grain surface features (as shown in Fig. 6.1) were evaluated statistically using the χ^2 distribution to test for significant differences in surface features (i) between horizons in the same profiles (Table. 6.2), (ii) between the same horizons in different profiles (Table 6.3) and (iii) between the two minerals in the same horizon (Table 6.4), for all soils. In order that the effects of pedogenesis on grain surface features (see Table 5.1) could be distinguished from depositional effects, it was a prerequisite that the nature of the ^{relatively} unaltered parent material of the soils of the chronosequence be defined. Ordinarily the C horizon of each soil could be taken as the parent material and a statistical comparison between surface features of sands from the C horizons would define the variability inherited from the sediment. Variability exceeding this value would be a measure of the influence of pedogenesis on mineral weathering as measured by differences in grain

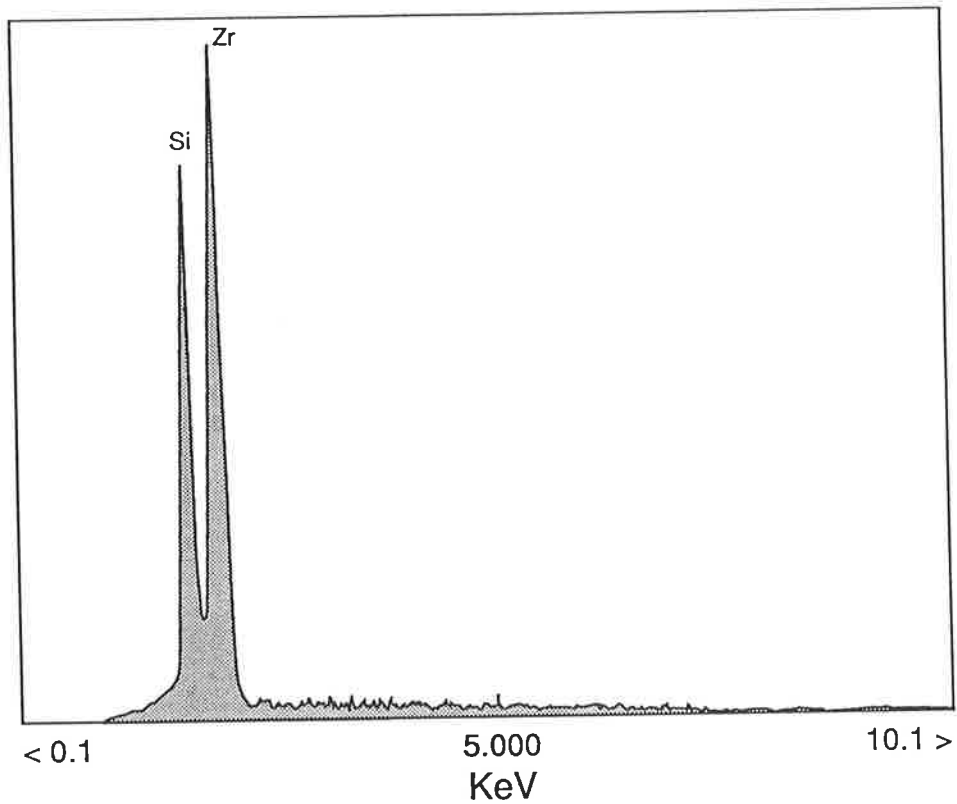


Fig. 6.21. EDAX spectrum for zircon from E horizon of Seacliffs profile.

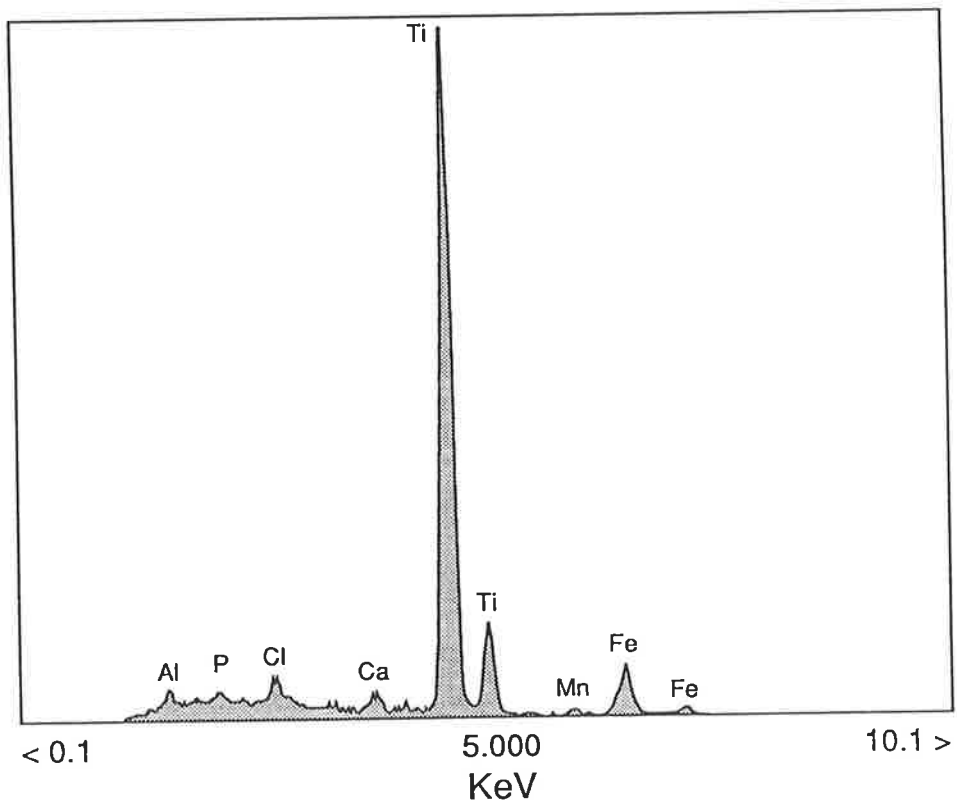


Fig. 6.22. EDAX spectrum for rutile containing iron from E horizon of Seacliffs profile.

Table 6.2. Comparison of surface features between grains within the same soil profile.

Surface feature number	Brief description†	Profile (Horizon‡)	Zircon			Rutile		
			Kings Bore (A1 to C)	Chalambar (A1 to C)	Seacliffs (A1 to C)	Kings Bore (A1 to C)	Chalambar (A1 to C)	Seacliffs (A1 to C)
1	High relief		ns	ns	****	ns	ns	*
2	Clean faces		ns	ns	ns	ns	****	ns
3	Steps		ns	ns	ns	ns	ns	ns
4	Angular grains		ns	**	****	ns	ns	ns
5	Conchoidal fractures		ns	ns	****	ns	ns	*
6	Solution		ns	ns	ns	ns	ns	ns
7	Rough surfaces		**	ns	***	ns	ns	ns
8	Etch pits		ns	ns	ns	ns	ns	ns
9	Rounded grains		ns	**	ns	ns	ns	ns
10	Hairline cracks		ns	ns	*	ns	ns	ns

*, **, *** and **** : significant at probabilities of 0.05, 0.025, 0.01 and 0.005 respectively; ns = non significant at 0.05.

† See Table 5.1 for full descriptions of surface features.

‡ Horizons for each profile are those listed in Table 6.1.

Table 6.3. Comparison of surface features between grains within the same horizons in different soil profiles using Carlo as reference profile.

Surface feature number	Brief description†	Horizon‡	Zircon					Rutile				
			A1	E	Bhs2	Bhs3	C	A1	A2	Bhs2	Bhs3	C
1	High relief		****	ns	ns	ns	****	*	***	*	ns	****
2	Clean faces		ns	*	****	ns	*	****	ns	ns	ns	ns
3	Steps		ns	ns	ns	ns	ns	ns	ns	ns	ns	ns
4	Angular grains		ns	***	ns	****	****	ns	****	***	*	ns
5	Conchoidal fractures		ns	ns	ns	**	****	ns	ns	ns	*	****
6	Solution		ns	ns	ns	ns	*	ns	ns	ns	ns	ns
7	Rough surfaces		ns	*	*	ns	ns	ns	ns	ns	ns	ns
8	Etch pits		ns	ns	ns	ns	ns	ns	ns	ns	ns	ns
9	Rounded grains		ns	ns	ns	ns	ns	ns	ns	ns	ns	ns
10	Hairline cracks		ns	ns	ns	ns	ns	ns	ns	ns	*	ns

* , ** , *** and **** : significant at probabilities of 0.05, 0.025, 0.01 and 0.005 respectively; ns = non significant at 0.05.

† See Table 5.1 for full descriptions of surface features.

‡ Horizons from Kings Bore, Chalambar 1, Seacliffs as shown in Table 6.1; Carlo is included as an AC horizon.

Table 6.4. Comparison of surface features on zircon and rutile in the same horizons of different soil profiles using Carlo as a reference profile.

Surface feature number	Brief description†	Profile‡				
		I	II	III	IV	V
1	High relief	ns	ns	ns	ns	ns
2	Clean faces	ns	ns	ns	ns	ns
3	Steps	ns	ns	ns	ns	ns
4	Angular grains	ns	ns	ns	ns	ns
5	Conchoidal fractures	ns	ns	ns	ns	ns
6	Solution	ns	ns	ns	ns	ns
7	Rough surfaces	ns	*	ns	ns	ns
8	Etch pits	ns	ns	ns	ns	ns
9	Rounded grains	ns	ns	ns	ns	ns
10	Hairline cracks	ns	ns	ns	ns	ns

* , ** , *** and ****: significant at probabilities of 0.05, 0.025, 0.01 and 0.005 respectively; ns, not significant at 0.05.

† See Table 5.1 for full descriptions of surface features.

‡ Same horizons in different profiles as:

I Carlo and A1 horizons of Kings Bore, Chalambar 1 and Seacliffs,

II Carlo and E horizons of Kings Bore, Chalambar 1 and Seacliffs respectively,

III Carlo and Bhs2 horizons of Kings Bore, Chalambar 1 and Seacliffs,

IV Carlo and Bhs3 horizons of Kings Bore and Chalambar, 1

V Carlo and C horizons of Kings Bore, Chalambar 1 and Seacliffs; Carlo is included as an AC horizon.

surface features. In view of the possibility of fluctuating water table effects on C horizons of the oldest soil (Seacliffs), it was decided that the Carlo profile was the most likely to represent the conditions of the parent materials of the other soils. Although referred to in this thesis as a profile, Carlo (at least where sampled) is a sedimentary deposit still actively accreting: there has been no pedogenesis, even to the extent of any organic matter accumulation.

Differences in surface features between horizons in the same profile.

In Table 6.2 the comparison of surface features on zircon and rutile grains within the same profile are presented. In explaining the observed differences in Tables

6.2, 6.3 and 6.4 the original frequency of occurrence of individual surface features on grains in horizons from the different profiles was referred to and used. There is a significant difference in the angularity of zircon grains between horizons in Chalambar and Seacliffs profiles. The Bhs2 horizon of Chalambar has the least number of angular grains, whilst the A1 horizon of Seacliffs has the highest number of angular grains. All horizons in the Kings Bore profile, except the Bhs3 and C, have slightly more conchoidal fractures/breakage blocks. The low number of subdued edge or rounded zircon grains in the C horizon of Chalambar accounts for the significant difference reported for this feature. In the oldest profile (Seacliffs) there are also significant differences between horizons for two other 'mechanical' features: high relief and conchoidal fractures/breakage blocks. The E and Bhs2 horizons show a significantly higher number of grains with high relief features, whereas the C horizon shows no evidence of grains with conchoidal fractures or breakage blocks. Zircon grains from the E horizon of Seacliffs have more hairline cracks than the other horizons. It is therefore suggested that soil development has led to both mechanical and chemical modification of zircon.

In the case of rutile (Table 6.2), there are significant differences for only a few features. There are significant differences for clean/smooth face features for horizons within Chalambar. The A1 horizon has far fewer clean/smooth faces compared to the other horizons. In the Seacliffs profile high relief and conchoidal fractures/breakage block features are significant. Very few high relief features were observed on grains from the C horizon. Most grains from the E horizon have conchoidal fractures or breakage blocks. As with zircon, rutile has been subjected to soil weathering processes leading to grain morphological modifications during pedogenesis.

Differences in surface features between the same horizons in different profiles.

For zircon grains there are significant differences in high relief, angularity, conchoidal fractures/breakage blocks and surface roughness for some of the horizons

(Table 6.3). Grains from the A1 and C horizons of the Seacliffs profile have a low number of high relief features recorded. In the E horizons more angular grains are recorded for the Chalambar profile. Similarly in the C horizons the Chalambar profile recorded about 40 % angular grains compared to zero for Seacliffs. For all horizons the Chalambar profile has more fractured grains than Carlo, Kings Bore and Seacliffs. In the C horizon, for example, 43 % of grains examined from Chalambar are fractured compared to zero for grains from Seacliffs. Hence, Seacliffs (the oldest soil) has a tendency to display surface features with smoother and more rounded attributes which could result from prolonged chemical and physical weathering. The values for surface roughness of zircon grains from E and Bhs2 horizons of Kings Bore, Chalambar and Seacliffs are marginally lower than for the youngest profile, Carlo. The main difference for solution features is between the C horizon of Seacliffs with 30 % occurrence (a well developed podzol) and the AC horizon of Carlo with ~ 7 % occurrence (mobile dune). The results indicate that pedogenesis has altered zircon.

Significant differences are reported between rutile grains with high relief from the A1, E, Bhs2 and C horizons (Table 6.3). The differences are due to rutile grains from Seacliffs having fewer high relief features than the other profiles, again indicating pedogenetic effects. The Chalambar A1 horizon has far fewer grains with clean smooth/fractured faces which accounts for the significant difference shown in Table 6.3. The E, Bhs2 and Bhs3 horizons show differences in grain angularity with Chalambar recording the highest occurrence of this feature on grains examined. Differences in the proportion of grains with conchoidal fractures/breakage blocks emanate from lower amounts of this feature on grains from the Bhs3 horizon of Kings Bore and Chalambar profiles and the C horizon of Seacliffs profile.

Differences in surface features between zircon and rutile in the same horizons of different profiles.

The statistical comparison of surface features on zircon and rutile in the same

horizons of different profiles showed that there were no significant differences between zircon and rutile grains, except for surface roughness in the E horizon (Table 6.4). It appears that rutile has been subjected to a greater degree of chemical weathering in this horizon than zircon.

6.4. Discussion

6.4.1. Chemical weathering features and pedogenic processes.

Chemical weathering is influenced primarily by solubility, atomic structure and intrinsic surface properties of the mineral (e.g. the number of defects per unit area), as well as the chemical environment of the medium. Pettijohn (1957) described chemical stability as the resistance of a mineral to intracrystal solution and/or weathering. The chemical agents which affect mineral surface reactions include water in the form of interstitial, rain and sea water. Except for feature 10 (hairline cracks), rutile shows more of the surface features indicative of chemical weathering (features 6 to 10 in Table 5.1)

Chemical weathering features after deposition which result in the formation of deep surface etching (Plate 6.7) and solution pits (Plates 6.8 and 6.9), show on rutile grains more intensely than on zircon grains. Even in the Bhs2 horizon where more of the rutile grains are coated with amorphous material (shown by micromorphology and SEM), there are larger amounts of solution pits on rutile grains than on zircons. In the literature there is controversy surrounding the role of amorphous grain coatings in protecting mineral grains from dissolution. Many researchers believe that dissolution of grains is surface-reaction controlled (through build up of ions at the crystal surface) rather than transport-controlled (through more rapid detachment of dissolving ions from the crystal surface). The bulk of the work has been done on iron-free silicate minerals (e.g. Berner and Schott, 1982). Studies on iron-bearing silicates (e.g. Schott and Berner, 1983) have suggested that in weathering conditions favouring oxidation the hydrous ferric oxide layer that forms is not protective enough. This is contrary to

another school of thought (e.g. Siever and Woodford, 1979) that iron hydroxide forms a protective surface layer on iron containing silicate minerals in oxidizing environments. The presence of more solution pits on rutile grains compared with zircon grains in the Bhs2 horizons suggests that iron-containing coatings which are common in this horizon (see Chapter 4 on micromorphology) are not protective enough to prevent dissolution. Selective surface dissolution leading to deep etch pit formation occurs at sites where there are structural dislocations. The presence of higher amounts of iron in the rutile compared with zircon may be responsible for more intense dissolution in the rutile. Wilson (1975) suggested that oxidation of structural ferrous iron is important in the early weathering stages of iron-containing minerals. Optical microscopic and electron probe work on the zircons showed hardly any evidence of crystalline inclusions and/or zoning of the grains. Such zircons are more chemically stable (Carroll, 1953) than those with either numerous inclusions or zoning. In general, it was found that the zircons were more corroded at broken ends of the prisms than at the prism surfaces and pyramid faces (e.g. Plate 6.1). Krinsley and Doornkamp (1973) concluded that the details of the surface imprints on quartz grains are a function of the number of previous chemical or mechanical episodes to which the grains have been subjected, the chemical reactivity of the surface, and the specific diagenetic environment into which the grains have been placed. Given that both minerals have had the same sedimentary history in any one horizon, it is clear that there is a greater difference between zircon and rutile grains in Seacliffs (the oldest profile) than in Carlo (the parent material) which is interpreted to mean that the surfaces of zircon grains have been less altered by pedochemical weathering than rutile.

Large scale chemical decomposition, resulting in friable cleavages or breakage plates with reduced bond strength between them (scaling) and very rough surfaces (feature 7, Table 5.1), which are indicative of a high energy chemical environment (Krinsley and Doornkamp, 1973), is a minor feature of both minerals (Fig. 6.1). If the interpretation for quartz relates to zircon and rutile, it may be that the microenvironment after deposition was high in sesquioxidic and humic compounds and

the climate hot and humid.

There are more coatings on the rutile grains than the zircon grains (Plate 6.10 for rutile) in the Bhs2 horizon. The coatings consist of Al, Si and some Fe. Such a composition could be related to imogolite and proto-imogolite allophanic materials which have been shown to coat grains in similar horizons of podzolic soils (Wilson, 1986). In the illuviated podzol Bhs horizon, the precipitation of amorphous products should occur initially on the most reactive sites, normally organic materials but, as the amorphous material becomes thicker, the mineral grains also become coated. Dissolved iron may be locally reprecipitated in and around the weathering grain wherever movement of the soil solution is relatively restricted, such as in an oxidizing environment with low biological activity. Therefore, zircon grains may have less coatings because of their very small iron content (up to 0.03 %), compared with rutile (up to 9 %).

6.4.2. Mechanical/physical weathering features and other environmental processes.

Surface textures 1 to 5 (Table 5.1) which are indicative of "freshness" tend to show up more on zircon than rutile. Zircon therefore appears to be more susceptible to mechanical breakdown than rutile. Most mechanically produced surface features are due to physical action during transportation, and the physical properties of a given mineral such as hardness, cleavage and tenacity, and physico-chemical properties such as shape, edges and corners determine the susceptibility of a grain to these physical processes (Lin *et al.*, 1974). Also of importance are the energy of the environment and the size distribution of the minerals concerned. Zircon has no cleavage, but is brittle and therefore prone to breaking into irregular fragments with conchoidal surfaces (Carroll, 1953). The weakness within the structure is often at the junction of the prism and pyramid faces.

Zircon and/or rutile grains in these podzols show an abundance of surface features such as high relief (Plates 6.2 and 6.11), semi-parallel or arc-shaped steps

(Plate 6.2), conchoidal fractures and breakage blocks (Plates 6.1, 6.2 and 6.11). If these features are interpreted on the basis of work done by Krinsley and Margolis (1971) and Setlow and Karpovich (1972), they can be interpreted as indicative of mechanical action in glacial environments. However, the possibility of a glacial event in this subtropical lowland region is very remote and the features can be indicative of other environmental conditions such as high energy conditions in surf zones, upper stretches of rivers and streams (Brown, 1973).

Grain angularity is more pronounced on zircon than rutile [compare Plates 6.3, 6.4 (left grain), with Plate 6.7]. The paucity of features having a chemical origin compared to features likely to be caused by mechanical effects indicates that the microtextural properties of zircon are due to conditions during transportation rather than *in situ* weathering.

6.4.3. Physico-chemical weathering features and other environmental processes.

There are some cases where it is difficult to separate chemical from physical or mechanical weathering. During chemical weathering, for instance, some alterations are accompanied by volume changes, with the product having a greater volume than the original. Hydration and oxidation seem to be the major agents of the chemical alteration process that causes physical weathering. The features described below tend to result from a combined action of physico-chemical processes in the weathering environment.

Rounded and subdued edges on grains are the result of mutual rubbing or impact and of pressure of large grains on smaller ones (Lin *et al.*, 1974) or solution (Krinsley and Doornkamp, 1973). Well rounded zircons showing little abrasion (Plate 6.4, grain on the left) can result from magmatic corrosion (Hollis *et al.*, 1986). The occurrence of well rounded grains, regardless of the grain surface textural characteristic (Plates 6.5 and 6.12) may be attributed to aeolian activity (Krinsley and Margolis, 1971). However, rounding of edges by solution in subaqueous environments in

which grains are transported, abraded and deposited by water may have also contributed to the rounding process (Plates 6.1 and 6.12). The grains in these Plates have few other features present on their surfaces.

Hairline cracks on fractured and unfractured grains [Plates 6.1, 6.4 (right grain), 6.5, 6.6 and 6.12] may have several causes. Krinsley and Doornkamp (1973) reported the occurrence of cracks on aeolian quartz grains with size $< 250 \mu\text{m}$. They believed this marked the beginning of chemical weathering in modern sand dunes. Hollis *et al.*, (1986) suggested that the cracks may result from rapid cooling and depressurization during transport in volcanic eruptions or reflect metamictization especially in zircon. It is possible that the cracks on grains in this were initiated in an earlier environmental setting, but the delicate nature of some of the microcrack patterns suggests them being formed *in situ* (Plates 6.1, 6.4, 6.5 and 6.6). Except for Plate 6.12 the other cracks are not associated with features resulting from strong chemical action. Therefore there is little likelihood of them being produced chemically. At the same time no obvious mechanical causes, such as salt crystal growth or heat effects, are evident in the crack formation.

Oriented and random etch pits occur to some degree on nearly all the grains observed for both minerals (see Plates). Lasaga and Blum (1986) have suggested that etch pits form on grain surfaces as a result of dislocations and line defects within the crystal. In energy terms the formation of an etch pit will depend on the stresses induced by the dislocations and the overall energy change for a transition from the solid to the solution. Impurities, fission tracks and alpha tracks may also serve as initiation sites for etching (Amelinckx, 1964). Etch pits form on grains in a range of environments, including subaqueous (Lin *et al.*, 1974), and soil (Raeside, 1959; Bateman and Catt, 1985). The ubiquity of this feature on grain surfaces from these soils renders it unsuitable as a means of environmental interpretation.

In discussing the likely environmental conditions and processes to which the minerals were once subjected, based on surface textural information, it is important to note that there are no simple diagnostic features for any one environmental

reconstruction. Different mechanical and chemical processes can produce similar surface features on mineral grains. For example (Whalley, 1985) reported that breakage textures such as conchoidal fractures, breakage blocks and semi-parallel step-like features, that are caused by brittle fracture, can be produced by a single mechanism.

6.5. Conclusions

Within profiles there are differences in the proportion of particular features between horizons. These differences become more pronounced with age. In the case of zircons, three out of five 'mechanical' features in the oldest profile (Seacliffs) show differences between horizons. Zircon and rutile grains in the oldest Spodosol (Seacliffs) showed significant differences in both mechanical and chemical surface features between E and B2 horizons compared with the C horizon. In all horizons of the oldest Spodosol (Seacliffs), zircon and rutile grains are more rounded and smoother in appearance than grains from the younger profiles. In the E horizons, rutile displays features indicative of greater chemical weathering than zircon. In the Bhs2, the rutile grains were more thickly coated with poorly crystalline iron and aluminosilicate compounds and also have higher amounts of solution pits than zircons. Zircon grains are less chemically altered during pedogenesis than rutile, probably because of the higher iron content in the rutiles, rendering them more susceptible to weathering. It appears that there has been loss of iron from rutiles by chemical etching and gain of iron, by deposition, in the form of discontinuous coatings. However, zircons tend to show more features which can be ascribed to processes of physical alteration.

The juxtaposition of euhedral, subhedral and unetched zircon and rutile grains with highly rounded and etched forms in the same profile indicates diverse provenance. Because of the high percentage of well-rounded and pitted grains, the soil parent materials are likely to have undergone considerable reworking. The occurrence,

in different proportions, of all the ten surface features on grains in the chronosequence suggests that the zircon and rutile grains have a complex environmental history, with no simple feature, or set of features, diagnostic for predepositional conditions. Nevertheless, microtextural features of zircons and rutiles are valuable for the interpretation of the extent and nature of post depositional weathering.

CHAPTER 7

MINERALOGY AND CHEMISTRY OF HEAVY MINERAL FRACTION

7.1. Introduction

In pedogenic studies, the origin of parent material and its degree of homogeneity are important in the assessment of soil development. The soils used in this study are derived either from aeolian or marine sediment sources. For this reason the heavy mineral distributions in these soils are mixtures of minerals, the type and proportion depending on the regional placement of source rocks, weathering (alteration) at exposure and transport. In quantitative pedological studies a major problem is the assessment of the degree of lithologic homogeneity of parent materials.

Several studies have been done to establish the uniformity of parent material (e.g. Chittleborough and Oades, 1980; Evans and Adams, 1975 a; Chittleborough *et al.*, 1984). Most of the methods (criteria) used are described in Barshad (1964). The most important are (i) total mineralogical analysis, (ii) particle-size distribution and the analysis of resistant minerals in one size fraction of the nonclay separate, (iii) ratio of the contents of two resistant minerals in any one size fraction. The most useful method in assessing uniformity depends on the nature of the parent material, but preferably the estimates of homogeneity should include as many methods as possible.

The second phase in mineralogical analysis, after assessment of parent material homogeneity, is to relate the mineral analyses to the genesis of soil profiles by interpreting mineralogical changes in the soil profile with depth due to pedochemical weathering and/or leaching (Brewer, 1976). Several methods are available for this analysis, including methods for assessing uniformity of parent material through the estimation of changes in volume or weight of stable (resistant to weathering) minerals.

The determination of the nature and magnitude of alteration of soil parent material during pedogenesis, and the subsequent evaluation of the fate of particular soil

constituents (in solution or colloidal form) depends on the assumption that certain minerals or groups of minerals are unaffected by pedogenic processes and can therefore remain stable and immobile. Even though no mineral is stable under all conditions (Wild, 1961; Berrow *et al.*, 1978), the stability sequences published by several workers (e.g. Matelski and Turk 1947; Weyl, 1951; Alias, 1961; Bateman and Catt, 1985) show that zircon, rutile, tourmaline, sphenc, magnetite and ilmenite have been shown to be satisfactory stable heavy minerals, with zircon, rutile and tourmaline as the most widely used minerals.

Heavy minerals can be can be quantitatively determined by a variety of methods including direct methods such as magnetic separation and grain counting or chemical determination of an element specific for a mineral or group of minerals (e.g. Zr for zircon, Ti for rutile or anatase). Direct quantification of mineral abundance and type through magnetic separation has been little used in soil studies (Mitchell, 1975). The bulk of work has concentrated on the use of the technique to separate mineral species into different groups based on their magnetic susceptibilities prior to chemical and/or mineralogical analysis. Little or no use has been made of the technique, on its own, as a tool in investigating the mineralogic homogeneity of soil profiles to verify either parent material uniformity or the degree of pedogenesis before mineral identification of the bulk magnetic fractions.

Most of the work involving the use of resistant minerals in soil development studies and, to lesser extent, parent material uniformity has been by individual grain counts under the petrographic microscope (e.g. Brewer, 1976). Both qualitative and quantitative differences in the heavy mineral suite of resistant minerals have been used to assess differences in parent material (Marshall and Jeffries, 1946). Comparison of the ratio of two resistant minerals in the whole soil or a specific size fraction with depth in a profile is an established method of assessing parent material uniformity. The constancy of the ratio with depth in a profile attests to homogeneity of the parent material. The application of this technique to transported soil materials in Australia is limited (Chittleborough *et al.*, 1984), despite an extensive and variable amount of soils

developed on transported parent materials. In most soils the resistant minerals occur in very low concentrations, and statistically valid interpretations can only be based on identifying and counting large numbers of grains separated from the bulk sample or from a specific particle-size fraction. Discrepancies in the results obtained from the resistant mineral ratio technique can be explained by using other methods such elemental chemistry of the resistant heavy minerals.

Another line of evidence used widely in pedogenic studies to verify parent material homogeneity and degree of weathering in soils is elemental chemistry of the light and heavy mineral fractions of soils. Several minerals have been selected as internal standards because of the difficulties with weathering resistance and mobility mentioned earlier in this chapter. The use of element concentrations specific for these resistant minerals to represent mineral abundance is widely used. Several workers (e.g. Smith and Wilding, 1972; Sudom and St. Armand, 1971; Chittleborough *et al.*, 1984) have used zirconium and titanium as measures of zircon and rutile respectively. Yttrium has also been used to estimate the amount of xenotime (Murad, 1978), boron for tourmaline (Marshall, 1977) and phosphorus for monazite (Chittleborough *et al.*, 1984).

The theory of an element specific for a mineral or group of minerals can also be used for the assessment of the degree of chemical weathering, using ratios of the concentration of weatherable to resistant minerals in the non-clay fraction of soils. CaO/ZrO_2 or $\text{Na}_2\text{O/ZrO}_2$ $\text{Fe}_2\text{O}_3/\text{ZrO}_2$ have been used on the assumption that Ca and Na occur almost exclusively in weatherable minerals (Beavers *et al.* 1963; Chittleborough and Oades, 1980; Chittleborough *et al.*, 1984). There is often a marked decrease in the ratios in the A horizon compared to the E which indicates that weathering and mobilization of Ca, Na and Fe are more intense in this part of the profile. In podzolic soils the development of bleached E horizon has been attributed to this process.

Weathering assessment based on calculation of losses and gains of less resistant constituents relative to a standard resistant mineral has also been used to assess soil

development. Values of losses and gains are essentially based on the choice of the parent material and the stable immobile constituent (Brewer, 1976). Various internal standards have been used by several workers, but by far the most widely used stable constituents are zirconium, quartz and titanium (Wilding *et al.*, 1971; Sudom and St. Armand, 1971; Evans and Adams 1975 b and Chittleborough *et al.*, 1984). Evidence of titanium mobility, from SEM analysis of particular soil fractions, has been reported, a fact which limits the use of this element as an indice.

Zircon is considered one of the most stable (i.e. least resistant to weathering) minerals in soils (Brewer, 1976; Marshall, 1977) and is an ubiquitous accessory heavy mineral in these environments. In geological studies, Hf/Zr (Kosterin *et al.*, 1960; Erlank *et al.*, 1978 b; Owen, 1987) ratios in zircons have been extensively used to determine source rocks for sediments. Detrital zircons of multicyclic nature may be from different proximate source rocks (rocks from which grain was recently eroded), and the use of zircon for provenance determination in such instances is limited to determining the petrogenetic relationship between the different rock types. The more acidic the rock, the less the Zr/Hf ratio (Erlank *et al.*, 1978 b).

In this chapter, an investigation is carried out in order to assess (i) the parent material uniformity and (ii) the extent of weathering of the soils using some of the techniques outlined above. Also the nature and origin of zircon is compared for selected soils.

7.2. Materials and methods

7.2.1. Materials

All soils from the fourteen profiles listed in Appendix 2 were subjected to heavy mineral separation and fractionation. Subsamples were analysed for zircon, rutile, zirconium and titanium contents. Twenty-three selected horizons were analysed for zirconium:hafnium ratios.

7.2.2. Methods

A general outline of the methods used is shown in the flow diagram in Chapter 5 (Fig. 5.1).

7.2.2.1. Heavy mineral separation and fractionation.

The methods used in this section have described in Chapter 5 (Section 5.2.2). The weights of the 53-125 μm fraction in the whole soil, total heavy mineral in the 53-125 μm fraction and different magnetic fractions in the total heavy mineral fraction were recorded as weight percentages.

7.2.2.2. Grain impregnation and mounting.

Subsamples of the non-magnetic fraction (NM) were impregnated using a mixture of polyester resin (Scotchcast No. 3) in the proportion of 2 parts of A to 3 parts of B by weight. The mixture was placed in an oven for about 10 minutes to lower the viscosity and remove entrapped air bubbles. Mineral grains were carefully added to the resin in plastic containers (15 mm diameter, 6.5 mm depth) on a hot plate. The mixtures were stirred to get maximum concentration of the grains at the bottom of the containers. The polyester resin polymerized after 12 hours at 75°C.

The mounted blocks of grains were gently ground flat (within a tolerance of 5 μm) using 600 grit silicon carbide paper. The flattened sides were thoroughly cleaned to remove any grinding residue and then rinsed with freon (carbon tetrafluoride). The blocks were fixed onto slides using epoxy resin (Araldite M:Araldite LC 234, 4:1). Uniform glue lines were obtained using spring loaded presses. Complete polymerization occurred after approximately 20 hours.

The mounted grain blocks were cut within 1 mm of the slide using a 250 mm diameter diamond saw, and ground on a surface grinder (Struers Discoplan-TS) until 40-50 μm thick. The sections were reduced to a final thickness of about 30 μm by polishing their surfaces using a Kent 3 automatic lapping and polishing machine.

7.2.2.3. *Electron microprobe analysis.*

The thin sections were eventually coated with carbon (after preliminary examination of slides with a petrographic microscope) by vacuum evaporation. Two sets of analyses were carried out on the coated samples.

First, grains were counted with a JEOL 733 electron microprobe under the control of a DEC computer and an automated point counting technique. Accelerating voltage was 15 kv, probe current 500 μ A and count time 1 second per point. The area of the slide to be covered was a function of the number of points to be counted and the distance between the points on the grid. More than 1000 points were counted on each slide. To reduce the possibility of double counting grains a 100 μ m spacing was preferred as the between point measurement. Spectra of minerals present on the slide and plastic (used for impregnation) were stored in the computer, and served as a reference by which the grain at a particular point could be assigned to a specific mineral class. The percentage mineral composition based on number of points counted for each phase was calculated. Because the particle-size was confined to a narrower range, concentrations of minerals were calculated directly from point counts with no adjustment for specific gravity.

Second, three positions (2 marginal and 1 central) on each of six zircon grains were analysed for five elements (Zr, Hf, Ti, Fe and Si). The analyses were performed using the same electron microprobe as above in the wavelength dispersive mode (WDS), at an accelerating voltage of 20 kv and a beam current of 30 ± 1.0 nA (regulated). Standards for the different elements were either pure metals or oxides. All analyses were carried out at $\times 10^3$ magnification. Data were analysed using Genstat 5 version 1.2 (1987) ANOVA procedures. As the concentration of Hf in detrital zircons is used as an indicator of petrogenetic relationships between rocks, the statistical evaluation of the data is reported for Zr and Hf contents of zircons in the selected profiles.

7.2.2.4. X-ray fluorescence spectroscopy.

Subsamples of the NM were ground in a McCrone micronising mill to a fine powder. After ignition in a furnace at 1000°C, 0.28 g of each sample was mixed with 1.52 g of lithium borate and lanthanum oxide and fused into a glass disc. Elemental concentrations were measured by x-ray fluorescence spectroscopy (XRF) using a Philips PW 1400 instrument and the sample preparation method of Norrish and Hutton (1969).

7.3. Results and discussion

7.3.1. Parent material uniformity.

The uniformity of the parent material was assessed by the following criteria viz

- (i) similarity of the proportion (by weight) of the 53-125 μm separate in the fine earth fraction of each horizon
- (ii) similarity of the proportion (by weight) of the total heavy mineral and different magnetic heavy fractions within the 53-125 μm fraction
- (iii) similarity of the ratio of zircon : rutile in the non-magnetic fraction of the 53-125 μm separate and
- (iv) similarity of the ratio of zirconium : titanium in the non-magnetic fraction of the 53-125 μm separate.

For rapid comparison between the four above criteria , a common scale (weight percent in the 2 mm fraction) was used in all Tables and some of the figures.

7.3.1.1. 53-125 μm fraction percent.

Horizons within profile.

The results for the 53-125 μm fraction by weight in the fine earth fraction indicate that, for horizons within a profile, the material is from a similar source. There are less inflections in figures (Figs. 7.101 to 7.122) and comparatively lower standard deviations (Table 7.1) compared to horizons between profiles (discussed later in this

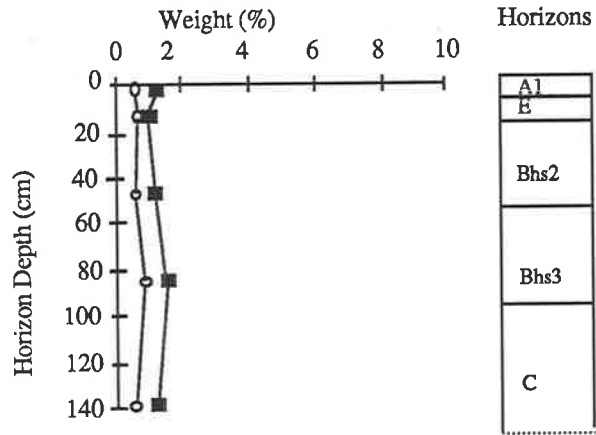


Fig. 7.101. Kings Bore profile.

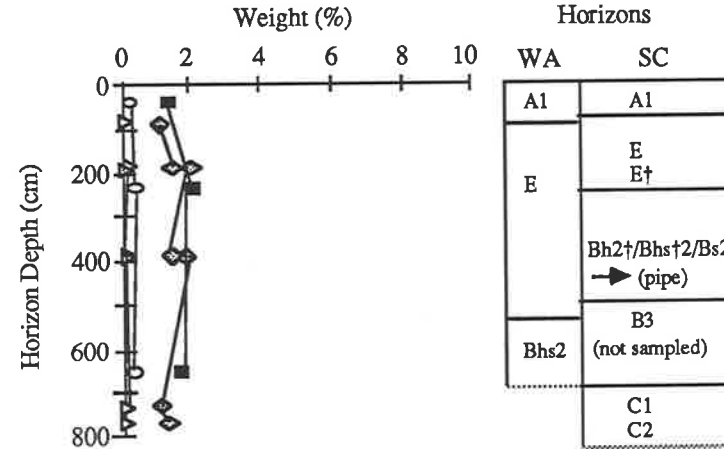


Fig. 7.103. Warrawonga (WA, ○, ■) and Seacliffs (SC, ▴, ◇) profiles. † = pipe.

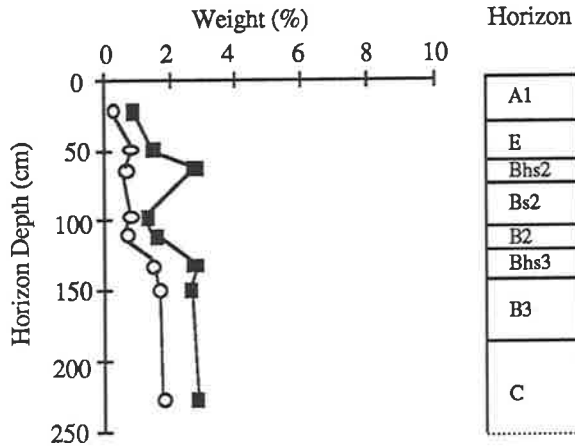


Fig. 7.102. Chalambar profile.

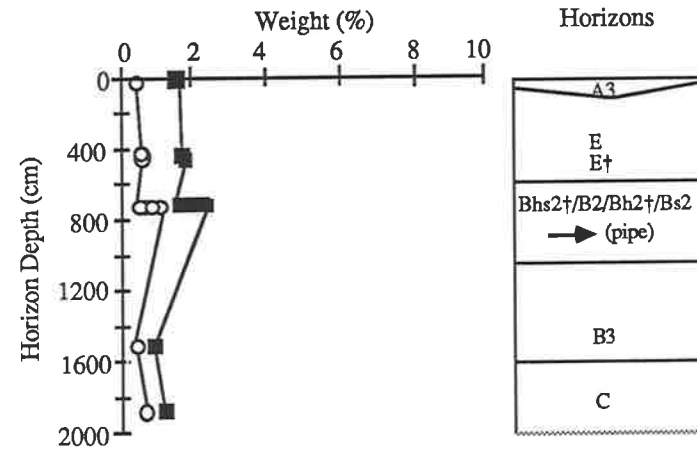
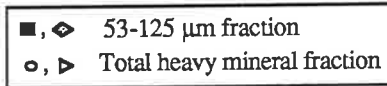


Fig. 7.104. Amity profile. † = pipe.

Fig. 7.10. Percent weight of 53-125 μm fraction and total heavy mineral fraction in the < 2 mm fraction of soils from the south east coast of Queensland.



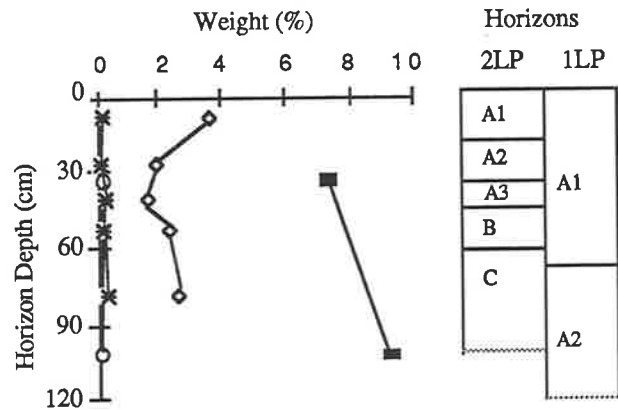


Fig. 7.111. LeFevre Peninsula 1 (1LP, O, ■) and LeFevre Peninsula 2 (2LP, ✖, ◇) profiles.

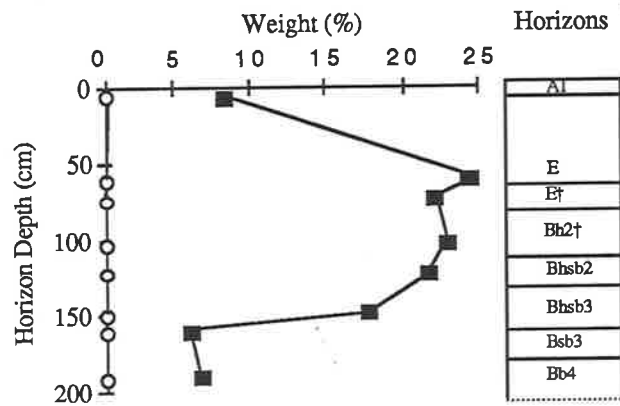


Fig. 7.112. Mount Compass profile. † = pipe.

Fig. 7.11. Percent weight of 53-125 μm fraction and total heavy mineral in the < 2 mm fraction of soils from the central South Australian coast.

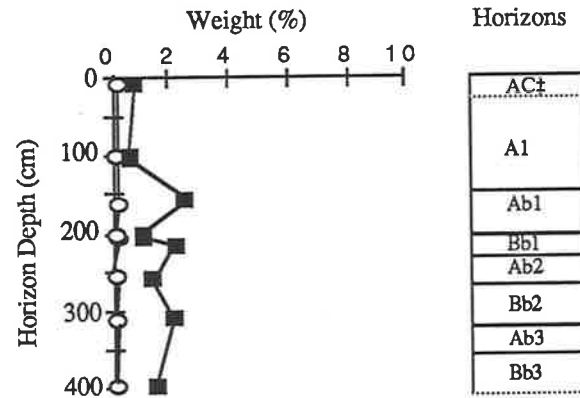


Fig. 7.121. Canunda site. † = beach deposit.

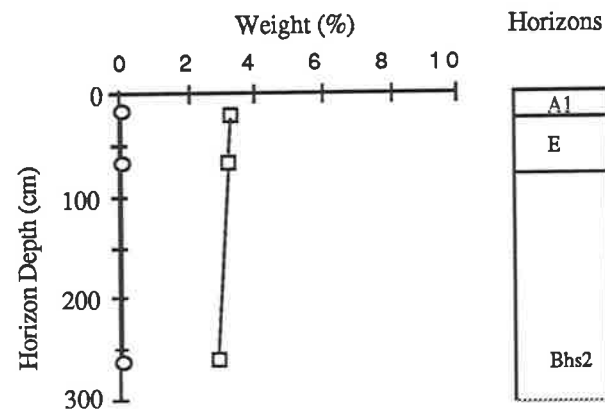


Fig. 7.122. Mount Burr profile.

Fig. 7.12. Percent weight of 53-125 μm fraction and total heavy mineral in the < 2 mm fraction of soils from the south east South Australian coast.

■, ◇ 53-125 μm fraction
O, ✖ Total heavy mineral fraction

Table 7.1. Percent 53-125 µm fraction particles and heavy minerals in the < 2 mm soil fraction, and ratio data for individual soil profiles. Means, standard deviations and coefficients of variation.

Horizon	Sampling depth (cm)	53-125 µm fraction	THM‡	Zi\$	Ru¶	Zi/Ru ratio	Zr	Ti	Zr/Ti ratio
Kings Bore Profile									
A1	0-10	1.05	0.54	0.112	0.088	1.27	0.077	0.117	0.66
E	15-20	0.94	0.51	0.109	0.102	1.07	0.067	0.099	0.68
Bhs2	30-60	1.18	0.78	0.142	0.149	0.95	0.127	0.141	0.90
Bhs3	60-110	1.57	1.00	0.175	0.187	0.94	0.154	0.215	0.72
C	130-150	1.25	0.74	0.133	0.134	0.99	0.101	0.180	0.56
Mean		1.20	0.71	0.134	0.132	1.04	0.105	0.150	0.70
Std.Dev.		0.24	0.20	0.027	0.039	0.14	0.036	0.047	0.12
CV %		20	28	20	30	13	34	31	18
Chalambar Profile									
A1	0-40	0.87	0.54	0.079	0.058	1.36	0.048	0.081	0.60
E	40-60	1.58	0.35	0.143	0.096	1.49	0.098	0.148	0.66
Bhs2	60-63	1.50	0.87	0.167	0.120	1.39	0.100	0.201	0.50
Bs2	80-120	1.52	0.66	0.130	0.107	1.21			
B2	100-120	1.30	0.76	0.155	0.112	1.38			
B3hs	120-140	2.75	1.47	0.370	0.182	2.03	0.207	0.274	0.76
B3	140-160	2.62	1.60	0.343	0.239	1.44			
C	200-250	2.92	1.63	0.330	0.231	1.43	0.242	0.294	0.82
Mean		1.883	0.99	0.215	0.143	1.47	0.139	0.200	0.67
Std.Dev.		0.766	0.51	0.114	0.066	0.24	0.082	0.088	0.13
CV %		41	51	53	46	17	59	44	19
Warrawonga Profile									
A1	0-80	1.15	0.15	0.023	0.034	0.68	0.017	0.040	0.43
E	210-260	2.02	0.33	0.050	0.067	0.75	0.038	0.081	0.47
Bhs2	625-690	1.72	0.21	0.032	0.049	0.65	0.024	0.057	0.42
Mean		1.63	0.23	0.035	0.050	0.69	0.026	0.059	0.44
Std.Dev.		0.44	0.09	0.014	0.017	0.05	0.011	0.021	0.03
CV %		27	40	40	33	7	40	35	6
Seacliffs Profile									
A1	55-110	1.22	0.12	0.020	0.027	0.74	0.015	0.032	0.47
E	150-250	2.10	0.26	0.043	0.049	0.88	0.028	0.070	0.40
E†	160-270	1.50	0.15	0.028	0.027	1.04			
Bh2†	310-470	1.65	0.14	0.024	0.022	1.09			
Bhs2†	310-470	1.80	0.16	0.025	0.026	0.96			
Bs2	310-470	1.70	0.24	0.035	0.057	0.61	0.026	0.061	0.43
C1	720-760	1.54	0.15	0.024	0.025	0.96	0.014	0.033	0.41
C2	780-800	1.30	0.24	0.033	0.034	0.97	0.022	0.049	0.45
Mean		1.60	0.18	0.029	0.033	0.91	0.021	0.049	0.43
Std.Dev.		0.28	0.05	0.008	0.013	0.16	0.006	0.017	0.03
CV %		17	30	26	38	17	30	34	6

Table 7.1 contd.

Horizon	Sampling depth (cm)	53-125 μ m fraction	THM†	Zi\$	Ru¶	Zi/Ru ratio	Zr	Ti	Zr/Ti ratio
Amity Profile									
A3	10-30	1.50	0.46	0.097	0.125	0.78	0.068	0.144	0.47
E	400-425	1.74	0.69	0.133	0.170	0.78	0.097	0.194	0.50
E†	415-440	1.72	0.59	0.115	0.156	0.74	0.074	0.180	0.41
Bh2†	700-900	1.69	0.55	0.105	0.149	0.70	0.076	0.156	0.49
Bhs2†	700-900	1.78	0.89	0.181	0.213	0.85	0.116	0.247	0.47
Bs2	700-900	2.15	0.69	0.131	0.174	0.75	0.079	0.209	0.38
B2	700-900	2.05	0.80	0.150	0.183	0.82	0.093	0.212	0.44
B3	1500-1550	0.98	0.34	0.145	0.150	0.97	0.077	0.152	0.51
C	1900-1930	1.25	0.48	0.166	0.215	0.77	0.118	0.246	0.48
Mean		1.65	0.61	0.136	0.171	0.80	0.089	0.193	0.46
Std.Dev.		0.37	0.17	0.028	0.030	0.08	0.018	0.039	0.04
CV %		22	29	20	17	10	21	20	9
LeFevre Peninsula 1 Profile									
A1	26-40	7.63	0.03	0.003	0.002	1.50			
A2	90-110	9.24	0.03	0.002	0.003	0.67			
Mean		8.44	0.03	0.003	0.003	1.08			
Std.Dev.		1.13	0	0.001	0.001	0.59			
CV %		13	0	33	25	54			
LeFevre Peninsula 2 Profile									
A1	0-15	3.87	0.10	0.006	0.005	1.20			
A2	15-30	1.99	0.12	0.007	0.008	0.88			
A3	30-49	1.82	0.18	0.007	0.010	0.70	0.006	0.014	0.43
B	49-60	2.45	0.02	0.002	0.003	0.67	0.002	0.003	0.67
C	60-100	2.48	0.22	0.013	0.015	0.87	0.011	0.020	0.55
Mean		2.52	0.13	0.007	0.008	0.86	0.006	0.013	0.55
Std.Dev.		0.80	0.08	0.004	0.005	0.21	0.004	0.009	0.12
CV %		32	60	57	57	25	69	68	22
Mount Compass Profile									
A1	0-10	8.14	0.03	0.010	0.005	2.00			
E	10-110	24.67	0.08	0.031	0.010	3.10	0.018	0.015	1.20
E†	30-100	21.79	0.07	0.031	0.011	2.82	0.019	0.014	1.36
Bh2†	90-120	22.35	0.08	0.027	0.013	2.08	0.019	0.014	1.36
Bhsb2	110-130	21.33	0.08	0.030	0.010	3.00	0.019	0.013	1.46
Bhsb3	135-150	17.79	0.08	0.033	0.008	4.13	0.020	0.012	1.67
Bsb3	155-175	5.63	0.06	0.007	0.002	3.50			
Bb4	160-220	6.85	0.07	0.020	0.006	3.33	0.012	0.007	1.71
Mean		16.07	0.07	0.024	0.008	3.02	0.015	0.013	1.46
Std.Dev.		7.87	0.02	0.010	0.004	0.84	0.007	0.003	0.20
CV %		49	25	43	46	28	47	22	14

Table 7.1 contd.

Horizon	Sampling depth (cm)	53-125 μ m fraction	THM†	Zi\$	Ru¶	Zi/Ru ratio	Zr	Ti	Zr/Ti ratio
Canunda Profile									
A1	90-110	0.58	0.01	0.0004	0.0002	2.00			
Ab1	155-170	2.82	0.02	0.0004	0.0004	1.00			
Bb1	185-200	0.96	0.01	0.004	0.004	1.00			
Ab2	205-220	2.45	0.03	0.004	0.003	1.33			
Bb2	240-260	1.40	0.04	0.004	0.004	1.00			
Ab3	310-318	2.31	0.02	0.001	0.001	1.00			
Bb3	340-370	1.55	0.02	0.001	0.001	1.00			
<i>Mean</i>		<i>1.72</i>	<i>0.02</i>	<i>0.002</i>	<i>0.002</i>	<i>1.19</i>			
<i>Std Dev.</i>		<i>0.83</i>	<i>0.01</i>	<i>0.002</i>	<i>0.002</i>	<i>0.38</i>			
<i>CV %</i>		<i>48</i>	<i>53</i>	<i>84</i>	<i>86</i>	<i>32</i>			
Mount Burr Profile									
A1	0-25	3.11	0.06	0.009	0.013	0.69			
E	60-80	3.09	0.07	0.010	0.013	0.77			
Bhs2	250-270	2.93	0.05	0.007	0.009	0.78			
<i>Mean</i>		<i>3.04</i>	<i>0.06</i>	<i>0.009</i>	<i>0.012</i>	<i>0.75</i>			
<i>Std Dev.</i>		<i>0.10</i>	<i>0.01</i>	<i>0.002</i>	<i>0.003</i>	<i>0.05</i>			
<i>CV %</i>		<i>3</i>	<i>17</i>	<i>19</i>	<i>22</i>	<i>7</i>			

† = Soil material associated with pipe.

‡ THM = total heavy mineral.

\$ Zi = zircon.

¶ Ru = rutile.

chapter). The MC profile (Fig. 7.112) is an exception, insofar as there are a greater number of inflections for the sub-horizons of E, B2 and Bhsb3, compared with the overlying A1 and underlying Bsb3 and Bb4 horizons. This may indicate either a boundary between depositional layers or more weathering of coarser to finer fractions. It should be pointed out that inflections may be due to either parent inhomogeneity, weathering *in situ* and/or statistical fluctuations. With respect to the latter, there is no agreed deviation beyond which one could say that a horizon was *not* pedogenetically related to another horizon. Except for LeFevre Peninsula 1 (Fig. 7.111) and Mount Compass (Fig. 7.112) profiles, the weight percentage of heavy minerals in the 53-125 μ m fraction of the fine earth fraction in horizons within profiles from the different locations is less than 5 %.

Horizons between profiles.

On a regional basis, comparable horizons from soil profiles in the same location showed evidence of similar size distribution which may imply homogeneity of source material (Figs. 7.131 to 7.135 and Table 7.2). For the 53-125 μm fraction, soils from Cooloola (CL, KB, BW, CH, SC, WA, MU and KL) and North Stradbroke Island (AM) have similar trends with depth for all horizons, but these trends are different from soils in other locations (1LP, 2LP, MC, CN and MB). Because of the overlap of results for fractions from different locations (separated both in time and space), further mineralogical proof of parent material uniformity using other methods is essential.

7.3.1.2. Total heavy mineral (THM) percent.*Horizons within profile.*

The THM in the < 2 mm fraction showed relatively consistent trends with depth (Figs. 7.101 to 7.104, 7.111 to 7.112 and 7.121 to 7.122, and Table 7.1). The percent weight varied widely: from 1.63 in the C horizon of Chalambar profile to 0.01 in the AC, A1 and Bb2 horizons of Canunda profile. There are variations in percentages of THM fraction, between profiles both from the same location (Cooloola - compare KB, CH, WA, and SC as in Figures 7.101 to 7.104; LeFevre Peninsula - compare 1LP and 2LP as in Figure 7.111); Mount Compass (Fig. 7.112); Canunda (Fig. 7.121) and Mount Burr (Fig. 7.122). In general there is a higher concentration of heavy minerals in soils from the south east coast of Queensland. This concentration ranges from 0.12-1.63 %, whereas in other locations, the concentrations are < 0.1%, except for 2LP (Table 7.1).

Horizons between profiles.

Comparable horizons from different profiles, both at location and regional levels, displayed wide disparity particularly amongst samples from the south east coast of Queensland (CL, KB, BW, CH, WA, SC, MU, KL and AM) as shown in Figs. 7.131 to 7.135, and Table 7.2. The differences in total heavy mineral content within

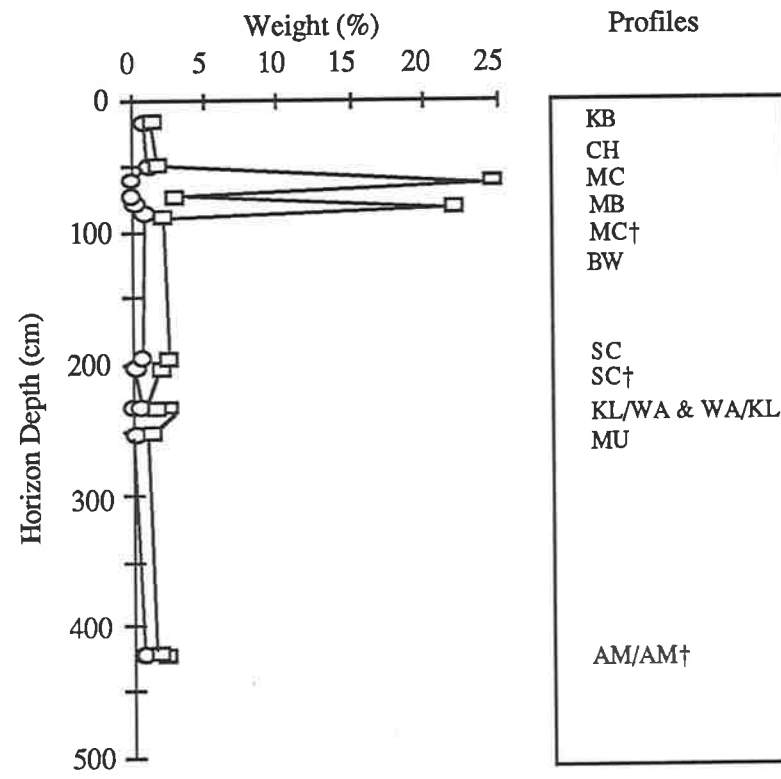
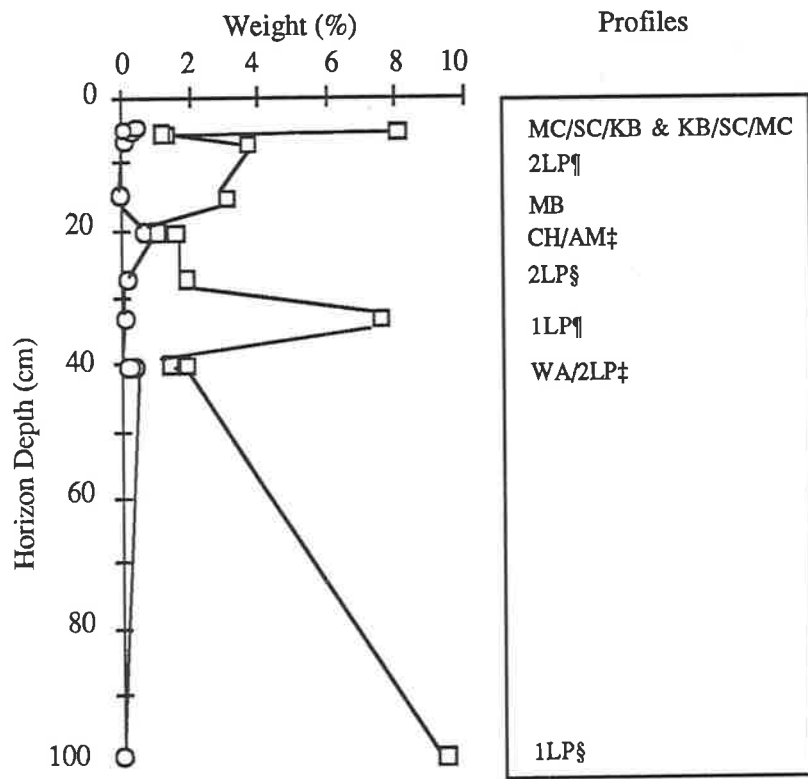


Fig. 7.131. A horizons of different profiles.

Fig. 7.132. E horizons of different profiles.

Fig. 7.13. Percent weight of 53-125 μm fraction and total heavy mineral fraction in the < 2 mm fraction of soils from comparable horizons of different profiles.

KB = Kings Bore, MC = Mount Compass, 2LP = LeFevre Peninsula 2, MB = Mount Burr, AM = Amity, CH = Chalambar, WA = Warrawonga, 1LP = LeFevre Peninsula 1, SC = Seacliffs, BW = Burwilla, KL = Kabali and MU = Mundu. ¶ = A1, § = A2, ‡ = A3 and † = pipe.

○ 53-125 μm fraction
 □ Total heavy mineral fraction

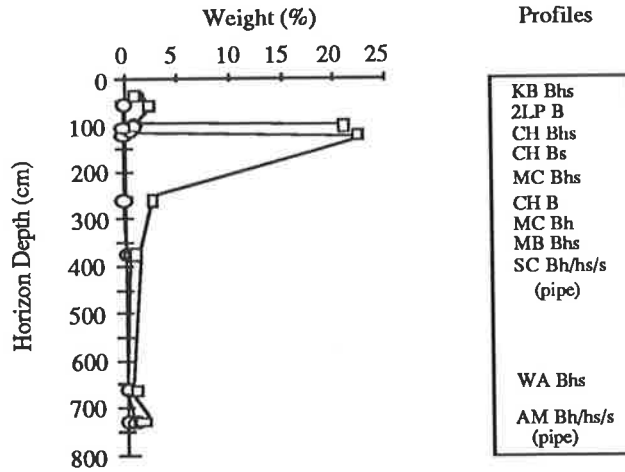


Fig. 7.133. B2 horizons of different profiles.

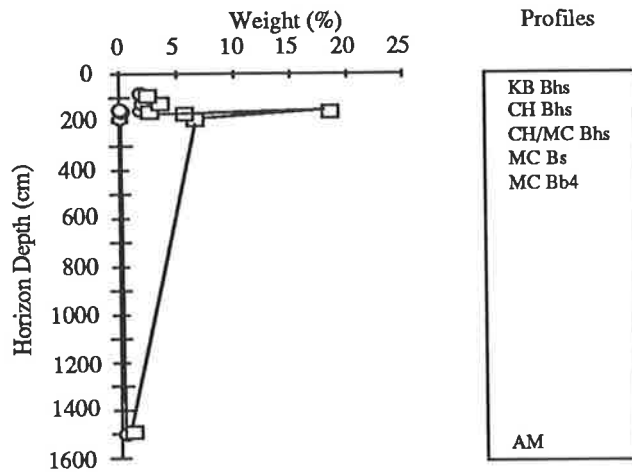


Fig. 7.134. B3 horizons of different profiles.

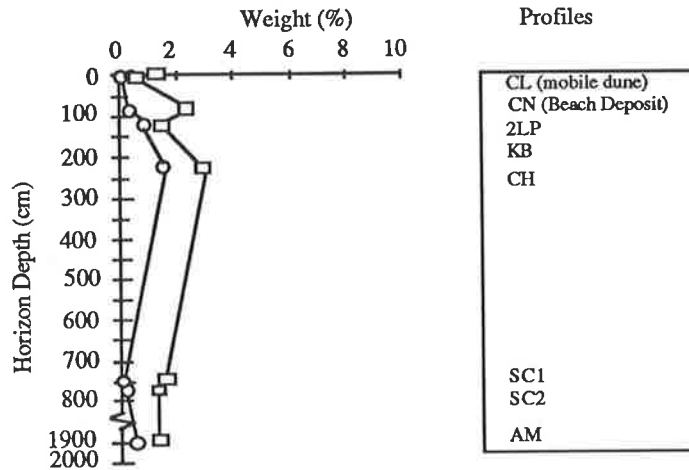


Fig. 7.135. C horizons of different profiles.

Fig. 7.13. contd. Percent weight of 53-125 μm fraction and total heavy mineral fraction in the < 2 mm fraction of soils from comparable horizons of different profiles.

KB = Kings Bore, CH = Chalambar, WA = Warrawonga, SC = Seacliffs, AM = Amity, 2LP = LeFevre Peninsula 2, MB = Mount Furr, MC = Mount Compass, CL = Carlo and CN = Canunda.

○ 53-125 μm fraction
 □ Total heavy mineral fraction

Table 7.2. Percent by weight of (a) 53-125 μm fraction, (b) total heavy mineral, (c) zircon and (d) rutile in the < 2 mm soil fraction, and ratio data for comparable horizons of different soil profiles. Means, Standard deviations and coefficients of variation.

Profile# (Horizon)	Sampling depth (cm)	53-125 μm fraction	THM†	Zi‡	Ru§	Zi/Ru ratio	Zr	Ti	Zr/Ti ratio
AC Horizon									
CL	0-5	1.45	0.35	0.058	0.066	0.88	0.036	0.084	0.43
CN	0-5	0.65	0.01	0.0006	0.0005	1.20			
<i>Mean</i>		<i>1.05</i>	<i>0.18</i>	<i>0.029</i>	<i>0.033</i>	<i>1.03</i>			
<i>Std.Dev.</i>		<i>0.57</i>	<i>0.24</i>	<i>0.040</i>	<i>0.046</i>	<i>0.22</i>			
<i>CV %</i>		<i>54</i>	<i>133</i>	<i>139</i>	<i>139</i>	<i>22</i>			
A Horizon									
KB (A1)	0-10	1.05	0.54	0.112	0.088	1.27	0.077	0.117	0.66
MC (A1)	0-10	8.14	0.03	0.010	0.005	2.00			
2LP (A1)	0-15	3.87	0.10	0.006	0.005	1.20			
MB (A1)	0-25	3.11	0.06	0.009	0.013	0.69			
CH (A1)	0-40	0.87	0.37	0.079	0.058	1.36	0.048	0.081	0.60
WA (A1)	0-80	1.15	0.15	0.023	0.034	0.68	0.017	0.040	0.43
AM (A3)	10-30	1.50	0.46	0.097	0.125	0.78	0.068	0.144	0.47
2LP (A2)	15-30	1.99	0.12	0.007	0.008	0.88			
1LP (A1)	26-40	7.64	0.03	0.003	0.002	1.50			
2LP (A3)	30-49	1.82	0.18	0.007	0.010	0.70	0.006	0.014	0.43
SC (A1)	55-110	1.22	0.12	0.020	0.027	0.74	0.015	0.032	0.48
1LP (A2)	90-110	9.24	0.03	0.002	0.003	0.67			
<i>Mean</i>		<i>3.47</i>	<i>0.18</i>	<i>0.031</i>	<i>0.032</i>	<i>1.04</i>	<i>0.039</i>	<i>0.071</i>	<i>0.51</i>
<i>Std.Dev.</i>		<i>3.08</i>	<i>0.18</i>	<i>0.040</i>	<i>0.039</i>	<i>0.43</i>	<i>0.030</i>	<i>0.051</i>	<i>0.09</i>
<i>CV %</i>		<i>89</i>	<i>96</i>	<i>128</i>	<i>125</i>	<i>41</i>	<i>78</i>	<i>72</i>	<i>19</i>
E Horizon									
MC (E)	10-110	24.67	0.08	0.031	0.010	3.10	0.018	0.015	1.20
KB (E)	15-20	0.94	0.51	0.109	0.102	1.07	0.067	0.099	0.68
MC (E†)	30-100	21.79	0.07	0.031	0.011	2.82	0.019	0.014	1.36
CH (E)	40-60	1.58	0.72	0.143	0.096	1.49	0.098	0.148	0.656
MB (E)	60-80	3.09	0.07	0.010	0.013	0.77			
BW (E)	70-90	1.61	0.54	0.081	0.101	0.80	0.064	0.130	0.49
SC (E)	150-250	2.10	0.26	0.043	0.049	0.88	0.028	0.070	0.40
SC (E†)	160-270	1.50	0.15	0.028	0.027	1.04			
KL (E)	210-260	2.81	0.27	0.049	0.046	1.06	0.029	0.071	0.41
WA (E)	210-260	2.02	0.33	0.050	0.067	0.75	0.038	0.081	0.47
MU (E)	220-280	1.92	0.38	0.066	0.063	1.045	0.041	0.084	0.49
AM (E)	400-425	1.74	0.59	0.133	0.170	0.78	0.097	0.194	0.50
AM (E†)	415-440	1.72	0.55	0.115	0.156	0.74	0.074	0.180	0.41
<i>Mean</i>		<i>5.19</i>	<i>0.35</i>	<i>0.068</i>	<i>0.070</i>	<i>1.26</i>	<i>0.052</i>	<i>0.099</i>	<i>0.64</i>
<i>Std.Dev.</i>		<i>8.05</i>	<i>0.22</i>	<i>0.044</i>	<i>0.053</i>	<i>0.78</i>	<i>0.029</i>	<i>0.059</i>	<i>0.33</i>
<i>CV %</i>		<i>155</i>	<i>63</i>	<i>64</i>	<i>75</i>	<i>62</i>	<i>56</i>	<i>60</i>	<i>51</i>
Bhs2 Horizon									
KB (Bhs2)	30-60	1.18	0.78	0.142	0.149	0.95	0.127	0.141	0.90
CH (Bhs2)	60-63	1.50	0.87	0.167	0.120	1.39	0.100	0.201	0.50
MC (Bhs2)	110-130	21.33	0.08	0.027	0.013	3.00	0.019	0.014	1.35
MB (Bhs2)	250-270	2.93	0.05	0.007	0.009	0.78			
SC (Bhs2†)	310-470	1.80	0.16	0.004	0.004	0.96			
WA (Bhs2)	625-690	1.73	0.21	0.032	0.049	0.65	0.024	0.057	0.42
AM (Bhs2†)	700-900	1.78	0.89	0.181	0.213	0.85	0.116	0.247	0.47
<i>Mean</i>		<i>4.61</i>	<i>0.43</i>	<i>0.089</i>	<i>0.081</i>	<i>1.22</i>	<i>0.077</i>	<i>0.132</i>	<i>0.75</i>
<i>Std.Dev.</i>		<i>7.39</i>	<i>0.39</i>	<i>0.083</i>	<i>0.084</i>	<i>0.81</i>	<i>0.052</i>	<i>0.097</i>	<i>0.44</i>
<i>CV %</i>		<i>160</i>	<i>90</i>	<i>98</i>	<i>104</i>	<i>66</i>	<i>67</i>	<i>74</i>	<i>59</i>

Table 7.2 contd.

Profile# (Horizon)	Sampling depth (cm)	53-125 μ m fraction	THM‡	Zi\$	Ru¶	Zi/Ru ratio	Zr	Ti	Zr/Ti ratio
B Horizons (except Bhs2)									
2LP (B)	49-60	2.45	0.02	0.002	0.003	0.67	0.002	0.003	0.67
CH (Bs2)	80-120	1.52	0.66	0.130	0.107	1.21			
MC (Bh2†)	90-120	22.35	0.08	0.030	0.010	2.08	0.019	0.014	1.36
CH (B2)	100-120	1.30	0.76	0.155	0.112	1.38			
SC (Bh2†)	310-470	1.65	0.14	0.024	0.022	1.09			
SC (Bs2)	310-470	1.70	0.24	0.035	0.057	0.61	0.026	0.061	0.43
AM (Bh2†)	700-900	1.69	0.55	0.105	0.149	0.70	0.076	0.156	0.49
AM (Bs2)	700-900	2.15	0.69	0.131	0.174	0.75	0.079	0.209	0.38
AM (B2)	700-900	2.05	0.80	0.150	0.189	0.82	0.093	0.212	0.44
<i>Mean</i>		<i>4.09</i>	<i>0.44</i>	<i>0.079</i>	<i>0.083</i>	<i>1.03</i>	<i>0.049</i>	<i>0.109</i>	<i>0.63</i>
<i>Std.Dev.</i>		<i>6.85</i>	<i>0.31</i>	<i>0.060</i>	<i>0.071</i>	<i>0.47</i>	<i>0.038</i>	<i>0.095</i>	<i>0.37</i>
<i>CV %</i>		<i>167</i>	<i>72</i>	<i>73</i>	<i>75</i>	<i>46</i>	<i>77</i>	<i>87</i>	<i>59</i>
B3 Horizon									
KB (Bhs3)	60-110	1.57	1.00	0.175	0.187	0.94	0.154	0.215	0.72
CH (Bhs3)	120-140	2.75	1.47	0.370	0.182	2.03	0.207	0.274	0.76
MC (Bhsb3)	135-150	17.79	0.08	0.033	0.008	4.13	0.020	0.012	1.67
CH (B3)	140-160	2.62	1.60	0.343	0.239	1.44			
MC (Bsb3)	155-175	5.63	0.06	0.007	0.002	3.50			
MC (Bb4)	160-220	6.85	0.07	0.020	0.006	3.33	0.012	0.007	1.67
AM (B3)	1500-1550	0.98	0.34	0.077	0.079	0.97	0.041	0.080	0.51
<i>Mean</i>		<i>5.46</i>	<i>0.66</i>	<i>0.146</i>	<i>0.100</i>	<i>2.33</i>	<i>0.087</i>	<i>0.118</i>	<i>1.07</i>
<i>Std.Dev.</i>		<i>5.84</i>	<i>0.68</i>	<i>0.154</i>	<i>0.101</i>	<i>1.31</i>	<i>0.088</i>	<i>0.121</i>	<i>0.57</i>
<i>CV %</i>		<i>107</i>	<i>103</i>	<i>105</i>	<i>100</i>	<i>56</i>	<i>101</i>	<i>103</i>	<i>52</i>
C Horizon									
2LP (C)	60-100	2.48	0.22	0.013	0.015	0.87	0.011	0.020	0.55
KB (C)	130-150	1.25	0.74	0.133	0.134	0.99	0.101	0.180	0.56
CH (C)	200-250	2.92	1.63	0.330	0.231	1.43	0.242	0.294	0.82
SC (C1)	720-760	1.54	0.15	0.024	0.025	0.96	0.014	0.033	0.41
SC (C2)	780-800	1.30	0.24	0.033	0.034	0.97	0.022	0.049	0.45
AM (C)	1900-1930	1.25	0.48	0.079	0.103	0.77	0.056	0.118	0.48
<i>Mean</i>		<i>1.79</i>	<i>0.58</i>	<i>0.102</i>	<i>0.090</i>	<i>1.00</i>	<i>0.074</i>	<i>0.116</i>	<i>0.54</i>
<i>Std.Dev.</i>		<i>0.73</i>	<i>0.56</i>	<i>0.120</i>	<i>0.083</i>	<i>0.22</i>	<i>0.089</i>	<i>0.106</i>	<i>0.14</i>
<i>CV %</i>		<i>40</i>	<i>97</i>	<i>117</i>	<i>92</i>	<i>22</i>	<i>120</i>	<i>92</i>	<i>26</i>

CL = Carlo, CN = Canunda, KB = Kings Bore, MC = Mount Compass, 2LP = LeFevre Peninsula 2, MB = Mount Burr, CH = Chalambar, WA = Warrawonga, AM = Amity, 1LP = LeFevre Peninsula 1, SC = Seacliffs, BW = Burwilla, KL = Kabali and MU = Mundu.

† = Soil material associated with pipe; ‡ THM = total heavy mineral; \$ Zi = zircon; ¶ Ru = rutile.

and between profile can be explained by the fact that many of the mineral species are not particularly resistant to weathering in the soil environment. This has been clearly demonstrated by the numerous weathering stability indices published by different workers mentioned earlier (e.g. Matelski and Turk 1947; Weyl, 1951; Alias, 1961; Bateman and Catt, 1985). As a result, the proportions and total amounts of the different mineral species may change markedly with depth in profiles formed even on

uniform parent material (Haseman and Marshall, 1945). Also *in situ* weathering can alter mineral proportions within different size fractions in the various horizons of a profile with homogeneous source material (Brewer, 1955). The differences in quantitative bulk mineral content is characteristic (a) differences in geological materials and (b) differences in conditions of deposition. Almost certainly both have been contributors to between sample variation especially in view of the geology and mode of deposition of the parent materials. A quantitative and qualitative determination of the magnetic fraction was carried out to further investigate the geological and depositional aspects of the parent sediments.

7.3.1.3. Magnetic mineral fraction percent.

Horizons within profile.

The weight percent of minerals in the non-magnetic (NM), slightly magnetic (SM) and strongly magnetic (VM) fractions in the < 2 mm separate is shown for individual profiles (Figs. 7.201 to 7.222) in the three regions. For soils from Cooloola (KB, BW, CH, WA, SC, MU and KL) and North Stradbroke Island (AM) the proportion of NM and VM fractions are similar and are much higher in concentration than the SM (Figs. 7.201 to 7.205). Soils from 1LP and 2LP have proportions in the order VM > NM > SM (Figs. 7.211 to 7.212), whereas the Mount Compass soil (MC) has a rather inconsistent trend of abundance with mostly NM > SM > VM (Fig. 7.213). In soils from the south east of South Australia the magnetic mineral fraction abundance followed the order Canunda = VM ≥ NM > SM and Mount Burr = NM > VM > SM (Figs. 7.221 and 7.222). Values far less than 0.01% were not recorded in the figures at the scales used.

Horizons between profiles.

On a regional basis the mineral distribution of the magnetic fractions were similar for profiles from Cooloola (CL, KB, CH, BW, SC, WA, MU and KL), because of comparable source materials (Figs. 7.231 to 7.235). The mineral

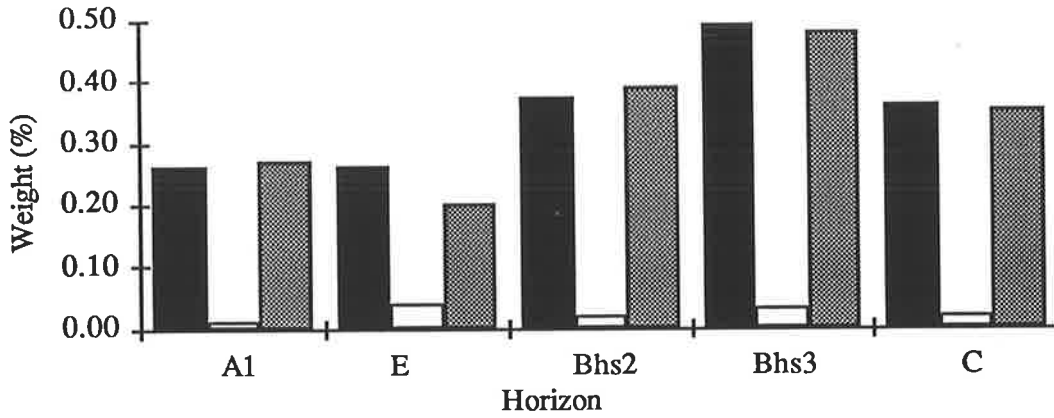


Fig. 7.201. Kings Bore profile.

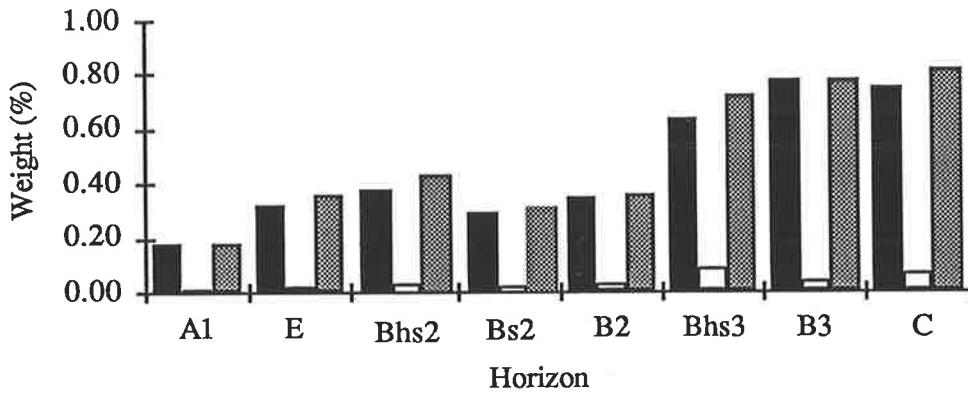


Fig. 7.202. Chalambar profile.

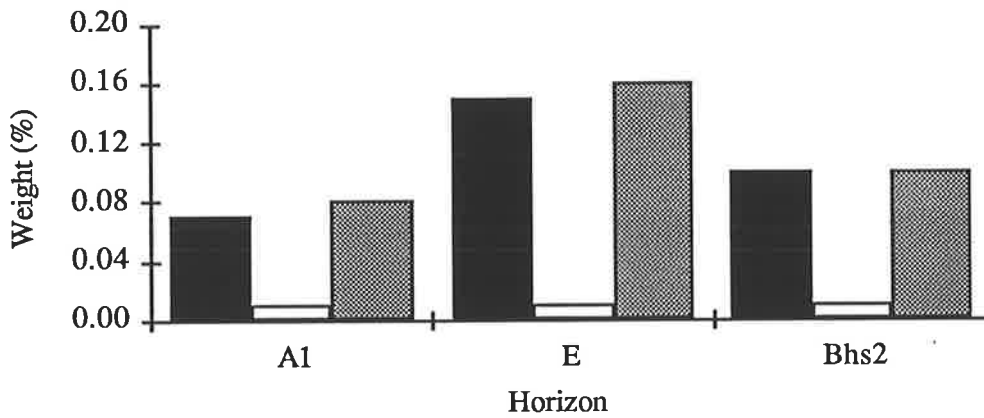


Fig. 7.203. Warrawonga profile.

Fig. 7.20. Percent weight of NM, SM and VM heavy mineral fraction in the < 2 mm fraction of soils from the south east coast of Queensland.



NM, SM and VM = non-, slightly- and strongly-magnetic fractions respectively.

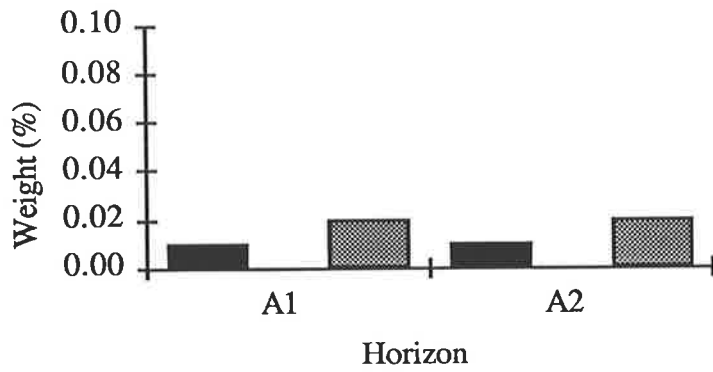


Fig. 7.211. LeFevre Peninsula 1 profile.

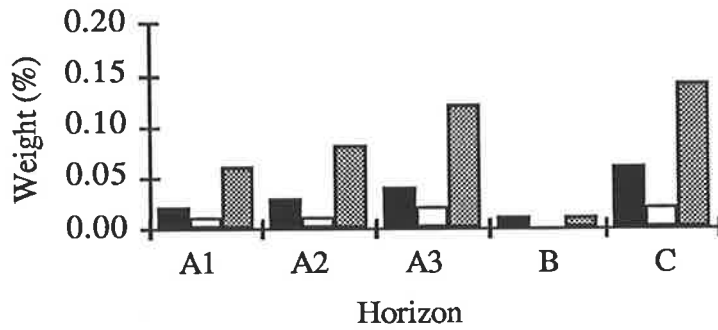


Fig. 7.212. LeFevre Peninsula 2 profile.

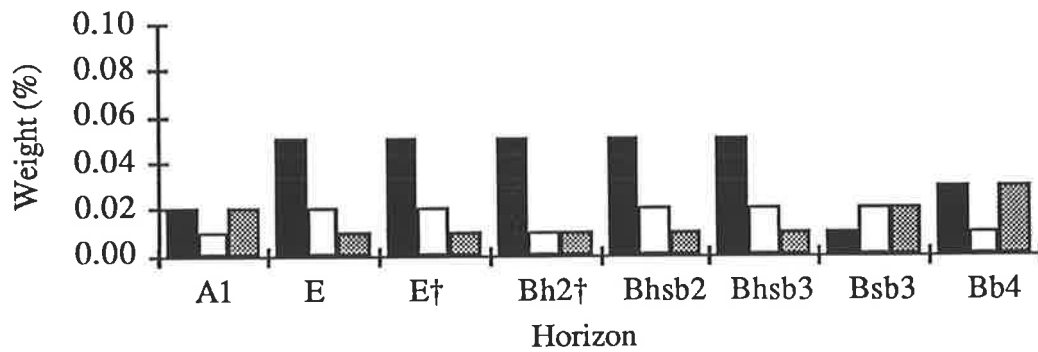


Fig. 7.213. Mount Compass profile. † = pipe.

Fig. 7.21. Percent weight of NM, SM and VM heavy mineral fraction in the < 2 mm fraction of soils from the central South Australian coast.



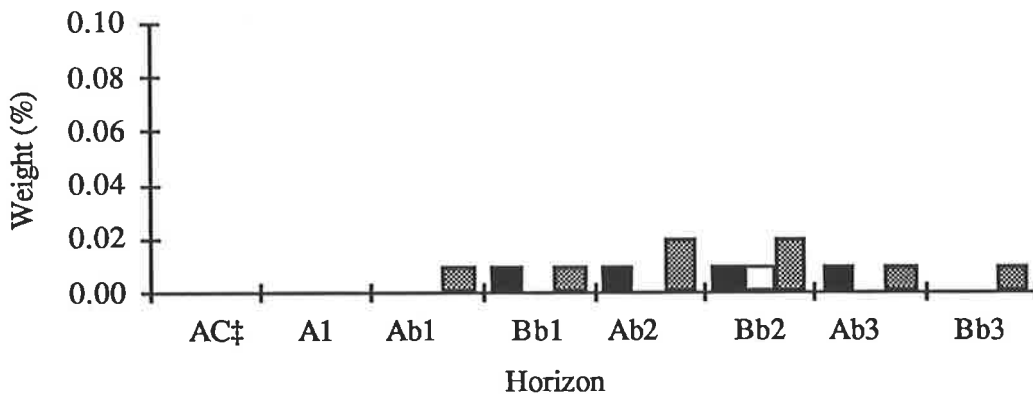


Fig. 7.221. Canunda site. ‡ beach deposit.

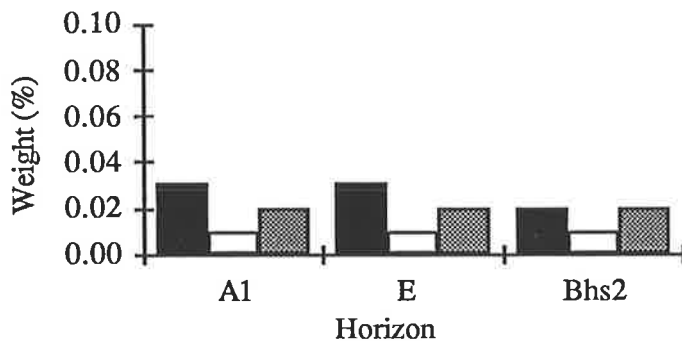


Fig. 7.222. Mount Burr profile.

Fig. 7.22. Percent weight of Nm, SM and VM heavy mineral fraction in the < 2 mm fraction of soils from the south east South Australian coast.



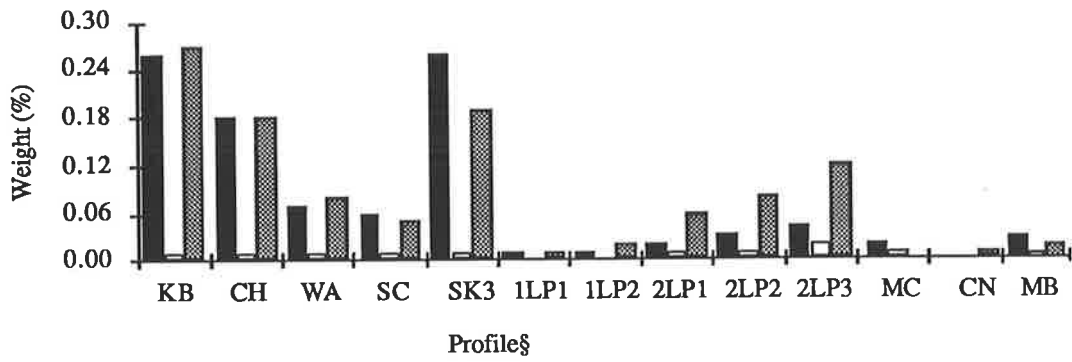


Fig. 7.231. A horizons of different profiles.

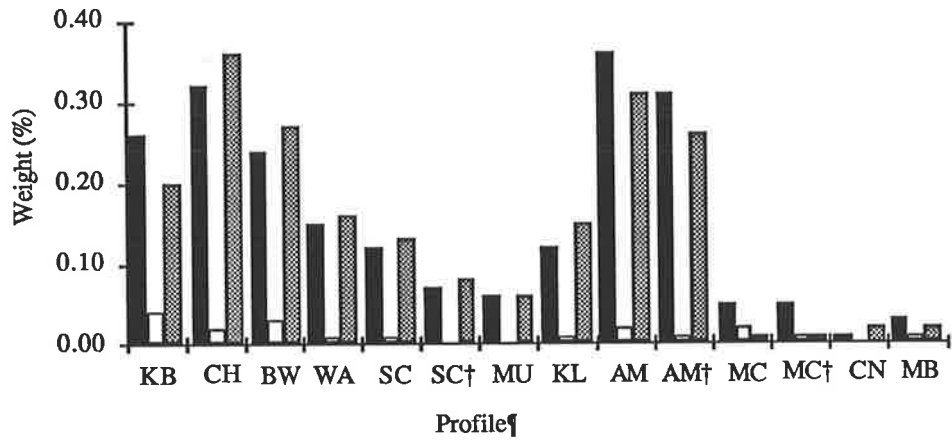


Fig. 7.232. E horizons of different profiles.

Fig. 7.23. Percent weight of NM, SM and VM heavy mineral fraction in the < 2 mm fraction of soils from comparable horizons of different profiles.

KB = Kings Bore, CH = Chalambar, BW = Burwilla, WA = Warrawonga, SC = Seacliffs, MU = Mundu, KL = Kabali, AM = Amity, 1LP = LeFevre Peninsula 1, 2LP = LeFevre Peninsula 2, MB = Mount Burr and MC = Mount Compass.

§ 1 = A1, 2 = A2 and 3 = A3.

¶ † = pipe.



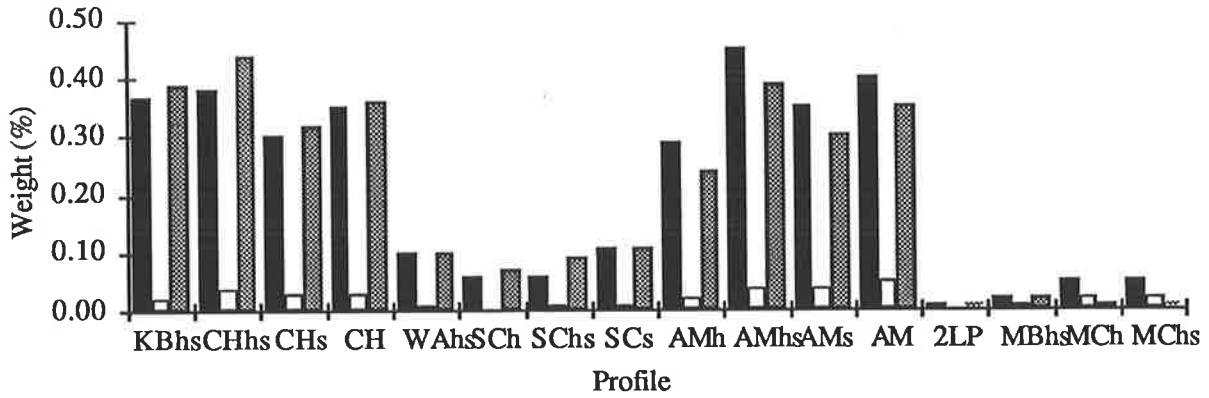


Fig. 7.233. B2 horizons of different profiles.

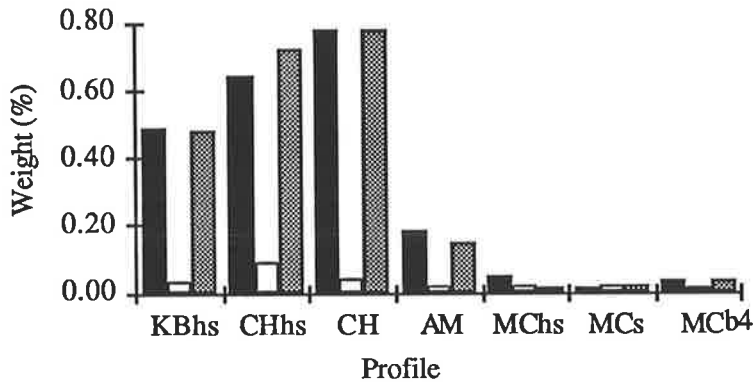


Fig. 7.234. B3 horizons of different profiles.

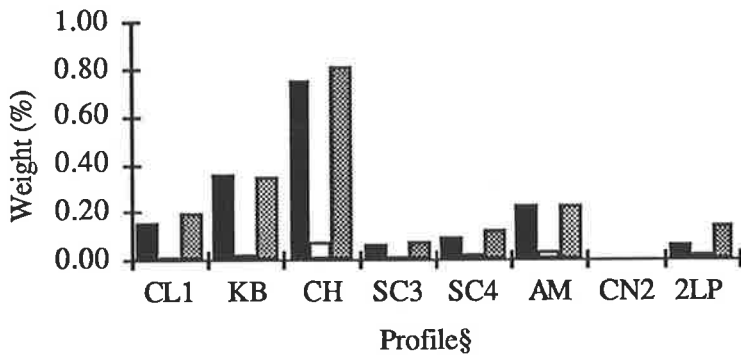
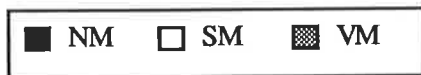


Fig. 7.235. C horizons of different profiles.

Fig. 7.23 contd. Percent weight of NM, SM and VM heavy mineral fraction in the < 2 mm fraction of soils from comparable horizons of different profiles.

KB = Kings Bore, CH = Chalambar, WA = Warrawonga, SC = Seacliffs, AM = Amity, 2LP = LeFevre Peninsula 2, MB = Mount Burr, MC = Mount Compass. § 1 = mobile dune, 2 = beach deposit, 3 = C1 and 4 = C2. .



distribution in soils from Cooloola was more or less similar to North Stradbroke Island profile (AM) (Figs. 7.231 to 7.235), because the profiles are from adjacent coastal sequences albeit with slight differences in source rocks (there has been more igneous input at North Stradbroke Island). This similarity was shown qualitatively by the predominance of zircon and rutile in the NM, garnet, epidote, spinel and monazite in the SM and ilmenite in the VM fractions of soils from the two locations. Within the central South Australian coastal region, mineral distributions in soils from the LeFevre Peninsula profiles (1LP and 2LP) and Mount Compass profile (MC) were different between locations (Figs. 7.231 to 7.233). In the LeFevre Peninsula profiles, 1LP was similar to 2LP in terms of the overall mineral distribution pattern (VM > NM > SM; similar source rocks), but different in actual proportions (1LP had more of NM and 2LP had more of VM; probably due to irregularities in the sediment source and changes in transporting conditions through time for these two profiles. Between LeFevre Peninsula and Mount Compass the distribution patterns showed that the source materials were completely different as shown in Figs. 7.231 and 7.233 for comparable horizons. This was supported by a qualitative analysis of the dominant heavy minerals which showed zircon, rutile and sillimanite in the NM fraction of both LeFevre Peninsula and Mount Compass profiles. However, differences occurred in the SM and VM suites, with the following:-

SM - garnet, amphibole, tourmaline, monazite and staurolite for LeFevre Peninsula;

tourmaline, garnet and staurolite for Mount Compass

VM - garnet (pink) and ilmenite for LeFevre Peninsula; ilmenite, leucoxene, iron oxide/

hydroxide for Mount Compass.

Soils from the south eastern coastal region of South Australia have a more complicated pattern of mineral distribution, with the Canunda (CN) and Mount Burr (MB) profiles high in VM and NM respectively (Figs. 7.231 and 7.232). Mineralogically the dominant minerals in the magnetic fractions of the two profiles were zircon, rutile and sillimanite (NM), and garnet, epidote, staurolite, tourmaline and amphibole (SM) and ilmenite, leucoxene and magnetite (VM). The observed differences in the proportions

can be ascribed to the influence of pedochemical weathering which is more intense in the Mount Burr soil profile. See further discussion in a latter section of this chapter.

On a regional basis, comparable horizons from the Queensland profiles were different from the central and south eastern South Australia profiles because of completely different proximate source materials. Based on sedimentary environments, the inland soils from Mount Compass and Mount Burr were different because of contrasting geologic and depositional histories between the two locations (see comparable horizons for MC and MB in Figs. 7.231 and 7.232). However, the coastal soils at LeFevre Peninsula and Canunda appeared to be somewhat similar in mineral distribution with $VM > NM > SM$ (Figs. 7.231-7.232), presumably due to a variety of source materials, but similar coastal distribution processes.

7.3.1.4. Zircon : rutile ratio.

The ratio of two resistant minerals for a specific fraction is considered to be a more reliable criterion than percentage values for evaluating depositional variations. Ratio data is a relative measure which is better for comparative work, provided the numerator and denominator are clearly and directly related.

Horizons within profile.

The ratios of zircon : rutile in the 53-125 μm fraction show little variation with depth in the different profiles (Table 7.1; Figs. 7.301 to 7.304, 7.311, 7.321 and 7.322), except for MC profile (Fig. 7.312). The constancy of the within profile ratio with depth is an indication that the two minerals remained unaffected by soil formation, assuming no decomposition, and the constant ratio throughout the profile reflects the degree of uniformity of the parent material (Grossman *et al.*, 1959; Barshad, 1964). The accuracy of the technique depends on the number of grains counted which is related to the probable percentage error, confidence interval and percentage of the mineral species in the sample (Brewer, 1976). Where the number of grain counts were

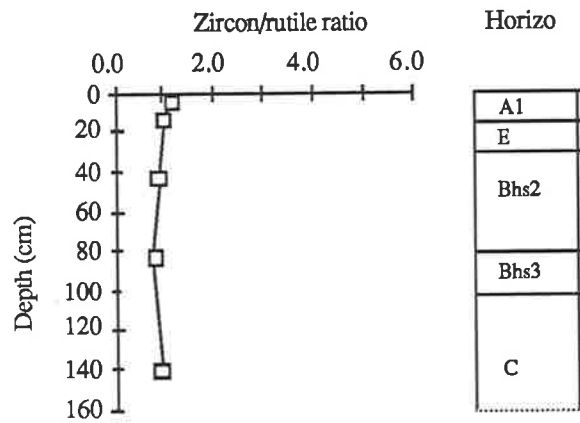


Fig. 7.301. Kings Bore profile.

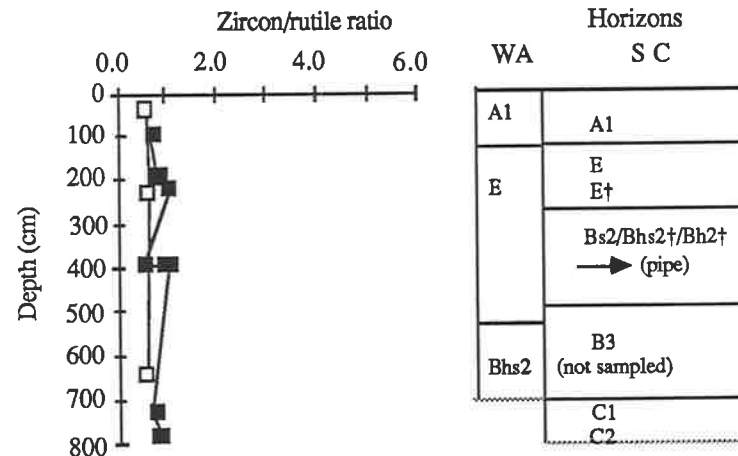


Fig. 7.303. Warrawonga (WA, □) and Seacliffs (SC, ■) profiles. † = pipe.

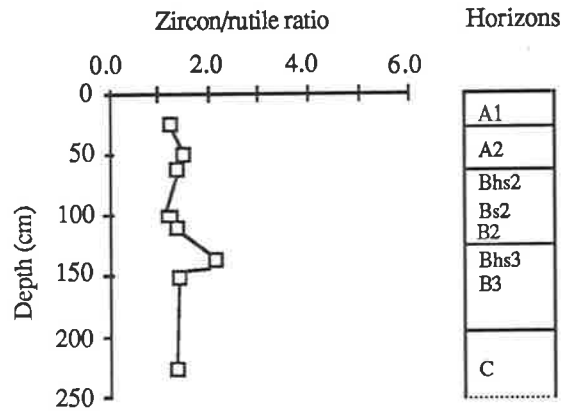


Fig. 7.302. Chalambar profile.

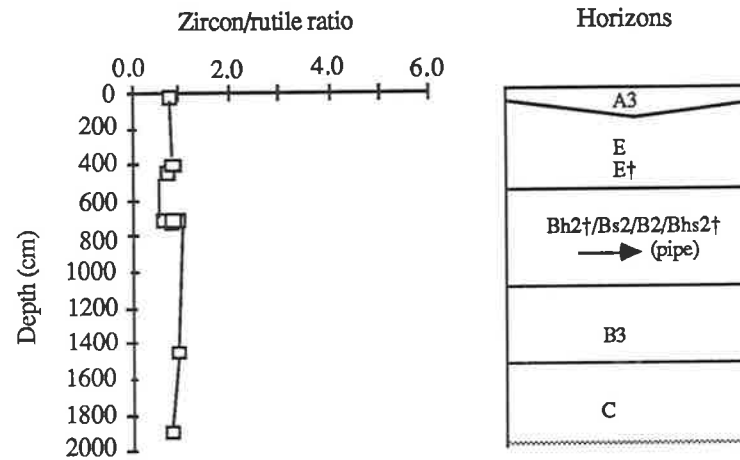


Fig. 7.304. Amity profile. † = pipe.

Fig. 7.30. Zircon : rutile ratio of the 53-125 μ m fraction of soils from the south east coast of Queensland.

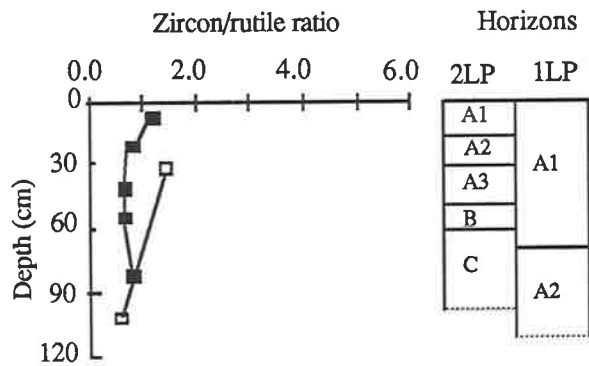


Fig. 7.311. LeFevre Peninsula 1 (1LP, □) and LeFevre Peninsula 2 (2LP, ■) profiles.

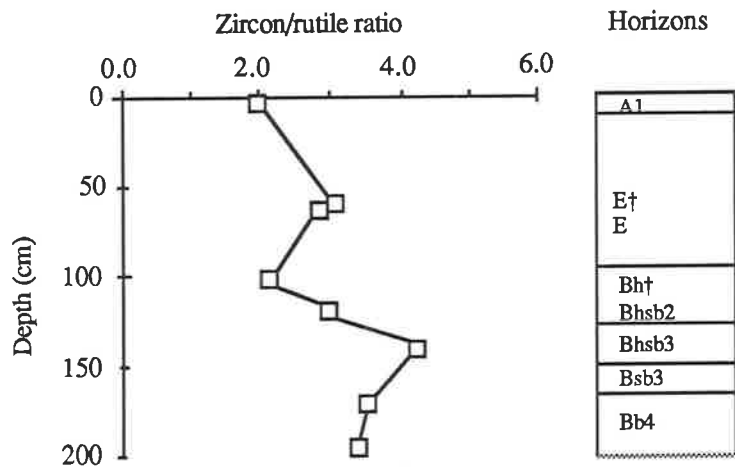


Fig. 7.312. Mount Compass profile. † = pipe.

Fig. 7.31. Zircon:rutile ratio of the 53-125 μm fraction of soils from the central South Australian coast.

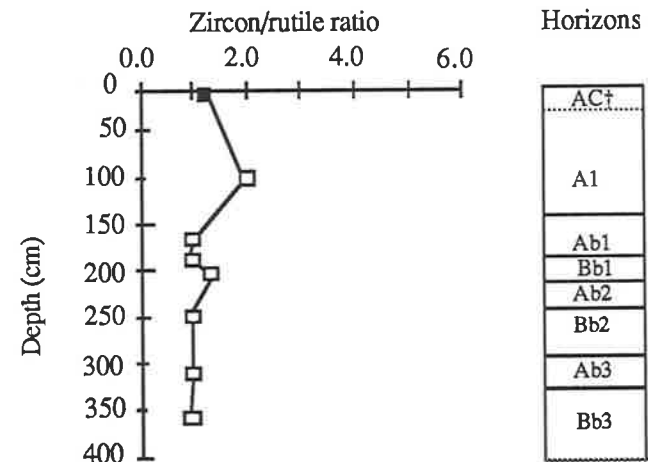


Fig. 7.321. Canunda site. †beach deposit (■).

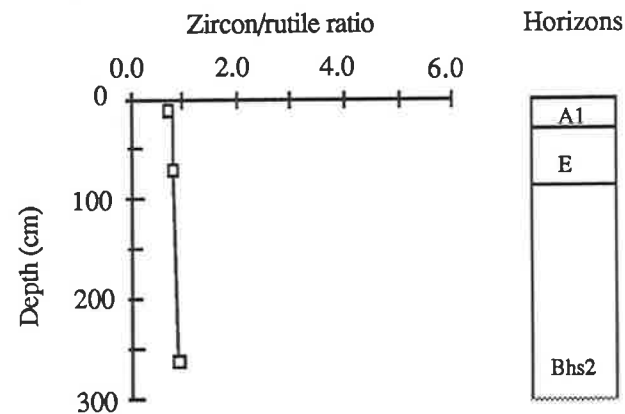


Fig. 7.322. Mount Burr profile.

Fig. 7.32. Zircon:rutile ratio of the 53-125 μm fraction of soils from the south east South Australian coast.

small (mainly in the B horizons of the Queensland samples and all horizons in soils from the other regions) the conclusions are more tentative.

Horizons between profiles.

The between profile variations for comparable soil horizons showed inflections (Figs. 7.331 to 7.336), particularly for the MC soils compared to the rest of the other soils. The higher ratios for the MC soil could be explained by either one of two mechanisms viz - more input of zircon from source material or greater weathering of the relatively less resistant mineral (rutile) in the profile. The close relationship amongst the other profiles from Queensland (e.g. KB, CH, SC, WA) and South Australia (e.g. 1LP, 2LP, MB), based on the ratio of the zircon : rutile again strengthens the argument that complementary methods of assessing parent material uniformity should be used wherever possible.

7.3.1.5. Zirconium : titanium ratio.

As key stable elements in the sand fraction, most of the Zr is in zircon (a resistant mineral) and Ti is in rutile (also a resistant mineral). The ratios of zirconium to titanium in the sand fraction have been used to estimate parent material uniformity in soils.

Horizons within profile.

The $ZrO_2 : TiO_2$ ratios within profiles (Table 7.1 and Figs. 7.401 to 7.404 and 7.411) do not indicate a lithological discontinuity between the upper and lower horizons. The data in Fig. 7.412 for MC profile, however, again shows the possibility of a stratigraphic break between the B2 and B3 horizons. In the KB, CH, WA, AM (Figs 7.401 to 7.404) and 2LP profiles (Fig. 7.411) the $ZrO_2 : TiO_2$ ratios are less than 1, between 0.38 and 0.72 (Table 7.1). The ratios for the MC profile (Fig. 7.412) exceed 1 (Table 7.1). There could be two reasons for this. First, and perhaps more likely, is source material differences, the mineralogical composition of MC is more

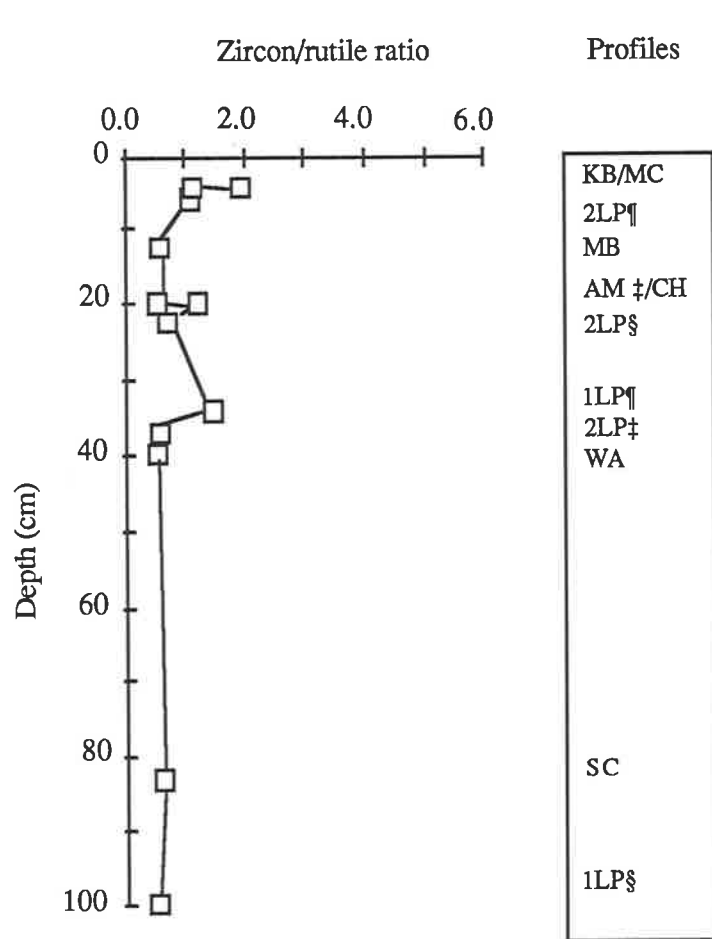


Fig. 7.331. A horizons of different profiles.

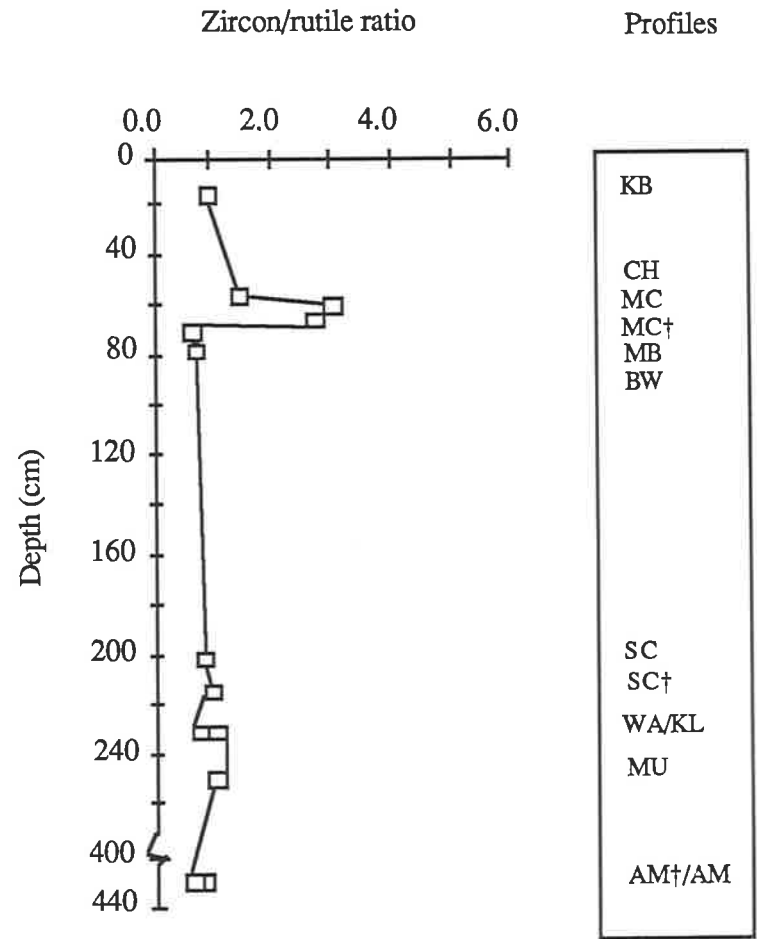


Fig. 7.332. E horizons of different profiles.

Fig. 7.33. Zircon:rutile ratio of the 53-125 μ m fraction of soils from comparable horizons of different profiles.

KB = Kings Bore, MC = Mount Compass, 2LP = LeFevre Peninsula 2, MB = Mount Burr, AM = Amity, CH = Chalambar, WA = Warrawonga, 1LP = LeFevre Peninsula 1, SC = Seacliffs, BW = Burwilla, KL = Kabali, and MU = Mundu. ¶ = A1, § = A2, ‡ = A3 horizons and † = pipe.

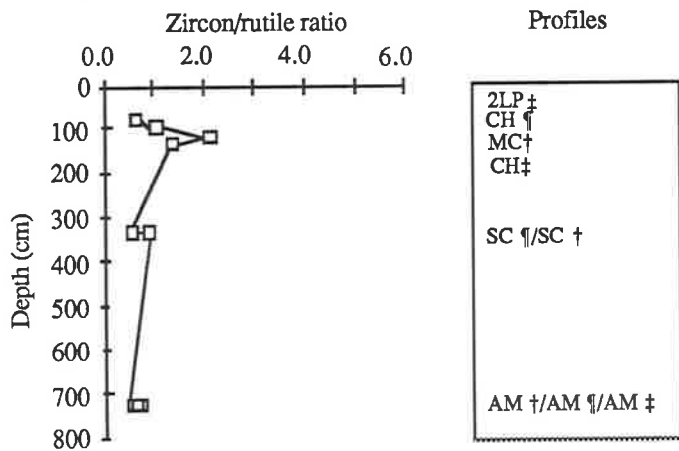


Fig. 7.333. B2* horizons of different profiles. † = Bs, ‡ = B and † = Bh.

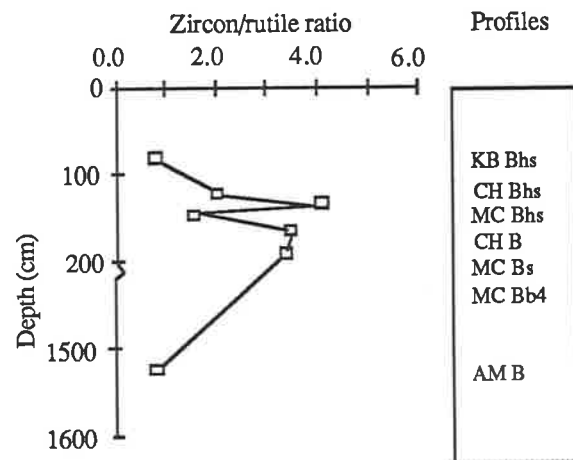


Fig. 7.335. B3 horizons of different profiles.

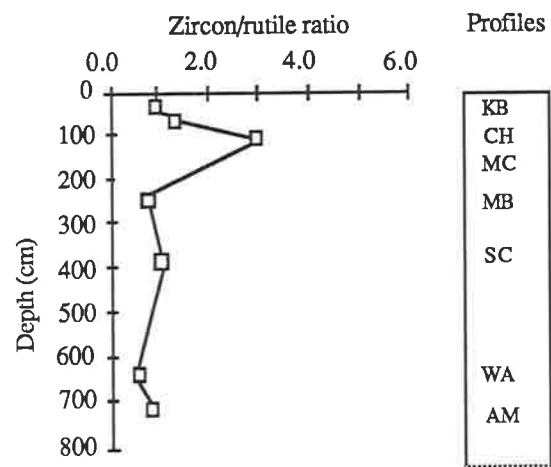


Fig. 7.334. Bhs2 horizons of different profiles.

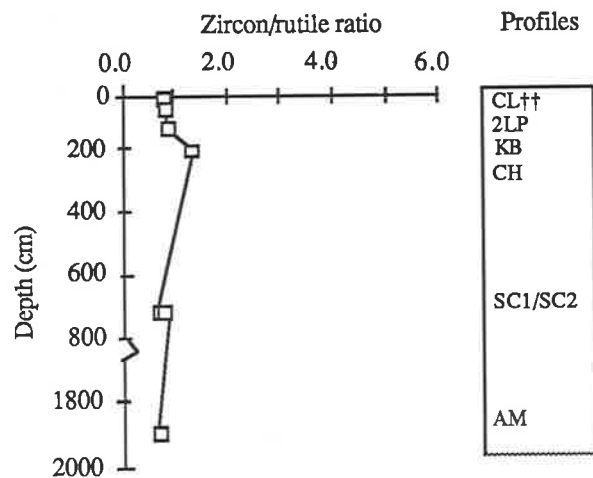


Fig. 7.336. C horizons of different profiles.

Fig. 7.333. contd. Zircon:rutile ratio of the 53-125 µm fraction of soils from comparable horizons of different profiles.

CH = Chalambar, 2LP = LeFevre Peninsula 2, MC = Mount Compass, SC = Seacliffs, AM = Amity, KB = Kings Bore, WA = Warrawonga, MB = Mount Burr and CL†† = Carlo beach deposit. *B = all B horizons except Bhs.

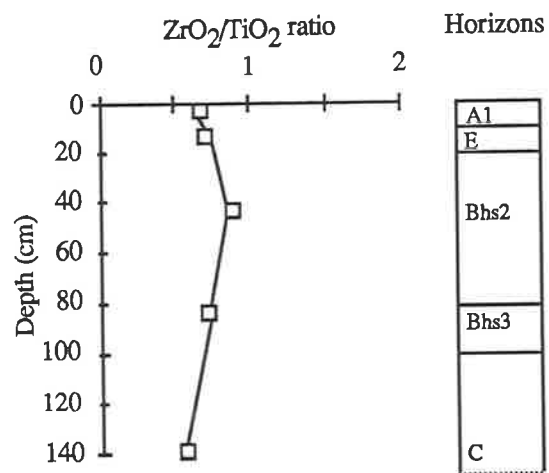


Fig. 7.401. Kings Bore profile.

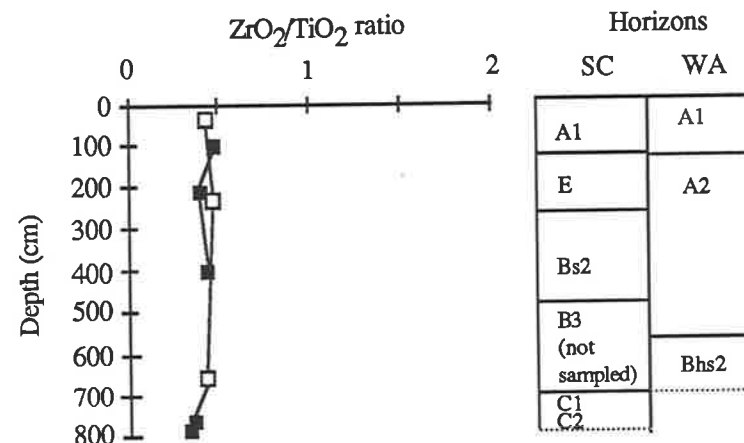


Fig. 7.403. Seacliffs (SC, ■) and Warrawonga (WA, □) profiles.

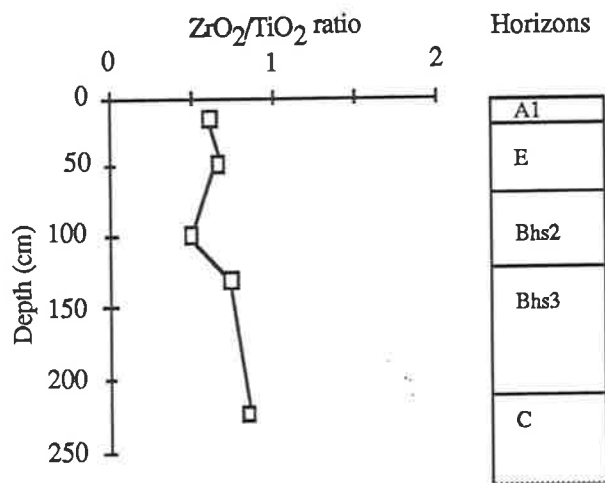


Fig. 7.402. Chalambar profile

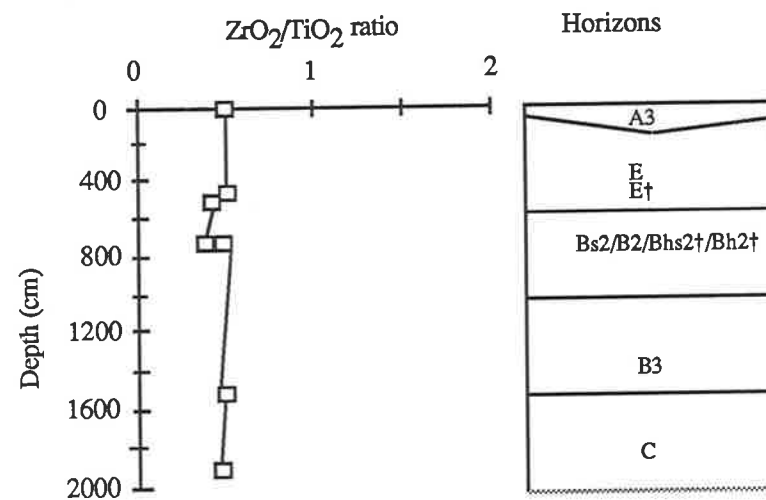


Fig. 7.404. Amity profile. † = pipe.

Fig. 7.40. Zirconium:titanium ratio of the 53-125 μm fraction of soils from the south east coast of Queensland.

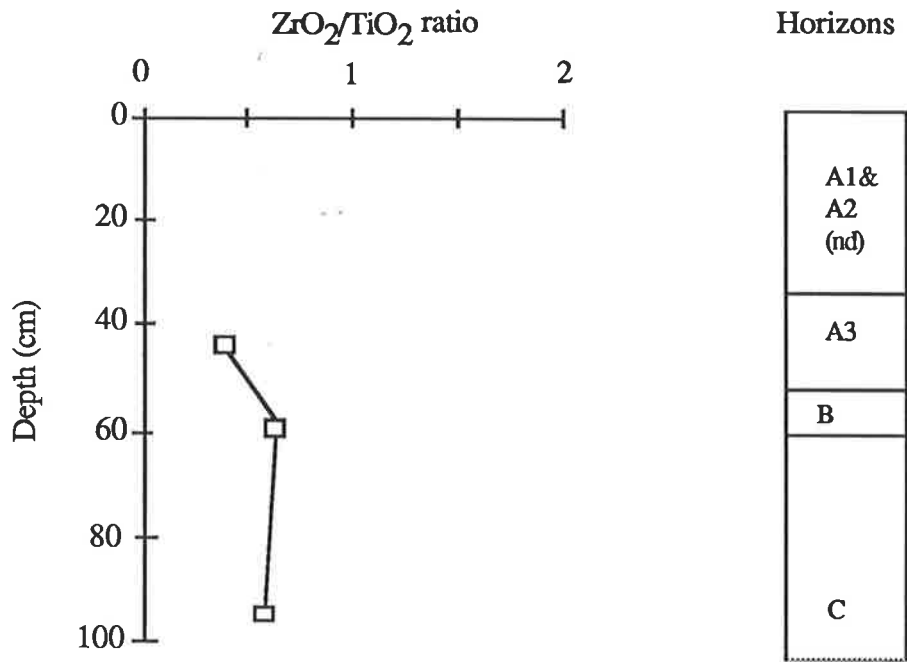


Fig. 7.411. LeFevre Peninsula 2 profile. nd = not determined.

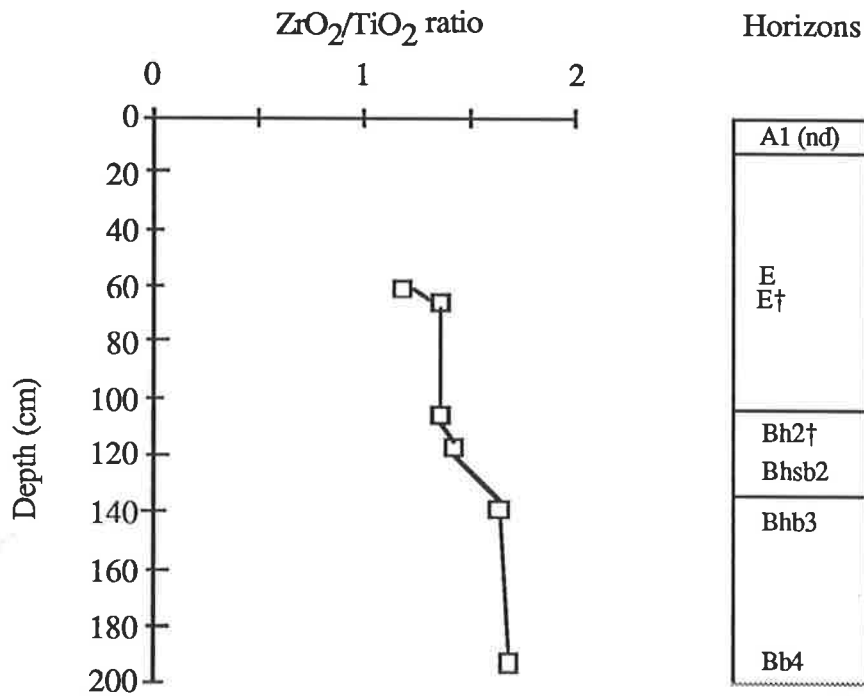


Fig. 7.412. Mount Compass profile. nd = not determined. † = pipe.

Fig. 7.41. Zirconium:titanium ratio of the 53-125 μm fraction of soils from the central South Australian coast.

matured (reworked Permian sediments) and from different source rocks. In contrast, KB, CH, WA and AM profiles are from relatively younger sediments (Mesozoic and Tertiary rocks) which have abundance of relatively less resistant minerals primary (e.g. ilmenite) in the VM fraction. The VM fraction of MC profile on the other hand is dominated by secondary iron oxide minerals. The 2LP profile is comprised of old reworked Palaeozoic sediments and fresh mineral input from younger rocks derived from much older rocks (see Chapter 5). Second is the loss of Ti, present mainly in rutile, during pedogenesis. It is possible that in the oldest profile (MC) some TiO_2 had been lost by complete dissolution of rutile grains during pedogenesis. As pointed out by Bain (1976) there are greater chances of titanium concentrating in the finer fraction of the soil as secondary minerals. Other researchers have noted losses of Ti during pedogenesis (e.g. Sudom and St. Arnaud, 1971; Evans and Adams, 1975 b; Busacca and Singer 1989), occurring predominantly in the clay fraction. However, within soil profiles Ti mobility was minimal as indicated by the extent and depth of Ti loss relative to Zr. Yaalon *et al.* (1974) showed similar within profile trend. Because of the above reason, each profile can be considered as having been formed from a mineralogically similar parent material.

Horizons between profile.

The ZrO_2/TiO_2 ratios for comparable horizons from different soil profiles showed variable trends (Figs. 7.421 to 7.423 and Table 7.2). In the A1 horizon the constancy of the ZrO_2/TiO_2 for soils from the Queensland region (KB, CH, SC, WA and AM) might indicate similar parent material for these soils (Fig. 7.421). However, the 2LP profile fits in even better than CH profile, but the two materials are clearly from different sources as indicated earlier. In the E horizon (Fig. 7.422), except for the MC profile, the ZrO_2/TiO_2 ratios are again similar for the profiles from the south east coast of Queensland (KB, CH, BW, SC, WA, MU, KL and AM). However, comparison with similar profiles from other regions (except for MC) could not be made because of lack of sufficient samples. Because of the good agreement that could occur

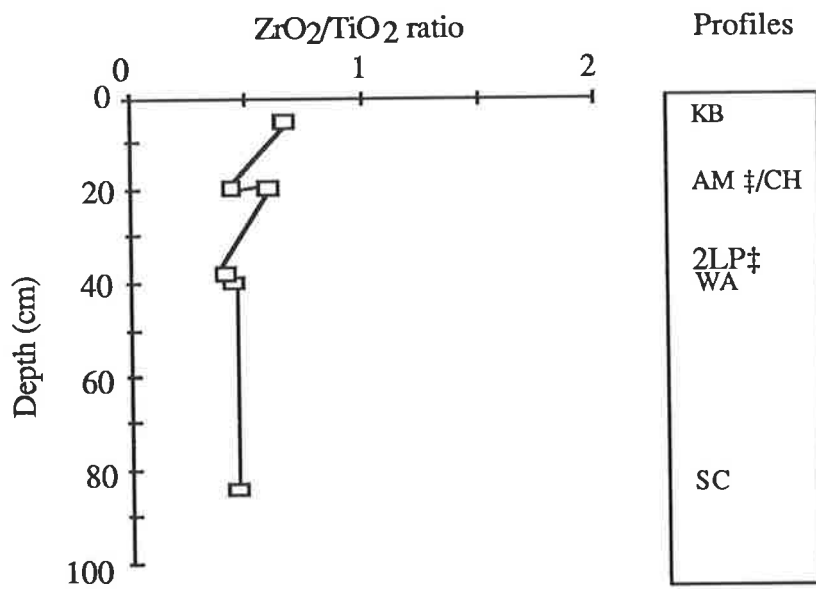


Fig. 7.421. A horizons of different profiles.

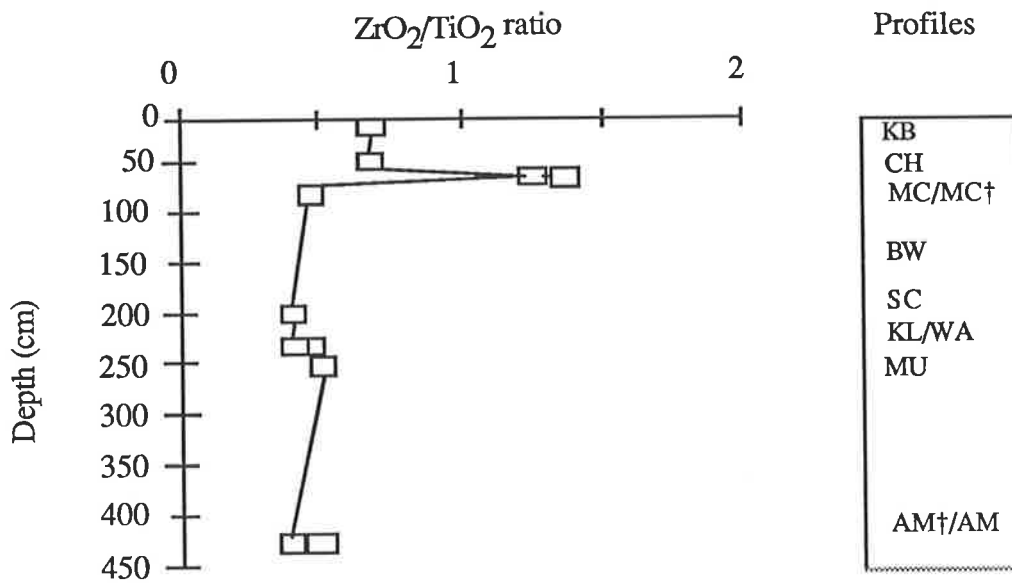


Fig. 7.422. E horizons of different profiles. ‡ = pipe.

Fig. 7.42. Zirconium:titanium ratio of the 53-125 μ m fraction of soils from comparable horizons of different profiles.

KB = Kings Bore, CH = Chalambar, BW = Burwilla, AM = Amity, 2LP = LeFevre Peninsula 2, MC = Mount Compass, WA = Warrawonga, SC = Seacliffs, MU = Mundu and KL = Kabali. ‡ = A3.

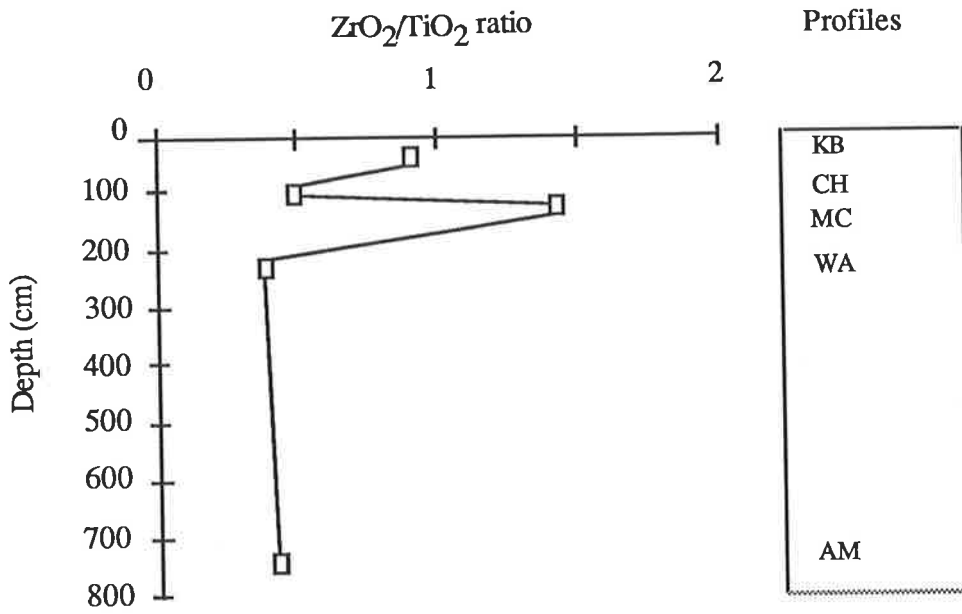


Fig. 7.423. Bhs2 horizons of different profiles.

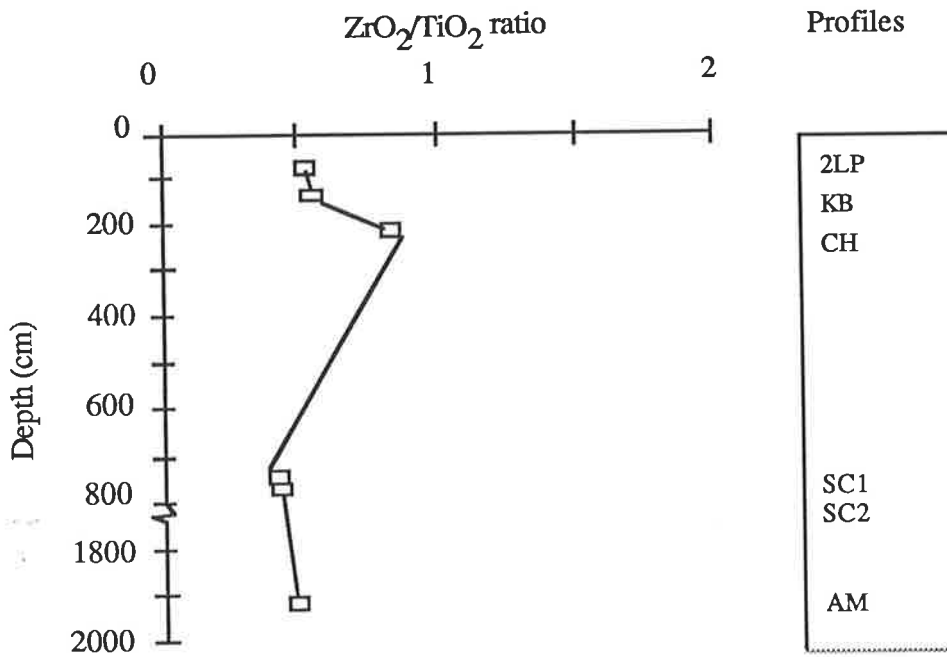


Fig. 7.424. C horizons of different profiles.

Fig. 7.42. contd. Zirconium:titanium ratio of the 53-125 μm fraction of soils from comparable horizons of different profiles.

KB = Kings Bore, 2LP = LeFevre Peninsula 2, CH = Chalambar, MC = Mount Compass, WA = Warrawonga, SC = Seacliffs and AM = Amity

between samples from different parent materials, it is obviously advantageous to select as many methods as possible for assessing parent material uniformity. The scattered inflections in the Bhs2 horizons could show either depositional differences in this horizon (since soils are from similar parent materials, except for MC) or preferential weathering of the two minerals in the 53-125 μm fraction. Assuming that rutile is less stable than zircon (at least from the qualitative surface microtextural feature investigations in Chapters 5 and 6), the latter suggestion is less likely because *in situ* weathering should be higher with age of profile in a chronosequence (youngest to oldest = KB < CH < WA/SC), but this was not shown in either Figs. 7.421 to 7.423 or Table 7.2. A similar explanation can be given for the C horizon of different profiles (Fig. 7.424).

7.3.1.6. Summary.

The plots of the index constituents (% 53-125 μm fraction and the % stable mineral and element ratios) against depth for horizons within profiles (Figs. 7.101 to 7.122; 7.301 to 7.322 and 7.401 to 7.412) show detectable differences in the percentage of the stable constituents between horizons as shown by the inflections in the curves at the various depths. For the recognition of the parent material the values of the % stable constituent in the parent material should coincide with the depth axis at a very low angle (Brewer 1976). This condition is fulfilled by some profiles using some of the methods (e.g. zircon/rutile ratio in Chalambar). The curves for 53-125 μm , THM in Chalambar and Kings Bore and Zircon/rutile ratio in Kings Bore show slight inflections going down to the C horizon. This could be due to experimental error in estimating these constituents or else the true parent material has not been reached. The problem was resolved by carrying out qualitative mineralogical analysis on the samples.

In general the ratio of zircon : rutile is greater than zirconium : titanium in all the soils. The probable reasons for this are:-

(a) error associated with grain counting- according to (Brewer, 1976) the probable percent error associated with counting 1000 grains and for a mineral species comprising 60 % or more of sample is about 5 % at 95 % confidence interval;

(b) the relative shapes and sizes of the different minerals, with the possibility of longer and larger grains counted more than once.

On the other hand the TiO_2 (XRF result) is greater than rutile (mineral count result) presumably because some unidentified grains were actually rutile but, because the reference spectra was pure Ti, rutile grains with some Fe, Si or allophanic coatings may not have been counted. This would depend on the portion of the grain probed. By the same token, the proportion of true rutile could have been overestimated (probe detecting Ti rich zones of other Ti containing minerals). The possibility of contaminated zircon (either crusted grains or grains with other mineral inclusions) was very much smaller. The XRF therefore took into account the total TiO_2 in the NM heavy mineral fraction, though not necessarily all from rutile *per se*.

7.3.1.7. *Statistical evaluation.*

The means, standard deviations (std. dev.) and coefficients of variation (CV) for the 53-125 μm and THM fractions in the < 2mm size particles; zircon and rutile, ZrO_2 and TiO_2 , and ratios of zircon to rutile and zirconium to titanium in the 53-125 μm fraction of soils are presented in Tables 7.1 to 7.4. If all the samples (Tables 7.1 to 7.4) are regarded as parts of a normally distributed population, the CV is used as a measure of variation within populations with different means. The higher the CV % the greater the variation. The general uncertainty that surrounds variation in the mineralogical composition and extent of sorting (of the parent material) made it impossible to agree on any particular standard percentage variation in methods for assessing uniformity. Chapman and Horn (1968) regarded differences of 100 % or more in Ti/Zr ratio between two or more horizons of a profile, whereas Drees and Wilding (1973) considered a variation of 60 % in Ti/Zr ratio to detect lithologic

Table 7.3. Percent 53-125 μm fraction particles and heavy minerals in the < 2 mm soil fraction, and ratio data for soil sequences based on locations. Means, standard deviations and coefficients of variation.

Profile# (Horizon)	Sampling depth (cm)	53-125 μm fraction	THM†	Zi‡	Ru¶	Zi/Ru ratio	Zr	Ti	Zr/Ti ratio
Cooloola sequence									
CL-AC	0-5	1.45	0.35	0.058	0.066	0.88	0.036	0.084	0.43
KB-A1	0-10	1.05	0.54	0.112	0.088	1.27	0.077	0.117	0.66
E	15-20	0.94	0.51	0.109	0.102	1.07	0.067	0.099	0.68
Bhs2	30-60	1.18	0.78	0.142	0.149	0.95	0.127	0.141	0.90
Bhs3	60-110	1.57	1.00	0.175	0.187	0.94	0.154	0.215	0.72
C	130-150	1.25	0.74	0.133	0.134	0.99	0.101	0.180	0.56
CH-A1	0-40	0.87	0.37	0.079	0.058	1.36	0.048	0.081	0.60
E	40-60	1.58	0.72	0.143	0.096	1.49	0.098	0.148	0.66
Bhs2	60-63	1.50	0.87	0.167	0.120	1.39	0.100	0.201	0.50
Bs2	80-120	1.52	0.66	0.130	0.107	1.21			
B2	100-120	1.30	0.76	0.155	0.112	1.38			
Bhs3	120-140	2.75	1.47	0.370	0.182	2.03	0.207	0.274	0.75
B3	140-160	2.62	1.60	0.343	0.239	1.44			
C	200-250	2.92	1.63	0.330	0.231	1.43	0.242	0.294	0.82
WA-A1	0-80	1.15	0.15	0.023	0.034	0.68	0.017	0.040	0.43
E	210-260	2.02	0.33	0.050	0.067	0.75	0.038	0.081	0.46
Bhs2	625-690	1.73	0.21	0.032	0.049	0.65	0.024	0.057	0.42
SC-A1	55-110	1.22	0.12	0.020	0.027	0.74	0.015	0.032	0.47
E	150-250	2.10	0.26	0.043	0.049	0.88	0.028	0.070	0.40
E†	160-270	1.50	0.15	0.028	0.027	1.04			
Bh2†	310-470	1.65	0.14	0.024	0.022	1.09			
Bhs2†	310-470	1.80	0.16	0.025	0.026	0.96			
Bs2	310-470	1.70	0.24	0.035	0.057	0.61	0.026	0.061	0.43
C1	720-760	1.54	0.15	0.024	0.025	0.96	0.014	0.033	0.41
C2	780-800	1.30	0.24	0.033	0.034	0.97	0.022	0.049	0.45
<i>Mean</i>		<i>1.61</i>	<i>0.57</i>	<i>0.111</i>	<i>0.091</i>	<i>1.08</i>	<i>0.076</i>	<i>0.119</i>	<i>0.57</i>
<i>Std.Dev.</i>		<i>0.53</i>	<i>0.46</i>	<i>0.103</i>	<i>0.065</i>	<i>0.329</i>	<i>0.067</i>	<i>0.080</i>	<i>0.15</i>
<i>CV %</i>		<i>33</i>	<i>81</i>	<i>93</i>	<i>71</i>	<i>30</i>	<i>88</i>	<i>68</i>	<i>27</i>
Cooloola-North Stradbroke Island sequence									
CL-AC	0-5	1.45	0.35	0.058	0.066	0.88	0.036	0.084	0.43
KB-A1	0-10	1.05	0.54	0.112	0.088	1.27	0.077	0.117	0.66
E	15-20	0.94	0.51	0.109	0.102	1.07	0.067	0.099	0.68
Bhs2	30-60	1.18	0.78	0.142	0.149	0.95	0.127	0.141	0.90
Bhs3	60-110	1.57	1.00	0.175	0.187	0.94	0.154	0.215	0.72
C	130-150	1.25	0.74	0.133	0.134	0.99	0.101	0.180	0.56
CH-A1	0-40	0.87	0.37	0.079	0.058	1.36	0.048	0.081	0.60
E	40-60	1.58	0.72	0.143	0.096	1.49	0.098	0.148	0.66
Bhs2	60-63	1.50	0.87	0.167	0.120	1.39	0.100	0.201	0.50
Bs2	80-120	1.52	0.66	0.130	0.107	1.21			
B2	100-120	1.30	0.76	0.155	0.112	1.38			
Bhs3	120-140	2.75	1.47	0.370	0.182	2.03	0.207	0.274	0.76
B3	140-160	2.62	1.60	0.343	0.239	1.44			
C	200-250	2.92	1.63	0.330	0.231	1.43	0.242	0.294	0.82
WA-A1	0-80	1.15	0.15	0.023	0.034	0.68	0.017	0.040	0.43
E	210-260	2.02	0.33	0.050	0.067	0.75	0.038	0.081	0.47
Bhs2	625-690	1.73	0.21	0.032	0.049	0.65	0.024	0.057	0.42
SC-A1	55-110	1.22	0.12	0.020	0.027	0.74	0.015	0.032	0.47
E	150-250	2.10	0.26	0.043	0.049	0.88	0.028	0.070	0.40
E†	160-270	1.50	0.15	0.028	0.027	1.04			
Bh2†	310-470	1.65	0.14	0.024	0.022	1.09			
Bhs2†	310-470	1.80	0.16	0.025	0.026	0.96			
Bs2	310-470	1.70	0.24	0.035	0.057	0.61	0.026	0.061	0.43
C1	720-760	1.54	0.15	0.024	0.025	0.96	0.014	0.033	0.41
C2	720-760	1.30	0.24	0.033	0.034	0.97	0.022	0.049	0.45
AM-A3	10-30	1.50	0.46	0.097	0.125	0.78	0.068	0.144	0.47
E	400-425	1.74	0.69	0.133	0.170	0.78	0.097	0.194	0.50
E†	415-440	1.72	0.59	0.115	0.156	0.74	0.074	0.180	0.41

Table 7.3 contd.

Profile# (Horizon)	Sampling depth (cm)	53-125 μ m fraction	THM‡	Zi\$	Ru¶	Zi/Ru ratio	Zr	Ti	Zr/Ti ratio
Cooloola-North Stradbroke Island sequence contd.									
Bh2†	700-900	1.69	0.55	0.105	0.149	0.70	0.076	0.156	0.49
Bhs2†	700-900	1.78	0.89	0.181	0.213	0.85	0.116	0.247	0.47
Bs2	700-900	2.15	0.69	0.131	0.174	0.75	0.079	0.209	0.38
B2	700-900	2.05	0.80	0.150	0.183	0.82	0.093	0.212	0.44
B3	1500-1550	0.98	0.34	0.077	0.079	0.97	0.041	0.080	0.51
C	1900-1930	1.25	0.48	0.079	0.103	0.77	0.056	0.118	0.48
Mean		1.62	0.58	0.115	0.108	1.01	0.078	0.137	0.54
Std.Dev.		0.49	0.41	0.091	0.065	0.32	0.056	0.076	0.14
CV %		30	69	79	60	31	72	55	26
LeFevre Peninsula Sequence									
1LP-A1	26-40	7.64	0.03	0.003	0.002	1.50			
A2	90-110	9.24	0.03	0.002	0.003	0.67			
2LP-A1	0-15	3.87	0.10	0.006	0.005	1.20			
A2	15-30	1.99	0.12	0.007	0.008	0.88			
A3	30-49	1.82	0.18	0.007	0.010	0.70	0.006	0.014	0.43
B	49-60	2.45	0.02	0.002	0.003	0.67	0.002	0.003	0.67
C	60-100	2.48	0.22	0.013	0.015	0.87	0.011	0.020	0.55
Mean		4.21	0.10	0.006	0.007	0.93	0.006	0.013	0.55
Std.Dev.		3.00	0.08	0.004	0.005	0.31	0.004	0.009	0.12
CV %		71	79	66	72	34	69	68	22
LeFevre Peninsula-Mount Compass sequence									
1LP-A1	26-40	7.64	0.03	0.003	0.002	1.50			
A2	90-110	9.24	0.03	0.002	0.003	0.67			
2LP-A1	0-15	3.87	0.10	0.006	0.005	1.20			
A2	15-30	1.99	0.12	0.007	0.008	0.88			
A3	30-49	1.82	0.18	0.007	0.010	0.70	0.006	0.014	0.43
B	49-60	2.45	0.02	0.002	0.003	0.67	0.002	0.003	0.59
C	60-100	2.48	0.22	0.013	0.015	0.87	0.011	0.020	0.52
MC-A1	0-10	8.14	0.03	0.010	0.005	2.00			
E	10-110	24.67	0.08	0.031	0.010	3.10	0.018	0.015	1.20
E†	30-100	21.79	0.07	0.031	0.011	2.82	0.019	0.014	1.36
B2h†	90-120	21.33	0.08	0.027	0.013	2.08	0.019	0.014	1.36
Bhsb2	110-130	22.35	0.08	0.030	0.010	3.00	0.019	0.013	1.46
Bhsb3	135-150	17.79	0.08	0.033	0.008	4.13	0.020	0.012	1.67
Bsb3	155-175	5.63	0.06	0.007	0.002	3.50			
Bb4	160-220	6.85	0.07	0.020	0.006	3.33	0.012	0.007	1.71
Mean		10.54	0.08	0.015	0.008	2.03	0.014	0.013	1.14
Std.Dev.		8.50	0.06	0.012	0.004	1.20	0.007	0.005	0.50
CV %		81	67	77	56	59	48	38	44
Canunda-Mount Burr sequence									
CN-AC	0-5	0.65	0.01	0.0006	0.0005	1.20			
A1	90-110	0.58	0.01	0.0004	0.0002	2.00			
Ab1	155-170	2.82	0.02	0.0004	0.0004	1.00			
Bb1	185-200	0.96	0.01	0.004	0.004	1.00			
Ab2	205-220	2.45	0.03	0.004	0.003	1.33			
Bb2	240-260	1.40	0.04	0.004	0.004	1.00			
Ab3	310-318	2.31	0.02	0.001	0.001	1.00			
Bb3	340-370	1.55	0.02	0.001	0.001	1.00			
MB-A1	0-25	3.11	0.06	0.009	0.013	0.69			
E	60-80	3.09	0.07	0.010	0.013	0.77			
Bhs2	250-270	2.93	0.05	0.007	0.009	0.78			
Mean		1.99	0.03	0.004	0.005	1.07			
Std.Dev.		0.99	0.02	0.003	0.005	0.36			
CV %		50	68	94	110	33			

Profile names same as given in Table 7.2.

† = Material associated with pipe.

‡ THM = total heavy mineral.

\$ Zi = zircon.

¶ Ru = rutile.

Table 7.4. Percent 53-125 μm fraction and heavy minerals in the < 2 mm soil fraction, and ratio data for soil horizons from all locations combined. Means, standard deviations and coefficients of variation.

Profile TM (Horizon §)	Sampling depth (cm)	53-125 μm fraction	THM†	Zi‡	Ru‡	Zi/Ru ratio	Zr	Ti	Zr/Ti ratio
CL-AC	0-3	1.45	0.35	0.058	0.066	0.88	0.036	0.084	0.43
KB-A1	0-10	1.05	0.54	0.112	0.088	1.27	0.077	0.117	0.66
E	15-20	0.94	0.51	0.109	0.102	1.07	0.067	0.099	0.68
Bhs2	30-60	1.18	0.78	0.142	0.149	0.95	0.127	0.141	0.90
Bhs3	60-110	1.57	1.00	0.175	0.187	0.94	0.154	0.215	0.72
C	130-150	1.25	0.74	0.133	0.134	0.99	0.101	0.180	0.56
BW-E	70-90	1.61	0.54	0.081	0.101	0.80	0.064	0.130	0.49
CH-A1	0-40	0.87	0.37	0.079	0.058	1.36	0.048	0.081	0.60
E	40-60	1.58	0.72	0.143	0.096	1.49	0.098	0.148	0.66
Bhs2	60-63	1.50	0.87	0.167	0.120	1.39	0.100	0.201	0.50
Bs2	80-120	1.52	0.66	0.130	0.107	1.21			
B2	100-120	1.30	0.76	0.155	0.112	1.38			
Bhs3	120-140	2.75	1.47	0.370	0.182	2.03	0.207	0.274	0.76
B3	140-160	2.62	1.60	0.343	0.239	1.44			
C	200-250	2.92	1.63	0.330	0.231	1.43	0.242	0.294	0.82
WA-A1	0-80	1.15	0.15	0.023	0.034	0.68	0.017	0.040	0.43
E	210-260	2.02	0.33	0.050	0.067	0.75	0.038	0.081	0.47
Bhs2	625-690	1.73	0.21	0.032	0.049	0.65	0.024	0.057	0.42
SC-A1	55-110	1.22	0.12	0.020	0.027	0.74	0.015	0.032	0.47
E	150-250	2.10	0.26	0.043	0.049	0.88	0.028	0.070	0.40
E†	160-270	1.50	0.15	0.028	0.027	1.04			
Bh2†	310-470	1.65	0.14	0.024	0.022	1.09			
Bhs2†	310-470	1.80	0.16	0.025	0.026	0.96			
Bs2	310-470	1.70	0.24	0.035	0.057	0.61	0.026	0.061	0.43
C1	720-760	1.54	0.15	0.024	0.025	0.96	0.014	0.033	0.41
C2	780-800	1.30	0.24	0.033	0.034	0.97	0.022	0.049	0.45
MU-E	220-280	1.92	0.38	0.066	0.063	1.04	0.041	0.084	0.49
KL-E	210-260	2.81	0.27	0.049	0.046	1.05	0.029	0.071	0.41
AM-A3	10-30	1.50	0.46	0.097	0.125	0.78	0.068	0.144	0.47
E	400-425	1.74	0.69	0.133	0.170	0.78	0.097	0.194	0.50
E†	415-440	1.72	0.59	0.115	0.156	0.74	0.074	0.180	0.41
Bh2†	700-900	1.69	0.55	0.105	0.149	0.70	0.076	0.156	0.49
Bhs2†	700-900	1.78	0.89	0.181	0.213	0.85	0.116	0.247	0.47
Bs2	700-900	2.15	0.69	0.131	0.174	0.75	0.079	0.209	0.38
B2	700-900	2.05	0.80	0.150	0.183	0.82	0.093	0.212	0.44
B3	1500-1550	0.98	0.34	0.077	0.079	0.97	0.041	0.080	0.51
C	1900-1930	1.25	0.48	0.079	0.103	0.77	0.056	0.118	0.48
1LP-A1	26-40	7.64	0.03	0.003	0.002	1.50			
A2	90-110	9.24	0.03	0.002	0.003	0.67			
2LP-A1	0-15	3.87	0.10	0.006	0.005	1.20			
A2	15-30	1.99	0.12	0.007	0.008	0.88			
A3	30-49	1.82	0.18	0.007	0.010	0.70	0.006	0.014	0.43
B	49-60	2.45	0.02	0.002	0.003	0.67	0.002	0.003	0.67
C	60-100	2.48	0.22	0.013	0.015	0.87	0.011	0.020	0.55
MC-A1	0-10	8.14	0.03	0.010	0.005	2.00			
E	10-110	24.67	0.08	0.031	0.010	3.10	0.018	0.015	1.20
E†	30-100	21.79	0.07	0.031	0.011	2.82	0.019	0.014	1.36
Bh2†	90-120	21.33	0.08	0.027	0.013	2.08	0.019	0.014	1.36
Bhsb2	110-130	22.35	0.08	0.030	0.010	3.00	0.019	0.013	1.46
Bhsb3	135-150	17.79	0.08	0.033	0.008	4.13	0.020	0.012	1.67
Bs3	155-175	5.63	0.06	0.007	0.002	3.50			
Bb4	160-220	6.85	0.07	0.020	0.006	3.33	0.012	0.007	1.71
CN-AC	0-5	0.65	0.01	0.0006	0.0005	1.20			
A1	90-110	0.58	0.01	0.0004	0.0002	2.00			
Ab1	155-170	2.82	0.02	0.0004	0.0004	1.00			
Bb1	185-200	0.96	0.01	0.004	0.004	1.00			
Ab2	205-220	2.45	0.03	0.004	0.003	1.33			

Table 7.4 contd.

Profile # (Horizon)	Sampling depth (cm)	53-125 μ m fraction	THM‡	Zi\$	Ru¶	Zi/Ru ratio	Zr	Ti	Zr/Ti ratio
Bb2	240-260	1.40	0.04	0.004	0.004	1.00			
Ab3	310-318	2.31	0.02	0.001	0.001	1.00			
Bb3	340-370	1.55	0.02	0.001	0.001	1.00			
MB-A1	0-25	3.11	0.06	0.009	0.013	0.69			
E	60-80	3.09	0.07	0.010	0.013	0.77			
Bhs2	250-270	2.93	0.05	0.007	0.009	0.78			
Mean		3.83	0.36	0.069	0.064	1.26	0.060	0.105	0.66
Std.Dev.		5.56	0.39	0.083	0.068	0.76	0.054	0.082	0.36
CV %		145	109	121	107	61	89	78	55

Profile names same as given in table 7.2.

† = Material associated with pipe.

‡ THM = total heavy mineral.

\$ Zi = zircon.

¶ Ru = rutile.

discontinuity. Murad (1978) and Chittleborough *et al.* (1984) chose CVs of elemental ratios of 30 % and < 25 % respectively to account for parent material uniformity.

Horizons within profile.

Within different soil profiles (Table 7.1) the range of CVs is as follows: 3 % in MB to 49 % in MC for the 53-125 μ m fraction; 0 % in 1LP to 60 % in 2LP for the THM fraction; 19 % in MB to 84 % in CN for zircon content; 17 % in AM to 86 % in CN for rutile content; 7 % in WA and MB to 54 % in 1LP for zircon : rutile ratio; 21 % in AM to 69 % in 2LP for zirconium content; 20 % in AM to 68 % in 2LP for titanium content and 6 % in WA and SC to 22 % in 2LP for zirconium : rutile ratio. If the soil parent materials within profiles are homogeneous (as shown from previous discussions), then the individual CVs for the different techniques complements the non-standardization of CVs for assessing parent material uniformity. As suggested by Marsan *et al.* (1988), for a uniform parent material the content of the elements used in the ratio should vary in a parallel manner and the CV of the ratio should be lower than, or equal to, that of the CV of the absolute content of at least one of the two elements. In this study the individual elements vary in an almost parallel manner with depth in the profile (see Figs. 7.101 to 7.122), and the CVs of the ratios are lower than any of the

two minerals or elements (Table 7.1). This complements the work of Marsan *et al.* (1988) and suggests that the parent materials are uniform in individual soil profiles, except in the MC profile which has been shown (both qualitatively and quantitatively) to have a stratigraphic break. In this profile the contents of the individual elements are not parallel with depth, even though the CV of their ratios is lower than that of the individual elements. This further enhances the fact that no single criteria is good enough, on its own, for the assessment of parent material uniformity.

Horizons between profiles.

The CVs for the various measured variables (53-125 μm , THM, etc) for comparable horizons in different profiles are presented in Table 7.2. The variation in the 53-125 μm fraction ranged from 40 % in C horizons to 167 % in B horizons (other than Bhs2). For the total heavy mineral fraction the range of variation was from 63 % in E horizons to 133 % in AC horizons. The range of variations for the zircon, rutile and zircon : rutile ratios were 64 % in the E to 139 % in the AC, 75 % in E and B horizons to 139 % in AC and 22 % in AC and C to 66 % in Bhs2 respectively. Furthermore, zirconium content, titanium content and zirconium : titanium ratios were shown to range as follows:- 56 % in E to 120 % in C for zirconium, 60 % in E to 103 % in B3 for titanium and 19% in A1 horizon to 59 % in B2 horizon for the zirconium : rutile ratios. The CVs in Table 7.2 are mostly higher than for horizons within the same profile. This complements previous sections of this chapter that the parent sediments are from different sources for profiles from the south east Queensland, central and south east South Australian regions.

Regional and overall comparisons.

In Tables 7.3 and 7.4 the fractionation, mineral and elemental criteria were used to assess the degree of variation in soils on a regional scale (Table 7.3) and all the soils combined (Table 7.4). If the maximum CVs for the within profile measurement (Table 7.1) are used as a guide for establishing parent material uniformity on the account of

their relatively low values compared with the other Tables (7.2, 7.3 and 7.4), and the other evidences from techniques such as magnetic fractionation and mineral identification, then the results in Tables 7.3 and 7.4 have considerable implications in establishing the concept of a chronosequence of soils. From Table 7.1, the maximum CVs for the different criteria were 49 % for the 53-125 μm fraction, 60 % for the THM fraction, 84 % for the zircon content, 86 % for the rutile content, 54 % for the zircon : rutile ratio, 69 % for the zirconium content, 68 % for the titanium content and 22 % for ZrO_2 : TiO_2 ratio. Ignoring the very high CVs for zircon and rutile contents and the ratio value associated with them in the CN, 1LP and 2LP profiles (Table 7.1) because of the high errors connected with them, based on the closeness of their means to zero, the next highest values of acceptable merit are 53 %, 46 %, 17 %, 59 %, 44 % and 19 % for zircon, rutile, zircon : rutile ratio, Zr, Ti and Zr:Ti ratio respectively. Also the use of CV values from MC profile as a standard was not justified because of the proposed evidence of depositional break between the B2 and B3 horizon boundary. Using the latter maximum CV values as standards for the different criteria for establishing the concept of a chronosequence in the different soils on regional basis (Table 7.3) the following deductions were made:-

1. In profiles from Cooloola and the south east coast of Queensland (Cooloola and North Stradbroke Island) only the 53-125 μm fraction attested to the concept of a chronosequence. Nevertheless, the separation (in space) of Cooloola from North Stradbroke Island does not exactly conform to the chronosequence concept.
2. The profiles at CN and MB in the south east coastal region of South Australia (within statistical limits) form a chronosequence based only on the CV of the 53-125 μm fraction. Thus it seems that the 53-125 μm fraction analysis is a more discriminating criterion for ascertaining the occurrence of chronosequences in these regions. The other criteria cannot be effectively used because of the wide variations in their absolute values both within and between profiles in a given sequence. This suggests differences in the mode of deposition (layering) of the minerals, particularly in

regions where it has been shown that there is qualitative similarity of the suite of resistant heavy minerals (uniform parent material) e.g. LeFevre Peninsula.

When all the horizons are considered as part of the same population, i.e. with similar parent material, the overall CVs increase (Table 7.4), indicating an even greater variability between profiles than that presented in Table 7.3. None of the criteria gave an indication of uniform parentage for all soils combined.

7.4.1. Weathering.

Comparative quantitative mineral analyses can be applied to the study of genesis of soil profiles which can be shown by changes in the mineralogy or particle-size fraction with depth in the profile due to weathering. Such a study is complemented by the establishment of parent material uniformity of the soil profiles investigated. This has been substantiated in the previous section, for the individual profiles from different regions.

7.4.1.1. 53-125 μm and THM fractions.

Horizons within profile.

The proportion of the 53-125 μm fraction and total heavy mineral fraction in the < 2 mm fraction of soils from different horizons within the same soil profile are given in Fig. 7.101 to 7.104, 7.111 to 7.112 and 7.121 to 7.122. In the south east Queensland coastal sequence (Figs. 7.101 to 7.104) the patterns of distribution of both the 53-125 μm and THM fractions with depth within the individual profiles showed very weak and subtle trends. The 53-125 μm and total heavy mineral fractions followed similar distribution patterns in all the profiles (i.e. occurrence of higher 53-125 μm fraction matches correspondingly higher THM fraction presence). This implies that the bulk of the heavy mineral occurred in the 53-125 μm fraction. Also, in the older profiles (WA, SC and AM), the two fractions were shown to be slightly more abundant in the upper horizons (A, E & B2), but in the younger profiles (KB and CH) there was a tendency towards an increased proportion of the two fractions with depth in

the profile. The possible explanation for this is that, initially, the proportion of 53-125 μm fraction in the source material was unevenly distributed (as shown in younger profiles) and with increasing age the coarser sand fraction was weathered in the upper horizons of the older profiles to cause an increase in the proportion of these fractions in these horizons. The situation is even more complicated in profiles from the central South Australian coastal region (Figs. 7.111 and 7.112) and the Canunda profile (Fig. 7.121) from the south east of South Australia. In these soils there is no detectable pattern between the 53-125 μm and THM fractions, meaning that the THM fraction is mostly not concentrated in this fraction. Again, for the younger soils (1LP, 2LP and CN) the trends in the proportion of the two fractions with depth are not uniform and are inconsistent. However, in the older soils (MC and MB) the trend for the 53-125 μm fraction showed higher proportions in the upper horizons of the profiles (Figs. 7.112 and 7.122) where there has been relatively more intense weathering of coarser particles to finer forms. The trends for the THM for all soils in the South Australia region are obscured due to the appreciably low values of this fraction in these soils and the greater errors associated with estimating the correct percentages (highest amount approximately 0.08 % in MC).

Horizons between profiles.

For comparable horizons in profiles constituting a chronosequence (i.e. Cooloola, LeFevre Peninsula and Canunda/Mount Burr) the proportion of the 53-125 μm and THM fractions also showed very weak and inconsistent trends with age. In Figs. 7.131 to 7.135 the Cooloola (1), LeFevre Peninsula (2) and Canunda/Mount Burr (3) chronosequences are represented by the following profiles where appropriate (1) KB, CH, BW, WA, SC, MU & KL profiles, (2) 1LP and 2LP profiles and (3) CN and MB profiles respectively. In soils formed *in situ* on parent rocks it is generally known that with increasing age the proportions of the finer fraction increase and that of the THM decreases due to increasing weathering. However, this relationship is

unattainable in the soils studied due to the nature of the parent materials and the processes of their accumulation (see later section of this chapter).

7.4.1.2. *Magnetic fractions.*

Differences in the degree of mineral weathering in a profile can be measured by (a) qualitative and quantitative similarity in the heavy mineral suite and (b) qualitative similarity but quantitative differences in the more easily weathered minerals (Marshall, 1977).

Horizons within profile.

In Figs. 7.201 to 7.205, 7.211 to 7.213 and 7.221 to 7.222 the proportions of the NM, SM and VM heavy mineral fractions in horizons within individual soil profiles showed no definite pattern in the distribution of the respective mineral fractions with horizonation. This means that weathering of the minerals within profiles cannot be precisely assessed using this technique.

Horizons between profiles.

In comparable horizons of different profiles (Figs. 7.231 to 7.235) weathering has somewhat modified the heavy mineral assemblages in the older, more inland deposits of MC and MB profiles. In samples from Canunda and Mount Burr, and LeFevre Peninsula and Mount Compass, the effect of weathering was evident. There was a higher proportion of the more resistant non magnetic minerals (zircon, rutile and sillimanite) in the older soils at Mount Burr and Mount Compass. The younger deposits close to the coast (Canunda and LeFevre Peninsula) consisted of higher proportions of less resistant minerals, viz. pink garnet, magnetite and ilmenite (strongly magnetic minerals). In soils from Cooloola (KB, BW, CH, WA, SC, MU & KL) the effect of weathering with increasing age (youngest = KB and oldest = KL) showed better with the SM mineral fraction (a general decrease with age).

7.4.1.3. *Zircon:rutile and zirconium:titanium ratios.*

Given that zircon is more resistant to weathering than rutile (as shown, at least qualitatively, in Chapters 5 and 6)) the zircon : rutile ratios were used to explore the possibility of discerning weathering patterns in the different horizons within profiles and between profiles.

Horizons within profile.

Within profile, zircon : rutile ratios for soils from the south east coast of Queensland (Figs. 7.301 to 7.304) gave no consistent indication of weathering pattern with depth in the profiles. Likewise the zircon : rutile ratios for the LeFevre Peninsula (Fig. 7.311), Canunda (Fig. 7.321) and Mount Burr (Fig. 7.322) profiles showed no confirmable pattern of weathering with depth. Similar observations were made for the zirconium : titanium ratios in horizons for those profiles in which analysis were done (Figs. 7.401 to 7.404, 7.411). The curves for zircon : rutile ratio in Mount Compass profile (Fig. 7.312) and zirconium : titanium ratio (Fig. 7.412) show significantly higher ratios for the two analyses in the B3 horizon. This quantitative difference between the lower horizon and the upper A, E and B2 horizons suggests parent material heterogeneity. This difference might be accounted for by changes in the mode of depositional and/or weathering pattern in the profile. As suggested in Chapter 5 sillimanite grains were absent from the B3 horizon, which may suggest that weathering has depleted the original concentration. However, there is more evidence for parent material heterogeneity in this profile, from both this chapter and Chapter 4. The higher concentration of zircon with respect to rutile could thus be explained by a depositional time break with the underlying material being relatively older in age (matured sediment with higher amounts of the more resistant mineral, zircon). It is possible that soil development occurred in the parent sediment during a period of landscape stability but later during an unstable phase the soil was partially truncated by erosion. Stones present in the upper Bhsb3 horizon (see morphological description in Appendix 2) were concentrated on the erosion surface and buried by relatively stone free sediments.

Some differentiation has occurred in the overlying horizons; mobile constituents such as organic matter and clay (Chapter 4 and Appendix 3) have eluviated and partially replenished the buried horizons or parts of them.

Horizons between profiles.

Similarly, the zircon : rutile ratios (Figs. 7.331 to 7.336) and zirconium : titanium ratios (Figs. 7.421 to 7.424) showed no definite patterns or trends (for comparable horizons of different profiles) with age (for soils comprising a chronosequence). It is likely that the effects of depositional differences as is affected by mineral concentration exceed those that may be due to weathering. Also the use of two very resistant minerals to measure weathering may not be too sensitive in most of these soils which are of Pleistocene age at the most. Where trends were non-uniform and somewhat inconsistent the nature of the sediment build up process could explain the inconsistencies. Intermittent aeolian and wave actions (depending on the deposit) generate irregular depositional layers, some with a high concentration of heavy minerals. This is shown by the degree of variation in proportion of mineral fractions in individual profiles (Figs. 7.201 7.205, 7.211 to 7.213 and 7.221 to 7.222). In soils with uniform parent materials (formed from *in situ* weathering rock), there is often a strong correlation between abundance of certain heavy mineral grains (e.g. zircon) and age of soils : as the age of the profile increases, the proportion of resistant heavy minerals (as determined by grain counting or elemental analysis) increases (e.g. Barshad, 1964). In soils derived from transported sediments this relationship may be obscured by the degree of inherent variability (Marsan *et al.*, 1988; Busacca and Singer, 1989).

Oertel and Giles (1966) showed that depositional layers in parent sediments may leave a strong impression on some properties of the soil while leaving no detectable evidence in presumably closely related properties. They further suggested the use of properties selected for identifying depositional layers in pedological study of profile, if the layers have a important pedogenetic function. The 53-125 μm fraction

and various heavy mineral data have been used to detect parent material uniformity, depositional variations and weathering. However, the more the lithologic variability in the source material the less efficient these methods are in assessing parent material uniformity and degree of weathering of the soil. In this study, even though the methods showed that the parent materials were uniform for all the profiles, except MC, the use of the different criteria to assess the extent of weathering within and between profiles showed minimal prospect. This could be due to the high depositional difference amongst the individual profiles as shown by higher concentrations of individual minerals in the younger soil profiles compared with the older soils. Changes in heavy mineral contents with time in such soils may have to be measured by criteria other than percentage abundance, e.g. by analysis of grain surface microtextural features as described in Chapters 5 and 6.

7.5.1. Nature of zircons in soils.

Several workers (e.g. Marshall, 1967; Speer, 1980 and Milnes and Fitzpatrick, 1989) have reported on the use of zircon as a source indicator in provenance studies. This is because zircon has been considered to be amongst the most resistant mineral species occurring in rocks and to have the ability to survive several erosional cycles, sedimentary transport, diagenesis, metamorphism and other processes which transform rocks within the earth's crust. This resistant characteristic of zircon, in addition to its relative ubiquity, in parent sediments has made it a useful mineral in pedological studies. Techniques used in such studies are different and include both qualitative and quantitative measurements. In assessing parent material uniformity, for example, the genetic record may be qualitatively evaluated by the external morphology or physical properties of the individual grains. This qualitative analysis is often complemented by quantitative estimates of common occurring trace elements (e.g. Hf, U, Th and Pb) in selected zircon grains (Bossart *et al.*, 1986; Owen, 1987). In this section elemental composition of zircon grains was used to assess the differences in zircon populations in soils, and hence the parent sediment differences, between the various regions.

7.5.1.1. Zirconium and hafnium contents, and Zr:Hf ratios of zircon grains

The Zr, Hf contents, and Zr:Hf ratios of zircons from selected soil horizons in profiles from the different regions are shown in Table 7.5. The range of Zr:Hf ratio is between 39.82 for Mount Burr to 46.92 for Mount Compass. The Zr:Hf ratios in Table 7.5 may represent those found in zircons from a wide range of rocks (Erlank *et al.*, 1978 b) including igneous (diorites, granodiorites and granites), metamorphic (gneisses, pegmatites) and sedimentary (beach sands and placer deposits). The geology of the areas sampled attests to this complex composition of rocks from which the zircons may have been derived (see Chapter 2 for the geology). The basement rocks which are the ultimate sources in these regions include igneous and metamorphic rocks which have undergone one or several uplifts, structural deformations, erosion and deposition to give rise to overlying younger rocks (igneous, metamorphic and sedimentary) with compositional and structural modifications. Variations in the Zr:Hf ratios have been reported for rocks in the same general group (igneous, metamorphic or sedimentary). These variations have been ascribed to the relative movement (addition or removal) of Zr⁴⁺ and Hf⁴⁺ ions in the zircon structure during petrogenesis (Erlank *et al.*, 1978 b).

Although the average Zr:Hf ratios appear to somewhat resolve the origin of the zircons, there is no guarantee that these ratios will display the same level of uniformity between and within individual soil horizons, and within individual grains. An indication of the variability of the measurements between and within units (horizon and grains) were obtained from the F-test (Tables 7.6 and 7.7). The basic assumption in the analysis was that the samples were randomly drawn from normally distributed populations having equal variances. The variances in the Zr content in the tested horizons decreased as follows: A > B > C ; i.e. the lowest variance C occurred for the within grain measurements, followed by B (between grains within horizons) and A (between grain between horizons). Variations in the Hf contents followed the order

Table 7.5. The zirconium and hafnium content and the zirconium:hafnium ratio of zircon in selected horizons from different sites.

Location	Site	Horizon	Percent conc. †		Zr/Hf † ratio	
			ZrO ₂	HfO ₂		
Cooloola (southeast Qld. coast)	Carlo	AC	65.59	1.49	43.93	
	Kings Bore	E	62.29	1.51	41.28	
		Bhs2	62.39	1.55	40.26	
	Burwilla	E	63.19	1.55	40.71	
	Chalambar	E	63.89	1.38	46.38	
		Bhs2	62.82	1.48	42.41	
	Warrawonga	E	61.23	1.50	40.79	
		Bhs2	65.84	1.42	46.20	
	Seacliffs	E	66.65	1.43	46.69	
		Bhs2	64.32	1.38	46.66	
	Mundu	E	65.95	1.54	42.77	
	Kabali	E	62.87	1.52	41.40	
	North Strad. Is. (southeast Qld. coast)	Amity	E	62.97	1.49	42.33
			Bhs2	64.18	1.53	41.94
LeFevre Peninsula (central S.A. coast)	LeFevre Peninsula 2	A3	62.97	1.46	43.14	
		B	66.14	1.47	44.82	
Mt. Compass (central S.A. coast)	Mt. Compass	E	67.78	1.44	46.92	
		Bhsb2	62.05	1.40	44.34	
		Bhsb3	66.12	1.57	42.19	
Canunda (southeast S.A. coast)	Canunda	Ab1	65.26	1.52	42.79	
		Bb3	60.46	1.41	42.88	
Mt. Burr (southeast S.A. coast)	Mt. Burr	E	64.18	1.61	39.82	
		Bhs2	61.38	1.38	44.54	

† average values of three measurements each on 6 grains.

Table 7.6. Comparison of variances of zirconium and hafnium contents, and Zr:Hf ratios of zircon grains in selected horizons of soils from south east coastal region of Queensland.

Location	Horizon (Test No. †)	Source of variation ‡	df	Mean square (variance) and F-test					
				Zr content		Hf content		Zr/Hf ratio	
				M.S.	F-test	M.S.	F-test	M.S.	F-test
Coolooloa	E(1)	A	7	58.19	**	0.07	ns	143.57	ns
		B	40	1.37	*	0.10	**	122.74	**
		C	96	0.85		0.02		24.00	
	Bhs2(2)	A	4	44.17	**	0.08	ns	162.27	ns
		B	25	3.80	**	0.09	**	90.60	**
		C	60	1.06		0.02		18.20	
Nth. Strad. Is.	E&Bhs2(3)	A	1	13.09	ns	0.02	ns	6.60	ns
		B	10	3.43	**	0.17	**	161.89	**
		C	24	0.59		0.02		19.21	
Coolooloa - Nth. Strad. Is.	E(4)	A	8	57.37	**	0.09	ns	142.61	ns
		B	45	1.40	ns	0.12	**	121.85	**
		C	108	0.79		0.02		22.96	
Coolooloa - Nth. Strad. Is.	Bhs2(5)	A	5	45.02	**	0.09		161.34	ns
		B	30	3.99	**	0.10		89.94	**
		C	72	1.18		0.02		17.96	

* Significant at 5 % level; ** significant at ≤ 1 % level; ns, not significant.

† Horizons tested (see Table 7.5 for locations, sites and horizons)

(1) = AC and E horizons of soils from sites at Coolooloa.

(2) = AC and Bhs2 horizons of soils from sites at Coolooloa.

(3) = E and Bhs2 horizons of soils from Amity site at North Stradbroke Is.

(4) = AC and E horizons of soils from Coolooloa, and E horizon from Amity.

(5) = AC and Bhs2 horizons of soils from Coolooloa, and Bhs2 horizon from Amity.

‡ A = between sites (horizons).

B = between grains within horizon.

C = between points within grains.

(starting with the highest) : $B > A > C$. For the Zr:Hf ratios the variations followed two paths viz in Table 7.6, $A > B > C$ (except for the E and Bhs horizons of the AM profile) and in Table 7.7, $B > A > C$. This means that for soils from the south east coast of Queensland (Table 7.6) there is more variation in zircon grains between profiles than within profiles or within grains. This greater between profile heterogeneity is probably due to the spatial variability of the heavy mineral contents of the sands during the formation of the horizons. In soils from the central and south east coastal region of South Australia and in all the soils tested (Table 7.7) the within

Table 7.7. Comparison of variances of zirconium and hafnium contents, and Zr:Hf ratios of zircon grains in selected horizons of soils from central and south east coastal region of South Australia, and in all horizons analysed.

Location	Horizon (Test No.†)	Source of variation ‡	df	Mean square (variance) and F-test					
				Zr content		Hf content		Zr/Hf ratio	
				M.S.	F-test	M.S.	F-test	M.S.	F-test
LeFevr.- Mt.Compass	A 3& E(6)	A	1	208.26	**	0.002	ns	108.27	ns
		B	10	2.60	**	0.25	**	235.67	**
		C	24	0.60		0.02		31.93	
	B(7)	A	29	9.88	**	0.13	ns	11.78	ns
		B	15	1.60	*	0.15	*	106.41	*
		C	36	0.57		0.06		43.04	
Canunda- Mt.Burr	A&B(8)	A	39	2.51	**	0.21	ns	79.91	ns
		B	20	5.57	**	0.10	**	87.10	**
		C	48	0.24		0.03		22.24	
All	All(9)	A	22	65.78	**	0.08	ns	108.87	ns
		B	115	2.98	**	0.12	**	121.87	**
		C	276	0.72		0.03		25.99	

* significant at 5% level; ** significant at $\leq 1\%$ level; ns, not significant

† Horizons tested (see Table 7.5 for locations, sites and horizons)

(6) = A3 and E horizons of soils from sites at LeFevre Peninsula 2 and Mt. Compass respectively.

(7) = B and Bhsb2 horizons of soils from sites at LeFevre Peninsula 2 and Mt. Compass respectively.

(8) = Ab1 and Bb3 horizons of soils from Canunda, and E and Bhs2 horizons of soils from Mt. Burr site.

(9) = All the horizons from all sites as listed in Table 7.5.

‡ A = between sites (horizons).

B = between grains within horizons.

C = between points within grains.

horizon variation is much more than the between horizon or profile variation. The profile (AM) from North Stradbroke Island showed similar trends. The high variability of the within horizon measurements is probably due to the more complex and heterogeneous source of the zircons in profiles from these regions. At North Stradbroke Island the higher within profile and yet lower between profile variability (compared with Cooloola profiles) cannot be explained quite easily.

The significant F-test values imply that the evidence is sufficiently strong for all the treatments (horizons and grains) not to belong to populations with a common mean. However, it does not indicate which differences may be considered statistically

significant. For example the differences may not be solely attributable to the differences in locations or profiles (as shown for the North Stradbroke Island profile), but rather to some unknown mixtures of differences in the several inputs that contributed to the formation of the present parent sediment. Owen (1987) suggested that for such studies to be more meaningful it is essential to acquire knowledge about most of the likely sources of limitations, e.g. regional geology, stratigraphy and palaeogeographic reconstruction. However, because of diverse proximate provenance of the zircon grains a reliable petrogenetic relationship, based on these analyses, is reduced. Since the zircon grains are known to have been derived from a variety of rock types, it is impossible to isolate the influence of any one rock type using the Zr:Hf ratios of the zircons. As such this technique is insensitive to distinguishing between the source rock types in the different regions or locations more accurately.

In summary even though a small number of analyses were carried out for each sample the results showed that there were differences between zircons from profiles within the same location (e.g. Cooloola) and between profiles from different locations (e.g. LeFevre Peninsula and Mount Compass or Canunda and Mount Burr). For the sample size used the risk of a type I error was controlled at the 5 % level of significance. The degree of heterogeneity of the proximate source material for the sediments is greater for soils from the South Australian than the Queensland region, because of the higher within horizon variability for zircons from the former region. In all samples zircon grains showed least variability for within grain measurements, which may mean that compositionally the grains were more uniform.

7.6. Conclusions

Four different quantitative criteria were used to assess parent material uniformity and degree of weathering of soils. These criteria were based on (i) proportions of the 53-125 μm fraction, (ii) proportions of total heavy mineral and different magnetic fractions in the < 2 mm fraction of soils; (iii) zircon:rutile ratio and

(iv) zirconium: titanium ratio in the 53 -125 μm fraction. In addition qualitative mineralogical analyses were performed to identify individual mineral species within a given soil profile. It was concluded that, except for the Mount Compass profile, the other individual soil profiles consisted of uniform parent materials with depositional layering. In such instances it is vital to supplement quantitative analysis (e.g. petrographic microscopy) with qualitative investigation (e.g. Zircon:rutile and Zr:Ti ratios).

The nature of the zircons (Zr:Hf ratios) in the soils indicated that the proximate sources for the sediments in the different profiles were from several different rocks.

CHAPTER 8

GENERAL DISCUSSION AND CONCLUSIONS

8.1. Introduction

The purpose of this chapter is to consolidate the findings reported on in the various sections of this thesis with those results published in the literature. The goal is to ascertain on the one hand the differences and/or similarities in research findings which will help improve understanding of heavy mineral weathering characteristics and distribution in profiles from different locations and of different ages in sandy podzols (Spodosol) and other related soils. From these discussions, certain conclusions will be drawn and general recommendations for future research direction suggested. It is clear from Chapters 1 and 5 that while the use of heavy minerals as pedogenic indices is widely acceptable, the nature and weathering characteristics of these key index minerals (particularly zircon and rutile) in different soil weathering environments is not well documented. These shortcomings in our knowledge of susceptibility of heavy minerals to weathering raises uncertainties in the assessment of quantitative pedological processes in different soils. Though in many soils zircon and rutile are amongst the most resistant mineral types, in some soils there may be present other minerals that are far more resistant. Therefore it is better for the minerals to be assessed first before using them indiscriminately as pedogenic indices or internal standards in quantitative studies involving certain pedological processes.

As outlined in Chapter 1 it was important to develop new and/or modify existing techniques for the assessment of mineral weathering and to endeavour to relate weathering features and characteristics to known soil macro and micro-morphological properties, and mechanical and chemical properties, soil age and parent material source. Because physical and chemical processes are involved in the weathering of minerals it was important to consider relatively common grain surface features which are indicative

of both processes. The importance of physical and chemical weathering features on the minerals could be considered in the light of some of their mineralogical properties.

It was also important to investigate changes in mineralogical and elemental patterns and also to study the distribution of the zircon and rutile both of which were present in all samples and were found to be on the more resistant side of the susceptibility-to-weathering scale. Magnetic separation techniques have simply been used for separating mineral species into different groups based on their magnetic susceptibilities. However, use of these magnetic separation techniques, on their own, as a tool for investigating possible mineralogic homogeneity of soil profiles to verify either parent material uniformity or the degree of pedogenesis has not been carried out (Mitchell, 1975). The different magnetic groups, the dominant mineral species contained in them and the chemistry of the most common and resistant minerals (zircon and rutile) were considered here.

8.2. Thermoluminescence dating and related studies, and weathering rates with time

Generally the ages of most soils are still a matter of guesswork mainly because of the lack of absolute ages; undated deposits are commonly correlated with dated deposits in other areas. Rates of weathering of heavy minerals can therefore not be placed in a very accurate framework. It has been recognised for many years that the Cooloola sands constitute a soil chronosequence (Thompson, 1981). Much of the early work on these sands was governed by inferred ages, by merely demonstrating the relationship between them and other nearby dated sequences as outlined in Section 3.2. It was believed that these sands spanned the Quaternary, despite the fact that this geologic period, although being the shortest, was marked by several changes of climate, sea level, floras and faunas. To understand the dune building processes and the associated events which may affect mineral weathering, there was need to more precisely date some of the sands. For this reason thermoluminescence dating was

conducted (Section 3.2) and proved most useful especially in the absence of suitable materials for ^{14}C dating and the fact that some of the dunes are older than 40 ka BP (upper limit for ^{14}C dating). The oldest soil at Kabali was found to be about 730 ka BP, a period associated with major dune formations in other parts of Australia (Idnurm and Cook, 1980; An *et al.*, 1986). The TL ages of the Warrawonga and Amity samples, which were found to be 90 and 120 ka BP respectively, together with that of Kabali, were consistent with the inferred pedological/geomorphological ages for all samples and the isotope age of Amity (as revised by Pickett *et al.*, 1989). However, for the younger dune sampled at Kings Bore the TL age of 11 ka BP arrived at was much greater than the inferred pedological/geomorphological age. This clearly suggested that either the C horizon material sampled at Kings Bore was much older than the apparent field evidence or that there was insufficient exposure time of the quartz grains for the TL to be reset before they were deposited where they are now. It is, therefore, apparent that the TL and inferred dates for Kings Bore are discrepant and fail to give a clear indication of the definite age of the dune building period, and hence the inception of the podzolization process.

Several studies (e.g. Hay, 1960; Ruxton, 1968; Birkeland, 1973; Colman 1981) have deduced relationships between weathering trends (based on chemical analysis) and age of deposits. Douglas and Platt (1977) and Setlow (1978) attempted to use quartz and other heavy mineral surface morphologies to establish a time base for soil development. They observed some trends in weathering with age of the soil material. This study, in part, looked at weathering trends (based on grain surface microtextures) and ages (both absolute and inferred). Even though there were weak consistent trends in weathering in profiles constituting a sequence from the same location (see Sections 5.3.2.3 and 6.3.1.1), the general tendency was commonly inconsistent. This confirms the results of other workers (some mentioned above) and stresses the fact there are factors other than time which appear to have strong influence on the weathering of minerals in soils (Whalley 1985).

The DTA and TGA techniques applied to the different quartz samples to my knowledge were new methods used in the field of TL dating. Since differences and similarities were observed between samples for their absolute sensitivity to radiation it was considered that the DTA method could be used to investigate those differences (see Section 3.2.3.2). The DTA curves described in Section 3.2.3.2 showed narrow and sharp endothermic peaks near 573 °C, with no clear differences that could be attributed to different quartz sources. The TGA data, nevertheless, showed differences between samples which were ascribed to different levels of water sorbing substances present as coatings on the grain surfaces and/or in cracks. Perhaps a more sensitive technique to be used for differentiating quartz from various sources would be a complementary thermal analysis technique referred to as differential scanning calorimetry (DSC) method. Bartenfelder and Karathanasis (1989) used DSC on twelve quartz samples of geologic and soil materials and concluded that the ΔH of inversion showed more sensitivity than inversion temperature, to structural substitutions or deformations. They also found that igneous and metamorphic samples had the highest, whereas the soil samples had the lowest ΔH with values ranging from 1.70 to 5.86 J/g. In their experiment, Bartenfelder and Karathanasis (1989) further showed that the activation energy (E_a) was more promising for distinguishing materials with respect to quartz origin, environment of deposition and extent of weathering.

8.3. Stages of soil development based on micromorphology and SEM

Micromorphological description of the soils as discussed in Chapter 4 were similar to those conducted by other workers on related soil types (e.g. Gile *et al.*, 1966 on calcareous soils; Brewer *et al.*, 1983 on siliceous and calcareous sands, and Podzols). The experiment described in this section of the thesis was carried out to give an *in situ* microscopic view of the arrangement of the soil constituents which could be useful in interpreting mineral weathering trends. Two groups of soil micropedological developments were identified in the thin sections studied (see Section 4.4.4): (i)

calcareous sands with little or no pedogenesis, marked by the presence of segregated faunal excrements and/or very minor micro crystalline calcite pedofeatures in various horizons; (ii) siliceous sands with different stages of podzol developments marked by variations in the arrangement and organisation of organic and inorganic coarse and fine fragments. The accumulation of coatings and infillings around grains and in voids are believed to have an effect on the weathering characteristics of the mineral grains (as discussed in Chapters 5 and 6). The degree and extent of coating and infilling development on grains and in voids seems to depend on the nature of the fine material, its abundance and age of the soil. Organic rich coatings seemed to be irregular and somewhat fragmented, whereas sesquioxide rich types were more uniform and complete around the mineral grains in soils of similar age. The results of Chapter 4 showed that infilling of voids was highest in the B3 horizon of Mount Compass profile because of relatively higher proportion of fine material in this section of the profile.

Observations made under the SEM to describe the surface morphology of mineral grains revealed marked differences between grains from different horizons. Following pre-treatment of samples (see Section 5.2.2) it was observed that mineral grains in all Bhs horizons were more thickly coated with poorly crystalline sesquioxidic compounds having a variety of chemical compositions. Energy dispersive x-ray analysis indicated the following order of abundance of chemical elements within the coatings: $\text{Si} > \text{Al} > \text{Fe} > \text{Mg} > \text{Ca} > \text{Na} > \text{Ti}$. It is clearly apparent that not only more coatings form around the grains in the Bhs2 and B3 horizons of (e.g. Mount Compass profile) as shown in thin sections, but that these coatings persist strongly on grain surfaces, even after agitation following physical and chemical pre-treatments. It may well be that the bonding forces between the precipitated amorphous products (coatings) and the grain surfaces are quite substantial, and may require more rigorous chemical pre-treatments to remove them. In studies involving mineral examination the use of strong chemical pretreatments may introduce artefacts into the analysis leading to errors in interpretation. As suggested by Hunter and Busacca (1989) ultrasonic vibration was sufficient to disaggregate soils without significantly damaging primary structures in the

sand, silt or clay fractions. However, the use of calgon and/or NaOH (see Section 5.2.2) as dispersants in this study could not have had any significant effect on the original grain surface features as has been shown earlier (e.g. Darmody, 1985). The influence of mineral coatings, on grains, in mineral weathering studies certainly makes interpretations complex and may play a controversial role in interpretation (as discussed in Section 6.4.1). Several workers, amongst them, Siever and Woodford (1979), Velbel (1984), Jouany and Chassin (1987), have suggested that coatings protect grain surfaces from weathering mainly through their water-proofing action. However, this study has shown that the poorly crystalline mineral coatings do not appear to protect the mineral grains from dissolution by pore fluids, as the coatings were found to be too patchy or discontinuous, in (for example) Bhs horizons, and did not prevent selective diffusion of weathering agents into parts of the mineral grains. This finding supports those of other researchers such as Schott and Berner (1983) who found that thin hydrous ferric oxide layers formed on grain surfaces were not protective enough. However, the protective role of coatings in weathering could be limited, and, as suggested by Colman (1981) this could lead to a decrease in the rate of change of most weathering features with time. In surface horizons the rate of destruction of the residual layer is commonly small or negligible and the residues appear to slow movement of water to unaltered material and impede chemical transport away from it. An equilibrium thickness of the chemically more stable residue (coatings and infillings) promotes a constant rate of weathering. This could be the situation in the B3 horizon of Mount Compass where there is relatively less weathering even though the material is suggested to be much older than the overlying soil.

8.4. Environmental effects of mineral weathering based on SEM studies

The point value score (PVS) and value assessment score (VAS) methods of assessing mineral weathering were adopted as modified techniques to study the weathering characteristics of heavy minerals in soils (Chapter 5). The VAS method

was markedly more efficient in differentiating between weathered and less weathered mineral types both between profiles and between horizons within profile. The results showed that weathering of minerals in the different profiles were complex and dependent on a wide range of factors that contributed to soil forming processes. The established weathering sequence of zircon > sillimanite \geq spinel \geq rutile > garnet > epidote > monazite agreed largely with those suggested by other workers (e.g. Dryden and Dryden, 1946; Nickel, 1973). One of the physical limitations to a more ordered weathering pattern was the inherent grain shapes and surfaces. Irregular shaped etch pits were found on zircon, rutile, spinel, monazite and epidote whereas geometrical pits could be seen on sillimanite and garnet. Cleavage was present on sillimanite. Rounded and rough surfaced grains showed greater evidence of weathering which was marked by abundant chemically oriented features. Mechanical or "freshness" features were either still preserved on some areas or were extremely rare to absent. This was clearly displayed by monazite grains. The chemical composition of the mineral could also influence its relative stability to weathering. As shown in Section 5.4, a mineral containing more chemically reactive cation such as Fe^{2+} weathered much faster. Velbel (1984) showed that the mineralogy of garnet weathering products could be determined by the availability of Fe and Al. In the case of almandine Velbel (1984) also showed that there is congruent breakdown of the parent garnet, with localized precipitation of most of the Fe (as goethite) and some of the Al (as gibbsite), and the removal of the remaining constituents in solution. This localised precipitation phenomenon occurred mainly in restricted (densely compacted) rock environments. In freely drained sands the dominant weathering process could well be due to removal of constituents in solution. According to Wilson (1986) the removal, movement and precipitation of Fe and Al rich constituents in solution results in the crystallization of secondary weathering products such as imogolite, proto-imogolite allophane and iron oxide minerals mainly in the Bs horizons of podzols. The probable source of iron oxide rich stains and coatings on grains and infilled voids that were seen in the undisturbed thin sections (Chapter 4) is due to the weathering of Fe and Al bearing

heavy minerals in the sands studied. In energy terms it has been demonstrated that the persistence of a mineral in the weathering environment correlates very much with the total energy released by its breakdown into weathering products (Curtis, 1976; Lasaga and Blum 1986). Extensive studies to catalog the standard free energy of formation values (ΔG°_f) for different minerals have been carried out by Curtis (1976). Curtis observed that the greater the negative value of ΔG°_f , the greater should be the tendency to "react" and this should be reflected in instability. He noted particularly the rapid weathering of almost any minerals rich in ferrous iron. The ΔG°_f values for zoisite, grossular and spinel were - 78.7, - 61.0 and - 22.8 kcalmol⁻¹. In terms of stability therefore (starting with the least stable) : zoisite < grossular < spinel, which is the order found for these minerals in this study. The situation, however, can be more complex than this, and may involve other parameters such as Burgers vectors, Poisson ratios and isotropic shear moduli (Lasaga and Blum, 1986). The latter workers propounded the theory of etch pit formation and applied the theory to predict critical undersaturation values for various defects in different minerals. Their values ranged from - 500 calmol⁻¹ to - 8000 calmol⁻¹, with further results indicating etch pit formation depending on the value of ΔG between the solution and the mineral phases. It appears therefore that the thermochemical properties of minerals and the surrounding solution are important in mineral weathering studies, in addition to other physico-chemical properties.

Not all grains were severely etched in any one horizon. Even horizons that had chemically unstable constituents such as Fe²⁺ had some remarkably fresh grains. For instance, fresh garnet or rutile containing Fe existed along side highly weathered types. The following suggestions are proposed: (i) the grains could have been derived from different sources, with fresh inputs from younger rocks or recently weathered from older rocks, (ii) differential weathering due to the contribution of other factors which control chemical weathering, e.g. pH, permeability and sorting could account for the differences observed. Section 2.1.3 shows that the grains were derived from a variety of rock sources, including igneous, metamorphic and sedimentary types with ages

ranging from Cainozoic to Palaeozoic. There are indications in Section 5.4.2.3 that the sediments constituting the present soils might have been through more than one cycle of erosion, transportation and deposition. In Section 5.4.2.4 the pH conditions in the different soils were compared with relative mineral stabilities. Mineral stability sequences in this study were comparable to some of those mentioned in Nickel (1973). However, the small differences in pH between horizons within profiles, and between horizons for profiles with comparable soil reaction made unclear any relationship that may exist between severity of weathering and soil pH. Also the degree of sorting and permeability as influenced by redistribution of secondary minerals through translocation and redeposition have been discussed earlier. Poorly sorted soils tend to be less permeable to percolating fluids (more fine material as coatings and/or infillings) and in regions of higher rainfall the reduction in porosity could result in greater retention of moisture in the B horizon. This promotes hydrolytic reactions for longer periods of the year, which in these instances can cause greater mineral weathering in the B horizons as shown in Section 5.4. At shallower depths (in the A and E horizons) there were marginally more weathering recorded for grains, particularly zircon and rutile. The combination of hydration and oxidation processes may be responsible for these results. In these horizons, though, the soils are better sorted with little or no fine material as coatings or infillings (see Chapter 4). Under such conditions, given the same rainfall, oxidation reactions are better favoured than hydration.

The governing factors explaining the presence or absence data on surface microtextural features on grains described in Chapter 6 integrates some of the environmental factors already discussed above, including the chemical composition of the minerals and their physico-chemical characteristics. The significance of the occurrence of the different surface features to pedogenesis and provenance is the key factor in Chapter 6. The two most common and resistant minerals (zircon and rutile) were considered while limiting the within-sample variability by concentrating on only four of the profiles at Cooloola, where a definite age sequence has been established and the parent material known to be homogeneous (Chapter 7). There were a few

interesting findings from this study. First an order of frequency of occurrence of the surface features on the grains was established viz etch grain > subdued/rounded grain > clean/smooth fractured or cleavage faces (featureless faces) \approx high relief > conchoidal fractures/breakage blocks > sharp edges and angular grains > solution \approx scaling or surface roughness > hairline cracks \approx arc-shaped/parallel or semi-parallel steps. Second, the statistical evaluation presented data to support the influence of pedogenesis in the different soils, by accounting for significant changes in the proportion of different surface features. Third, the contribution to the various surface features by various environmental and energy conditions was discussed. The main difficulty in this study was how to best discriminate inherited (pre-depositional) features from those due to *in situ* pedogenesis. Since the source material was diverse it was impossible to examine and check that some of the textures observed were due to weathering of the grains *in situ* and not merely inherited from a previous erosional cycle. Despite this difficulty the microtextural imprints on the zircons and rutiles suggested some effects of post depositional weathering and were valuable in this respect.

8.5. Mineral distribution and characteristics in soils

Several different lines of evidence were used to assess the uniformity of the parent material as discussed in Chapter 7 (Section 7.4.1). The techniques are based on the similarity of the proportion in each horizon, of the different criteria used. These criteria were the 53-125 μm fraction, the total heavy mineral and different magnetic heavy fractions within the 53-125 μm , the ratio of zircon:rutile in the non-magnetic fraction of the 53-125 μm fraction and ratio of zirconium:titanium in the non-magnetic fraction of the 53-125 μm fraction.

In the present study, it was observed that weight fraction analyses of 53-125 μm separate gave indications of uniform parent material for soils in individual profiles, except at Mount Compass. At Mount Compass the B3 horizon could either have undergone more weathering to accumulate a higher amount of the 53-125 μm fraction

or this horizon could be a truncated remain of an older profile. Thin section studies from Chapter 4 point towards there being a depositional break at the B2 /B3 boundary (see Section 4.4.2). Also as shown in Section 7.4.1.1 the proportion of 53-125 μm fraction was similar for soils from the same location, again except for the LeFevre Peninsula and Mount Compass samples.

Analysis of the total heavy mineral in the 53-125 μm fraction documented disordered changes in heavy mineral concentration over the entire range of sequences studies (Section 7.4.1.2). There were within and between profile differences in total heavy mineral contents which could be explained by the fact that many of the mineral species were not particularly resistant to weathering in the soil environment. This has been demonstrated by several workers (e.g. Brewer, 1976; Bateman and Catt, 1985) who reported different mineral stability sequences in different soil environments. The quantitative differences in total heavy mineral proportion in the 53-125 μm fraction is characteristic of differences in geologic materials and/or differences in conditions of deposition. The geology and geomorphology of the sands as discussed in Chapter 2 substantiates the occurrence of both process in these samples.

Further quantitative and qualitative determination of the magnetic fraction was carried out to investigate the geological and depositional claims (Section 7.4.1.3). In quantitative and qualitative terms, the order of occurrence of minerals in the non-, slightly- and strongly-magnetic fractions suggested similar parent sediments for soils from Cooloola and North Stradbroke Island, but different for soils from LeFevre Peninsula and Mount Compass. The results for Canunda and Mount Burr profiles suggested differences in magnetic mineral proportions which were ascribed to pedochemical weathering. Qualitative analysis suggested similar suites of minerals for these profiles, which indicated they were derived from similar source(s).

The ratios of zircon:rutile in profiles from the different regions also indicated uniformity of parent material as discussed in Section 7.4.1.4. In all profiles, Mount Compass again showed greater variations in the ratio of the two minerals especially between the 0-120 cm and 120-200 cm depth. In the B3 horizons (~ 120-200) the

zircon content was higher relative to rutile with two possible explanations viz either there was more zircon contribution from the source material or greater weathering of the relatively less resistant mineral (rutile) in this part of the profile. Previous evidences and interpretations in other chapters and this support the theory of inhomogeneity of parent sediments at the B2/B3 horizon boundary.

Zirconium:titanium ratio results (Section 7.4.1.5) showed constant ratio (within statistical uncertainties) for horizons within profiles, except for Mount Compass (B2/B3 boundary, Fig. 7.412). Even though titanium in rutile and other minerals in the finer fractions (fine silt and clay) of soils is lost during pedogenesis (e.g. Sudom and St. Arnaud, 1971; Busacca and Singer, 1989), the constancy in the 53-125 μm fraction suggests either uniform soil parent material and/or minimal weathering and therefore inconsiderable mobility in the different profiles. Comparable horizons (Bhs2 and C) from different profiles within Cooloola and North Stradbroke (Figs 7.423 and 7.424) illustrated significant differences in the $\text{ZrO}_2 : \text{TiO}_2$. This suggested either depositional differences in these horizons (since it has been shown that the parent sediments are (similar) or preferential weathering of zircon and rutile. From results discussed in Chapters 5 and 6, rutile was shown to be less stable than zircon (at least qualitatively) and if the latter suggestion is true, then *in situ* weathering (with greater loss of rutile) should be higher with age in a chronosequence (youngest to oldest = KB < CH < WA/SC). However, Figs. 7.422 and 7.423 do not show this type of trend, indicating depositional differences as more likely.

Obviously comparable horizons from different profiles in different locations had different parent materials - the geologic provinces were different as discussed in Chapter 2. However, it was interesting to speculate what difference could occur if uniformity of parent material in these horizons were assessed purely based on values of the different quantitative criteria above, using the concept of parameter value coinciding with the depth axis at a very low angle (Brewer, 1976). The results using this concept *per se* showed remarkable similarity in parent material for soils as far apart as at Cooloola and LeFevre Peninsula (see Chapter 7 and Figs. 7.131 to 7.135, 7.331 to

7.336 and 7.421 to 7.424). This study and others (e.g. Haseman and Marshall, 1945; Barshad, 1964 and Brewer, 1976) have shown that for the establishment of uniformity of parent material several possible lines of evidence including both quantitative and qualitative mineralogical analyses should be used and very carefully assessed.

Simple statistical evaluation using the coefficient of variation (CV), which is a measure of the relative dispersion between two or more entire sets of data, has been used (e.g. Chapman and Horn, 1968; Murad, 1978 and Chittleborough *et al.*; 1984) to assess parent material uniformity. The general idea is the samples are considered as parts of a normally distributed population and the lower the CV the less variation in the parameters used as criteria for establishing parent material uniformity. Different workers have suggested their own CV limits to substantiate parent material homogeneity because of overall uncertainties linked with variations in mineralogical composition and extent of sorting of the parent material (see Section 7.4.1.6). In this section, the maximum CV values for the different criteria (e.g. 53-125 μm fraction, total heavy mineral fraction, zircon:rutile ratio, etc) for the within profile variations were used as a guide for establishing parent material uniformity. This decision formed the complement to earlier evidences using other techniques such as magnetic fractionation and mineral identification. As stated in Section 7.4.1.6 the 53-125 μm fraction was the only useful parameter that supported the concept of a chronosequence for Cooloola and North Stradbroke Island, and Canunda and Mount Burr sands. The other criteria were ineffective in establishing the soils as a chronosequence, because variations in their absolute values were wide both within and between profiles in a given sequence. This suggested differences in the deposition of the minerals especially in regions where at least, qualitatively, the suite of heavy minerals were shown to be similar, denoting homogeneous parent material.

After establishing parent material uniformity in the different profiles and sequences in the different locations, the next step was to estimate the degree of weathering in these soils using the same criteria as in the parent material studies (Section 7.4.2). It was difficult to select a true unaltered parent material in the soils

studied due to the great depths at which soil-forming processes were still operating (e.g. fluctuating water tables at depth > 20 m in some of the older podzols at Cooloola and at North Stradbroke Island). This prompted the study of individual heavy mineral grains to assess weathering patterns as described in Chapters 5 and 6. However, in this section weathering was basically considered to give estimates of absolute weathering (Brewer, 1976).

It was suggested that weathering had modified the proportion of the 53-125 μm and THM fractions in soils from Cooloola and North Stradbroke, to the extent that there were more of these fractions present in the upper A and B horizons of the older profiles than the younger sections of the sequence. Such a relationship was not established for soils from LeFevre Peninsula, Mount Compass, Canunda and Mount Burr, particularly for the THM fractions which varied widely in these soils. The older profiles at Mount Compass and Mount Burr showed some trend for the 53-125 μm fraction that indicated more weathering in the upper horizon (higher proportion of 53-125 μm fraction in E horizon of Mount Compass, and A and E horizons of Mount Burr, Figs. 7.112 and 7.122).

In the established chronosequences at Cooloola, LeFevre Peninsula and Canunda/Mount Burr no definite relationship was found between the proportion of the 53-125 μm and THM fraction with age of the profiles (Section 7.4.2.1).

Estimates of different magnetic mineral fractions did not give any indication of weathering trends within profiles (Section 7.4.2.2). However in comparable horizons of different profiles the effects of weathering were slightly more evident. Soils from the South Australia region (LeFevre Peninsula, Mount Compass, Canunda and Mount Burr) showed higher proportions of the more resistant, non-magnetic minerals (zircon, rutile and sillimanite) in the older soils at Mount Compass and Mount Burr. The slightly magnetic mineral fraction was more sensitive to demonstrating weathering trends in soils from Cooloola, in which the proportion of this fraction in comparable horizons of the different profiles generally decreased with increasing age.

Usually ratios of the concentration of weatherable to resistant minerals or specific elements associated with such minerals in the non-clay fraction of soils are used to assess the degree of weathering. In such cases ratios such as feldspars:zircon, $\text{CaO}:\text{ZrO}_2$, $\text{Na}_2\text{O}:\text{ZrO}_2$ and $\text{Fe}_2\text{O}_3:\text{ZrO}_2$ are considered (Section 7.1). However, in this study I was hampered in my attempt to precisely measure the concentration of these weatherable components indirectly by XRF analysis. This was because there were very low K_2O and/or CaO values for samples, particularly from Cooloola (see Table 3.2): this has been shown by other workers (e.g. Little *et al.*, 1978; Thompson, 1981). Total elemental composition, except for SiO_2 , in < 2 mm fraction indicated considerable variation between and within profiles (Skjemstad *et al.*, 1990). This was partly due to translocation of some elements within profiles, but was mainly influenced by the natural variations within horizons due to banding of heavy minerals. At Cooloola and North Stradbroke Island, this latter process is a result of the dune building processes (over-lapping dune building events, producing large parabolic compound dunes as discussed in Chapter 2). The total Fe_2O_3 contents were a little higher (Table 3.2; Skjemstad *et al.*, 1990) and were mainly from ilmenite and/or pseudorutile, but their use could not have been very meaningful because of the general difficulty in evaluating depositional, weathering, translocation processes within each profile from such data. Given this background and, as shown in Chapters 5 and 6, zircon was more resistant to weathering than rutile (at least qualitatively), I decided to explore the possibility of assessing weathering trends within and between profiles using zircon:rutile and zirconium:titanium ratios. However, both approaches failed to give any clues on mineral weathering trends (Section 7.4.2.3). It was likely that either the effects of depositional differences exceeded those that could be due to weathering or these minerals did not weather sufficiently enough to show any definite trends. Both suggestions are supported by a recent work (Skjemstad *et al.*, 1990) where they found that chemical extraction techniques gave relatively low yields of Ti from heavy minerals and that heavy minerals contributed to a highly variable background of Ti and Zr levels in soils from the Queensland region. Also these workers could not show any evidence

of Zr movement or accumulation in the soils studied, using various chemical extraction methods.

Since all the studies in this thesis showed that zircon was the most stable mineral to weathering, it was decided to investigate individual zircon grains more closely (Section 7.4.3.1). This study included analysing for Zr and Hf in individual zircon grains to investigate the differences in the zircon population in regard to source rocks. The results showed differences existed between zircon grains from profiles within the same location (e.g. Cooloola) and between profiles from different locations (e.g. LeFevre Peninsula and Mount Compass or Canunda and Mount Burr). As stated in section 7.4.3.1 the degree of heterogeneity of the proximate source material for the sediments is greater for soils from the South Australian than the Queensland region.

8.6. General conclusions

1. Parent materials of all soils sampled are believed to have been deposited during the Quaternary period. Thermoluminescence ages (19-700 ka BP) of quartz samples from Cooloola and North Stradbroke Island are in the same chronological order as indicated by field relationships.
2. Micromorphological investigation showed close relationship between field macromorphological properties, age of profile and degree of profile development. In both calcareous and siliceous soils there were different levels and zones of organo-mineral complex formations around mineral grains and in voids between grains, which became more intricate with prolonged soil development.
3. Two semi-quantitative scaling methods (mean point value score and value assessment score) were used to assess and classify surface microtextural features on grains of heavy minerals. These methods were sensitive enough to enhance the development of a resistance-to-weathering scale for these minerals.

4. Mineral weathering studies in soils, through analysis of surface microtextural features on heavy mineral grains, provide useful means of relating changes associated with grain surfaces to pedogenesis.
5. The relationship between heavy mineral weathering (using surface microtextural features) and soil development is a complex open process which is affected by a range of environmental, pedogenic and geogenic factors.
6. The development of individual surface microtextures on grains are strongly affected by the interaction between both the mechanical and chemical processes in the environment, as well as the provenance, crystallographical, mineralogical, physical and chemical properties of the mineral. The influence of all these factors on the microtextural features of zircon and rutile grains showed that zircon is less chemically altered during pedogenesis ^{than} rutile. However, zircons exhibited more features that can be ascribed to processes of physical alteration.
7. Parent material uniformity and stratification within profiles were established by a range of mineralogical methods (including weight fraction, mineral and elemental ratio of the 53-125 μm fraction, and heavy mineral analysis), as well as micromorphology.
8. Analysis of surface microtextures of zircon and rutile grains, and elemental investigations of zircon grains suggested a multiple grain source for these minerals in all the soils studied.

8.7. Suggestions for future work

1. More thermoluminescence work to include all the dune systems and more samples within each dune system to further verify the time gap and/or stratigraphic variations within profiles.
2. Use of other thermal analysis techniques (e.g. DSC) to more closely examine the nature and origin of quartz grains from the different dune systems. This could help to understand why different quartz samples have different TL response curves.
3. More work should be done on mineral resistance to weathering, to include SEM and chemical analytical techniques. This may clarify the influence of chemical composition on mineral weathering, and may enhance the understanding of mechanisms that govern reactions and translocation of elements such as Fe within the soil profile.
4. The surface etching and pitting on zircon mineral grains suggest some solution effects and consequently loss of constituent elements from the mineral. These soils thus provide the opportunity to study the fate of Zr. Appropriate techniques will have to be used in order to account for pedogenic phases of zircon.
5. More information on the influence of geogenic as opposed to pedogenic weathering on mineral grains is required. This would help define the relative importance of various soil microenvironmental factors, in particular how they affect the degree and nature of mineral weathering, and would clarify what now appears to be a complex interaction between the soil microenvironment and weathering of mineral grains.

Appendix 1. Monthly and annual climatic data for stations nearby sampling sites (Bureau of Meteorology, 1988).

Station Name	DOUBLE ISLAND POINT											Commenced	1891	QUEENSLAND			
Number	Lighthouse											Lat. 25° 56' S		Long. 153° 12' E		Elevation 77.0m	
	Jan.	Feb.	Mar.	Apr.	May	Jun.	Jul.	Aug.	Sep.	Oct.	Nov.	Dec.	Year				
													95 Years of record				
Rainfall (mm)														92	135	1446	
Mean	177	173	178	139	147	124	91	61	55	74	73	123	1388				
Median	139	132	156	117	138	105	76	60	50	55	73	123	1388				
													95 Years of Record				
Raindays (no.)														10	11	145	
Mean	13	15	17	15	15	12	10	9	9	9	10	11	145				
													28 Years of Record				
Daily maximum temperature (°C)														25.5	26.8	23.8	
Mean	27.3	27.3	26.5	24.7	22.3	19.9	19.2	20.4	22.2	24.0	25.5	26.8	23.8				
86 Percentile	29.0	29.1	28.2	26.7	24.4	21.7	21.5	22.4	24.2	26.1	27.6	28.6					
14 Percentile	25.5	25.6	24.6	22.8	20.3	18.3	17.2	18.3	20.0	21.9	23.6	25.0					
													28 Years of Record				
Daily minimum temperature (°C)														20.1	21.3	18.5	
Mean	22.2	22.3	21.6	19.8	17.2	14.7	13.6	14.5	16.4	18.4	20.1	21.3	18.5				
86 Percentile	23.9	23.9	23.3	21.6	19.5	17.0	16.1	16.7	18.3	20.0	21.8	23.1					
14 Percentile	20.6	20.8	20.0	18.0	15.0	12.2	10.8	12.2	14.4	16.6	18.3	19.4					
													28 Years of Record				
Humidity														73	75	74	
9am mean relative humidity (%)	76	78	78	75	75	73	71	68	70	70	73	75	74				
3pm mean relative humidity (%)	75	75	74	72	69	67	63	63	65	68	72	73	70				

Appendix 1 contd. Monthly and annual climatic data for stations nearby sampling sites (Bureau of Meteorology, 1988).

Station Name BRISBANE REGIONAL OFFICE											Commenced 1840		QUEENSLAND	
Number 040214		Lat. 27° 28' S				Long. 153° 2' E				Elevation 38.0m				
	Jan.	Feb.	Mar.	Apr.	May	Jun.	Jul.	Aug.	Sep.	Oct.	Nov.	Dec.	Year	
Rainfall (mm)											138 Years of record			
Mean	163	158	141	87	73	68	56	47	47	77	98	134	1149	
Median	131	116	109	60	51	44	38	29	40	64	84	116	1107	
Raindays (no.)											138 Years of Record			
Mean	13	14	15	11	10	8	7	7	8	9	10	11	123	
Daily maximum temperature (°C)											99 Years of Record			
Mean	29.4	29.0	28.0	26.1	23.2	20.9	20.4	21.8	24.0	26.1	27.8	29.1	25.5	
86 Percentile	32.1	31.6	30.4	28.6	25.5	23.1	22.6	24.2	26.8	29.1	30.7	31.9		
14 Percentile	26.7	26.4	25.5	23.9	20.9	18.6	18.2	19.5	21.4	23.0	24.8	26.2		
Daily minimum temperature (°C)											99 Years of Record			
Mean	20.7	20.6	19.4	16.6	13.3	10.9	9.5	10.3	12.9	15.8	18.1	19.8	15.7	
86 Percentile	22.7	22.4	21.3	19.0	16.1	13.8	12.7	13.1	15.5	18.3	20.4	21.9		
14 Percentile	18.7	18.7	17.5	14.1	10.4	7.7	6.3	7.4	10.2	13.1	15.7	17.7		
Humidity											35 Years of Record			
9am mean relative humidity (%)														
	66	69	70	69	70	70	68	63	60	60	59	61	65	
3pm mean relative humidity (%)														
	58	60	58	53	51	49	45	43	45	51	53	57	52	

Appendix 1 contd. Monthly and annual climatic data for stations nearby sampling sites (Bureau of Meteorology, 1988).

Station Name ADELAIDE (WEST TERRACE)		Commenced 1839 Ceased 1980		SOUTH AUSTRALIA									
Number 023000	Lat. 34° 56' S	Long. 138° 35' E		Elevation 40.0m									
	Jan.	Feb.	Mar.	Apr.	May	Jun.	Jul.	Aug.	Sep.	Oct.	Nov.	Dec.	Year
												140 Years of record	
Rainfall (mm)													
Mean	20	21	24	44	68	72	67	62	51	44	31	26	530
Median	13	10	17	38	62	65	65	59	47	42	24	21	526
												140 Years of Record	
Raindays (no.)													
Mean	4	4	5	9	13	15	16	16	13	11	8	6	120
												92 Years of Record	
Daily maximum temperature (°C)													
Mean	28.5	28.5	26.0	22.1	18.6	15.7	14.9	16.1	18.4	21.3	24.4	26.8	21.8
86 Percentile	35.9	35.4	32.0	27.6	22.3	18.1	17.1	19.1	23.2	27.8	31.7	34.2	
14 Percentile	22.4	22.5	20.9	17.9	15.4	13.6	12.8	13.4	14.6	16.4	18.7	20.6	
												92 Years of Record	
Daily minimum temperature (°C)													
Mean	1.61	16.8	1.52	12.8	10.4	8.5	7.5	8.0	9.2	11.1	13.2	15.1	12.0
86 Percentile	12.6	21.7	19.3	16.0	13.1	11.1	9.8	10.5	12.2	14.8	17.5	19.9	
14 Percentile	12.6	12.8	11.6	9.5	7.4	5.5	4.9	5.2	6.2	7.6	9.4	11.3	
												24 Years of Record	
Humidity													
9am mean relative humidity(%)	47	50	54	59	69	73	75	71	61	55	50	49	59
3pm mean relative humidity (%)	37	38	42	47	56	59	62	58	51	45	41	39	48

Appendix 1 contd. Monthly and annual climatic data for stations nearby sampling sites (Bureau of Meteorology, 1988).

Station Name	MYPONGA POST OFFICE											Commenced	1914		SOUTH AUSTRALIA		
Number	023738					Lat. 35° 24' S					Long. 138° 28' E					Elevation 226.0m	
	Jan.	Feb.	Mar.	Apr.	May	Jun.	Jul.	Aug.	Sep.	Oct.	Nov.	Dec.	Year				
													71 Years of record				
Rainfall (mm)														37	29	759	
Mean	24	28	25	59	94	109	113	98	82	61	28	24	768				
Median	17	16	17	51	88	103	103	102	79	57	28	24	768				
													71 Years of Record				
Raindays (no.)														8	6	117	
Mean	4	4	4	9	14	14	16	15	13	10	8	6	117				
													11 Years of Record				
Daily maximum temperature (°C)														22.1	23.7	19.5	
Mean	27.1	25.5	24.0	20.5	16.2	14.3	12.6	13.6	15.7	18.9	22.1	23.7	19.5				
86 Percentile	35.0	33.1	30.0	26.1	19.7	16.7	14.4	16.4	20.0	25.0	29.5	32.2					
14 Percentile	20.6	19.4	18.9	16.1	13.3	11.7	11.1	11.3	12.7	14.4	16.1	17.8					
													11 Years of Record				
Daily minimum temperature (°C)														8.6	10.1	7.7	
Mean	11.6	11.7	10.2	7.4	6.5	4.8	4.2	4.7	5.4	7.1	8.6	10.1	7.7				
86 Percentile	15.0	14.4	14.4	11.7	11.1	10.0	8.3	8.3	8.9	10.6	12.6	13.9					
14 Percentile	8.3	8.9	5.8	2.8	1.7	-0.6	-0.5	0.6	1.7	2.8	3.9	6.7					
													1 Years of Record				
Humidity														59	56	68	
9am mean relative humidity (%)	49	54	59	69	80	82	84	82	73	66	59	56	68				
3pm mean relative humidity (%)	40	43	47	56	66	71	72	70	64	58	49	48	57				

Appendix 1 contd. Monthly and annual climatic data for stations nearby sampling sites (Bureau of Meteorology, 1988).

Station Name MOUNT BURR FOREST RESERVE Commenced 1924 SOUTH AUSTRALIA													
Number 026019	Lat. 37° 34' S				Long. 140° 26' E				Elevation 64.0m				
	Jan.	Feb.	Mar.	Apr.	May	Jun.	Jul.	Aug.	Sep.	Oct.	Nov.	Dec.	Year
											61 Years of record		
Rainfall (mm)													
Mean	29	29	37	69	85	96	112	102	80	63	48	39	789
Median	22	20	29	61	78	91	106	101	80	56	47	33	789
											61 Years of Record		
Raindays (no.)													
Mean	8	8	10	14	18	19	22	21	18	16	13	11	178
											28 Years of Record		
Daily maximum temperature (°C)													
Mean	25.3	25.6	23.0	20.1	16.3	14.2	13.3	14.3	15.7	18.1	20.5	22.7	19.1
86 Percentile	33.3	33.2	29.4	25.5	19.5	16.1	15.2	16.7	19.6	23.6	27.2	30.1	
14 Percentile	19.6	19.4	18.2	15.9	13.6	12.1	11.6	12.0	12.8	14.0	15.6	17.4	
											28 Years of Record		
Daily minimum temperature (°C)													
Mean	12.2	12.7	11.6	9.8	7.6	5.9	5.0	5.7	6.4	7.7	9.4	10.8	8.7
86 Percentile	16.4	16.6	15.3	13.4	10.8	8.9	7.8	8.4	9.7	11.6	13.0	14.3	
14 Percentile	7.9	8.7	7.6	6.4	4.4	2.6	2.1	2.4	2.9	3.9	5.4	7.1	
											28 Years of Record		
Humidity													
9am mean relative humidity(%)	61	63	69	76	85	88	89	84	78	72	68	63	75
3pm mean relative humidity (%)	43	43	50	57	68	74	74	70	67	62	56	49	59

Appendix 2. Selected morphological data for samples associated with profiles studied.

Sample No.	Horizon†	Sampling depth (cm)	Colour‡	Texture\$	Structure\$	Consistence\$	Boundary\$
COOLOOLA PROFILES							
<u>Carlo - CL¶ (Siliceous sand#; Typic Quartzipsamment††)</u>							
MS 1.10	AC\$\$	0-5	10YR 6/5	s	0sg	ml	-
<u>Kings Bore - KB¶ (Siliceous sand#; Typic Quartzipsamment††)</u>							
MS 2.10	A1	0-10	10YR 4/2	s	0sg	mvfr	dw
MS 2.20	E	15-20	10YR 7/3	s	0sg	mvfr	dw
MS 2.30	Bhs2	30-60	10YR 4/3	s	0sg	mvfr	cs
MS 2.40	Bhs3	60-110	10YR 6/4	s	0sg	mvfr	cs
MS 2.50	C	130-150	10YR 6/4	s	0sg	mvfr	
<u>Chalambar 1 - CH¶ (Podzol#; Troporthod††)</u>							
MS 3.10	A1	0-40	10YR 6/1	s	0sg	mvfr	dw
MS 3.20	E	40-60	10YR 5/1	s	0sg	ml	cw
MS 3.31	Bhs2	60-63	10YR 4/4	s	0sg	mfr	cw
MS 3.32	Bs2	80-120	7.5YR 4/3	s	0sg	mvfr	gw
MS 3.33	B2	100-120	7.5YR 5/6	s	0sg	mvfr	gw
MS 3.41	Bhs3	120-140	10YR 5/4	s	0sg	mvfr	gw
MS 3.42	B3	140-160	10YR 6/6	s	0sg	mvfr	gw
MS 3.50	C	200-250	10YR 7/5	s	0sg	mvfr	
<u>Burwilla 1 - BW¶ (Podzol#; Troporthod††)</u>							
MS 10.20	E	70-90	10YR 5/2	s	0sg	ml	-
<u>Warrawonga 1 or Seacliffs - SC¶ ("Giant" Podzol#; Spodic Quartzipsamment††)</u>							
MS 4.10	A1	55-110	10YR 6/1	s	0sg	mvfr	dw
MS 4.20	E	150-250	10YR 5/2	s	0sg	ml	ds
MS 4.21	E‡‡	160-270	10YR 5/1	s	0sg	ml	as
MS 4.31	Bh2‡‡	310-470	10YR 2.5/1	s	0sg	mvfr	gw
MS 4.32	Bhs2‡‡	310-470	10YR 3/2	s	0sg	mvfr	gw
MS 4.33	Bs2	310-470	10YR 3/3	s	0sg	mvfr	dw
MS 4.41	C1	720-760	10YR 4/4	s	0sg	mvfr	ds
MS 4.42	C2	780-800	10YR 6/4	s	0sg	mvfr	
<u>Warrawonga 2 - WA¶ ("Giant" Podzol#; Spodic Quartzipsamment††)</u>							
MS 11.10	A1	0-80	10YR 5/1	s	0sg	mvfr	dw
MS 11.20	E	210-260	10YR 7/2	s	0sg	mvfr	cw
MS 11.30	Bhs2	625-690	10YR 4/4	s	0sg	mvfr	

Appendix 2 contd.

Sample No.	Horizon†	Sampling depth (cm)	Colour‡	Texture§	Structure§	Consistence§	Boundary§
<u>Mundu 4 - MU¶ ("Giant" Podzol#: Spodic Quartzipsamment††)</u>							
MS 12.20	E	220-280	10YR 9/1	s	Osg	ml	-
<u>Kabali 2- KL¶ ("Giant" Podzol#: Spodic Quartzipsamment††)</u>							
MS 13.20	E	210-260	10YR 8/1	s	Osg	ml	-
NORTH STRADBROKE ISLAND PROFILE							
<u>Amity - AM¶ ("Giant" Podzol#: Spodic Quartzipsamment††)</u>							
MS 14.13	A3	10-30	10YR 5/2	s	Osg	ml	dw
MS 14.20	E	400-425	10YR 8/2	s	Osg	ml	ds
MS 14.21	E‡‡	415-440	10YR 7/2	s	Osg	ml	as
MS 14.31	Bh2‡‡	700-900	10YR 3/1	s	Osg	mfr	dw
MS 14.32	Bhs2‡‡	700-900	7.5YR 4/4	s	Osg	mfr	dw
MS 14.33	Bs2	700-900	7.5YR 4/3	s	Osg	mvfr	di
MS 14.34	B2	700-900	10YR 6/2	s	Osg	mvfr	di
MS 14.40	B3	1500-1550	10YR 3/2	s	Osg	mvfr	di
MS 14.50	C	1900-1930	10YR 6/4	s	Osg	mvfr	
LEFEVRE PENINSULA PROFILES							
<u>LeFevre Peninsula 1 - 1LP¶ (Calcareous sand#: Typic Xeropsamment††)</u>							
MS 5.10	A1	26-40	7.5YR 5/2	s	Osg	mvfr	di
MS 5.20	A2	90-110	7.5YR 6/1	s	Osg	ml	
<u>LeFevre Peninsula 2 - 2LP¶ (Calcareous sand#: Typic Xeropsamment††)</u>							
MS 6.10	A1	0-15	7.5YR 3/1	s	Osg	mvfr	di
MS 6.20	A2	15-30	7.5YR 3/2	s	Osg	ml	cs
MS 6.30	A3	30-49	10YR 5/4	s	Osg	ml	gs
MS 6.40	B	49-60	7.5YR 4/3	s	Osg	ml	gs
MS 6.50	C	60-100	10YR 8/3	s	Osg	ml	
MOUNT COMPASS SEQUENCE							
<u>Mount Compass - MC¶ (Podzol#: typic Haplorthod††)</u>							
MS 7.10	A1	0-10	7.5YR 4/1	s	Osg	mvfr	dw
MS 7.20	E	10-110	10YR 8/2	s	Osg	ml	ds
MS 7.21	E‡‡	30-100	10YR 6/6	s	Osg	ml	aw
MS 7.30	Bh2‡‡	90-120	7.5YR 3/4	s	Osg	mfi	cw
MS 7.31	Bhsb2	110-130	10YR 6/8	s	Osg	mfi	gw
MS 7.41	Bhsb3	135-150	10YR 4/6	s, g	Osg	mfr	di
MS 7.42	Bsb3	155-175	10YR 4/8	s	Osg	mvfr	di
MS 7.43	Bb4	160-220	10YR 7/4	ls	Osg	mvfr	

Appendix 2 contd.

Sample No.	Horizon†	Sampling depth (cm)	Colour‡	Texture\$	Structure\$	Consistence\$	Boundary\$
------------	----------	---------------------	---------	-----------	-------------	---------------	------------

CANUNDA PROFILE

Canunda - CN¶ (Calcareous sand#; Typic Xeropsamment††)

MS 8.10	AC¶¶	0-5	2.5Y 7/4	s	Osg	ml	-
MS 8.20	A1	90-110	2.5Y 8/4	s	Osg	ml	ds
MS 8.21	Ab1	155-170	10YR 2/2	s	Osg	ml	aw
MS 8.22	Bb1	185-200	10YR 5/4	s	Osg	ml	aw
MS 8.23	Ab2	205-220	10YR 2/2	s	Osg	mvfr	aw
MS 8.24	Bb2	240-260	2.5Y 8/4	s	Osg	ml	aw
MS 8.25	Ab3	310-318	10YR 5/3	s	Osg	mvfr	aw
MS 8.26	Bb3	340-370	2.5Y 8/4	s	Osg	ml	

MOUNT BURR PROFILE

Mount Burr - MB¶ (Podzol#; Entic Haplorthod††)

MS 9.10	A1	0-25	10YR 4/1	s	Osg	mvfr	dw
MS 9.20	E	60-80	10YR 8/1	s	Osg	ml	gw
MS 9.30	Bhs2	250-270	10YR 4/4	s	Osg	mfr	

† Horizon nomenclature is that designated in the field.

‡ Munsell colour notation for moist soil.

\$ Abbreviations are those assigned to texture, structure, consistence and boundary in soil Survey Staff Manual (1951), where s = sand; 0 = structureless, sg = single grain; ml = loose, mvfr = very friable, mfr = friable, mfi = firm; a = abrupt, c = clear, g = gradual, d = diffuse, s = smooth, w = wavy, i = irregular.

¶ Profile symbol used in the thesis.

Stace *et al.*, (1968).

†† Soil Survey Staff (1987). Keys to Soil Taxonomy.

\$\$ Mobile dune.

‡‡ materials associated with a pipe.

¶¶ Beach deposit.

Appendix 3.

Physical data for selected soil profiles.

Horizon	Depth (cm)	CO ₃ CaCO ₃	Acid treated samples					Untreated samples					Total soil		Total
			Clay	Silt	Fine Sand	Crse Sand	Total	Clay	Silt	Fine Sand	Crse Sand	Total	Fine Sand	Crse Sand	
Canunda - CN¶ (Calcareous sand#; Typic Xeropsamment††)															
A1	90-110	90	0.0	0.1	4	5	100	11.0	1.5	19	71	103	22	78	100
Ab1	155-175	90	0.0	0.0	5	4	99	10.2	1.8	17	71	100	16	84	100
Bb1	185-200	90	0.2	0.1	5	5	100	9.8	1.2	18	70	99	19	81	100
Ab2	205-220	84	0.3	0.3	8	6	99	10.3	2.5	32	53	98	33	68	100
Bb2	240-265	90	0.0	0.1	3	4	97	10.0	0.2	13	78	101	17	84	100
Ab3	310-318	86	0.0	0.5	6	6	98	12.5	2.5	25	63	103	19	81	100
Bb3	340-370	90	0.0	0.2	4	5	99	9.5	1.8	27	63	101	21	79	100
Mount Burr - MB¶ (Podzol#; Entic Haplorthod††)															
A1	0-25							2	2	10	85	100			
E	60-80							1	1	9	88	100			
Bhs2	250-270							3	2	12	84	100			
LeFevre Peninsula 1 - 1LP¶ (Calcareous sand#; Typic Xeropsamment††)															
A1	26-40	20						2	1	10	65	97			
A2	90-110	27						2	1	14	56	99			
LeFevre Peninsula 2 - 2LP¶ (Calcareous sand#; Typic Xeropsamment††)															
A1	0-15	3.3						5	4	29	55	96			
A2	15-30	2.0						1	1	31	64	99			
A3	30-49	0.6						2	0	28	70	100			
B	49-60	0.3						2	0	28	67	97			
C	60-100	0.9						1	1	32	66	101			
Mount Compass - MC¶ (Podzol#; Typic Haplorthod††)															
A1	0-10							1	3	32	62	98			
E	10-110							2	0	31	67	100			
E‡‡	30-100							3	1	26	71	101			
E/B1	80-100							3	1	31	67	101			
Bh2‡‡	90-120							4	1	25	70	100			
Bhsb2	110-130							3	1	34	62	100			
Bhsb3	135-150							5	2	12	82	100			
Bsb3	155-175							12	0	3	85	100			
Bb4	160-220							6	2	7	86	100			
Amity - AM¶ ("Giant" Podzol#; Spodic Quartzipsamment††)															
A3	10-30							1	2	11	86	100			
E	400-425							<1	1	10	87	98			
C	1900-1930							1	1	7	92	101			

¶ Profile symbol used in this study.

Stace *et al.* (1968).

†† Soil Management Support Service (1987), Keys to Soil Taxonomy.

‡‡ Materials associated with a pipe.

Appedix 3 contd.

Chemical data for selected soil profiles.

Horizon	Depth (cm)	Moist %	pH†	E.C. dSm ⁻¹	Total		Org. C. %	Sol.P ugg ⁻¹	-----Exch. cations-----					Total CEC
					Cl ⁻ ugg ⁻¹	C %			Ca	Mg	Na	K	Total mmol(+)/kg ⁻¹	
Canunda - CN¶ (Calcareous sand#; Typic Xeropsamment††)														
A1	90-110	0.11	9.4	0.09	6	10.3		4	6.0	0.7	0.1	<0.1	7	16
Ab1	155-175	0.31	9.0	0.12	17	10.3		6	16.0	5.3	3.4	<0.1	25	28
Bb1	185-200	0.11	9.3	0.09	10	10.0		9	7.3	1.4	0.8	<0.1	10	21
Ab2	205-220	0.21	9.2	0.12	33	9.6		9	8.7	2.5	1.1	<0.01	12	21
Bb2	240-265	0.15	9.4	0.09	15	10.2		6	5.3	0.9	3.8	<0.1	10	7
Ab3	310-318	0.17	9.2	0.11	28	9.8		7	10.0	1.9	0.9	<0.1	13	13
Bb3	340-370	0.08	9.4	0.09	9	9.9		4	6.7	0.8	2.1	<0.1	9	16
Mount Burr - MB¶ (Podzol#; Entic Haplorthod††)														
A1	0-25	0.39	4.2	0.04	<2	0.6		3	6.1	2.4	0.5	0.4	9	29
E	60-80	0.22	4.9	0.03	<2	0.1		2	1.4	<0.2	<0.1	<0.1	1	<2
Bhs2	250-270	0.25	5.1	0.04	<2	0.3		1	1.1	<0.2	<0.1	<0.1	1	23
LeFevre Peninsula 1 - 1LP¶ (Calcareous sand#; Typic Xeropsamment††)														
A1	26-40	1.21	8.9	1.77	2012	3.6	1.2	14						
A2	90-110	1.69	8.6	3.46	4924	3.8	0.6	17						
LeFevre Peninsula 2 - 2LP¶ (Calcareous sand#; Typic Xeropsamment††)														
A1	0-15	1.60	8.2	0.19	179	4.5	4.1	55						
A2	15-30	0.39	8.4	0.13	52	1.3	1.1	16						
A3	30-49	0.15	8.9	0.08	20	0.2	0.1	5						
B	49-60	0.14	9.0	0.10	23	0.4	0.4	5						
C	60-100	0	9.1	0.09	20	0.2	0.1	2						
Mount Compass - MC¶ (Podzol#; Typic Haplorthod††)														
A1	0-10	0.24	6.7	0.04	11	1.2	1.2	4	8.9	2.3	0.4	0.9	13	21
E	10-110	0.03	6.8	0.04	7	<0.1	<0.1	1	0.0	0.3	0.0	0.1	0	4
E‡‡	30-100	0.14	6.9	0.03	7	0.2	0.2	3	0.7	0.4	0.4	0.2	2	8
E/B1	80-100	0.08	6.7	0.03	7	0.2	0.2	2	0.7	0.6	0.5	0.1	2	6
Bh2‡‡	90-120	0.33	6.1	0.04	7	0.3	0.3	2	5.2	0.9	0.6	0.4	7	14
Bhsb2	110-130	0.18	6.5	0.04	7	0.2	0.2	0	0.0	0.5	0.2	0.1	1	7
Bhsb3	135-150	0.88	6.1	0.03	7	0.8	0.8	2	0.7	1.0	0.3	0.4	2	34
Bsb3	155-175	0.89	5.9	0.03	6	0.1	0.1	0	1.5	2.0	0.7	0.4	5	14
Bb4	160-220	0.30	6.0	0.03	7	0.1	0.1	0	0.7	0.5	0.7	0.2	2	6
Amity - AM¶ ("Giant" Podzol#; Spodic Quartzipsamment††)														
A3	10-30	0.34	5.0	0.04	<2	0.4		4	3.2	0.8	<0.1	0.5	5	21
E	400-425	0.24	5.3	0.03	<2	<0.1		1	1.1	<0.2	<0.1	<0.1	1	<2
C	1900-1930	0.32	5.6	0.03	<2	<0.1		1	1.1	<0.2	<0.1	<0.1	1	<2

† (1:5, soil:water suspension)

¶ Profile symbol used in this study.

Stace *et al.* (1968).

†† Soil Management Support Service (1987), Keys to Soil Taxonomy.

‡‡ Materials associated with a pipe.

Appendix 3 contd.

Sand fractionation data for Canunda profile.

		Sand fractionation of untreated samples														
		Sieve size (μm)														
Horizon	53	75	102	125	150	180	225	250	300	355	400	500	600	850	1000	2000
	Accumulative %															
A1	0.1	0.2	0.4	0.8	2.9	19.5	37.6	57.5	74.6	86.9	92.0	95.9	97.7	99.6	99.9	100
Ab1	0.6	0.9	1.8	2.4	5.5	17.9	29.3	40.3	52.2	65.1	75.2	83.6	90.5	98.1	99.5	100
Bb1	0.1	0.3	0.5	1.1	3.6	20.8	36.1	53.6	67.9	80.2	87.3	92.0	95.3	99.2	99.9	100
Ab2	0.5	1.1	2.4	3.7	9.3	32.3	52.9	68.8	80.8	89.1	93.0	96.2	97.7	99.5	99.9	100
Bb2	0.1	0.2	0.4	0.6	1.9	14.9	30.4	48.9	64.1	76.8	84.4	89.6	93.6	98.7	99.6	100
Ab3	0.5	1.1	1.9	3.0	6.4	27.7	44.2	62.8	76.0	87.0	92.1	95.9	97.7	99.7	99.6	100
Bb3	0.4	0.8	1.9	2.7	6.0	25.7	44.9	59.3	70.7	79.0	84.9	89.1	92.7	97.2	98.8	100
		Sand fractionation of acid treated samples														
	53	75	102	125	150	180	225	250	300	355	400	500	600	850	1000	2000
A1	0.7	0.8	2.0	2.5	6.5	38.5	73.4	91.5	96.4	98.3	98.8	99.5	99.6	99.8	99.8	100
Ab1	1.6	2.8	4.4	6.1	12.9	49.9	77.0	89.1	93.0	94.9	96.2	97.2	98.2	99.6	99.8	100
Bb1	0.6	1.3	2.2	3.6	7.7	40.9	70.8	87.6	93.6	96.2	97.2	98.3	98.9	99.7	99.9	100
Ab2	1.4	3.2	1.7	6.1	10.5	59.6	81.1	95.7	98.1	99.0	99.3	99.6	99.8	100	100	100
Bb2	0.9	1.4	2.4	3.2	6.5	37.4	72.0	89.5	94.6	96.8	97.1	98.2	98.2	99.4	99.6	100
Ab3	0.9	1.8	3.1	4.1	9.9	45.9	76.6	92.0	96.5	98.2	98.6	99.3	99.5	100	100	100
Bb3	1.1	1.8	3.2	5.3	8.9	31.5	76.6	82.5	94.7	91.7	97.1	94.0	98.6	95.7	99.8	100

REFERENCES

- Aitchison, G.D., Sprigg, R.C. and Cochrane, G.W. 1954. The soils and geology of Adelaide and suburbs. Geol. Surv. S. Aust. Bull. 32.
- Aitken, M.J. 1985. Thermoluminescence dating. Academic Press, London.
- Alias, L.J. 1961. Weathering process in a humic podzol profile. *Agrochimica* 5 : 338-351.
- Allan, J.F., Sack, R.O. and Batiza, R. 1988. Cr-rich spinels as petrogenetic indicators: MORB-type lavas from the Lamont Seamount Chain, eastern Pacific. *Am. Min.* 73 : 741-753.
- Allison, G.B., Colville, J.S. and Greacen, E.L. 1983. Water balance and ground water studies. p. 531-548. *In* Soils: an Australian viewpoint. Div. Soils, CSIRO. CSIRO, Melbourne/Academic Press, London.
- Amelinckx, S. 1964. The observations of dislocations. *Solid State Phy. Suppl.* 6 : 1-53.
- An, Z., Bowler, J. M., Opdyke, N. D., Macumber, P. G. and Firman, J. B. 1986. Palaeomagnetic stratigraphy of Lake Bungunna: Plio-Pleistocene precursor of aridity in the Murray Basin, southeastern Australia. *Palaeogeog. Palaeoclim. Palaeoecol.* 54 : 219-240.
- Anand, R.R. and Gilkes, R.J. 1984. Weathering of ilmenite in a lateritic pallid zone. *Clays Clay Min.* 32 : 363-374.
- Andrews, J.T. and Miller, G.H. 1972. Chemical weathering of tills and surficial deposits in east Baffin Island, N.W.T. paper 0102 p. 5-7. *In* W.P. Adams and F.H. Helleimer (ed.) *Int. Geog. Vol. 1.* Univ. Toronto Press, Toronto.
- Bain, D.C. 1976. A titanium-rich soil clay. *J. Soil Sci.* 27 : 68-70.
- Baker, H.W. 1976. Environmental sensitivity of submicroscopic surface textures on quartz sand grains- a statistical evaluation. *J. Sed. Petr.* 46 : 871-880.
- Ball, L.C. 1924. Report on oil prospecting near Tewantin. *Qd. Govt. Min. J.* 25 : 354-62.
- Barshad, I. 1964. Chemistry of soil development. p. 1-70. *In* F.E. Bear (ed.) *Chemistry of the soil.* 2nd ed. Reinhold Publ. Co., New York.
- Bartenfelder, D.C. and Karathanasis, A.D. 1989. A differential scanning calorimetry evaluation of quartz status in the geogenic and pedogenic environments. *Soil Sci. Soc. Am. J.* 53 : 961-967.
- Bateman, R.M. 1989. Interpretation of heavy mineral assemblages: outmoded art or undervalued science? p. 97-98. *Abstr. Vol. 1.* 28th Int. Geol. Congr., July 1989. Washington DC.
- Bateman, R.M. and Catt, J.A. 1985. Modifications of heavy mineral assemblages in English coversands by acid podochemical weathering. *Catena* 12 : 1-21.

- Beasley, A. W. 1948. Heavy mineral beach sands of southern Queensland. Proc. R. Soc. Qd 59 : 109-140.
- Beasley, A.W. 1950. Heavy mineral beach sands of southern Queensland. II. Physical and mineralogical composition, mineral descriptions and origin of the heavy minerals. Proc. R. Soc. Qd. 61 : 59-104.
- Beavers, A.H., Fehrenbacher, J.B., Johnson, P.R. and Jones, R.L. 1963. CaO - ZrO₂ molar ratios as an index of weathering. Soil Sci. Soc. Am. Proc. 27 : 408-412.
- Bell, W. T. (1979). Thermoluminescence dating: radiation dose rate data. Archaeometry 21 : 243-245.
- Bell, W. T. and Zimmerman, D. W. 1978. The effect of HF etching on the morphology of quartz inclusions for thermoluminescence dating. Archaeometry 20 : 63-65.
- Belperio, A.P. and Bluck, R.G. 1988. Heavy mineral sand exploration targets in the western Murray Basin, South Australia- Geological Survey. South Australian Dept. Mines and Energy. Rep. Book 88/72.
- Benussi, G. 1975. Genesis of North Stradbroke Island. Proc. R. Soc. Qd. 86 : 3-8.
- Berger, G.W. 1988. Dating Quaternary events by thermoluminescence. Geol. Soc. Am. Special Pap. 227 : 13-49.
- Berner, R.A. and Schott, J. 1982. Mechanism of pyroxene and amphibole weathering: II. Observations of soil grains. Am. J. Sci. 282 : 1214-1231.
- Berrow, M.L., Wilson, M.J. and Reaves, G.A. 1978. Origin of extractable titanium and vanadium in the A horizon of Scottish podzols. Geoderma 21 : 80-103.
- Bøtter-Jensen, L., Bundgaard, J. and Mejdahl, V. (1983). An HP-85 microcomputer controlled automated reader system for TL dating. PACT 9 : 343-349.
- Bird, E.C.F. 1973. Australian coastal barriers. p. 410-426. In M.L. Schwartz (ed.) Barrier islands. Dowden, Hutchinson, Ross, Stroudsburg, Pennsylvania.
- Bird, E.C.F. 1976. Coasts. 2nd ed. Aust. Nat. Univ. Press, Canberra.
- Birkeland, P.W. 1973. Use of relative age-dating methods in a stratigraphic study of rock glacier deposits, Mt. Sopris, Colorado. Artic and Alpine Res. 5 : 401-416.
- Blackburn, G. 1959. The soils of the County Grey, South Australia. CSIRO Div. Soils Aust. Soils and Land Use Series 33.
- Blackburn, G. 1966. Radiocarbon dates relating to soil development, coast-line changes, and volcanic ash deposition in south-east South Australia. Aust. J. Sci. 29 : 50-52.
- Blackburn, G., Bond, R.D. and Clark, A.P.R. 1965. Soil development associated with stranded beach ridges in south-east South Australia. CSIRO Aust. Soil Publ. 22.

- Bossart, P.J., Meier, M., Oberli, F. and Steiger, H. 1986. Morphology versus U-Pb systematics in zircon : a high-resolution isotopic study of a zircon population from a Variscan dike in the Central Alps. *Earth Plan. Sci. Letts.* 78 : 339-354.
- Bowler, J.M., Hope, G.S., Jennings, J.N., Singh, G. and Walker, D. 1976. Late Quaternary climates of Australia and New Guinea. *Quat. Res.* 6 : 359-394.
- Bowman, G. and Harvey, N. 1985. Holocene sediment budget: LeFevre Peninsula. Report prepared for the Coast Protection Board, Dept. of Environment and Planning, Adelaide, Australia.
- Bowman, G.M. and Harvey, N. 1986. Geomorphic evolution of a Holocene beach - ridge complex, LeFevre Peninsula, South Australia. *J. Coastal Res.* 3 : 345-362.
- Brewer, R. 1955. Mineralogical examination of a yellow podzolic soil formed on granodiorite. *CSIRO Aust. Soil Publ.* 5.
- Brewer, R. 1960. Cutans: their definition, recognition and interpretation. *J. Soil Sci.* 11 : 280-293.
- Brewer, R. 1972. The basis of interpretation of soil micromorphological data. *Geoderma* 8 : 81-94.
- Brewer, R. 1976. Fabric and mineral analysis of soils. John Wiley, New York.
- Brewer, R. 1979. Relationship between particle size, fabric and other factors in some Australian soils. *Aust. J. Soil Res.* 17 : 29-41.
- Brewer, R. and Sleeman, J.R. 1960. Soil structure and fabric: their definition and description. *J. Soil Sci.* 11 : 172-185.
- Brewer, R. and Thompson, C.H. 1980. Morphology of two subtropical podzols formed on siliceous dune in coastal Queensland. p. 116-123. *In* K.T. Joseph (ed.) *Proc. Int. Conf. on classification and management of tropical soils, 1977.* Malaysian Soc. Soil Sci., Kuala Lumpur.
- Brewer, R., Sleeman, J.R. and Foster, R.C. 1983. The fabric of Australian soils. p. 439-498. *In* *Soils: an Australian viewpoint.* Div. Soils, CSIRO. CSIRO, Melbourne/ Academic Press, London.
- Bull, P.A. 1978. A quantitative approach to scanning electron microscope analysis of cave sediments. p. 201-226. *In* W.B. Whalley (ed.) *Scanning electron microscopy in the study of sediments.* Geabstract, Norwich.
- Bull, P. A. 1981. Environmental reconstruction by electron microscopy. *Progr. Phys. Geog.* 5 : 368-397.
- Bull, P.A., Goudie, A.S., Williams, D.P. and Watson, A. 1987. Colluvium: a scanning electron microscope analysis of a neglected sediment type. p 16-35. *In* J.R. Marshall (ed.) *Clastic particles: scanning electron microscopy and shape analysis of sedimentary and volcanic clastics.* Reinhold, New York.
- Bullock, P., Federoff, N., Jongerius, A., Stoops, G. Tursina, T. and Babel, U. 1985. Handbook for soil thin section description. *Waine Res. Publ., England.*
- Buol, S.W., Hole, F.D. and McCracken, R.J. 1980. Soil genesis and classification. 2nd ed. Iowa State Univ. Press, Ames.

- Bureau of Meteorology 1975. Climatic atlas of Australia map set 3 - Evaporation. Dept. Sci. Bureau Met. Aust. Govt. Services, Canberra.
- Bureau of Meteorology 1979. Climatic atlas of Australia map set 8 - Wind roses. Dept. Sci. Bur. Met. Aust. Govt. Publ. Services, Canberra.
- Bureau of Meteorology 1988. Climatic averages Australia - meteorological summary. Dept. Admin. Services. Aust. Govt. Publ. Services, Canberra.
- Burne, R.V. 1982. Relative fall of Holocene sea level and coastal progradation north western Spencer Gulf, South Australia. *BMR J. Aust. Geol. Geophys.* 7 : 35-45.
- Busacca, A.J. and Singer, M.J. 1989. Pedogenesis of a chronosequence in the Sacramento Valley, California, U.S.A. II. Elemental chemistry of the silt fraction. *Geoderma* 44 : 43-75.
- Carroll, D. 1953. Weatherability of zircon. *J. Sed. Petr.* 23 : 100-116.
- Chapman, S.L. and Horn, M.E. 1968. Parent material uniformity and origin of silty soils in northwest Arkansas based on zirconium and titanium contents. *Soil Sci. Soc. Am. Proc.* 32 : 265-271.
- Chittleborough, D.J. 1989. Genesis of a Xeralf on a feldspathic sandstone, South Australia. *J. Soil Sci.* 40 : 235-250.
- Chittleborough, D.J. and Oades J.M. 1980. The development of a Red-brown earth. II Uniformity of the parent material. *Aust. J. Soil Res.* 18 : 375-382.
- Chittleborough, D.J., Oades, J.M. and Walker, P.H. 1984. Textural differentiation in chronosequences from eastern Australia. III. Evidence from elemental chemistry. *Geoderma* 32 : 227 - 248.
- Churchward, H.M. 1963. Soil studies at Swan Hill, Victoria, Australia. III. Some aspects of soil development on aeolian materials. *Aust. J. Soil Res.* 1 : 117-128.
- Coaldrake, J.E. 1961. The ecosystem of the coastal lowlands ('wallum') of southern Queensland. *CSIRO Aust. Bull.* 283.
- Coaldrake, J.E. 1962. The coastal sand dunes of southern Queensland. *Proc. R. Soc. Qd.* 72 : 101-116.
- Cogen, W.M. 1935. Some suggestions for heavy mineral investigations of sediments. *J. Sed. Petr.* 5 : 3-8.
- Coleman, N.T. and G.W. Thomas, 1967. The basic chemistry of soil acidity. *In* R.W. Pearson and F. Adams (ed.) *Soil acidity and liming.* *Agronomy* 12 : 1-41. Am Soc. Agron. Inc. Madison, Wisconsin.
- Colman, S.M. 1981. Rock weathering rates as a function of time. *Quat. Res.* 15:250-264.
- Colwell, J.B. 1976. Heavy minerals in the Late Cainozoic sediments of southeastern South Australia. *BMR Geol. and Geophys. Record* 1976/89.
- Colwell, J.B. 1979. Heavy minerals in the Late Cainozoic sediments of southeastern South Australia and western Victoria. *BMR J. Aust. Geol. Geophys.* 4 : 83 - 97.

- Cook, P.J., Colwell, J.B., Firman, J.B., Lindsay, J.M., Schwebel, D.A. and von der Borch, C.C. 1977. Late Cainozoic sequence of south east of South Australia and Pleistocene sea level changes. *BMR J. Aust Geol. Geophys.* 2 : 81-88.
- Correns, C. W. 1978. Titanium. Sections 22B-22O. *In* K.H.Wedepohl (ed.) *Handbook of geochemistry*. Vol. II-2. Springer-Verlag, Berlin.
- Creemeens, D.L., Darmody, R.G. and Jansen, I.J. 1987. SEM analysis of weathered grains: Pretreatment effects. *Geology* 15 : 401-404.
- Crocker, R.L. and Cotton B.C. 1946. Some raised beaches of the lower south-east of South Australia and their significance. *Trans. R. Soc. S. Aust.* 70 : 64-82.
- Curtis, C.D. 1976. Stability of minerals in surface weathering reactions; a general thermochemical approach. *Earth Surface Processes* 1 : 63-70.
- Daily, B., Firman, J.B., Forbes, B.G. and Lindsay, J.M. 1976. *Geology*. p. 5-42. *In* C.R. Twidale, M.J. Tyler and B.P. Webb (ed.) *Natural history of the Adelaide region, Adelaide, Australia*. R. Soc. S. Aust. Inc.
- Darmody, R.G. 1985. Weathering assessment of quartz grains: a semiquantitative approach. *Soil Sci. Soc. Am. J.* 49 : 1322-1324.
- Douglas, L.A. and Platt, D.W. 1977. Surface morphology of quartz and the age of soils. *Soil Sci. Soc. Am. J.* 41 : 641-645.
- Dragovich, D. 1988. A preliminary electron probe study of microchemical variations in desert vanish in western New South Wales, Australia. *Earth Surface Processes and Landforms* 13 : 259-270.
- Drees, L.R. and Wilding, L.P. 1973. Elemental distribution in the light mineral isolate of soil separates. *Soil Sci. Soc. Am. J.* 42 : 976-978.
- Dryden, L. and Dryden, C. 1946. Comparative rates of weathering of some heavy minerals. *J. Sed. Petr.* 16 : 91-96.
- Durbidge, E. 1975. Introduction to the Island. *Proc. R. Soc. Qd.* 86 : 1-2.
- Eggleton, R.A. and Fitzpatrick, R.W. 1988. New data and a revised structural model for ferrihydrite. *Clays Clay Min.* 36 : 111-124.
- Erlank, A.J., Smith, H.S., Marchant, J.W., Cardoso, M.P. and Ahrens, L.H. 1978 a. Zirconium. Sections 40A-40O. *In* K.H.Wedepohl (ed.) *Handbook of geochemistry*. Vol. II-4. Springer-Verlag, New York.
- Erlank, A.J. Smith, H.S. Marchant, J.W. Cardoso, M.P. and Ahrens, L.H. 1978 b. Hafnium. Sections 72B-72O. *In* K.H.Wedepohl (ed.) *Handbook of geochemistry*. Vol. II-5. Springer-Verlag, New York.
- Eswaran, H. and Banos, C. 1976. Related distribution patterns in soils and their significance. *Ans. Edaf. Agrobiol.* 35 : 33-45.
- Eswaran, H. and Stoops, G. 1979. Surface textures of quartz in tropical soils. *Soil Sci. Soc. Am. J.* 43 : 420-424.

- Evans, L.J. and Adams, W.A. 1975 a. Quantitative pedological studies on soils derived from Silurian mudstones. IV. Uniformity of parent material and evaluation of internal standards. *J. Soil Sci.* 26 : 319-326.
- Evans, L.J. and Adams, W.A. 1975 b. Quantitative pedological studies on soils derived from Silurian mudstones. V. Redistribution and loss of mobilized constituents. *J. Soil Sci.* 26 : 327-335.
- F.A.O. 1974. FAO-Unesco soil map of the world 1:5,000,000. Vol. 1. Legend. UNESCO, Paris.
- Farmer, V.C. 1987. The role of inorganic species in the transport of aluminium in podzols. p.187-194. *In* D. Righi and A. Chauvel (ed.) Podzols and podzolization. Plaiser: Assoc. Franc. Etude Sol.
- Farmer, V.C., Skjemstad, J.O. and Thompson, C.H. 1983. Genesis of humus B horizons in hydromorphic humus podzols. *Nature* 304 : 342-344.
- Firman, J.B. 1966. Stratigraphic units of Late Cainozoic age in the St. Vincent Basin, South Australia. *Quarterly Geol. Notes. Geol. Surv. S. Aust.* 17 : 6-9.
- Firman, J.B. 1973. Regional stratigraphy of surficial deposits in the Murray Basin and the Gambier Embayment. *Geol. Surv. S. Aust. Rep.* 39.
- FitzPatrick, E.A. 1980. Soils: their formation, classification and distribution. Longman, London.
- FitzPatrick, E.A. 1984. Micromorphology of soils. Chapman and Hall, London.
- Flinter, B.H. 1959. The magnetic separation of some alluvial minerals in Malaya. *Am. Min.* 44 : 738-751.
- Fordham, A.W. and Norrish, K. 1979. Electron microprobe and electron microscope studies of soil clay particles. *Aust. J. Soil Res.* 17 : 283-306.
- Fransan, M.A. (ed.). 1976. Standard methods for the examination of water and wastewater. 14th ed. American Public Health Assoc. Washington, D.C.
- Gandolfi, G. 1967. Discussion upon methods to obtain x-ray "powder pattern" from a simple crystal. *Miner. Petwgr. Acta.* 13 : 67-74.
- Gardner, D.E. 1955. Beach-sand heavy mineral deposits of eastern Australia. *Bull. Bur. Min. Resour. Aust.* 28 : 1-103.
- Gardner, G.J., Mortlock, A.J., Price, D.M., Readhead, M.L. and Wasson, R.J. 1987. Thermoluminescence and radiocarbon dating of Australian desert dunes. *Aust. J. Earth Sci.* 34 : 343-357.
- Genstat 5. 1987. Reference Manual. Oxford University Press.
- Gile, I.H., Peterson, F.F. and Grossman, R.B. 1966. Morphological and genetic sequences of carbonate accumulation in desert soils. *Soil Sci.* 101 : 347-360.
- Golding, H.G. 1955. Leucoxenitic grains in dune sands at North Stradbroke Island, Queensland. *J. R. Soc. NSW* 89 : 219-231.

- Gostin, V.A., Hails, J.R. and Polach, H.A. 1981. Quaternary sea levels in upper Spencer Gulf, South Australia. *Search* 12 : 43-45.
- Gravenor, C.P. 1979. The nature of the Late Paleozoic glaciation in Gondwana as determined from an analysis of garnets and other heavy minerals. *Can. J. Earth Sci.* 16 : 1137-1153.
- Gravenor, C.P. 1980. Chattermarked garnets and heavy minerals from the Late Paleozoic glacial deposits of southern Brazil. *Can. J. Earth Sci.* 17 : 156-159
- Gravenor, C.P. and Gostin, V.A. 1979. Mechanisms to explain the loss of heavy minerals from the Upper Palaeozoic tillites of South Africa and Australia and the Late Precambrian tillites of Australia. *Sedimentology* 26 : 707-717.
- Green, P. 1966. Mineralogical and weathering study of a Red-brown earth formed on granodiorite. *Aust. J. Soil Res.* 4 : 181-197.
- Grimes, K.J. 1979. Carbon-14 dates and the evolution of Fraser Island. *Qd. Govt. Min. J.* 80 : 79-82.
- Grossman, R.B., Stephen, I., Fehrenbacher, J.B., Beavers, A.H. and Parker, J.M. 1959. Fragipan soils in Illinois. II. Mineralogy in reference to parent material uniformity of Hosmer silt loam. *Soil Sci. Soc. Am. Proc.* 23 : 70-73.
- Hails, J.E., Salama, M.S., Gostin, V.A., Sargent, G.E.C. and von der Borch, C.C. 1982. Nearshore sediment dynamics and sedimentation in the Gulf of St. Vincent, South Australia. Adelaide. Coast Protection Board of South Australia Report.
- Hails, J.R. 1964. The coastal depositional features of south eastern Queensland. *Aust. Geogr.* 9 : 207-217.
- Hails, J.R., Belperio, A.P., and Gostin, V.A. 1983. Holocene sea levels of Upper Spencer Gulf, South Australia. *In* D. Hopley (ed.) Australian sea levels in the last 15,000 years : a review. Townsville Dept. of Geography, James Cook University. Monograph Series, Occasional Pap. 3 : 48-53.
- Harris, W. K. 1983. Geology. p. 1-6. *In* M.J. Tyler, C. R. Twidale, J. K. Ling and J. W. Holmes (ed.) Natural history of the south east. R. Soc. S. Aust. Inc.
- Haseman, J.F. and Marshall, C.E. 1945. The use of heavy minerals in studies of the origin and development of soils. University of Missouri Agricultural Experimental Station Research Bulletin 387.
- Hay, R.L. 1960. Rate of clay formation and mineral alteration in a 4000-year old volcanic ash soil on St. Vincent, B.W.I. *Am. J. Sci.* 258 : 354-368.
- Hemingway, J.E. and Tamar-Agha, M.Y. 1975. The effects of diagenesis on some heavy minerals from the sandstones of the Middle Limestone Group in Northumberland. *Proc. Yorkshire Geol. Soc.* 40 : 537-544.
- Hollis, J.D., Sutherland, F.L. and Gleadow, A.J. 1986. The occurrence and possible origins of large zircons in alkali volcanics of eastern Australia. p.565-578. *In* J. Mincera-Stefanova, I. Bonev, B.K. Kamenov, D. Stefanova, and T. Todorova (ed.) Crystal chemistry of minerals. Proc. 13th General Meeting Int. Min. Soc. (IMA), Varna. Bulgarian Academy of Sciences, Sofia.

- Holmgren, G.G.S., Juve, R.L. and Geschwender, R.C. 1977. A mechanically controlled variable rate leaching device. *Soil Sci. Soc. Am. J.* 41 : 1207-1208.
- Hossfeld, P.S. 1950. The Late Cainozoic history of the south east of South Australia. *Trans. R. Soc. S. Aust.* 73 : 232-279.
- Horwitz, R.C. 1960. Géologie de la région de Mt. Compass (feuille Milang), Australie Méridionale. *Ecolog. Geol. Helv.* 53 : 211-263.
- Howchin, W. 1888. Remarks on a geological section at the New Graving Dock, Glanville, with special reference to a supposed old land surface now below sea level. *Trans. R. Soc. S. Aust.* 10 : 31-35.
- Hunter, C.R. and Busacca, A.J. 1989. Dispersion of three Andic soils by ultrasonic vibration. *Soil Sci. Soc. Am. J.* 53 : 1299-1302.
- Hutton, J.T. 1976. Chloride in rainfall in relation to distance from the sea. *Search* 7 : 207-208.
- Idnurm, M. and Cook, P.J. 1980. Palaeomagnetism of beach ridges in South Australia and the Milankovich theory of ice ages. *Nature* 286 : 699-702.
- Jenny, H. 1941. Factors of soil formation - a system of quantitative pedology. McGraw-Hill Inc. New York.
- Jensen, H.I. 1914. The soils of New South Wales. Govt. Printer, Sydney.
- Jouany, C. and Chassin, P. 1987. Wetting properties of Fe and Ca humates. *The Sci. Total Env.* 62 : 267-270.
- Jung, H.A. and Peacor, D.R. 1987. Kaolinitization of biotite: TEM data and implications for an alteration mechanism. *Am. Min.* 72 : 353-356.
- Keller, J.M. 1986. Thermoluminescence dating of sediments: application of C-14 dated Holocene sand dunes of LeFevre Peninsula. Unpublished Honours thesis, Dept. Physics, University of Adelaide.
- Kosterin, A.V., Shevaleevskii, I.D. and Rybalova, E.K. 1960. The Zr/Hf ratio in the zircons of some igneous rocks of the northern slope of the Kuramin Mountain range. *Geochemistry* 5 : 541-545.
- Krinsley, D.H. and Donahue, J. 1968. Environmental interpretation of sand grain surface textures by electron microscopy. *Geol. Soc. Am. Bull.* 79 : 743-748.
- Krinsley, D.H. and Doornkamp, J.C. 1973. Atlas of quartz sand surface textures. Cambridge Univ. Press, Cambridge.
- Krinsley, D.H. and Margolis, S.V. 1971. Grain surface texture. p. 151-180. *In* R.E. Carver (ed.) *Procedures in sedimentary petrology*. John Wiley and Sons Inc., New York.
- Krinsley, D.H. and McCoy, F. 1978. Aeolian quartz sand and silt. p. 249-260. *In* W.D. Whalley (ed.) *Scanning electron microscopy in the study of sediments*. Geo Abstr., Norwich.
- Kruskal, W.H. and Wallis, W.A. 1952. Use of ranks in one criterion variance analysis. *J. Am. Stat. Assoc.* 47 : 583-621.

- Kubiena, W.L. 1938. *Micropedology*. Collegiate Press, Inc., Ames, Iowa.
- Lasaga, A.C. and Blum, A.E. 1986. Surface chemistry, etch pits and mineral-water reactions. *Geochim. et Cosmochim. Acta* 50 : 2363-2379.
- Laycock, J.W. 1971. North Stradbroke Island. p. 143-151. In G. Playford (ed.) *Geological excursion handbook*. Aust and N.Z. Ass. Advmt. Sci. 43rd Congr. Brisbane, and Geol. Soc. Aust. Inc. Qd. Div.
- Lin, I.J., Rohrlich, V. and Slatkine, A. 1974. Surface microtextures of heavy minerals from the Mediterranean coast of Israel. *J. Sed. Petr.* 44 : 1281-1295.
- Lindsay, W.L. and Moreno, E.C. 1960. Phosphate phase equilibria in soils. *Soil Sci. Soc. Am. Proc.* 24 : 177-182.
- Little, I.P., Armitage, T.M. and Gilkes, R.J. 1978. Weathering of quartz in dune sands under subtropical conditions in eastern Australia. *Geoderma* 20 : 225-237.
- Lu, Y.C., Prescott, J.R., Robertson, G.B. and Hutton, J.T. 1987. Thermoluminescence dating of the Malan loess at Zhaitang, China. *Geology* 15 : 603-605.
- Manickam, S. and Barbaroux, L. 1987. Variations in the surface texture of suspended quartz grains in the Loire River: an SEM study. *Sedimentology* 34 : 495-570.
- Marel, H.W. van der 1949. Mineralogical composition of a heath podzol profile. *Soil Sci.* 67 : 193-207.
- Margolis, S.V. 1968. Electron microscopy of chemical solution and mechanical abrasion features on quartz sand grains. *Sed. Geol.* 2 : 243-256.
- Margolis, S.V. and Krinsley, D.H. 1973. Depositional histories of sand grains from surface textures: comment. *Nature* 245 : 30-31.
- Marsan, F.A., Bain, D.C. and D.M.L. Duthie 1988. Parent material uniformity and degree of weathering in a soil chronosequence, north western Italy. *Catena* 15 : 507-517.
- Marshall, B. 1967. The present status of zircon. *Sedimentology* 9 : 119-136.
- Marshall, C.E. 1977. *The physical chemistry and mineralogy of soils*. Vol II. Soils in place. John Wiley and Sons, New York.
- Marshall, C.E. and Jeffries, C.D. 1946. Mineralogical methods in soil research. I. The correlation of soil types and parent materials with supplementary information on weathering processes. *Soil Sci. Soc. Am. Proc.* 10 : 397-406.
- Matelski, R.P. and Turk, L.M. 1947. Heavy minerals in some podzol soil profiles in Michigan. *Soil Sci.* 64 : 469-487.
- Maud, R.R. 1972. *Geology, geomorphology and soils of Central Country Hindmarsh (Mount Compass-Milang), South Australia*. CSIRO (Aust.) Soil Publ. 29.
- McKeague, J.A., DeConinck, F. and Franzmeier, D.P. 1983. Spodosols. p. 217-252. *In* L.P. Wilding, N.E. Smeck and G.F. Hall (ed.) *Pedogenesis and soil taxonomy II. The soil orders*. Elsevier, Amsterdam

- McKeague, J.A., Ross, G.J. and Gamble, D.S. 1978. Properties, criteria of classification and genesis of Podzolic soils in Canada. p. 27-60. *In* W.C. Mahoney (ed.) Quaternary soils. Geo Abstr., Norwich.
- McLeod, S. 1982. Notes on soil techniques No. 4. Division of Soils, CSIRO, Australia.
- McLeod, S. and Zarcinas, B.A. 1976. The determination of ammonium and chloride by an autoanalyser for the measurement of cation exchange capacity of soils. *Comm. Soil Sci. Plant. Anal.* 7 : 743-750.
- Merry, R.H. and Spouncer, L.S. 1988. The measurement of carbon in soils using a microprocessor-controlled resistance furnace. *Comm. Soil Sci. Plant Anal.* 19 : 707-720.
- Milnes, A.R. and Farmer, V.C. 1987. Micromorphological and analytical studies of the fine matrix of an Australian humus iron podzol. *J. Soil Sci.* 38 : 593-605.
- Milnes, A.R. and Fitzpatrick, R.W. 1989. Zirconium and titanium minerals. p. 1131-1205. *In* J.B. Dixon and S.B. Weed (ed.) Minerals in the soil environment. 2nd ed. Soil Sci. Soc. Am., Madison, Wisconsin.
- Milnes, A.R. and Hutton, J.T. 1974. The nature of microcryptocrystalline titania in 'silcrete' skins from the Beda Hill area of South Australia. *Search* 5 : 153-154.
- Mitchell, W.A. 1975. Heavy minerals. p. 449-480. *In* J.E. Gieseking (ed.) Soil components Vol. 2. Inorganic components. Springer-Verlag, Berlin.
- Morris, B.J. 1978. Heavy mineral sands; resume of South Australian occurrences and partial bibliography. South Australian Dept. Mines and Energy. Rep. Book 78/28.
- Morton, A.C. 1979. Surface features of heavy mineral grains from Palaeocene sands of the central North Sea. *Scottish J. Geol.* 15 : 293-300.
- Morton, A.C. 1984. Stability of detrital heavy minerals in Tertiary sandstones from the North Sea basin. *Clay Min.* 19 : 287-308.
- Morton, A.C. 1985. A new approach to provenance studies: electron microprobe analysis of detrital garnets from Middle Jurassic sandstones of the northern North Sea. *Sedimentology* 32 : 553-566.
- Murad, E. 1978. Yttrium and zirconium as geochemical guide elements in soil and stream sediment sequences. *J. Soil Sci.* 29 : 219-223.
- Murphy, C.P., McKeague, J.A., Bresson, L.M., Bullock, P., Kooistra, M.J., Miedema, R. and Stoops, G. 1985. Description of soil thin sections : an international comparison. *Geoderma* 35 : 15-37.
- Nagasawa, K. 1953. Differential thermal analysis studies on the high-low inversion of vein quartz in Japan. *J. Earth Sci.* 1 : 156-176.
- Nickel, E. 1973. Experimental dissolution of light and heavy minerals in comparison with weathering and intrastratal solution. *Contr. Sed.* 1 : 1-68.

- Norrish, K. and Chappell, B. W. 1977. X-ray fluorescence spectrography. p. 201-272. *In* J. Zussman (ed.) *Physical methods in determinative mineralogy*. Academic Press: London.
- Norrish, K. and Hutton, J. T. 1969. An accurate X-ray spectrographic method for the analysis of a wide range of geological samples. *Geochim. et Cosmochim. Acta* 33 : 431-453.
- Norrish, K. and Rosser, H. 1983. Mineral phosphate. p. 335-388. *In* *Soils : an Australian viewpoint*, Div. Soils CSIRO. CSIRO, Melbourne/Academic Press, London.
- Northcote, K.H. 1979. A factual key for the recognition of Australian soils. 4th ed. CSIRO Aust. Div. Soils., Rellim, Adelaide, South Australia.
- Oertel, A.C. and Giles, J.B. 1966. Quantitative study of a layered soil. *Aust. J. Soil Res.* 4 : 19-28.
- Olsen, S.R., Cole, C.V., Watanabe, F.S. and Dean, L.A. 1954. Estimation of available phosphorus in soils by extraction with sodium bicarbonate. U.S. Dept. Agric. Circ. 939.
- Owen, M.R. 1987. Hafnium content of detrital zircons, a new tool for provenance study. *J. Sed. Petr.* 57 : 824-830.
- Pawluk, S. 1960. Some podzol soils of Alberta. *Can. J. Soil Sci.* 40 : 1-14.
- Pettijohn, F.J. 1941. Heavy minerals and geologic age. *J. Geol.* 49 : 610-625.
- Pettijohn, F.J. 1957. *Sedimentary rocks*. Harper, New York.
- Pickett, J.W., Ku, T.L., Thompson, C.H., Roman, D., Kelley, R.A., and Huang, Y.P. 1989. A review of age determinations on Pleistocene corals in eastern Australia. *Quat. Res.* 31 : 392-395.
- Pickett, J.W., Thompson, C.H., Kelley, R.A. and Roman, D. 1985. Evidence of high sea level during Isotope stage 5C in Queensland, Australia. *Quat. Res.* 24, 103-114.
- Pickett, J.W., Thompson, C.H., Martin, H.A. and Kelley, R.A. 1984. Late Pleistocene fossils from beneath a high dune near Amity, North Stradbroke Island, Queensland. p. 167-177. *In* R. J. Coleman, J. Covacevich and P. Davie. (ed.) *Focus on Stradbroke Island*. Boolarong Publs., Brisbane.
- Piper, C.S. 1942. *Soil and plant analysis - a laboratory manual of methods for the examination of soils and the determination of the inorganic constituents of plants*. Interscience Publ. Inc., New York.
- Prescott, J.A. 1929. The vegetation map of South Australia. *Trans. R. Soc. S. Aust.* 53 : 7-9.
- Prescott, J.A. 1931. The soils of Australia in relation to vegetation and climate. *Common. Sci. Industr. Res. Aust. Bull.* 52.
- Prescott, J. R. 1983. Thermoluminescence dating of sand dunes at Roonka, South Australia. *Council of Europe J. PACT* 9 : 505-512.

- Prescott, J. R. and Hutton, J. T. 1988. Cosmic ray and gamma ray dosimetry for TL and ESR. *Nuclear Tracks and Rad. Meas.* 14 : 223-230.
- Pye, K. 1983. Formation and history of Queensland coastal dunes. *Zeits. Geomorph. Suppl. Bd.* 45 : 175-204.
- Radtke, U. 1988. How to avoid 'useless' radiocarbon dating. *Nature* 333 : 307-308.
- Raeside, J.D. 1959. Stability of index minerals in soils with particular reference to quartz, zircon and rutile. *J. Sed. Petr.* 29 : 493-502.
- Rahmani, R.A. 1973. Grain surface etching features of some heavy minerals. *J. Sed. Petr.* 43 : 882-888.
- Readhead, M. L. 1988. Thermoluminescence dating study of quartz in aeolian sediments from south eastern Australia. *Quat. Sci. Review* 7 : 257-264.
- Ruxton, B.P. 1968. Rates of weathering of Quaternary volcanic ash in north-east Papua. *J. Geol.* 76 : 518-527.
- Schott, J. and Berner, R.A. 1983. X-ray photoelectron studies of the mechanism of iron silicate dissolutions during weathering. *Geochim. et Cosmochim. Acta* 47 : 2233-2240.
- Schwebel, D.A. 1983. Quaternary dune systems. p. 15-24. *In* J. Tyler, C.R. Twidale, J.K. Long and J.W. Holmes (ed.) *Natural history of the South East*. R. Soc. S. Aust. Inc.
- Schwebel, D.A. 1984. Quaternary stratigraphy and sea-level variation in the south east of South Australia. p. 291-311. *In* B.G. Thom (ed.) *Coastal geomorphology in Australia*. Academic Press, Sydney.
- Sehgal, J.L. and Stoops, G. 1972. Pedogenetic calcite accumulation in arid and semi-arid regions of the Indo-gangetic alluvial plains of Erstwhile Punjab (India): their morphology and origin. *Geoderma* 8 : 59-72.
- Setlow, L.W. 1978. Age determination of reddened coastal dunes in northwest Florida, USA, by use of scanning electron microscopy. p. 283-305. *In* W.D. Whalley (ed.) *Scanning electron microscopy in the study of sediments*. Geo Abstr., Norwich.
- Setlow, L.W. and Karpovich, R.P. 1972. "Glacial" micro-textures on quartz and heavy mineral sand grains from the Littoral environment. *J. Sed. Petr.* 42 : 864-875.
- Shackleton, N. J. and Opdyke, N. D. 1976. Oxygen isotopes and palaeomagnetic stratigraphy of Pacific core V 28-239 late Pliocene to latest Pleistocene. *Geol. Soc. Am. Memoir* 145 : 449-464.
- Siegel, S. 1956. *Nonparametric statistics for the behavioural sciences*. McGraw- Hill, New York.
- Siever, R. and Woodford, N. 1979. Dissolution kinetics and the weathering of mafic minerals. *Geochim. et Cosmochim. Acta* 43 : 717-724.
- Simonson, R.W. 1959. Outline of a generalized theory of soil genesis. *Soil Sci. Soc. Am. Proc.* 23 : 152-156.

- Skjemstad, J.O., Fitzpatrick, R.W., Thompson, C.H. and Zarcinas, B.A. 1990. The pedogenesis of giant dune podzols and other related soils in eastern Australia. I. Translocation of elements. *Aust. J. Soil Sci.* (in press).
- Sleeman, J.R. 1964. Structure variation within two Red-brown earth profiles. *Aust. J. Soil Res.* 2 : 146-161.
- Smith, B. W. and Prescott, J.R. 1987. Thermoluminescence dating of the eruption at Mt. Schank, South Australia. *Aust. J. Earth Sci.* 34 : 335-342.
- Smith, H. and Wilding, L.P. 1972. Genesis of argillic horizons in ochraqualfs derived from fine textured till deposits of north western Ohio and south eastern Michigan. *Soil Sci. Soc. Am. Proc.* 36 : 808-815.
- Smith, L.H. and Tiller, K.G. 1977. A modified procedure for the more rapid determination of the clay content ($< 2\mu\text{m}$) of soils. *Div. Soils Divl. Rep.* 19. CSIRO, Australia.
- Soil Survey Staff 1987. *Keys to Soil Taxonomy*. 3rd printing. Soil Manage. Support Serv. Tech. Monog. No. 6 Cornell Univ., Ithaca, N.Y.
- Soil Survey Staff 1951. *Soil Survey Manual*. USDA-SCS Agric. Handb. 18. U.S. Govt. Print. Office, Washington D.C.
- Speer, J.A. 1980. Zircon. p. 67-112. *In* P.H. Ribbe (ed.) *Reviews in mineralogy*. Vol. 5. Orthosilicates. *Min. Soc. Am.*
- Sprigg, R.C. 1952. Geology of the southeast province of South Australia, with special reference to Quaternary coastline migrations and modern beach developments. *Geol. Surv. S. Aust. Bull.* 29.
- Stace, H.C.T., Hubble, G.D., Brewer, R., Northcote, K.H., Sleeman, J.R., Mulcahy, M.J. and Hallsworth, E.G. 1968. *A handbook of Australian soils*. Rellim, Glenside, South Australia.
- Steiglitz, R.D. 1969. Surface textures of quartz and heavy mineral grains from fresh water environments: an application of scanning electron microscopy. *Geol. Soc. Am. Bull.* 80 : 2091-2094.
- Stephens, C.G. 1962. *A manual of Australian soils*. 3rd ed. CSIRO Australia, Melbourne.
- Stephens, C.G., Crocker, R.L., Butler, B and Smith, R. 1941. A soil and land use survey of the Hundreds of Riddoch, Hindmarsh, Grey, Young and Nangwarry, County Grey, South Australia. *Common. Sci. Industr. Res. Aust. Bull.* 142.
- Stevens, P.R. and Walker, T.W. 1970. The chronosequence concept and soil formation. *Quat. Rev. Biol.* 45 : 333-350.
- Stobbe, P.C. and Wright, J.R. 1959. Modern concepts of the genesis of Podzols. *Soil Sci. Soc. Am. Proc.* 23 : 161-164.
- Stoops, G. and Jongerius, A. 1975. Proposal for a micromorphological classification of soil materials. I. A classification of the related distributions of fine and coarse particles. *Geoderma* 13 : 189-199.

- Sudom, M.D. and St. Arnaud, R.J. 1971. Use of quartz, zirconium and titanium in pedological studies. *Can. J. Soil Sci.* 51 : 385-396.
- Suzuki, H., Uesugi, Y., Endo, K., Ohmori, H., Takeuchi, K. and Iwasaki, K. 1982. Studies on the Holocene and Recent climatic fluctuations in Australia and New Zealand. Tokyo.
- Symkartz-Kloss, W. 1974. Differential thermal analysis. Springer-Verlag, New York.
- Thom, B.G. 1978. Coastal sand deposition in southeast Australia during the Holocene. p. 197-214. *In* J.L. Davies and M.A.J. Williams (ed.) Landform evolution in Australasia. Aust. Nat. Univ. Press, Canberra.
- Thom, B.G., Bowman, G.M., Gillespie, R., Polach, H.A. and Barbetti, M. 1981. Radiocarbon dating of Holocene beach-ridge sequences in south-east Australia. Monograph 11. Geogr. Dept. Univ. NSW, Duntroon.
- Thom, B.G., Palach, H.A. and Bowman G.M. 1978. Holocene age structure of coastal sand barriers in New South Wales, Australia. Geogr. Dept. Univ. NSW, Duntroon.
- Thompson, C.H. 1981. Podzol chronosequences on coastal dunes of eastern Australia. *Nature* 291 : 59-61.
- Thompson, C.H. 1983. Development and weathering of large parabolic dune systems along the sub-tropical coast of eastern Australia. *Zeit. Geomorph. Suppl. Bd.* 45 : 205-225.
- Thompson, C.H. and Bowman, G.M. 1984. Subaerial denudation and weathering of vegetated coastal dunes in eastern Australia. p. 263-290. *In* B. G. Thom.(ed.) Coastal geomorphology in Australia. Academic Press, Sydney.
- Thompson, C.H. and Hubble, G.D. 1980. Sub-tropical Podzols (Spodosols and related soils) of coastal eastern Australia. p. 203-213. *In* K.T. Joseph (ed.) Proc. Conf. on classification and management of Tropical soils 1977. Malaysian Soc. Soil Sci., Kuala Lumpur.
- Thompson, C.H. and Moore, A.W. 1984. Studies in landscape dynamics in the Cooloola-Noosa River area, Queensland. 1. Introduction, general description and research approach. CSIRO (Australia) Div. Soils, Divl. Rep. 73.
- Thompson, C.H. and Walker, J. 1986. Temporal changes in soils and vegetation on subtropical coastal dunes at Cooloola, Queensland, Australia - a synthesis. p. 1-7. *In* P. Stevens (ed.) Soils and the time factor. Proc. Welsh Soil Discussion Group Meeting. Aberystwyth, May 1983.
- Thompson, C.H. and Ward, W.T. 1975. Soil landscapes of North Stradbroke Island. *Proc. R. Soc. Qd.* 86 : 9-14.
- Tucker, B.M. 1983. Basic exchangeable cations. p. 401-416. *In* Soils: an Australian viewpoint. Div. Soils CSIRO. CSIRO, Melbourne/Academic Press, London.
- Twidale, C.R. 1976. Geomorphological evolution. p. 43-59. *In* C.R. Twidale, M.J. Tyler and B.P. Webb (ed.) Natural history of the Adelaide region. R. Soc. S. Aust. Inc.

- USDA Soil Conservation Service (1972, revised 1982). Soil survey laboratory methods and procedures for collecting soil samples. Soil survey investigations report No. 1. US Govt. Printing Office, Washington DC.
- Velbel, M.A. 1984. Natural weathering mechanisms of almadine garnet. *Geology* 12 : 631-634.
- von der Borch, C.C. 1979. Giant submarine canyons. p. 47-51. *In* M.J. Tyler, C.R. Twidale and J.K. Ling (ed.) *Natural history of Kangaroo Island, Adelaide, Australia*. R. Soc. S. Aust. Inc.
- Vreeken, W.J. 1975. Principal kinds of chronosequences and their significance in soil history. *J. Soil Sci.* 26 : 378-394.
- Walker, J., Thompson, C.H., Fergus, I.F. and Tunstall, B.R. 1981. Plant succession and soil development in coastal sand dunes of subtropical eastern Australia. p. 107-131. *In* D.C. West, H.H. Shugart and D.B. Botkin (ed.) *Forest succession: concepts and applications*. Springer-Verlag, New York.
- Walker, J., Thompson, C.H. and Lacey, C.J. 1987. Morphological differences in lignotubers of *Eucalyptus intermedia* R.T. Bak. and *E. Signata* F. Muell. associated with different stages of podzol development on coastal dunes, Cooloola, Queensland. *Aust. J. Bot.* 35 : 301-311.
- Ward, W.T. 1966. The geology, geomorphology and soils of south-western county Adelaide, South Australia. CSIRO Aust. Soil Publ. 23.
- Ward, W.T. 1977. Sand movement on Fraser Island: a response to changing climates. *Univ. Qd. Dept. Anthropol. Pap.* 8 : 113-126.
- Ward, W.T. 1978. Notes on the origin of Stradbroke Island. *Univ. Qd. Dept. Geol. Pap.* 8 : 97-104.
- Ward, W.T. and Grimes, K.G. 1987. History of coastal dunes at Triangle Cliff, Fraser Island, Queensland. *Aust. J. Earth Sci.* 34 : 325-333.
- Ward, W.T. and Jessup, R.W. 1965. Changes of sea level in Southern Australia. *Nature* : 205 : 791-792.
- Ward, W.T., Little, I.P. and Thompson, C.H. 1979. Stratigraphy of two sandrocks at Rainbow Beach, Queensland, Australia, and a note on humate composition. *Paleogeogr., Paleoclimat., Paleoecol.* 26 : 305-316.
- Weyl, R. 1951. Schwermineralkverwitterung in Schleswig-Holsteinischen Boden. *Schriften Naturwissenschaftlichen Vereins für Schleswig-Holstein* 25 : 157-165.
- Whalley, W. B. and Krinsley, D. H. 1974. A scanning electron microscope study of surface textures of quartz grains from glacial environments. *Sedimentology* 21 : 87-105.
- Whalley, W.B. 1985. Scanning electron microscopy and the sedimentological characterisation of soils. p. 183-201. *In* K.S. Richards, R.R. Arnett and S. ELLIS (ed.) *Geomorphology and soils*. George Allen and Unwin, London.
- Whitney, R.S. and Gardner, R. 1943. The effect of carbon dioxide on soil reaction. *Soil Sci.* 55 : 127-141.

- Whitworth, H.F. 1956. The zircon-rutile deposits on the beaches of the east coast of Australia with special reference to their mode of occurrences and the origin of the minerals. Dept. Mines NSW, Tech. Rep. 4 : 7-60.
- Wild, A. 1961 Loss of zirconium from 12 soils derived from granite. *Aust. J. Agric. Res.* 12 : 300-305.
- Wilding, L.P., Drees, L.R. Smeck, N.E. and Hall, G.F. 1971. Mineral and elemental composition of Wisconsin: age till deposits in West Central Ohio. p. 290-317. *In* R.P. Goldthwaite (ed.) Till: a symposium. Ohio State Univ. Press, Ohio.
- Wilson, M.J. 1975. Chemical weathering of some primary rock-forming minerals. *Soil Sci.* 119 : 349-355.
- Wilson, M.J. 1986. Mineral weathering processes in podzolic soils on granitic materials and their implications for surface water acidification. *J. Geol. Soc. Lond.* 143 : 691-697.
- Wintle, A.G. and Huntley, D.J. 1982. Thermoluminescence dating of sediments. *Quat. Sci. Review* 1 : 31-53.
- Wopfner, H. and Douglas, J.G. (ed.). 1971. The Otway Basin of southeastern Australia. Special Bull. Geol. Surv. S. Aust. and Victoria.
- Wynne, A.A., Fotheringham, D.G., Freeman, R., Moulds, B., Penney, S.W., Petrusevics, P., Tucker, R., and Ellis, D.P. 1984. Adelaide coast protection strategy review, Adelaide, Australia. Dept. Environment and Planning.
- Yaalon, D.H. and Ganor, E. 1973. The influence of dust on soils during the Quaternary. *Soil Sci.* 116 : 146-155.
- Yaalon, D.H., Brenner, I. and Koyumdjisky, H. 1974. Weathering and mobility sequence of minor elements on a basaltic pedomorphic surface, Galille, Israel. *Geoderma* 12 : 233-244.
- Zeuner, F.E. 1959. The Pleistocene Period. 2nd ed. Hutchinson and Co., London.